2006

DEEPER GROUNDWATER FLOW AND CHEMISTRY IN THE ARSENIC AFFECTED WESTERN BENGAL BASIN, WEST BENGAL, INDIA

Abhijit Mukherjee
University of Kentucky, amukh2@uky.edu

ABSTRACT OF DISSERTATION

Abhijit Mukherjee

The Graduate School

University of Kentucky

2006

DEEPER GROUNDWATER FLOW AND CHEMISTRY IN THE ARSENIC AFFECTED WESTERN BENGAL BASIN, WEST BENGAL, INDIA

ABSTRACT OF DISSERTATION

A dissertation submitted in partial fulfillment
of the requirements for the degree of Doctor of Philosophy in the
College of Arts and Sciences
at the University of Kentucky

By
Abhijit Mukherjee

Lexington, Kentucky

Director: Dr. Alan E. Fryar, Associate Professor of Earth and Environmental Sciences

Lexington, Kentucky

2006

ABSTRACT OF DISSERTATION

DEEPER GROUNDWATER FLOW AND CHEMISTRY IN THE ARSENIC AFFECTED WESTERN BENGAL BASIN, WEST BENGAL, INDIA

A regional-scale hydrogeologic study was conducted in a ~21,000-km^2 area of West Bengal (Murshidabad, Nadia, North and South 24 Parganas districts), India, with severe, natural arsenic contamination of shallow groundwater jeopardizing ~13.5 million inhabitants. The study evaluated the suitability of deeper water as an alternate drinking water source.

A hydrostratigraphic model (resolution: 1000 m × 1000 m × 2 m, ≤ 300 m below MSL) indicates a continuous, semi-confined sand aquifer (main aquifer) underlain by a thick clay aquitard. The aquifer deepens toward the east and south. In the south, there are several deeper, laterally connected, confined aquifers. Based on observed hydrostratigraphy, eight seasonal groundwater models (resolution: 1000 m × 1000 m × 15 m) were developed with presence of pumping (2001), absence of pumping (pre-1970s) and projected irrigational pumping (2011 and 2021). Simulations indicate topographically controlled, seasonally variable regional groundwater flow, which has been severely distorted by pumping.

Samples of deep groundwater, river water and rainwater were collected for major and minor solutes, dissolved gases and stable isotopes. A $\delta^{18}O$-$\delta^{2}H$ bivariate plot of groundwater falls subparallel to the constructed local meteoric water line ($\delta^{2}H = 7.24\ \delta^{18}O + 7.73$), suggesting a predominance of meteoric recharge (from monsoonal rainfall of present-day composition) with some evaporation. A trend of $\delta^{18}O$ depletion of groundwater was observed northward and westward from the Bay of Bengal, indicating a continental effect. Major solutes indicate the presence of hydrochemically distinct water bodies in the main and deeper isolated aquifers. Spatial trends of major and redox-sensitive solutes and geochemical modeling indicate that carbonate dissolution, silicate weathering, and cation exchange along with seawater and connate-water mixing control the major-ion chemistry. The suboxic main aquifer water exhibits partial redox equilibrium, with the possibility of oxidation in micro-scale environments. The redox processes are depth-dependent and hydrostratigraphically variable.

Deeper water was found unsafe with elevated (≥10 μg/L) As in ~60% of samples. The presence of As is related to coupled Fe-S redox cycles. Deeper water is probably polluted by groundwater flow though interconnected aquifers with reduced sediments. Deep irrigational pumping has potentially attracted shallower, polluted water to greater depths.

KEYWORDS: Arsenic Contamination, Hydrostratigraphy, Groundwater Flow Modeling, Hydrogeochemistry, West Bengal, India

Abhijit Mukherjee

3 July 2006

DEEPER GROUNDWATER FLOW AND CHEMISTRY IN THE ARSENIC AFFECTED WESTERN BENGAL BASIN, WEST BENGAL, INDIA

By

Abhijit Mukherjee

Alan E. Fryar
Director of Dissertation

Susan M. Rimmer
Director of Graduate Studies

3 July 2006

RULES FOR THE USE OF DISSERTATION

Unpublished dissertations submitted for the Doctor's degree and deposited in the University of Kentucky Library are as a rule open for inspection, but are to be used only with due regard to the rights of the authors. Bibliographical references may be noted, but quotations or summaries of parts may be published only with the permission of the author, and with the usual scholarly acknowledgements.

Extensive copying or publication of the thesis in whole or in part also requires the consent of the Dean of the Graduate School of the University of Kentucky.

DISSERTATION

Abhijit Mukherjee

The Graduate School

University of Kentucky

2006

DEEPER GROUNDWATER FLOW AND CHEMISTRY IN THE ARSENIC AFFECTED WESTERN BENGAL BASIN, WEST BENGAL, INDIA

DISSERTATION

A dissertation submitted in partial fulfillment
of the requirements for the degree of Doctor of Philosophy in the
College of Arts and Sciences
at the University of Kentucky

By
Abhijit Mukherjee

Lexington, Kentucky

Director: Dr. Alan E. Fryar, Associate Professor of Earth and Environmental Sciences

Lexington, Kentucky

2006

This dissertation is dedicated to my parents Kajali and Barindra Lal Mukherjee, my loving wife Abira, and my friend, philosopher, and guide Dr. Alan E. Fryar, without whose inspiration this work would not have been possible.

Acknowledgements

First of all, I would like to show my earnest gratitude and appreciation to my teacher and advisor Dr. Alan Fryar, through whom executing this research work and writing this dissertation has become possible. His endless support during laboratory analysis, computer modeling, and his travel to India for fieldwork in 2004 were invaluable assets for doing this work. My stay as his student at the University of Kentucky will remain as an unforgettable memory to me throughout my life.

I would also like to show my sincere gratitude to my advisory committee members Dr. William Thomas, Dr. Paul Howell (Earth and Environmental Sciences), and Dr. Steve Workman (Agricultural and Biosystems Engineering), and external examiner Dr. David Atwood (Chemistry), for their advice on various occasions.

This project could not have been executed without the cooperation of the Public Health Engineering Directorate (PHED), and State Water Investigation Directorate (SWID), Government of West Bengal. However, the ideas presented in this dissertation are those of the author and have not been officially endorsed by the Government of West Bengal or any other person or organization. Special thanks to P.K. De, A. Banerjee, A. Bhattacharya, and G. RoyChowdhury (PHED) for helping me with selection of sampling sites; Dr. S.P. SinhaRoy (Arsenic Core Committee) and the late Prof. A. Chakraborty (Indian Institute of Technology-Kharagpur) for their advice; and B.M. Engineering (KrishnaNagar) for supplying lithologs. I should especially mention the extensive help and cooperation that I received from Animesh Bhattacharya (PHED).

I also gratefully acknowledge the immense assistance provided by T. Datta and B. Hazra (PHED), Sudipta Rakshit (UK Agronomy), Basanmoy Moitra (Shantipur), and my "man Friday" Murali Singh (Calcutta) in sample collection; Trish Coakley, Bob King, John May (UK ERTL), Millie Hamilton (UK Forestry), Dr. Elisa D'Angelo (UK Plant and Soil Sciences), Jason Backus (KGS) and Dr. Chris Eastoe (University of Arizona) with sample analyses; Dr. Helena Truszczynska (UK SSTARS) with statistical analyses; Dr. Terry Lahm, Dr. Maura Metheny and Martin VanOort with groundwater modeling; Tom Sparks and Mark Thompson (KGS) for help

with GIS; and to Dr. Kevin Henke (UK CAER), Dr. Steve Fisher (KGS) and Dr. Sunil Mehta (Framatome ANP) for reviewing the manuscript. I would also like to show my special thanks to my colleagues Tao Sun, James Ward, Josh Sexton, Todd Aseltyne, Matt Surles and Niladri Gupta for their help on various occasions.

The project was financially supported by the University of Kentucky (Department of Earth and Environmental Sciences, College of Arts & Sciences, and the Graduate School), the Kentucky NSF-EPSCoR program, and the Geological Society of America. Thanks also to Pam Stephens and Rebecca Hisel for providing me help with the official procedures.

I wish to show my heartiest gratitude to my parents, brother and other family members and friends in India, and also my aunt, uncle and cousins in Pennsylvania, and the Ruthven-Fryar family for their constant emotional support and good wishes during my long stay for higher studies in the USA. Especially, I should mention the immense support provided by my father Barindra Lal Mukherjee during extremely strenuous fieldwork in 2005. Finally, I would like to thank my beloved wife Abira for her everlasting patience, inspiration, help and trust in me.

Last but not least, I am sincerely grateful to the inhabitants of West Bengal for their tremendous hospitality and cooperation during the fieldwork.

Table of Contents

List of Tables

List of Tables (continued)

List of Figures

List of Figures (continued)

List of Figures (continued)

List of Figures (continued)

List of Figures (continued)

List of Files

abmdissertation.pdf

Chapter 1: Introduction

1.1 Prelude

More than 2% (120 million) of the total population (6 billion) of this planet lives in an area of ~200,000 km^2 covering the eastern part of the state of West Bengal (India) and most of Bangladesh. This area, popularly known as the Bengal basin, is the world's largest fluvio-deltaic system (Coleman, 1981; Alam et al., 2003). The basin is drained jointly by the River Ganges, River Brahmaputra (also known as River Jamuna in Bangladesh), River Meghna and their numerous tributaries and distributaries, and hence is also known as the Ganges-Brahmaputra-Meghna (GBM) delta or basin.

Indiscriminate use of the rivers and streams as pathways of sewage and industrial waste by the Bengal basin inhabitants has made the surface water impotable. Moreover, the introduction of high-yielding dry-season rice (Boro) (Harvey et al., 2005) accelerated the demand for irrigation. This led to the shift of water policy from surface water to groundwater in both West Bengal and Bangladesh during the early 1970s. As a consequence, several million wells (ranging from low yielding hand-pumped to heavy-duty motor driven) were installed in order to meet drinking, irrigation, and industrial water demands (Smith et al., 2000; BGS/DPHE, 2001; Harvey et al., 2005; Horneman et al., 2004).

Unfortunately, arsenic concentrations exceeding the US Environmental Protection Agency (USEPA) maximum contaminant level of 50 μg/L were discovered in 1978 (Guha Mazumder et al., 1998) in some wells in the North 24 Parganas district of West Bengal, followed by detection of arsenicosis by 1984 (Garai et al., 1984). Arsenic, cited as the most hazardous contaminant by the U.S. Agency for Toxic Substance and Disease Registry (ATSDR, 2005), is a ubiquitous metalloid which, when ingested for extended periods, may cause severe health effects, including arsenical dermatitis, deformation of limbs, circulatory and respiratory problems, and various cancers, leading to untimely death. Soon, groundwater in other parts of West Bengal (mostly east of the River Bhagirathi-Hoogly [Figure 1.1], the main distributary of the Ganges in India) and, Bangladesh in 1993 (Swartz et al., 2004), were found to have groundwater with As concentrations exceeding the World Health Organization (WHO, 1993,

2001) drinking water safe limit of 10 μg/L. More than 50 million people may be at potential risk from As exposure in the Bengal basin (Figures 1.2a, b and c). Of these, at least 1 million are likely to be affected by arsenicosis, as calculated by Yu et al. (2003) based on dose-response data from Guha Mazumder et al. (1998). The contamination has been termed as the greatest mass poisoning in human history (Smith et al., 2000). Estimates show that at present about 25% (McArthur et al., 2004) to 33% (Horneman et al., 2004) of the wells have been identified to be contaminated by As. Since 1990, numerous studies by governmental and non-governmental agencies and researchers have tried to understand the causes and effects of this contamination. These studies have led to a detailed understanding of the water-sediment chemistry and proposition of several hypotheses on the occurrence and fate of arsenic in groundwater on both sides of the Indo-Bangladesh border (e.g. Saha, 1991; AIP/PHED, 1991, 1995; Mallick and Rajgopal, 1995; Das et al., 1995, 1996; Bhattacharya et al., 1997; CGWB, 1997; Mandal et al., 1998; Nickson et al., 1998, 2000; Ray, 1999; Acharyya et al., 1999, 2000; BGS/DPHE, 2001; McArthur et al., 2001, 2004; Ravenscroft et al., 2001, 2005; Harvey et al., 2002, 2005, 2006; Ghosh and Mukherjee, 2002; JICA, 2002; Smedley and Kinniburgh, 2002; Dowling et al., 2003; Stüben et al., 2003; van Geen et al., 2003, 2004; Horneman et al., 2004; Swartz et al., 2004; Polizzato et al., 2005).

1.2 Importance and objective of work

It has been hypothesized that the non-point source, geogenic As mostly occurs in the Holocene shallow aquifers of the Bengal basin and probably has been mobilized from the sediments by redox reactions. Various workers (e.g. BGS/DPHE, 2001; McArthur et al., 2001; JICA, 2002; van Geen et al., 2003; Ravenscroft et al., 2005, Zheng et al., 2005a) have suggested that deeper groundwater could be an alternate, safe drinking water source. Consequently, water-supply authorities have installed numerous deep community wells (Figure 1.3a) to provide As-free water to the huge urban and rural population, although the deeper water chemistry has received relatively little attention.

Because Bangladesh occupies most of the Bengal basin, it has received more attention than the part of the basin in West Bengal. Several comprehensive studies (e.g. BGS/DPHE/MML, 1999; BGS/DPHE, 2001; JICA, 2000, 2002) have examined the

contamination extent (Figure 1.3b), detailed regional hydrogeology and hydrogeochemistry of much of the eastern part of the basin. In West Bengal, however, in spite of district-level surveys of groundwater resources by the Central Ground Water Board (CGWB) (1994a, b, c, d, and e) and State Water Investigation Directorate (SWID) (1998), the regional hydrologic framework and detailed deeper hydrochemistry remain largely unrevealed. In most of the studies so far, the As concentration of the groundwater has been described in terms of absolute depth. However, for a proper understanding of the subsurface spatial distribution of As, geochemical processes, and possible future extent of the pollution, a detailed composite approach needs to be formulated.

This study is intended to characterize the deeper hydrogeology of the arsenic affected parts of the western Bengal basin (parts of four districts of West Bengal) with an estimated 13.5 million people at risk (Table 1.1). Of these at least 4 million rural residents are drinking deep water supplied from public water-supply schemes within the study area.

In the second chapter, a hydrostratigraphic model for the arsenic-contaminated areas of the western Bengal basin has been proposed with block-scale descriptions of the inferred aquifer-aquitard framework. In the third chapter, numerical simulations of regional-scale, seasonal groundwater flows through the proposed hydrostratigraphic framework have been described. The fourth chapter illustrates the stable isotopic composition of rainwater and regional trends in groundwater. The fifth chapter focuses on detailed characterization and geochemical modeling of the deeper water chemistry of the study area. The sixth and final chapter summarizes the extent of arsenic pollution in deeper water along with possible reasons for such pollution.

1.3 The study area

The study area (Table 1.2) consists of an area of about 21,000 km^2 in the western Bengal basin, including the districts of Murshidabad (eastern part) (Figure 1.4a), Nadia (Figure 1.4b), North 24 Parganas (Figure 1.4c) and South 24 Parganas (Figure 1.4d). The area is bounded in the north by the River Ganges, in the west by the River Bhagirathi-Hoogly (distributary of the River Ganges), in the east by the international border between India and Bangladesh and in the south by the Bay of Bengal. The study area includes the city of Kolkata (Calcutta) as well as a number

of smaller municipalities, including Behrampur, Krishna Nagar, Kalyani, Naihati, Barasat and Bashirhat.

1.4 Geologic overview of the Bengal basin

The Bengal basin represents world's largest sediment dispersal system (Kuehl et al., 1989; Milliman et al., 1995, Goodbred et al., 2003), with passage of an estimated 1060 million tons of sediments per year to the Bay of Bengal through a delta front of 380 km (Allison, 1998), thereby forming the world's biggest submarine fan, the Bengal fan (Kuehl et al., 1989; Rea, 1992), with an area of 3×10^6 km^2. Water discharge through the Bengal basin to the ocean is fourth largest in the world (Milliman and Meade, 1983). The total area of the GBM basin has been estimated to be about 200,000 km^2 (Alam et al., 2003). The maximum flow estimated for the River Ganges during the past century was on the order of 43,000 m^3/s, while the maximum flow for the Brahmaputra was on the order of 57,000 m^2/s (Chatterjee, 1949).

The Ganges enters the basin from the northwest after draining the Himalayas and most of north India for about 2500 km (Figure 1.5). The Ganges then divides into two distributaries. The main stream (River Padma) flows southeast toward the confluence with the River Brahmaputra in Bangladesh. The other part flows due south through West Bengal as the River Bhagirathi-Hoogly. For simplicity, both these distributaries are termed as the original stream, i.e., Ganges. The Ganges flows through a meandering course with very few braided reaches and occasional tributaries. It has been avulsing toward the northwest for the last 250 years (Brammer, 1996). The Brahmaputra enters the basin from the northeast (Figure 1.5) after draining Tibet and northeast India for about 2900 km. It has a palaeo-channel bifurcated along the east of the Madhupur forest. In general, the Brahmaputra is a braided stream characterized by multiple thalwegs, mid-channel bars and vegetated river islands. The channel belt shows a rapid lateral migration of up to 800 m/year (Allison, 1998). The Meghna drains the Sylhet basin and part of the Tripura hills before flowing into the Brahmaputra (Figure 1.6).

1.4.1 Boundaries of the basin: The Bengal basin is bounded (Figure 1.5) on the north and northwest by the Rajmahal Hills, which are composed of lower Jurassic to Cretaceous trap basalts of the Upper Gondowana system (Ball, 1877). From west to east they are known as the

Garo, Khasi and Jayantia hills, which stretch for about 97 km from north to south and 240 km from east to west (Morgan and McIntire, 1959). In the northeast the Shillong or Assam plateau acts as a boundary. The hills and the plateaus are composed of intensely stressed Precambrian quartzite and schist overlain by the Eocene Nummilitic limestone (Wadia, 1949). The Bengal basin's eastern limit is marked by the Tripura hills to the north and Chittagong hills to the south, which are composed of Paleocene-Pliocene age sediments of the Siwalik system (the Himalayan foredeep basin sediment system) (West, 1949). The Tripura hills include a series of plunging anticlines, which die out under overlapping recent sediments of the Sylhet basin (Morgan and McIntire, 1959). The Bangladesh-India border follows the base of the hills.

1.4.2 Geologic framework and history: The Bengal basin was initiated as a subsiding foredeep basin of the uprising Himalayan front and the Indo-Burma range formed by the collision of the Eurasian and Indian continental plates. By the mid-Miocene (Curray et al., 1982), the basin had become a huge sink of the sediments eroded from the rising mountain range (Allison, 1998). The basin has a complex evolutionary history. About 1 to 8 km of Permian to Recent clastic sediments rest on the stable shelf in the western part of the basin (Imam and Shaw, 1985) and up to 16 km of Tertiary to Quaternary alluvial sediment cover is present in the foredeep of the basin, which at present lies at the mouth of the Ganges and Brahmaputra rivers (Allison, 1998) (Figure 1.7). The ongoing Himalayan orogeny has kept the basin tectonically active, with most of its activity now focused in the foredeep region, as manifested by a number of vertical faults and folds. This has caused vertically displaced regional sedimentary blocks, which have divided the basin into numerous poorly connected sub-basins, which in turn caused conspicuous differences in sedimentary environment and lithology (Goodbred et al., 2003). On a larger scale, the basin is supposed to be divided into eastern and western portions, which are separated by a hinge zone marked by high magnetic and gravity anomalies (Sengupta, 1966).

Geologically, the basin is bounded in the west by the Peninsular shield of India, which has a Precambrian basement of metasediments with granitic, granophyric and doleritic intrusions. These are followed upward by scattered, east-west trending intracratonic Gondwana deposits like the Damodar basin with the Raniganj and Jharia coal basins and some Tertiary deposits like the Baripada and Durgapur beds, as well as the Mesozoic volcanics of the Rajmahal

trap. In the east the Naga-Lushai orogenic belt bound the basin. This belt consists of highly deformed Cretaceous-Tertiary sediments and is bordered in the north and northeast by the Dauki fault zone (Evans, 1964) and the Naga thrust (Sengupta, 1966), with a general movement direction of north-northeast. The Shillong Plateau, which borders the basin in the northeast, is most probably the continuation of the Indian shield through the Garo-Rajmahal gap (Sengupta, 1966).

Stratigraphic study of the Bengal basin shows that from the Cretaceous through the mid-Eocene, sedimentation was similar throughout the basin (Figures 1.8 and 1.9). The succession starts with the Gondwana sediments and volcanics, followed by a thick sequence of shallow marine clastics and carbonates in both the eastern and the western sub-basins. Arenaceous sediments dominate the clastics in both areas. The carbonate deposit, known as the Nummilitic Sylhet limestone, is found extensively throughout the basin. As a result of the basin configuration and nature of the submergence, the sequence is thinner in the western sub-basin. After the deposition of the Sylhet limestone, the sedimentation pattern of the basin changed to become more argillaceous, as marked by the Kopili Formation. After the Kopili, there occurred some significant movement of the basin-basement and -margin fault systems, which led to a completely different depositional environment and stratigraphic sequence in the two sub-basins. While thick marine sediments continued to be deposited in the deeper eastern sub-basin, successively resulting in the Bogra Formation, Barail Formation, Surma Group and Tipam Group, in the western sub-basin the Bhagirathi Group (consisting of the Memari-Burdwan, Pandua-Matla and Debagram-Ranaghat formations; Biswas, 1963), were deposited in a more near-shore environment. From the advent of the Pliocene, a similar style of sedimentation resumed throughout the basin, thereby depositing the voluminous and extensive Bengal alluvium over all the previous lithotypes.

Sequence-stratigraphic and seismic studies have established that there is a zone of flexure above the Sylhet limestone in the southeastern portion of the western part of the basin. This zone acts as a seismic reflector and has been interpreted as a hinge zone or a zone of faulting, which may be a shallow manifestation of a much more intense fault zone in the basement (Sengupta, 1966). The unconsolidated sediments deposited over it, because of bed instability and adjustment

of movement, have suffered from flexure, which gave the post-Sylhet deposits of the Bengal basin a broad synformal shape. The zone is not very wide, but it passes from east Calcutta to the town of Mymensinhga in northern Bangladesh. Thus the zone has been named as the Calcutta-Mymensinhga hinge zone (CMHZ) (Figure 1.6). The zone can be traced to its truncation by the Dauki fault zone in the Naga Hills of Assam (Sengupta, 1966). It occurs at a depth of about 4700 m below Calcutta, with a trend of N 30^{o} E. The presence of the CMHZ has been confirmed by the finding of a series of low-magnitude magnetic highs in northwest Calcutta and a steep gravity gradient in the west. Calcutta has been flanked by broad gravity highs to the east, indicating the presence of a gravity divide in-between (Sengupta, 1966).

The formation of the Bengal basin started with the break-up of Gondwanaland in the late Mesozoic, at about 126 Ma (Lindsay et al., 1991). Extrusion of basalt both in the Rajmahal areas and the south Shillong plateau (Banerjee, 1981) some time in the late Jurassic to early Cretaceous initiated the process of basin development. This was followed by the slow subsidence of the Bengal shelf in the late Cretaceous, leading to restricted marine transgression from the southeast in the proto-basin. The western part of the basin (mostly in West Bengal) records deposition of lagoonal argillaceous and arenaceous sediments, whereas the Assam front in the eastern and northeastern part was occupied by an open neritic sea (Sengupta, 1966). The proto-GBM delta started forming by sediments deposited by repeated submergence and transgression over a planar erosional surface, which exists at about 2200 m depth in the central part of the basin, with a dip toward the southeast (Lindsay et al., 1991).

During the middle to late Eocene, basin-wide subsidence initiated by movement along basin-margin faults caused an extensive marine transgression in the basin, which resulted in the deposition of the Sylhet limestone. Basement movement probably caused the formation of the CMHZ on top of this limestone (Sengupta, 1966). Subsequently, the sea began receding from the Bengal basin. At about 49.5 Ma, a major shift in the sedimentation pattern began. The carbonate-clastic platform sedimentary sequence was replaced by a predominantly clastic deposit (Lindsay et al., 1991). The process became conspicuous at about 40 Ma, when the basin became dominated by fluvial clastic sediments and the transitional delta prograded rapidly with frequent lobe switching. The sudden change in deltaic sedimentation and morphology was probably a

manifestation of the collision of the Indian plate with the Eurasian plate and rising of the Himalayas. Comparison of stratigraphic records from the eastern and western parts of the basin show a subsequent divergence in the sedimentary depositional history as a result of differential subsidence rate, tectonic movements and eustatic sea-level changes. From the early Oligocene onward, the eastern basin continued to experience marine conditions as marked by a thick arenaceous sequence, while the western part was under fresh to estuarine conditions, leading to a thinner sequence of argillaceous sediment (Sengupta, 1966). At about 10.5 Ma (Lindsay et al., 1991), in the middle to late Miocene, intense tectonic activity started along the Dauki fault zone and Naga thrust. The activity became more intense in the Pliocene (Sengupta, 1966). The result was basin-wide regression with a major eustatic low. Thus all parts of the basin, including the eastern part, saw a shift from a marine-estuarine environment to a predominantly fluvial-tidal dominated environment, which continues to the present. Deposition of the modern deltaic basin was thus initiated (Lindsay et al., 1991).

1.4.3 Physiography and Quaternary geomorphology: Physiographically, the Bengal basin can be divided into two major units, the Pleistocene uplands and deltaic lowlands (Morgan and McIntire, 1959). The divisions may be described as follows (Figure 1.10):

1) *Pleistocene uplands:* In the whole basin there are four main Pleistocene units along with several small outliers. Of these, two flank the basin. The Barind tract is in the east of the Cretaceous Rajmahal hills and the Madhupur Jungle is in the west of the early Tertiary Tripura hills (see Figure 1.10). The following description is based upon the classic study of Morgan and McIntire (1959).

These Pleistocene uplands are believed to be paleo-floodplains of the earlier GBM system. In terms of sediment characteristics and mineralogy, these deposits are very similar to their recent counterpart (Morgan and McIntire, 1959). For example, they have similar moderately well-sorted sand-size sediments. However, despite the similarities, there are some conspicuous differences. In contrast to the dark, loosely compacted, moist and organic-rich Recent sediments, the Pleistocene sediments are reddish, brown or tan, mottled, ferruginous or calcareous-nodule rich, relatively dry and organic-poor (Morgan and McIntire, 1959). Moreover,

there is a conspicuous difference in the landform features formed by the Pleistocene and the Recent sediments. The Pleistocene sediments form highlands, which are the manifestation of differential structural movements between the two units and also seaward subsidence with higher terrace formation during Pleistocene glaciations. Four such terraces have been identified (Morgan and McIntire, 1959). Also, the upland is characterized by only few prominent drainage systems, which also flow through deeply scoured, well-defined meanders.

The Barind is the largest Pleistocene unit in the Bengal basin, with an aerial extent of about 9400 km^2. It has been dissected into four separate units by recent fluvial systems, which include the north Bengal tributaries of the Ganges and Brahmaputra, namely the Mahananda, Karatoya, Atrai, Jamuna and Purnabhaba. The area is actively affected by orogenic movements, which are indicated by earthquakes, tilting of its eastern part, river course switching and visible major fault planes.

The 4100 km^2 of the Madhupur Jungle north of the city of Dhaka is the other important Pleistocene landform of the Bengal basin. The elevation of the upland increases from 6 m above mean sea level (MSL) in the south to more than 30 m above MSL in the north. The western side has a higher average elevation, while the whole upland dips toward the east, where ultimately it gets concealed under the thick Recent alluvium. The western margin marks an abrupt separation between the low-lying, flat, Recent flood plain in the east and the highly dissected older upland. The margin is bounded by six en-echelon faults ranging from 10 to 21 km in length and with the eastern side up-thrown by at least 6 to 18 m. It is believed by some workers that at least part of the uplift of the Madhupur forest took place during the 1762 catastrophic earthquake (Fergusson, 1863). The diversion of the Brahmaputra from its old course can be possibly attributed to the sudden uplift of the Madhupur Jungle and its gradual tilting toward the east and also the sudden diversion of the Tista from being a tributary of the Ganges to that of the Brahmaputra in 1787. Moreover, the presence of the lowland between the en-echelon fault system of the Madhupur and the Karatoya River fault system of the northeast Barind indicates ongoing subsidence/uplift.

2) *Recent Sediments:* The other main physiographic division is the Recent alluvial plain and delta of the GBM system (Morgan and McIntire, 1959), also known as the Recent alluvial lowland of

Bengal (Umitsu, 1987, 1993). These alluvial deposits are the most extensive part of the Bengal basin and cover almost the whole of the basin except the Pleistocene highlands.

Different workers have tried to classify this huge sedimentary basin in various ways. The classification described here is a combination of the two proposed by Morgan and McIntire (1959) and Umitsu (1987). According to this joint scheme, there are four physiographic subdivisions as described below:

a) The alluvial fans: These piedmont alluvial plains occur in the foothills of the eastern Himalayas and are formed by the deposition by the north Bengal tributaries of the Ganges and Brahmaputra such as the Tista, Atrai, Mahananda, and Purbabhaga. These rivers also have dissected the Pleistocene upland of the Barind, as mentioned earlier. Coarse-grained sediments like cobble and sand dominate these fans.

b) Tippera surface: This 7800-km^2 area in the easternmost part of the basin, near the Tripura hills in the Tippera district, has been classified as a different subdivision based on its characteristic drainage system (Morgan and McIntire, 1959). It is sometimes considered as a part of the GBM flood-delta plain (described later) (Umitsu, 1987). The rivers in this unit show a very well-defined rectangular pattern in contrast to the general braided or meandering pattern of the alluvial plains. How far this distinct pattern is a result of anthropogenic influence is a debatable issue. The surface is delineated in the north by an NE-SW trending fault. The sedimentological characteristics of the deposit are very similar to those of other recent alluvial deposits except a little more compacted and oxidized, but not as much as the Pleistocene uplands.

c) Sylhet basin: This small basin is located in the extreme northeastern portion of the main basin, surrounded by the Shillong plateau, Tripura hills and the Madhupur Jungle Pleistocene uplands. In the south a major fault scarp bounds it. The basin has an average altitude of about 4.5 m above MSL at its center. It was earlier considered as a part of the Ganges-Brahmaputra delta. The Old Brahmaputra River (the original channel of the Brahmaputra) passes through its westernmost limits. The present Brahmaputra course has an elevation of about 15 m above MSL, which shows that the Sylhet basin has subsided about 10.5 to 12 m during the last couple of hundred years.

The cause is certainly tectonic, associated with movements of the fault systems. Recent fossil wood fragments have been found at depths of 15 to 18 m below surface. The surface is inundated every year during monsoon season. The basin can be classified geomorphologically as having natural levees with dendritic drainage and continuously meandering levees (Umitsu, 1985). The sediment composition of the basin ranges from sandy to silty near the surface, grading to fine sand at a depth of about 12 m.

d) Ganges-Brahmaputra-Meghna flood and delta plain: This is the principal unit of the Bengal basin. This unit is so vast that many studies including the present work refer the Bengal basin as almost synonymous with the plain. It covers more than 10^5 km^2 of the alluvial plain in both Bangladesh and West Bengal, India, excluding the units that have already been mentioned.

The plain is bounded by the Pleistocene terraces in the west, the Barind and Madhupur Jungle in the north, the Tippera surface in the east (Morgan and McIntire, 1959) and the Bay of Bengal in the south. It is formed by two of the largest river systems of the world and thus is considered one of the best and most complex examples of fluvio-deltaic geomorphology. Like many of the large alluvial systems of the world, the GBM plain is also formed by overlapping of a number of sub-deltas (Morgan and McIntire, 1959) and alluvial flood plains. Moreover, avulsion of the major streams in the area, which are either tributaries or distributaries of the Ganges or Brahmaputra, within a time scale of 100 years, has resulted in a Recent sediment sequence of about 100 m of overbank silts and clays incised by channel sands (Coleman, 1969; Umitsu, 1987; Goodbred and Kuehl, 2000, Allison et al., 2003). The active delta area in the southernmost part of the plain, which supports the largest mangrove forest in the world, the Sunderban, can be demarcated from the flood plain by the furthest inland extent of ocean water from the Bay of Bengal during the dry season of October to April (Allison et al., 2003).

The GBM alluvial plain has an altitude of about 15 to 20 m in the northwest, which decreases to 1 to 2 m in the south near the coast. According to physiographic characteristics the plain can be divided into five distinct regions (Umitsu, 1987). These include a) the area in and around the city of Calcutta, b) the area of broad and indistinct natural levees (Umitsu, 1985) in the northwest part, also known as the moribund delta (Bagchi, 1944), c) the central part of the

plain, which includes areas with natural levees with dendritic distributary channels near the city of Khulna city (Umitsu, 1985) along with meandering and distinct natural levees, d) the Sunderban and e) the mouth of the Meghna with its active delta (Umitsu, 1987).

The oldest surface sediments in the GBM flood plain are recorded near the cities of Calcutta and Commila in northeastern Bangladesh, very near the Tippera surface, whereas the youngest sediments are all located in the active floodplain and the delta. The sediments in all the other places are of Holocene age. The Ganges alluvial deposits are divided into an upper silty or clayey part and a lower sandy part to a depth of about 50 m. In the northwestern part, near the Tippera surface, the sediments in the upper horizons are slightly oxidized and light gray in color. In the central and southern parts of the plain, organic and peaty materials are occasionally visible in near surface horizons. In the southernmost part, in and near the active delta region, alternating silt and sand are present with an upward fining sequence (Umitsu, 1987). The Brahmaputra-dominated alluvial plain is present in the area between the Barind and the Madhupur Jungle. This plain has a distinct basal gravel horizon overlain by a sequence of sandy sediments.

Umitsu (1987, 1993) classified the vertical sequence of the recent formations of the GBM plain into five units (lowest, lower, middle, upper, and uppermost). Each of these units is separated from its succeeding units by a difference in grain size, which is certainly a manifestation of depositional environment. The descriptions of the individual units are as follows, after Umitsu (1987). The lowest unit, which has a thickness of about 10 m, is composed predominantly of gravel. Near the northern portion of the plain, the bed occurs at a depth of more than 70 m below the surface, indicating that the sea level of the Bay of Bengal at the time of its deposition must have been about 100 m below the present level. The lower member is dominated by sand-sized sediments with few gravels. The unit contains two horizons near the middle and the top with a coarser grain size, probably resulting from a change in sediment size deposited by the rivers. An unconformity, probably caused by temporary marine regression, exists between the lower and the middle members. This is indicated by the presence of weathered and oxidized horizons at the top of the lower unit. The lower horizon in certain locations, mostly in the central plain, has sediments with occasional peat and organic material, indicating a swampy environment of deposition. The middle unit shows a coarsening upward sequence. The upper

member has a coarse-grained middle portion, sandwiched between fine-grained upper and lower portions. This oscillation of sedimentation pattern is believed to be caused by eustatic sea level change. Clay- and silt-sized sediments are characteristic of almost the entire uppermost horizon, with occasional peaty sediments.

The peaty materials in all these units are interpreted to have been deposited in mangrove swamps, which developed in the prograding delta over time (Vishnu-Mittre and Gupute, 1979; Umitsu, 1987; Islam and Tooley, 1999).

1.4.4 Age dating: Because of the presence of a large amount of organic material in the Recent sediments, radiometric age (mostly radiocarbon) dating of the sediments has been done by several workers. The lower unit organic remains of the central GBM plain near the city of Khulna (Bangladesh) at a depth of 46 m below MSL yield an age of 12,320 ± 240 years before present (BP) (Umitsu, 1993). Ages from shell fragments and wood remains from the middle unit at depths of 25 to 33 m below MSL range from 8910 ± 150 to 7640 ± 100 years BP (Umitsu, 1993). Peat layer ages determined from the upper unit are 7060 ± 120 years BP at 18 m below MSL and 6490 ± 130 year BP at 14 m below MSL (Umitsu, 1993).

Peat layers from the far western GBM plain (West Bengal, India) have been dated ~7100 to 9100 years BP at depths of 20 to 50 m in the coastal area (Hait et al., 1996) and, in inland areas, 6500 to 7500 years BP at depths of 6 to 12 m and 2000 to 5000 years BP at depths <5 m in inland areas (Banerjee and Sen, 1987). Mangrove remains from Calcutta have been dated at ~7000 years BP (Sen and Banerjee, 1990). The sediments from a location near Calcutta have been dated as 2615 ± 100 years BP at 1.37 m below surface to 5810 ± 120 years BP at 6.25 m below surface level (Vishnu-Mittre and Gupute, 1979).

Sediments from the Brahmaputra plain basal gravel at a depth of 101 m below sea level, in the south of the Barind, yield an approximate age of 28,320 ± 1550 years BP (Umitsu, 1987). Sylhet basin organics at depths of 36.6 m to 55 m below MSL yield ages of 6320 ± 70 years BP and 9390 ± 60 years BP respectively (Goodbred and Kuehl, 2000).

Radiocarbon dating of sediments from a depth of 25 to 30 m below surface at the active delta area near the main mouth of the GBM, records an age of 8400 years BP (Goodbred and Kuehl, 2000). Muddy sand about 50 m west of the aforementioned location and at a depth of 35 m below surface, yields an age in the range of 7500-8000 years BP (Goodbred and Kuehl, 2000).

1.4.5 Holocene landform evolution: As noted in section 1.4.3, the main lithostratigraphic and geomorphic units of the Bengal basin are mostly of Holocene age (Figure 1.11). Hence understanding the Holocene fluvio-dynamic processes along with the effects of eustatic sea level changes and tectonic impacts in this basin is critical for any further study. In the northwestern part of the basin, where tectonic processes are most active, fine-grained sediments dominate the stratigraphy. In the western part of the basin, near the stable shelf, the strong fluvio-dynamic processes have resulted in formation of extensive flood plains with a dominance of coarser grained sediments. The coastal region in the south has a mixture of fine-grained sand and mud deposits with peat layers, which have resulted from eustatic influence (Goodbred et al., 2003).

Deposition of the lowest unit of the GBM delta began at the onset of the Pleistocene glacial maximum in this part of the world (Islam and Tooley, 1999) (Figure 1.12). This is documented by the fact that the lowest unit was deposited at a depth of about 70 m below the present land surface, indicating that the glacial maximum sea level and the base level of land erosion must have been at least 100 m below the present MSL. Thus the rivers draining the plain during that time must have scoured through the earlier plains and deposited the basal gravel at a depth analogous to the sea level at that time (Umitsu, 1993). At that time the “Swatch of no ground” submarine canyon now in the center of the Bay of Bengal most probably was the estuary of the GBM plain (Chowdhury et al., 1985). If this hypothesis is true then most of the northern part of the Bay of Bengal during the Pleistocene glaciation was dry land (Islam and Tooley, 1999). The sediment supply at this time was low compared to the present (Milliman et al., 1995) and sediment inflow was low until the late Pleistocene, about 15,000 years BP (Weber et al., 1997).

Around 12,000 to 11,500 years BP, at the onset of the Holocene, the southwest monsoon, which determines the climate-controlled processes in southeast Asia, became stronger than at

present (Gasse et al., 1991), which led to a simultaneous increase in discharge and fluvial sedimentation. The sediment discharge has been estimated to be on the order of 2.5×10^9 t/yr (Goodbred and Kuehl, 2000). The lower unit of the GBM plain was probably deposited at this time as an extensive flood plain in the central region (Umitsu, 1993). As mentioned earlier, this unit coarsens upward, which may be correlated with increased discharge and aggravated erosion along the upper reaches of the main rivers.

The conditions of sedimentation and eustatic sea level rise that took place at about 10,500 years BP are a matter of debate because of the presence of apparently contradictory evidence. The sedimentary record at this time contains both dissected flood plains (Umitsu, 1993) caused by fluvial erosion and also drastic fining of sediments (Goodbred and Kuehl, 2000) further inland. It has been hypothesized that either there was a temporary (Umitsu, 1993) and most probably major (Lindsay et al., 1991) marine regression or the eustatic sea level rose to about –45 m MSL from the previous sea level (Fairbanks, 1989; Blanchon and Shaw, 1995), which caused extensive back-flooding and sedimentation. However, both these theories claim that the present GBM delta started forming and prograding into the bay at this time (Lindsay et al., 1991; Goodbred and Kuehl, 2000). The sharp decrease of sediment input to the submarine fan at this time (Weber et al., 1997) could be a manifestation of enhanced sediment trapping in the delta plain system. The fine sediment thus deposited would constitute the middle unit of the GBM plain (Umitsu, 1993). Hence, most probably there was a short-lived but effective marine regression followed by a marine transgression, which cumulatively initiated the modern delta-forming processes.

From about 10,000 years BP to about 7,000 years BP, in the mid-Holocene, a major and rapid transgression (Umitsu, 1993; Islam and Tooley, 1999; Goodbred and Kuehl, 2000) took place probably as a cause of glacial ice melting, which resulted in the deposition of fine sediments (the upper unit of the GBM plain) even in the north-central part of the basin. The coastline at that time transgressed up to the central delta, in the north of Khulna city (Umitsu, 1993). This continued transgression might also have had some short-lived regression cycles, for example, at about 9000 years BP. These are indicated by increased fluvial activity (Islam and Tooley, 1999). During the latter part of this transgression, the coastline probably receded slightly

toward the south causing the coarsening of the upper horizons of the upper unit. At this time mangrove vegetation (Vishnu-Mittre and Gupte, 1979) spread all over the central GBM plain and caused extensive deposition of peat. After ~7000 years BP, the gradient of the marine transgression curve decreased (Umitsu, 1993; Islam and Tooley, 1999; Goodbred and Kuehl, 2000). Nonetheless, the general trend of the eustatic sea-level curve shows continued transgression from the mid-Holocene onward (Figure 1.13). The decreased rate of transgression since 7000 years BP led to the deposition of the uppermost unit of the GBM plain, which contains clay, silt, and organic-rich layers throughout the southern Bengal basin. The continuation of these processes is the active delta formation and the mangrove vegetation in the Sunderban region.

Bengal Peat: These are extensive peat layers in the upper and uppermost units throughout the southern Bengal basin. These layers have been reported by various workers, including Vishnu-Mittre and Gupte (1979), Sen and Banerjee (1990), Barui and Chanda (1992), Umitsu (1987, 1993), and Islam and Tooley (1999), who have referred to the layers as the Bengal peat. Civil construction in Calcutta in recent past, even at shallow depths, have yielded remnants of peaty material. The above-mentioned authors have claimed the peat as in-situ in origin and mostly formed from mangrove (or mangal) vegetation. Studies near the city of Khulna have yielded five well-developed and generally thick layers of peat, each separated by inorganic layers (Islam and Tooley, 1999). The lowermost peat layer has been dated at 7000 to 6650 years old and contains remains of mangrove plants like *Acrostichum aureum, Heritiera spp.,* and *Avicennia spp.* Parts of the uppermost layer have been dated at 5000 to 2000 years old and contain abundant remains of freshwater peat-forming plants. The intercalation of mangrove and fresh water plant with mineral-rich layers have been interpreted to indicate deposition in a basin that was inundated by marine transgression with intermediate temporary regressions (Islam and Tooley, 1999).

1.4.6 Mineralogy, sedimentology and elemental distribution: The mineralogy and sedimentology of the Bengal basin are to a large extent dependent on the type of sediments eroded and transported by the Ganges, the Brahmaputra and their northern tributaries like the Tista, Meghna, Rangeet and Mahananda. Because of differences in sediment provenance, the two river systems have quite distinctive mineralogies (Heroy et al., 2002). The Brahmaputra flows

through various rock types, including Precambrian metamorphics (high grade schist, gneiss, quartzite, and marble), felsic intrusives, Paleozoic-Mesozoic sandstones, shales and limestones (Huizing, 1971). The Ganges drains terrains with similar kinds of lithologies, but also receives lower course and lowland tributaries which drain Mesozoic and Tertiary mafic extrusives and Precambrian-Cambrian shield (Huizing, 1971). The lowland tributaries also produce a kind of saline and alkaline soil, which contains calcareous concretions called "kankar" (Sarin et al., 1989). The sediments of the floodplains and the streambeds of all three river systems have been found to be very similar in sedimentary properties and mineralogy (Morgan and McIntire, 1959; Umitsu, 1993). Therefore the bank and floodplain sediments have been designated as major short-term river sediment sources (Meade and Parker, 1985).

More than 76% of bed sediments from the GBM river system are fine to very fine sand, with a mean grain size of 2.5 to 4 Φ (1/6 to 1/16 mm) (Datta and Subramanian, 1997). The grain size decreases from upper to lower reaches, and 66% of the sediments are moderately to well sorted according to the scale of Folk and Ward (1957) (Datta and Subramanian, 1997). All bed sediments are positively skewed (Goswami, 1985; Datta and Subramanian, 1997), and 95% of the suspended sediments are above 6 Φ (0.01 mm) and are well sorted (Datta and Subramanian, 1997).

The Bengal basin sediment mineralogy is dominated by detrital quartz and feldspar grains (Datta and Subramanian, 1997). The higher quartz content relative to feldspar is indicative of low-relief tropical weathering in the basin (Potter, 1978). The presence of very low amounts of carbonates is possibly an indication of differential deposition along the fluvial flow path (Datta and Subramanian, 1997).

Among the clay minerals, illite and kaolinite are profuse and occur in nearly equal proportions, while chlorite and montmorillonite are insignificant (Datta and Subramanian, 1997). The presence of high illite and low chlorite indicates the ongoing neotectonic activity that the basin is experiencing (Morgan and McIntire, 1959) and the enrichment of the parent rocks in muscovite mica (Griffin et al., 1968). The presence of a large amount of kaolinite signifies the intense kaolinization of the parent minerals (e.g. feldspars). The Ganges system has a higher

amount of smectite and a lower amount of kaolinite in comparison to the Brahmaputra (Sarin et al., 1989). Several studies have concluded that the smectite-kaolinite assemblage has been derived from the low-temperature alteration of the high-grade crystalline sediments of the Himalayas by pedogenic processes within the Bengal basin, while the illite-chlorite suite has been derived from direct erosion of the Himalayas. The amount of these assemblages derived from the cratonic part of the Indian subcontinent is insignificant (France-Lanord et al., 1993; Heroy et al, 2003).

The heavy mineral assemblages in all three river systems of the Bengal basin are similar (Datta and Subramanian, 1997). Among the heavy minerals, amphibole is most prominent, followed by garnet and epidote. There is a little enrichment of pyrope garnet in the Ganges system, while epidote is slightly higher in the Brahmaputra system (Huizing, 1971; Datta and Subramanian, 1997). Unstable minerals in general dominate the heavy mineral assemblage (e.g. hornblende, garnet, magnetite, and ilmenite), followed by semistable minerals like apatite, epidote, staurolite, and kyanite. There is a dearth of stable and ultrastable heavy minerals (Datta and Subramanian, 1997). The predominance of unstable heavy minerals is possibly a manifestation of lack of significant chemical alteration during their transport (Kumar and Singh, 1978). The high-grade metamorphic terrains are the provenance of 40 to 46% of the heavy minerals, followed by the igneous terrains with 21 to 29% (Huizing, 1971; Datta and Subramanian, 1997). There is a slight enrichment of amphibole in the Brahmaputra relative to the Ganges (Huizing, 1971; Datta and Subramanian, 1997), while the alluvium of the latter has more calcareous matter (Wadia, 1981). Pyrite is seldom found in the basin (BGS/DPHE, 2001). This range of heavy minerals is comparable to that of Miocene and younger sediments eroded from various orogenic sources, including the ophiolite suites of the Himalayas (Uddin and Lundberg, 1998).

The distributions of nitrogen and phosphorus in the basins of the Ganges, Brahmaputra and Meghna are similar and vary within a narrow range. The average total nitrogen (TN) of the three basins ranges from 0.1 mg/g to 0.6 mg/g (Datta et al., 1999). The average total phosphorus (TP) is about 0.7 ± 0.1 mg/g in the Meghna basin, 0.9 ± 0.2 mg/g in the Brahmaputra and 1.0 ± 0.4 mg/g in the Ganges (Datta et al., 1999). The total carbon (TC) content appreciably increases

from the Meghna basin to the Ganges. The values are 1.8 ± 0.5 mg/g in the Meghna, 2.0 ± 1.7 mg/g in the Brahmaputra and 8.2 ± 2.8 mg/g in the Ganges (Datta et al., 1999). While in the Meghna basin the total carbon consists primarily of total organic carbon (TOC) and there is little or no total inorganic carbon (TIC), the Ganges basin contains appreciable amounts of both TIC and TOC. In general, in the Bengal basin there is a very good correlation between TN and TOC and between TOC and grain size of the sediments (Figure 1.14). TN in the basin may be controlled by the organic sources and biogeochemical processes (Datta et al., 1999). The Ganges river sediments show higher concentrations of Na^+, HCO_3^- and Cl^- than the Brahmaputra (Sarin et al., 1989). The Ganges sediments are rich in Ca^{2+}, Mg^{2+} and HCO_3^- but poor in N and P. The Brahmaputra and Meghna sediments are typically characterized by noncalcareous, acidic soil (Saheed, 1995).

Common naturally-occuring trace metal contaminants reported in the Bengal basin include lead, arsenic, cadmium, mercury, and selenium (Aswathanarayana, 1995). The concentrations of trace elements like lead, arsenic and mercury are less in the Bengal basin than in standard shale and clay (Datta and Subrmanian, 1997). The index of geoaccumulation (Muller, 1979) is negative for lead, arsenic and mercury in the GBM system but is positive for cadmium in the Brahmaputra plains (Datta and Subrmanian, 1997).

1.4.7 Hydrogeology: The Bengal basin groundwater system is strongly influenced by the monsoonal rainfall caused by the southeast monsoon wind. It receives heavy rainfall during the monsoon period, which stretches from mid-June to mid-October. Annual rainfall varies from about 125 cm in the west-central part to more than 500 cm in the northeast part near the Shillong plateau and the Himalayas in the north. The average temperature is about 30^o in the summer and about 15^o in the winter. Everywhere on the delta plain precipitation exceeds annual potential evapotranspiration (Allison, 1998). The heavy rainfalls during the monsoon period together with the water from Himalayan snowmelt brought down by the Ganges and Brahmaputra cause extensive, damaging floods in the Bengal lowlands. There are distinct dry and wet seasons. During the dry months, severe groundwater exploitation for irrigation and other purposes becomes a necessity.

There have been various attempts to define the groundwater flow regimes in the basin. A common practice is to differentiate the aquifer materials between the older and more oxidized red-brown sediments and the younger gray sediments. On this basis five major aquifer systems have been identified in the Bengal basin (BGS/DPHE, 2001). These are:

a) late Pleistocene to Holocene Tista mega-fanglomerate and Brahmaputra channel basal gravel aquifers composed of coarse sand, gravels and cobbles;

b) late Pleistocene to Holocene Ganges, lower Brahmaputra and Meghna main-channel shallow aquifers composed of braided and meandering river sediments;

c) early to middle Pleistocene coastal and moribund Ganges delta deep aquifers composed of stacked, main-channel medium to coarse sands at depths more than 130 m;

d) early to middle Pleistocene Old Brahmaputra and Chandina deep aquifers composed of red-brown medium to fine sands underlying Holocene gray medium to fine sands;

e) early to middle Pleistocene Madhupur Jungle and Barind aquifers composed of coarse to fine fluvial sands of the Dupi Tila Formation, confined by near surface clay residuum.

Many workers have characterized the shallow aquifers but the deep aquifers have yet to be studied in detail. The estimate of average groundwater recharge made by ^{3}H-^{3}He isotope dating is in the range of 0.6 ± 0.2 m/year. The groundwater flux thus determined to the Bay of Bengal is on the order of 0.2×10^{15} liter/year, which is equal to about 19% of the total surface water flux (1.07×10^{15} liter/year) (Basu et al., 2002). However, these estimates are controversial because the high groundwater flux is implausible in a flat terrain like the GBM plain, where in a distance of 100 km, the land surface elevation only decreases by about 10 m (Harvey, 2002). The hydraulic conductivity (K) of the young gray sediments has been estimated in the range of 0.4 to 100 m/day. The older red-brown sediments have K in the order of 0.2 to 50 m/day (BGS/DPHE, 2001).

In general, the regional groundwater flow is from north to south with local variations in vicinity of the river systems, which are mostly effluent. However, the regional flow path has not previously been studied in detail. Locally, the high pumping rate through the shallow tubewells has a conspicuous effect on the shallow aquifer parameters. The hydraulic gradient in the northern part of the basin is about 1 m/km, which decreases in the southern Bengal basin to about 0.01 m/km (BGS/DPHE, 2001). This low gradient has led to a very slow flushing rate, which has had a significant effect on the hydrogeochemistry of the groundwater basin. Estimates show that Brahmaputra and Ganges basin sediments may have been flushed only once, if at all, since they have been deposited (BGS/DPHE, 2001).

1.5 Geochemistry of arsenic

Arsenic (As) is a ubiquitous element found in soils, rocks, natural waters, the atmosphere and organisms, mostly as a trace element. Its presence in the environment in abnormal amounts results mostly from natural conditions (Smedley and Kinniburgh, 2002), although As concentrations are sometimes aggravated by anthropogenic activities (Acharyya et al., 2000).

Arsenic is a member of the fourth group and fifth period (VB). It has an atomic number of 33 and atomic weight of 74.92. It is unique among the heavy metalloids in terms of its sensitivity to mobilization in groundwater at pH 6.5 to 8.5 under both oxidizing and reducing conditions (Smedley and Kinniburgh, 2002). Arsenic occurs in four oxidation states: arsenate (As[V]), arsenite (As[III]), arsenic (As[0]) and arsinic (As[-III]). The most common states of As in nature are As(V) and As(III), both as solids and in aqueous solution. As(III) is more mobile and stable than As(V) in aqueous solution, especially at pH >7. Stability of As(III) increases significantly in reducing conditions and it is about 100 times more toxic and hazardous than As(V) in solution (Ray, 1999). Arsenic is a sidero-chalcophile, i.e., it has a strong affinity for iron and sulfur. In nature it occurs mostly as sulfides, often being associated with Cu, Zn, Ni, and Ag. The major primary minerals of As are realgar (AsS), orpiment (As_2S_3) and arsenopyrite (FeAsS). These primary As minerals crystallize from hydrothermal solution formed in the last stage of magmatic crystallization, i.e., in the epithermal and mesothermal ranges and with volcanic emanation. Under oxidation they occasionally alter to secondary minerals like scorolite ($FeAsS{\cdot}2H_2O$), leucopyrite (Fe_3As_4), and pitticite (complex hydrated mixture of arsenate and

sulphate). Among all these minerals arsenopyrite is most abundant in nature and is regarded as the primary source of groundwater contamination**.** Derived from primary and secondary minerals, As also occurs as ionic sorbed phases on the surface of metal (Fe, Mg, Al) oxides in colloidal solutions and sometimes in geothermal springs (Ray, 1999)

1.5.1 Arsenic sorption kinetics: Redox reactions of major elements like Fe and Mn have a strong control on the behavior, concentration and speciation of trace elements like As in aqueous systems. One of the principal processes by which groundwater is enriched in As is reductive dissolution of hydrous Fe oxides [HFO (e.g. FeOOH)] along with release of sorbed As. The sequence begins with consumption of O_2 and reduction of SO_4^{2-}, being accelerated by accumulation of CO_2 derived from oxidation of organic matter. The liberated Fe and SO_4^{2-} will react with each other, ultimately forming pyrite (FeS_2) under reducing conditions. Excess Fe present in the system may be precipitated as authigenic magnetite (Fe_3O_4). However, under strongly reducing conditions, in the presence of H_2S, magnetite will transform into pyrite. Because the release or sorption of small amounts of As can have a major effect on the overall As concentration in the aquifer, understanding the coupled Fe-As-SO_4^{2-} reactions is of immense importance (Smedley and Kinniburgh, 2002).

Oxidation of As(III) and reduction of As(V) are other reactions that may influence the speciation behavior. The redox processes are slowest at a slightly acidic pH (around 5) and are catalyzed by microbial activities. This redox reactions lead to the release of adsorbed As(III) in groundwater (Masscheleyen et al., 1991). The reduction of As(V) takes place at a redox potential intermediate between those for Fe(III) and SO_4^{2-} reduction.

Equilibrium thermodynamics indicate that As(V) (as $H_2AsO_4^-$ and $HAsO_4^{2-}$) should predominate over As(III) (as $H_3As_3O_3^0$ and $H_2AsO_3^-$) under all conditions except where strong SO_4^{2-} reduction is taking place (Masscheleyen et al., 1991). However, under natural conditions, due to the interaction of multiple redox couples, the speciation process may be much more complex (Seyler and Martin, 1989), so that As(III) may predominate in less reducing environments (Seyler and Martin, 1989; Eary and Schramke, 1990; Kuhn and Sigg, 1993) or even oxidizing environments (Abdullah et al., 1995). Incubation studies of sediment from

Bangladesh showed that reductive dissolution of As can take place even in mildly oxic conditions (van Geen et al., 2004). The presence of naturally occurring organics (NOM) can have a profound effect on As movement as they can effectively hinder As(III) from reaching sorption equilibrium (Redman et al., 2001). This discussion shows that reduction of As will probably be the most effective mechanism of As mobilization in the subsurface of large fluvio-deltaic systems with reducing groundwater and large amounts of NOM (Smedley and Kinniburgh, 2002).

As(V) and As(III) have different adsorption isotherms, which implies that they travel through the aquifer with different velocities and increased separation along the flow path. Experiments show that As(III) moves five to six times faster than As(V) in acidic and mildly oxidizing conditions. At near neutral to neutral pH, As(V) moves faster than before but is still superseded by As(III). Under alkaline and reducing conditions both of them move rapidly (Gulen et al., 1979). Under similar conditions, in most natural systems, As(V) reacts much more rapidly with Fe oxides than As(III) does (Pierce and Moore, 1980). As(V) thus is preferentially adsorbed on Fe oxide and hydroxide (e.g., ferrihydrite [Figure 1.17]) surfaces (Ferguson and Anderson, 1974; Gulen et al., 1979, Pierce and Moore, 1980; Jain et al., 1999) and Mn oxide (Manning et al., 2002; Foster et al., 2003) at low concentrations. Alternately, As(III) can be scavenged by iron sulfides (Korte and Fernando, 1991; Rittle et al., 1995). Arsenic adsorption is more dependent on its oxidation state than on pH at near-neutral pH values. Oxidation of As(III) may lead to lowering of mobility and the oxidation rate can be radically increased by the presence of Mn oxides (Oscarson et al., 1981; Scott and Morgan, 1995). The rate of oxidation is independent of the concentration of dissolved O_2 (Scott and Morgan, 1995).

1.5.2 General mechanisms of arsenic mobilization in aqueous solution: Among aqueous systems, As is found in maximum concentration in groundwater, and also in the most varied concentration ranges. High-As groundwater is not common or typical in most aquifers but occurs only under very special biogeochemical conditions. Understanding the reason for As accumulation in hazardous amounts in groundwater systems requires a good understanding of the hydrodynamics, hydrogeochemistry and water-solid interaction potential of the aquifer. In most studied areas it has been seen that high-As groundwater is not related to areas of high As

concentration in the source rock. Two key factors have been identified. First, there should be very specific biogeochemical triggers, which lead to the mobilization of As from the solid/sorbed phase to groundwater, and second, the mobilized As should have sufficient time to accumulate and not be flushed away, i.e., it should be retained in the aquifer (Smedley and Kinniburgh, 2002). In other words, As release from the source should be quick, relative to the rate of groundwater flushing. Commonly five different mechanisms are identified for mobilization of As in groundwater. Each of them is described in brief as follows (after Smedley and Kinniburgh, 2002).

1) Mineral dissolution: The primary process by which As is introduced into the aqueous system is by dissolution of primary and secondary minerals (mentioned earlier) under extreme Eh-pH conditions. Fe-Mn oxides tend to dissolve at acidic pH values. The associated minor/trace elements like As that occur as adsorbed (labile) or bound (non-labile) phases tend to be released during the host mineral's dissolution. Similarly the sulfide minerals dissolve when oxidized, liberating As. This is the probable mechanism by which As is effectively mobilized from arsenopyrite/pyrite to many surface water and shallow groundwater systems.

2) Desorption of As under alkaline and oxidizing conditions: As tends to be strongly adsorbed by oxide minerals as arsenate under near-neutral to acidic conditions. However, as the pH becomes alkaline, As starts to rapidly desorb (Figure 1.18), increasing its concentration in groundwater along with other oxyanions like phosphate, vanadate, molybdenate and uranyl. The presence of HCO_3^- and $(PO_4)^{3-}$ may significantly modify the strongly non-linear adsorption isotherm of As, thereby affecting its mobilization in groundwater to some extent. Among the processes that may result from this change of pH are uptakes of protons by mineral weathering and ion-exchange reactions.

3) Desorption and dissolution of As under reducing conditions: The most widespread As contamination probably results from reduction of ferromagnesian oxides/hydroxides and SO_4^{2-} under anoxic aqueous conditions. Simultaneous with Fe(III) reduction to Fe(II), As(V) is reduced to more mobile and hazardous As(III), thereby increasing As concentrations in groundwater. The most common cause of this is rapid sediment accumulation and burial. This condition is ideal in fluvial systems with large meandering channels, where huge amounts of sediment are rapidly

deposited in the stream bed and in back-channel fills. The presence of a large quantity of NOM, which is very common in fluvial ecosystems, accelerates the reduction and mobilization cycle.

The reductive dissolution of FeOOH is enhanced by microbial activity of dissimilatory (respiratory) bacteria strains like *Shewanella* Br Y (Cumming et al., 1999). Microcosm studies by Islam et al. (2004) showed that anaerobic metal-reducing bacteria could play a catalytic role in mobilization of As from Bengal sediments. van Geen et al. (2004) suggested that the dissimilatory microbial reduction is stimulated by addition of substrate, possibly by the class of organisms responsible for sulfur reduction (Inskeep et al., 2002; Oremland et al., 2002).

4) Reduction of oxide mineral surface area: In the early stages of weathering and sedimentation, HFOs are generally deposited as fine-grained crystals of diameter ~5 nm and specific surface area of ~600 m^2/g (Smedley and Kinniburgh, 2002). As the age of the deposited sediments increases, the HFOs recrystallize to more ordered and large-grained minerals like hematite and goethite with specific surface areas of ~150 m^2/g. The result is significant surface-area reduction. Assuming that the total mass and volume of As remain constant in the system, this could lead to considerable mobilization of adsorbed species due to sorption-site deficiency (Figure 1.19).
5) Reduction in bond strength between As and host mineral surface: Under strong reducing conditions, the surfaces of HFOs are reduced to form Fe(II) from Fe(III). This, in addition to the above-described effects, will result in a significant decrease of net surface positive charge, thereby reducing the electrostatic attraction between the mineral surface and adsorbed species. This could result in substantial mobilization and enrichment of As in groundwater (BGS/DPHE, 2001).

1.6 Background

1.6.1 The contamination problem: As concentrations in groundwater of the Bengal basin vary widely, generally ranging from less than 0.005 mg/l to 3.2 mg/l (CGWB, 1999; BGS/DPHE, 2001), but in certain areas concentrations up to 4.1 mg/l have been identified (Ghosh and Mukherjee, 2002). The contaminated aquifers are of Quaternary age and are comprised of micaceous sand, silt and clay derived from the Himalayas and basement complexes of eastern India. They are sharply bounded by the River Bhagirathi-Hoogly (distributary of River Ganges)

in the west, the Rivers Ganges and Padma in the north, the flood plain of the River Meghna (tributary of the River Padma), and the River Jamuna in the northeast (Acharyya et al., 2000).

There has been much speculation about the primary source of As in this basin. The total amount of solid-phase As in the soil and sediment is not significant, ranging from 1 to 30 mg/kg (McArthur et al., 2001; Harvey, 2002). Several workers have confirmed that the contamination is natural and is intensified by anthropogenic interferences (Acharyya et al., 1999, 2000; Ray, 1999). Of the several hypotheses about the sources of As, the most convincing are as follows:

1) As is transported by the River Ganges and its tributaries from the Gondwana coal seams in the Rajmahal trap area, which are located to the west of the basin. As concentration of the coal can reach up to 200 ppm (Saha, 1991).

2) As is transported by the north Bengal tributaries of the River Bhagirathi and the River Padma from near the Gorubathan base-metal deposits in the eastern Himalayas (Ray, 1999).

3) As is a biogenic deposit in the paleo-channels of the River Bhagirathi and the River Padma under euxinic conditions (P. Chakrabarty, West Bengal State Remote Sensing Board, 1999, personal communication).

4) As is transported with the fluvial sediments from the Himalayas (e.g., McArthur et al., 2004). This is the most accepted hypothesis at present.

Four main mechanisms have been identified by various workers to explain the mechanism of As mobilization in groundwater of the Bengal basin. These are:

1) As is released by oxidation of As-bearing pyrite in the alluvial sediments (Mallick and Rajgopal, 1995; Das et al., 1996; Mandal et al., 1998). However, a general low concentration of SO_4^{2-} in the groundwater may not support this idea (McArthur et al., 2001).

2) Arsenic anions sorbed to aquifer material are displaced into solution by competitive exchange of PO_4^{3-} available from fertilizers of surface soils (Acharyya et al., 2000). Other workers have argued that dissolved PO_4^{3-} is contributed primarily by sources other than fertilizer (e.g., reductive dissolution of iron oxyhydroxide [FeOOH], degradation of human waste, and oxidation of peat) and that competitive exchange may be minor (McArthur et al., 2001).

3) As sorbed to FeOOH is released by reduction of peat under anoxic conditions during sediment burial (Bhattacharya et al., 1997; Nickson et al., 1998, 2000; McArthur et al., 2001, 2004; Ravenscroft et al., 2001) or by oxidation of NOM (Harvey et al., 2002, 2005).

4) As is released from HFOs or other sediment phases by complex redox reactions related to Fe and S cycling (Zheng et al., 2004) and is retained in the solution by partial redox equilibrium (see Chapter 5).

Many of the workers have agreed that one of the main mechanisms of transport of As across contaminated aquifers is indiscriminate agricultural and industrial pumpage.

1.6.2 Bengal basin hydrogeochemistry: The groundwater of the GBM floodplain is mostly dominated by Ca^{2+} and HCO_3^- with some Na^+, Cl^- and negligible SO_4^{2-} (BGS/DPHE, 2001; Dowling et al., 2002). Elevated concentrations of Sr and Ba are seven to nine times those of the local surface-water concentrations. Other trace metals like V, Ni, Mo, Ag, Cd, and Pb are at or near the detection limit (1–100 nmol/L) with detectable concentrations of U (Dowling et al., 2002). A distinct SW-NE divide of the hardness of the waters has been observed, with high Mg and Ca waters being particularly associated with Ganges sediments to the southwest (BGS/DPHE, 2001). In most places the ratios of V, Mn, Fe, Ni, Zn, As, Sr, Mo, Ag, Cd, Ba, Pb, and U to chloride are much greater than the seawater ratios, indicating that the dissolved trace metals in the groundwater may have been derived from the weathering of aquifer protoliths (Dowling et al., 2002). Positive correlations between Sr and Ca and between Sr and HCO_3^- suggest that the Sr in the groundwater may have been derived from the weathering of carbonates (Dowling et al., 2002). Most Bangladesh groundwater has high concentrations of Fe and As, which are often (though not always) found to be strongly correlated (BGS/DPHE, 2001). Strong

correlations ($r^2 = 0.6 – 0.9$) were observed between dissolved As and CH_4, Fe, and NH_4^+ (Dowling et al., 2002).

$^{87}Sr/^{86}Sr$ of Bengal groundwater (0.717– 0.735) indicates that the sediment source is mainly from the Ganges drainage basin (Dowling et al., 2002). The shallow groundwater (< 70 m bgl) has $\delta^{18}O$ values between –3.5 and –5.5 ‰ (VSMOW). This range is similar to that of the present precipitation in Bangladesh. Samples from deeper groundwater are scattered along the Global Meteoric Water Line (GMWL), but are either low (-6 ‰) or high (-3 ‰), suggesting recharge from precipitation in a different climatic regime from about 3,000 to 30,000 years ago (Aggarwal et al., 2000). $\delta^{13}C$ values range from –10 to –15 ‰ (VPDB). Tritium content of groundwater varies from 0 to 7 TU. Deeper wells have values of ~0.4 TU or less. Present-day rain and river water in Bangladesh has tritium concentrations of level of 5-10 TU (Aggarwal et al., 2000). ^{14}C ranges from 7.6 to 113.5 pmc, with deeper water having values less than 60 pmc. Water with ^{14}C values in the range of 7 to 60 pmc has been estimated to have an age of about 3000 to 15,000 years (Aggarwal et al., 2000).

1.6.3 Similar studies in North America: Several previous studies in North America have examined at regional hydrogeochemical evolution. These studies used various techniques in addition to traditional chemical analyses. The hydrogeochemical facies concept was introduced by Back and Hanshaw (1970) to study the mixing of groundwaters and water-sediment interaction along a flow path. Stable isotopes (e.g., ^{2}H, ^{13}C, ^{18}O, ^{34}S) and $^{87}Sr/^{86}Sr$ have been extensively used as tracers to identify groundwater sources and geochemical processes (Clark and Fritz, 1997). Radioisotopes (^{3}H, ^{14}C, ^{36}Cl) have been used to estimate residence time or age of groundwater as well as for investigation of recharge and discharge rates (Bentley et al., 1986; Lehmann et al., 1993; Johnson et al., 2000; Roback et al., 2001; Alley et al., 2002). Occasionally dissolved noble gases have also been used to understand paleo-recharge conditions (e.g., Andrews et al., 1991). Finally, modeling of flow and geochemistry has been used in many studies to assess the regional scale hydrogeochemistry (Plummer et al., 1990; Aravena et al., 1995a; Parkhurst et al., 1996; Plummer and Sprinkle, 2001).

The studies that are relevant to the present work have been undertaken in alluvial basins such as those of the Atlantic Coastal Plain, the High Plains, the Gulf Coastal Plain, and the Alberta basin in North America. One of the first regional studies of groundwater chemistry was conducted by the USGS in the Mississippi valley in 1957 to assess sustainability of the regional aquifer system (Boswell, 1996). Hendry et al. (1991) observed systematic patterns in Na^+, Cl^-, $HCO_3^- + CO_3^{2-}$, SO_4^{2-}, $\delta^{18}O$, δ^2H and pH along the groundwater flow path in the Milk River aquifer from Montana to Alberta. For a regional flow path ~100 km long in the Black Creek aquifer in South Carolina, Chapelle and McMahon (1991) concluded that SO_4^{2-} reduction appeared to be sustained by SO_4^{2-} diffusion from an adjoining aquitard, while S^{2-} concentrations are probably limited by pyrite precipitation at the aquifer-aquitard boundary. Fryar et al. (2001) used chemical analyses of precipitation, groundwater, soils, soil gas, and stable isotopes ($\delta^{13}C$, $\delta^{18}O$ and δ^2H), along with speciation calculations and groundwater flow modeling, to investigate sources of recharge and controls on regional-scale hydrochemical evolution of the Ogallala aquifer of the Texas High Plains. Reactions during recharge were inferred to include oxidation of organic matter, dissolution and exsolution of CO_2, dissolution of $CaCO_3$, silicate weathering, and cation exchange. Penny et al. (2003) noticed sequential peaks of Ca^{2+}, Mg^{2+}, K^+, and Na^+ along regional groundwater flow paths in Alabama, indicating separation of ions, possibly driven by cation exchange. Several discrete zones of Fe^{2+}, Mn^{2+}, Sr^{2+}, and SO_4^{2-} rich groundwater have formed along these flow paths, possibly related to microbial reduction of Fe and Mn. The modeled groundwater flow pattern indicates mixing of meteoric water, carbonate groundwater and saline basinal brines.

The present study selectively follows methodologies of the above-mentioned studies. However, it is distinct in that it tries to characterize the detailed hydrogeology of the Bengal basin in terms of aquifer-aquitard relationships, groundwater flow, regional hydrochemical patterns and chemical evolution to delineate the controls on nonpoint-source As contamination.

Table 1.1 Population details of arsenic-affected areas (by districts and administrative blocks) within the study area, excluding arsenic-affected parts of Calcutta (Kolkata) (Source: PHED, unpublished data).

District	As affected Administrative Blocks	Based on 2001 Census
		Total Population in each Block
Murshidabad	Raninagar-I	155000
	Raninagar-II	156000
	Domkal	312000
	Nawda	196000
	Jalangi	216000
	Hariharpara	222000
	Beldanga-I	259000
	Suti-I	139000
	Suti-II	213000
	Bhagwangola-I	163000
	Bhagwangola-II	130000
	Berhampur	379000
	Raghunathganj-II	193000
	Murshidabad-Jiaganj	200000
	Farakka	220000
	Lalgola	268000
	Beldanga-II	210000
	Raghunathganj-I	154000
	Sub-Total:	**3785000**
Nadia	Karimpur-I	167000
	Karimpur-II	192000
	Tehatta-I	218000
	Tehatta-II	134000
	Kaliganj	291000
	Nakashipara	335000
	Nabadwip	122000
	Hanskhali	261000
	Krishnaganj	133000
	Haringhata	208000
	Chakdaha	363000
	Santipur	216000
	Chapra	272000
	Ranaghat-I	207000
	Ranaghat-II	330000
	Krishnanagar-I	280000
	Krishnanagar-II	124000
	Sub-Total:	**3853000**

Table 1.1 (continued)

District	Blocks	Population in each block
North 24 Parganas	Habra-I	188000
	Habra-II	150000
	Barasat-I	238000
	Barasat-II	169000
	Deganga	276000
	Basirhat-I	147000
	Basirhat-II	194000
	Swarupnagar	226000
	Sandeshkhali-II	136000
	Baduria	248000
	Gaighata	300000
	Rajarhat	145000
	Amdanga	166000
	Bagda	274000
	Bongaon	344000
	Haroa	182000
	Hasnabad	177000
	Barrackpore-II	159000
	Barrackpore-I	157000
	Sub-Total:	**3876000**
South 24 Parganas	Baruipur	352000
	Sonarpur	167000
	Bhangar-I	204000
	Bhangar-II	207000
	Budge Budge-II	173000
	Bishnupur-I	206000
	Bishnupur-II	191000
	Joynagar-I	219000
	Mograhat-II	262000
	Sub-Total:	**1981000**
Grand Total:		**13495000**

Table 1.2: Geographical extent of the study area

End point	**Decimal degrees**		**Projection: Transverse Mercator** (UTM 45, Central Meridian 87), Spheroid: WGS 84	
	Latitude	Longitude	Northing	Easting
NW	24.66	88.01	2,725,439	600,000
SW	21.64	88.04	2,393,130	606,432
NE	24.30	88.71	2,690,042	675,641
SE	89.09	21.62	2,392,602	716,850

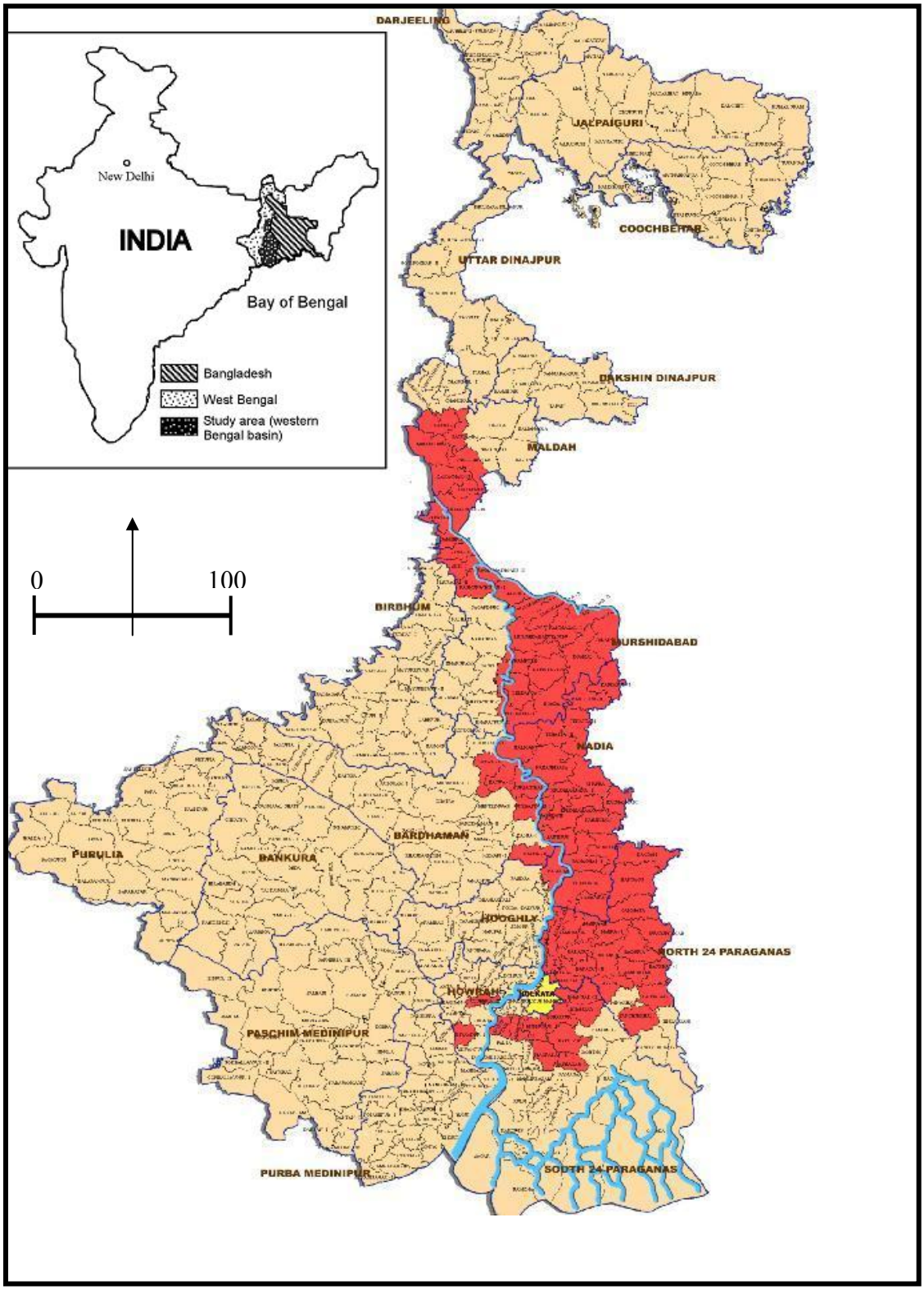

Figure 1.1: Map of West Bengal showing the arsenic-affected areas (red) (PHED, 2004).

Figure 1.2a: Montage of photographs taken (2003-2005) of patients suffering from arsenic contamination in the study area.

Figure 1.2b: Photo of one of the first known victims of As contamination (residing near our sample location at Kankphul, block Habra-II, North 24 Parganas).

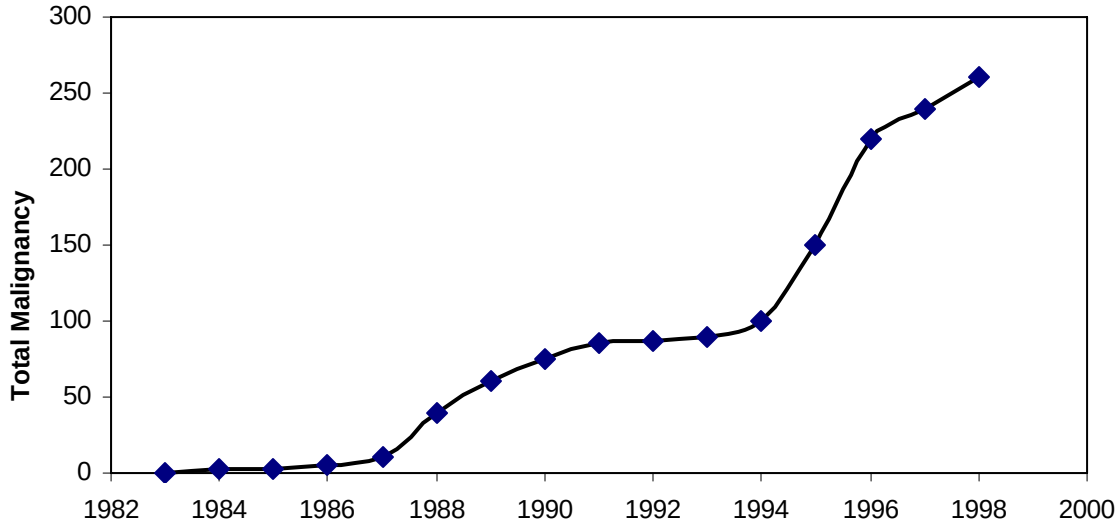

Figure 1.2c: Reported cases of malignancy (1983-1998) caused by arsenicosis in West Bengal (unspecified source).

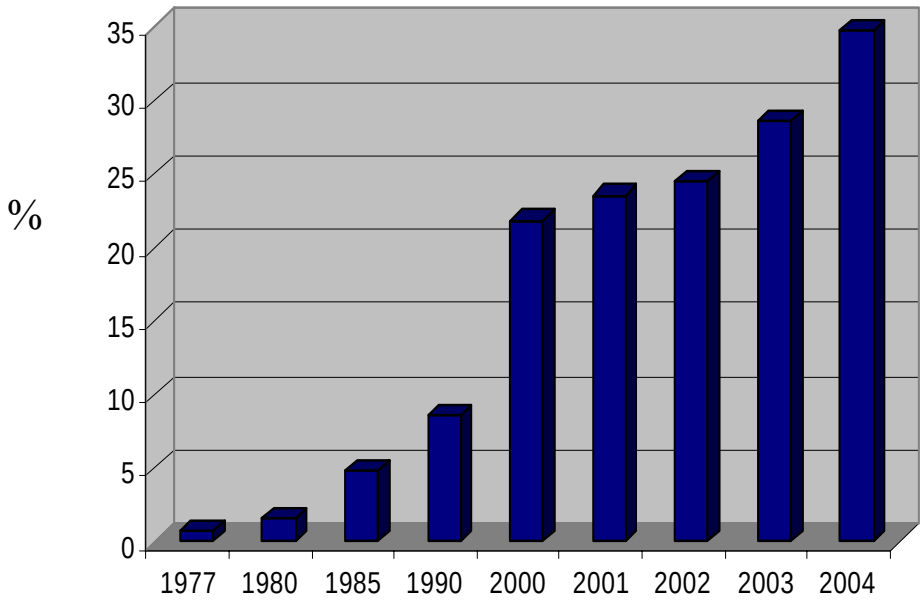

Figure 1.3a: Plot showing cumulative growth percentage of deep public water supply wells in West Bengal (PHED, unpublished data).

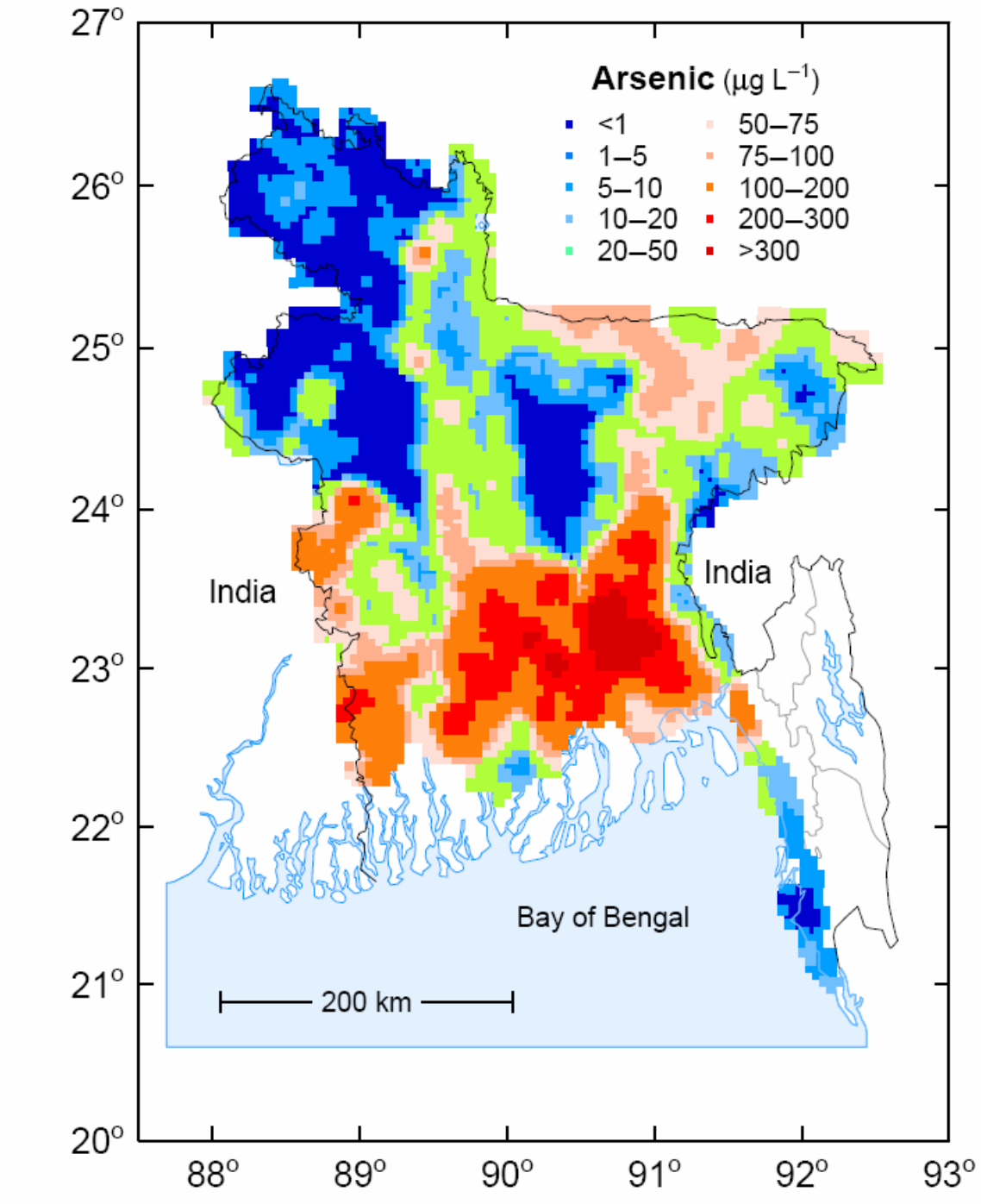

Figure 1.3b: Map (smoothed) showing extent of arsenic poisoning in the Bangladesh part of the Bengal basin (BGS/DPHE, 2001).

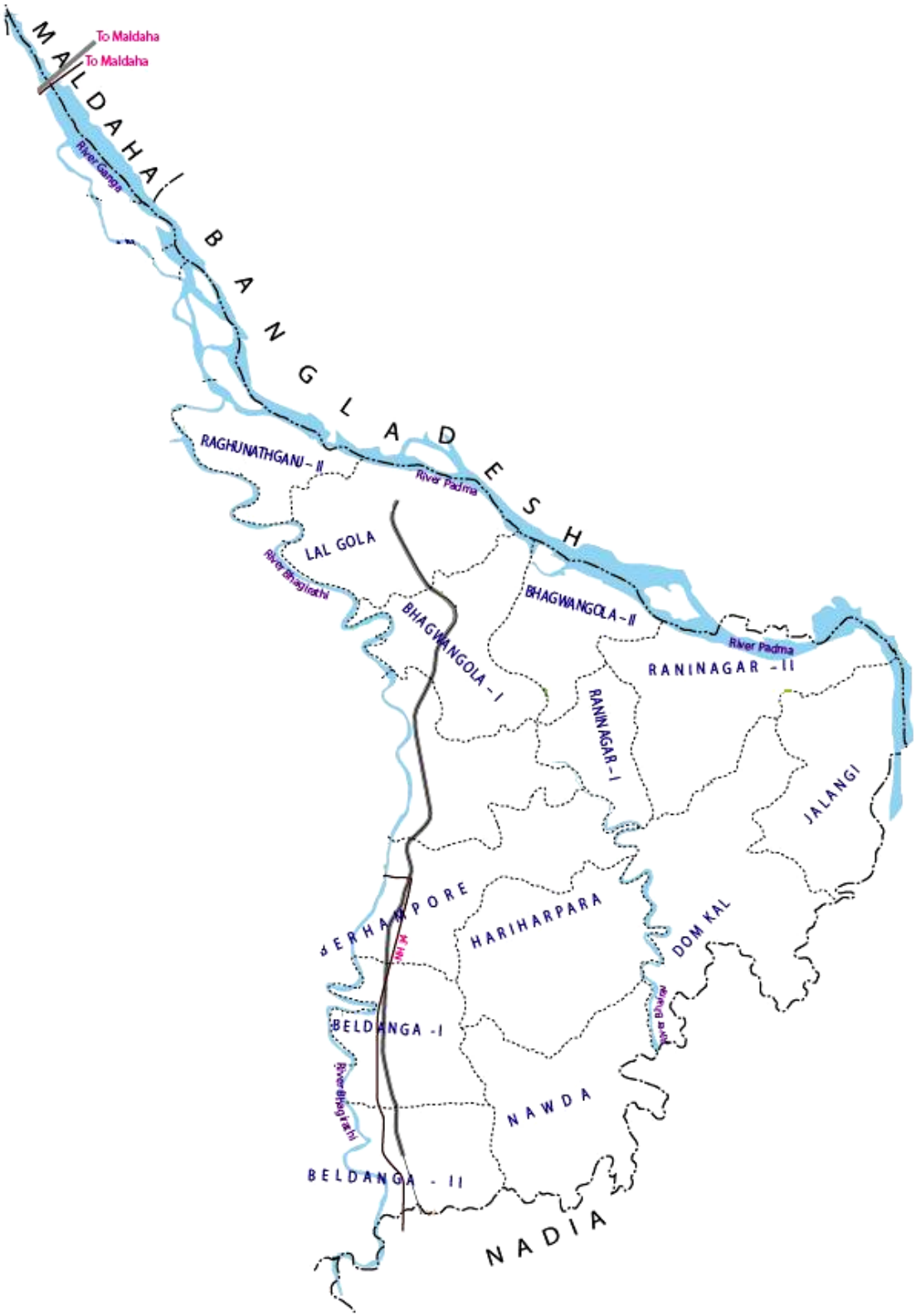

Figure 1.4a: Map of Murshidabad (eastern) showing the administrative blocks within the study area (PHED, unpublished map, as of 2004).

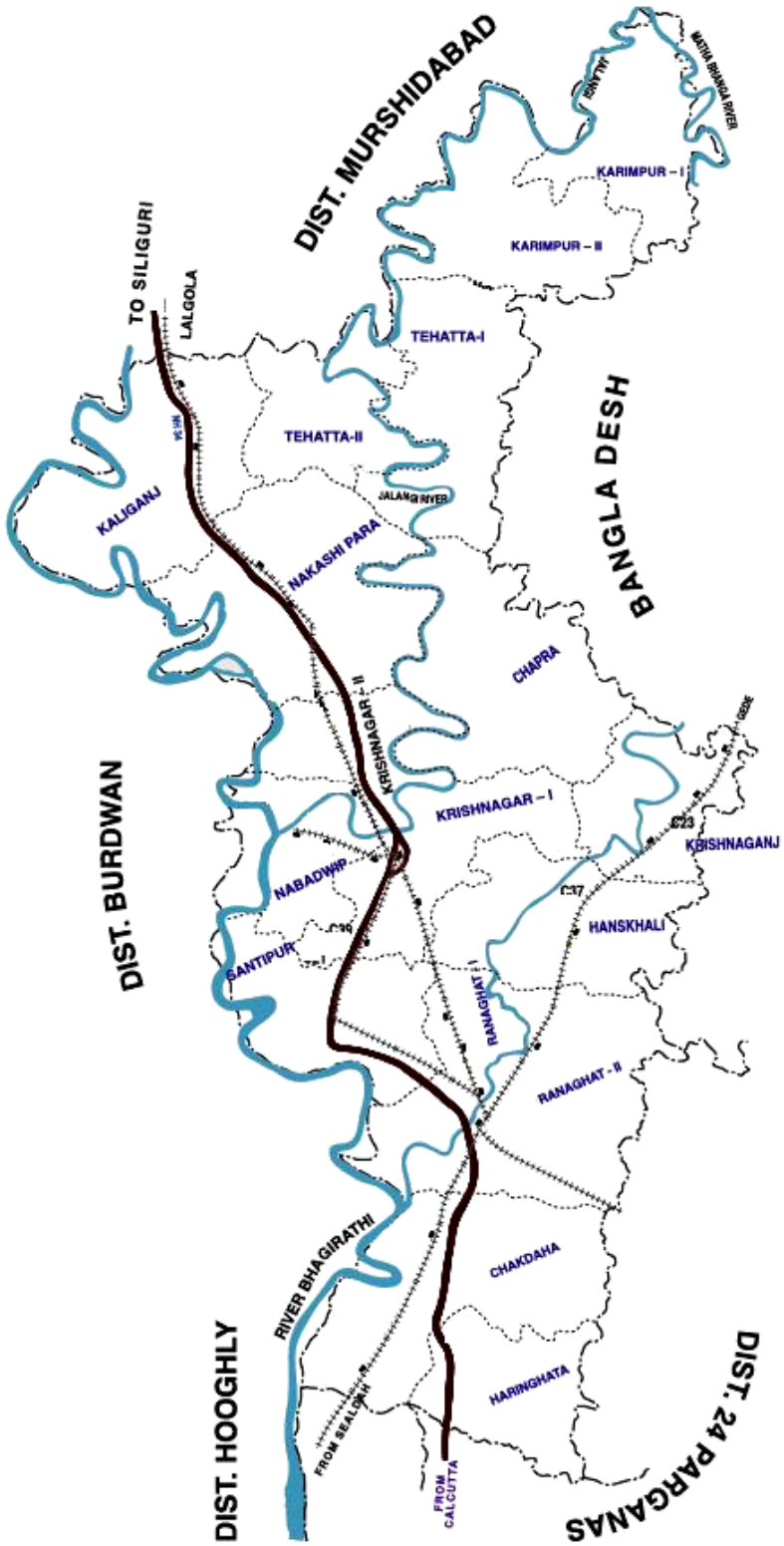

Figure 1.4b: Map of Nadia showing the administrative blocks within the study area (PHED, unpublished map, as of 2004).

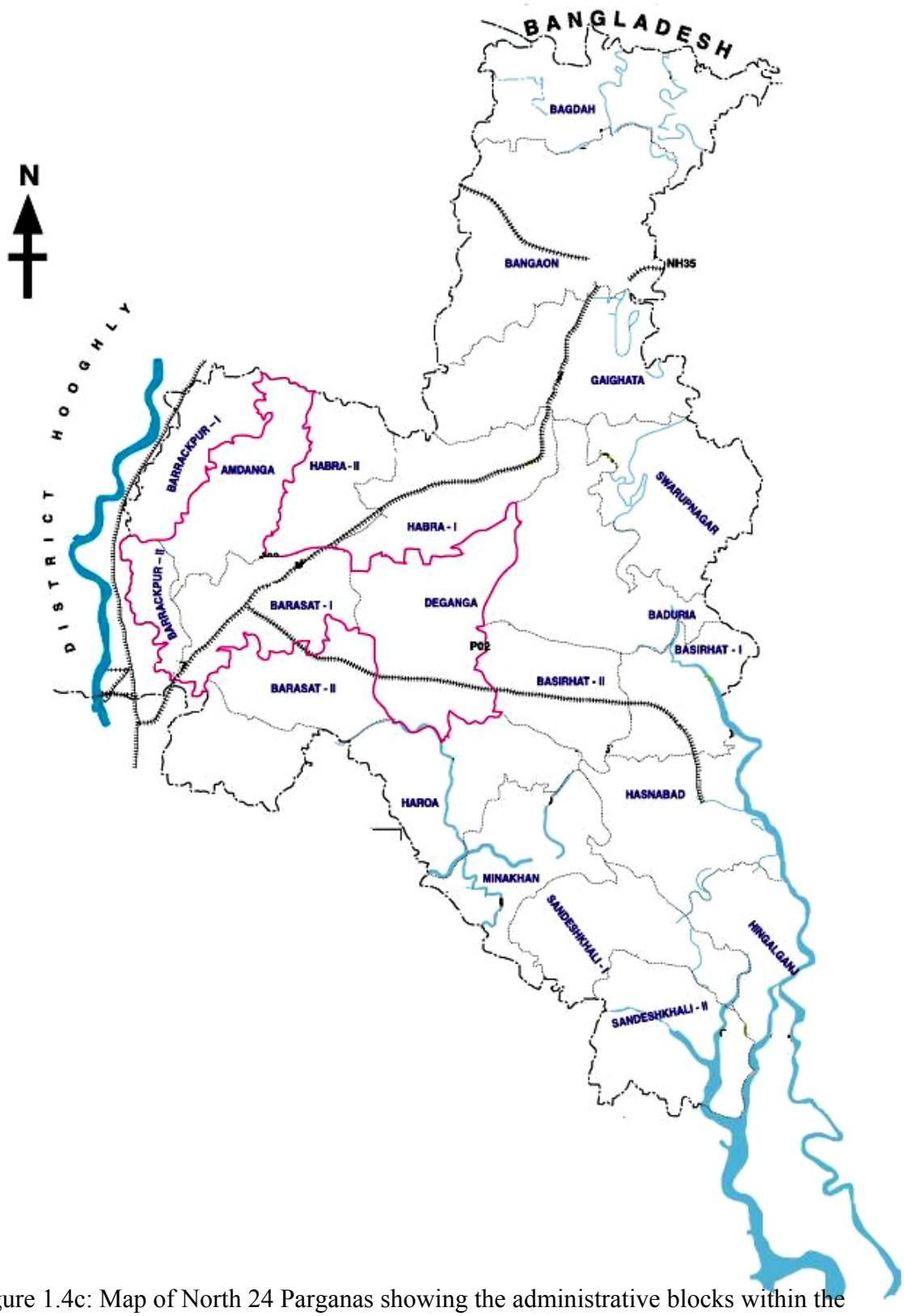

Figure 1.4c: Map of North 24 Parganas showing the administrative blocks within the study area. The red outline shows area with some surface water supply (PHED, unpublished map, as of 2004).

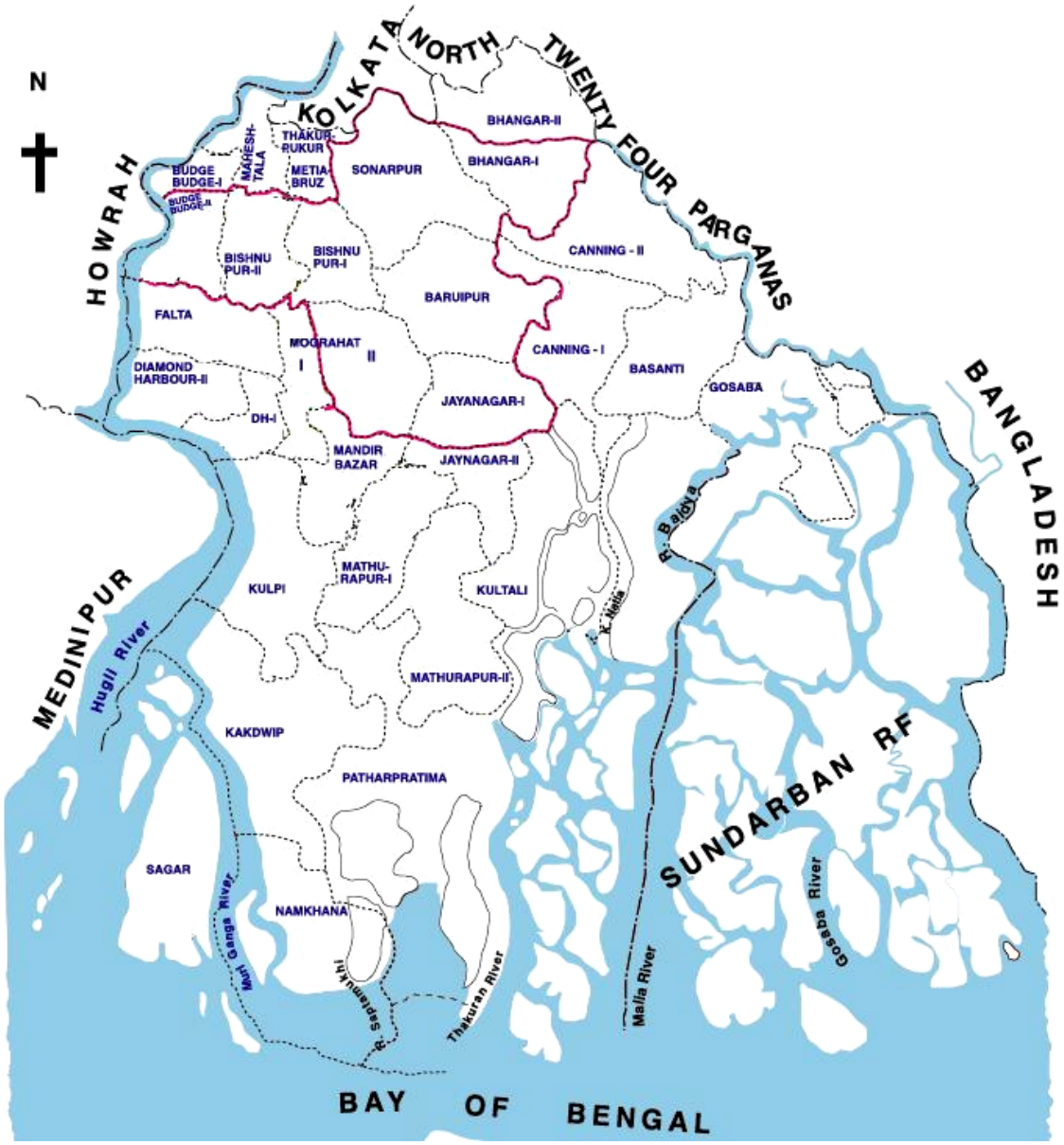

Figure 1.4d: Map of South 24 Parganas showing the administrative blocks within the study area. The red outline shows area with some surface water supply (PHED, unpublished map, as of 2004).

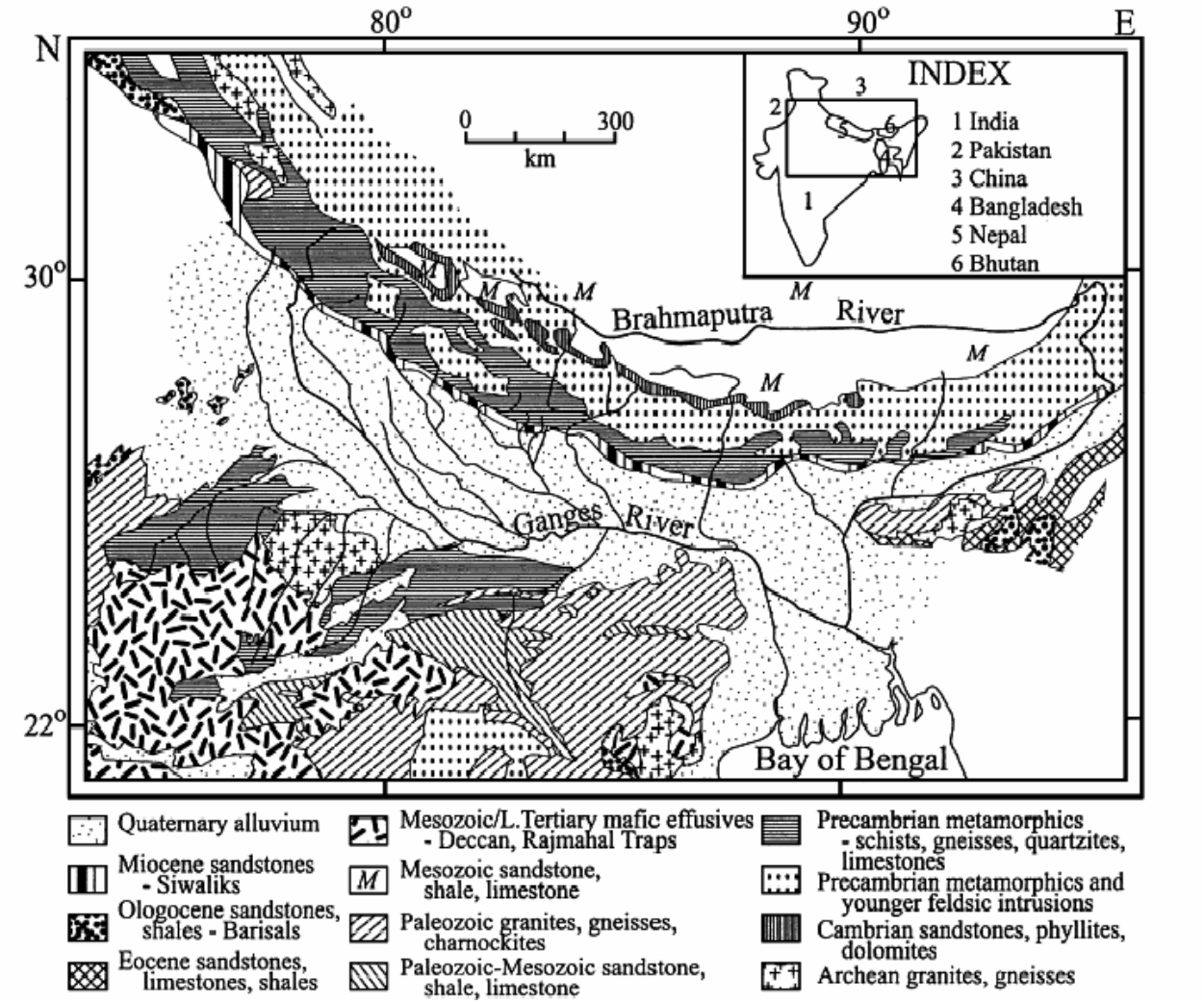

Figure 1.5: Geological map of Bengal basin and its surroundings (Segall and Kuehl, 1992).

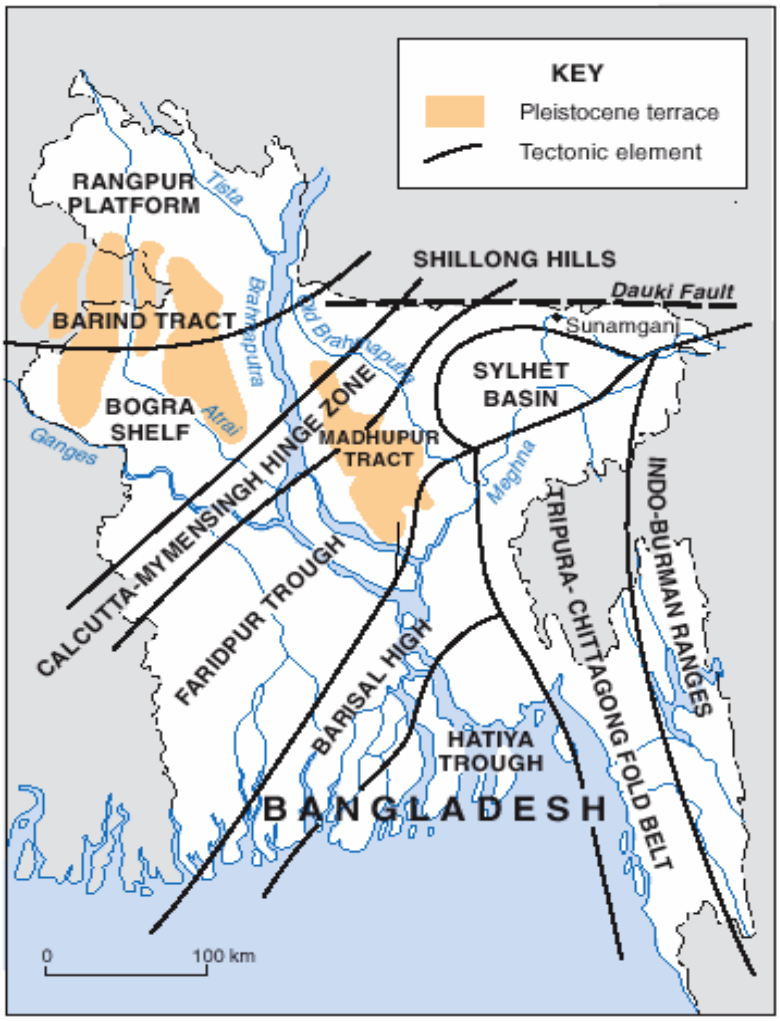

Figure 1.6: Map showing the tectonic elements of the Bengal basin (BGS/DPHE, 2001).

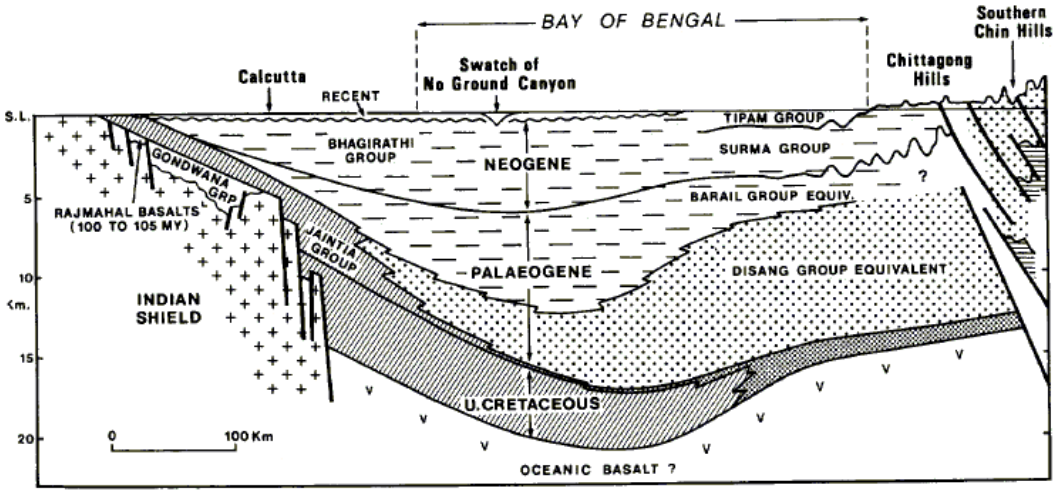

Figure 1.7: A cross-section of the Bengal basin from west to east boundary through the submarine canyon in the Bay of Bengal (Imam and Shaw, 1985).

Stage	Group	Formation	Lithology
Holocene		Alluvium	Silt, sand, gravel and clay
Pleistocene/Pliocene (up to 6375 m)	Madhupur	Dihing Formation/ Madhupur Clay	Yellow to yellowish grey, massive, fine to medium sandstone and claystone/sticky clay
		Dupi Tila Formation	Yellow to ochre, pink, light brown, light grey to greyish-white sandstone, siltstone and conglomerate. Several oxidised, iron-rich, clayey palaeosols. Petrified wood
Pleistocene/Neogene	Tipam Group (U. Jamalganj in NW)	Girujan Clay	Grey to greenish grey, red mottled, silty shale, shale and claystone
Neogene		Tipam Sandstone	Light yellow to yellowish grey, grey, brownish grey and orange fine to medium grained pebbly sandstone, siltstone and shale
	Surma Group (L. Jamalganj in NW)	Boka Bil Formation	Greenish to bluish grey and yellowish grey marine pyritic shale, siltstone and very fine to medium grained sandstone, marine fossils
Miocene (3100 m)		Bhuban Formation	Grey to bluish grey fine to medium sandstone, siltstone, claystone
Oligocene (800–1000 m)		Barail Formation Bogra Formation in the NW	Brown, yellow-brown, pink and grey sandstone, siltstone and carbonaceous shale
Late Eocene (Eocene 600–800 m) Middle–Early Eocene	Jaintia Group	Kopili Formation	Grey, greenish grey to black silty claystone, fossiliferous shale, thin beds of glauconitic sandstone and limestone
		Sylhet Limestone	Grey to greyish brown massive nummulitic limestone
Eocene and Palaeocene		Tura Formation	Grey, brown, pink and greyish-white ferruginous sandstone, coal and shale
Late-Middle Cretaceous	Upper Gondwana	Sibganj Trapwash	Coarse yellow brown sandstone; white clay; volcanic ash
Early Cretaceous–Jurassic		Rajmahal Traps	Amygdaloidal basalt; serpentinised andesite; shale; agglomerate
Late Permian	Lower Gondwana	Paharpur Formation	Sandstone; feldspathic greywacke; coal, shale; coarse sandstone
Early Permian	Lower Gondwana	Kuchma Formation	Coarse grained sandstone, shale; thick coal seams
Precambrian		Basement Complex	Gneiss and schist

Figure 1.8: General stratigraphic succession of the eastern part of the Bengal basin (Alam et al., 1990).

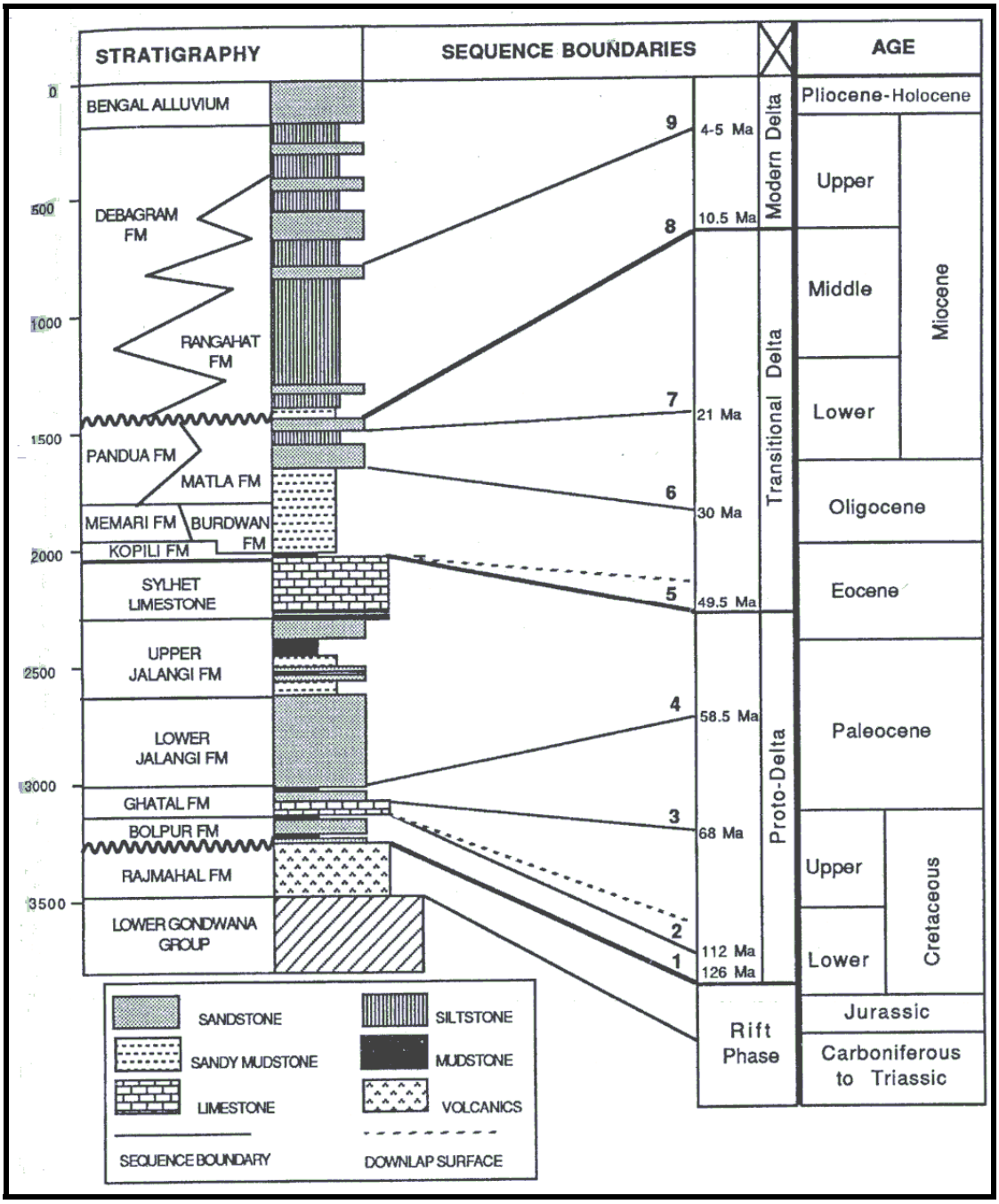

Figure 1.9: Lithostratigraphic succession of the western part of the basin with sequence boundaries and phases of delta formation (Lindsay et al., 1991).

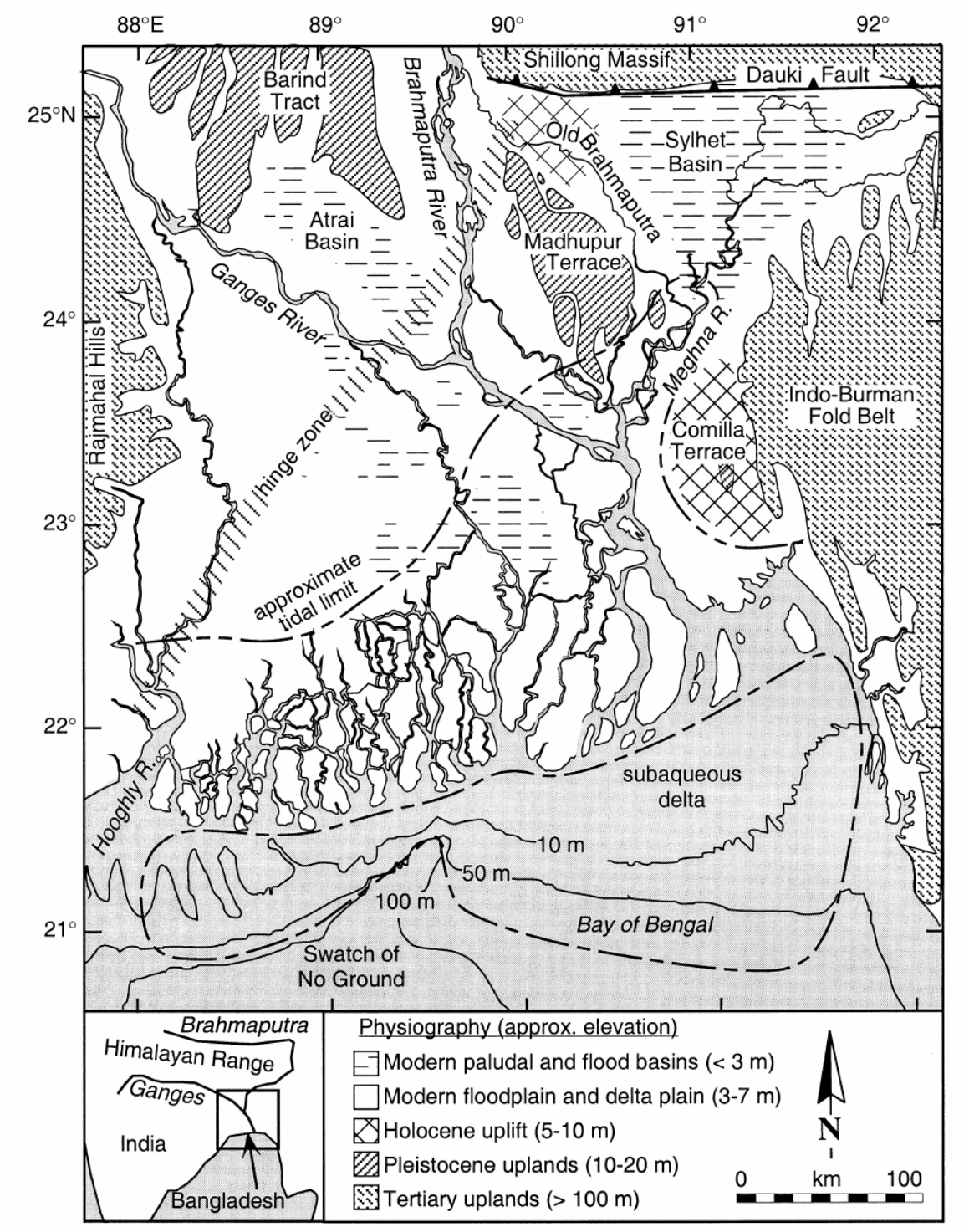

Figure 1.10: Physiographic map of the Bengal basin (Goodbred and Kuehl, 2000).

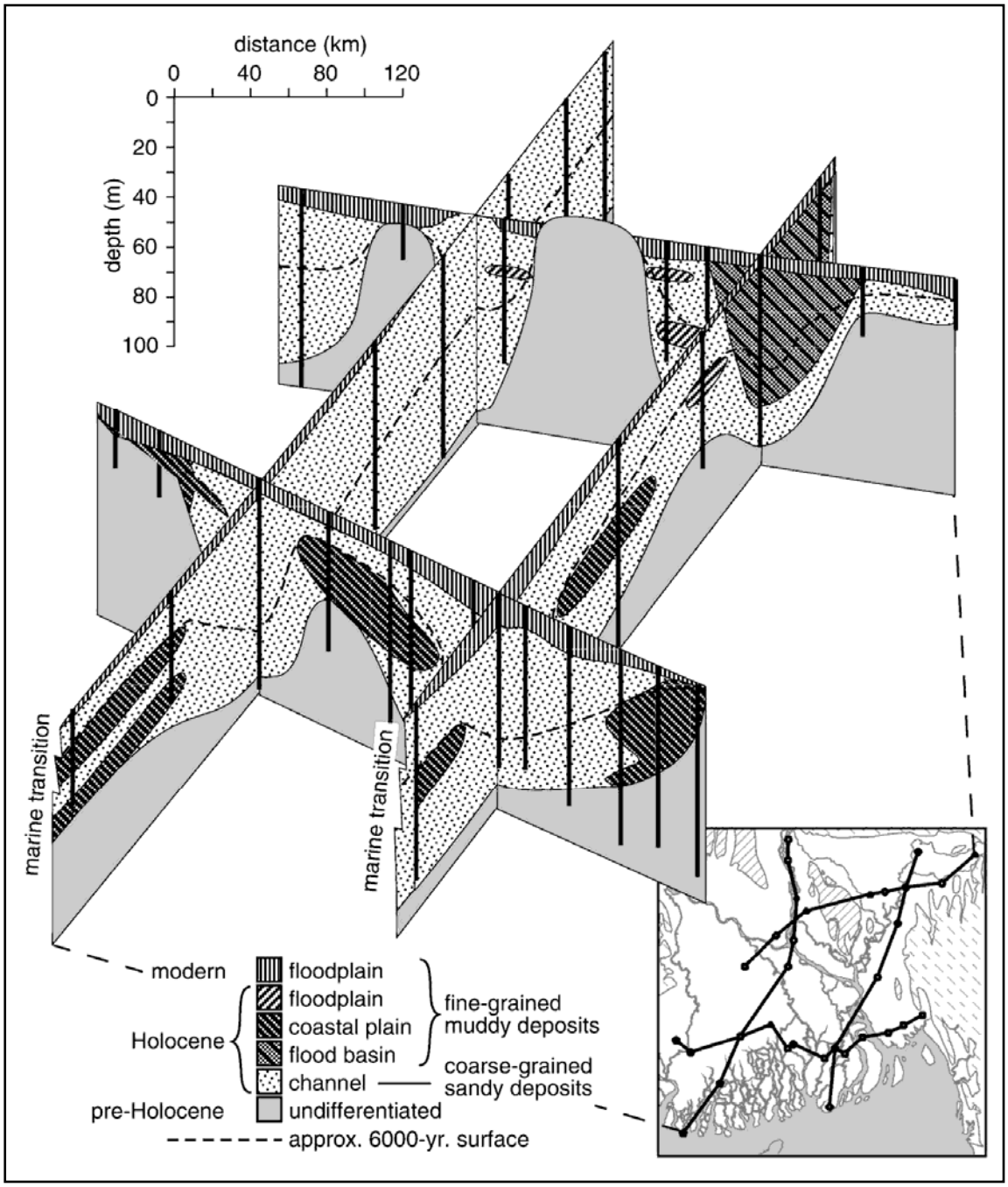

Figure 1.11: Fence diagram of lithology of the Bengal basin (Goodbred et al., 2003).

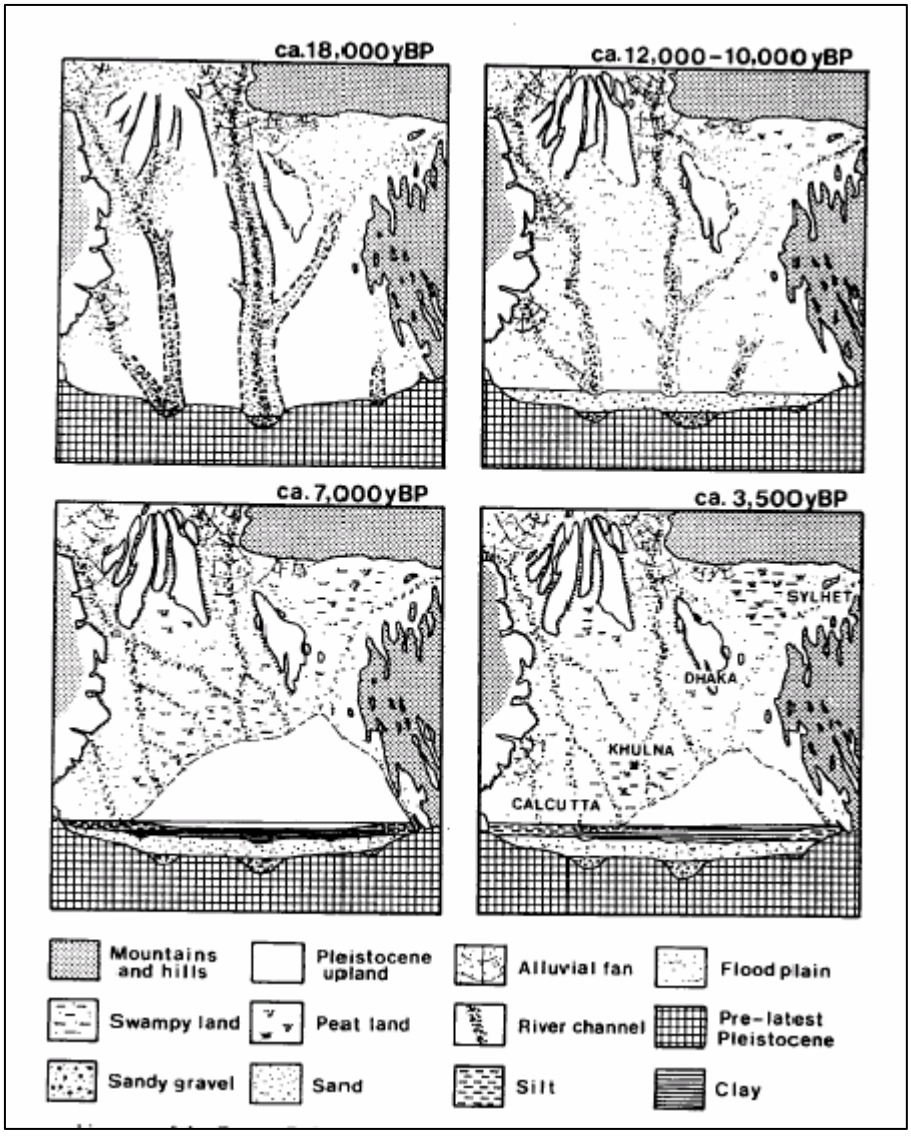

Figure 1.12: Major stages of Holocene landform evolution in the Bengal basin (Umitsu, 1993).

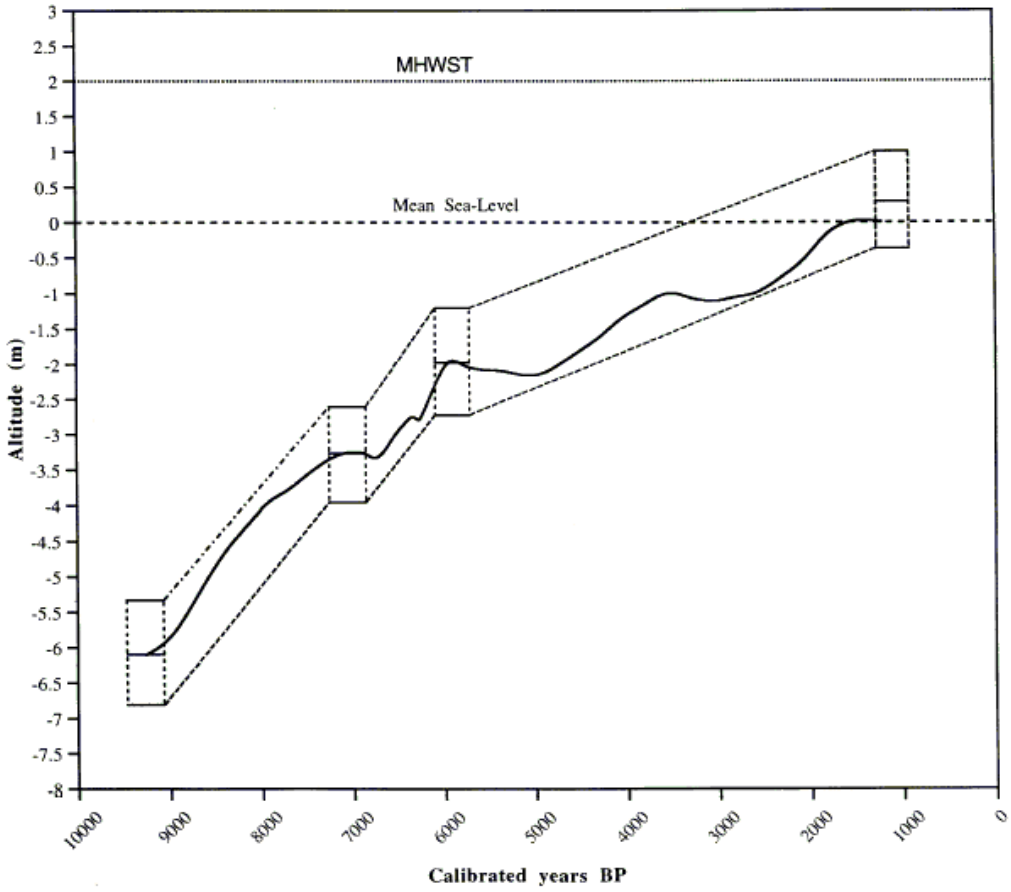

Figure 1.13: Eustatic sea level curve of the Bengal basin based on a study in the central GBM plain. The dashed boundary of the curve indicates limit of error (Islam and Tooley, 1999).

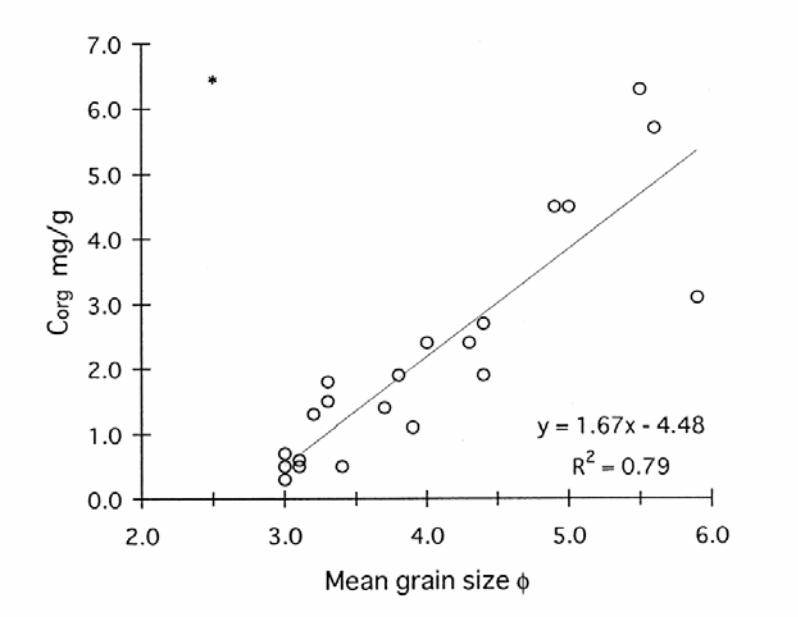

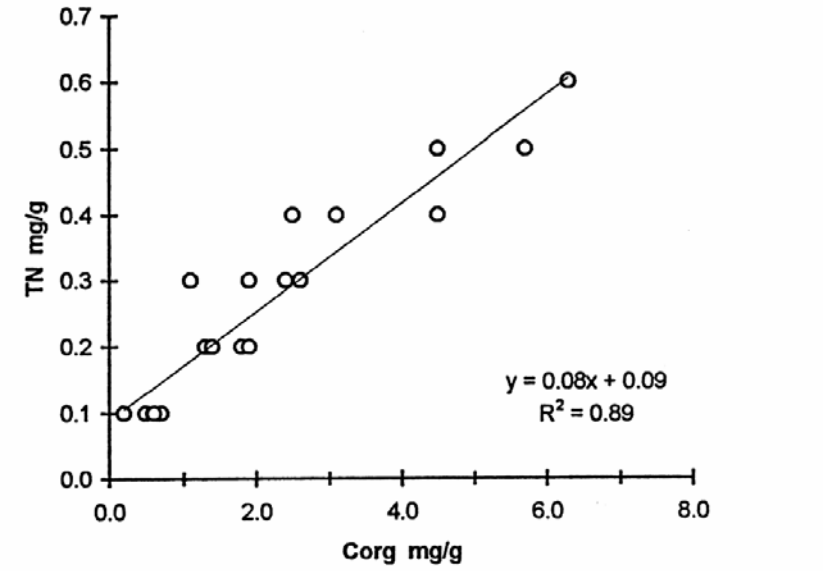

Figure 1.14: Plot showing the relation between a) mean grain size and organic carbon and b) organic carbon and total nitrogen in the Bengal basin (Datta et al., 1999).

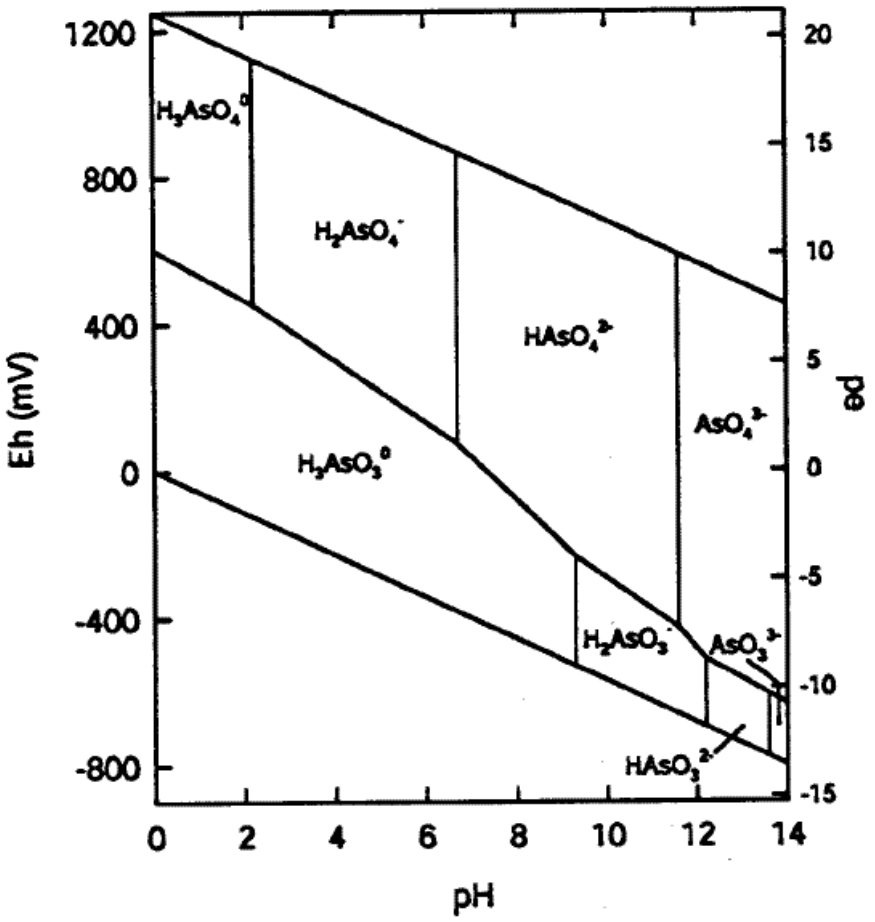

Figure 1.15: Eh-pH diagram for aqueous As in the system As-O_2-H_2O at 25^{o}C and 1 bar total pressure (Smedley and Kinniburgh, 2002).

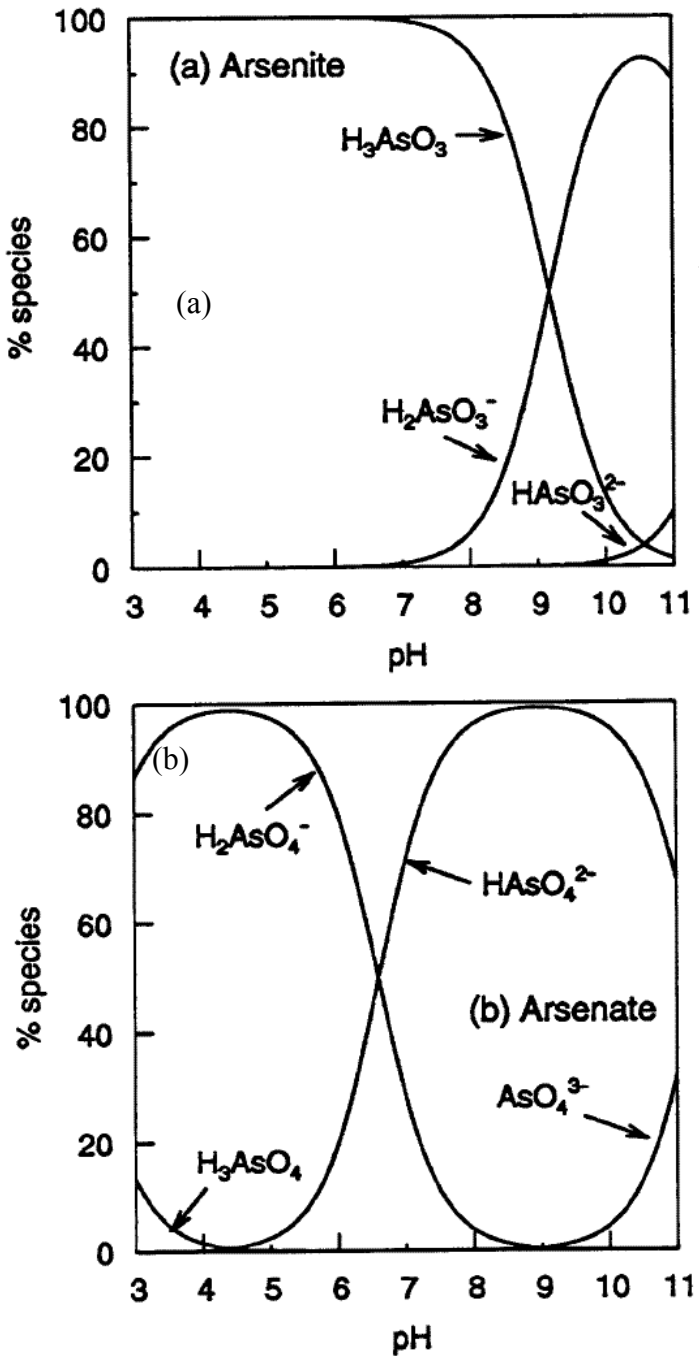

Figure 1.16: Plot showing (a) arsenite and (b) arsenate speciation as a function of pH and ionic strength of about 0.01 M (Smedley and Kinniburgh, 2002).

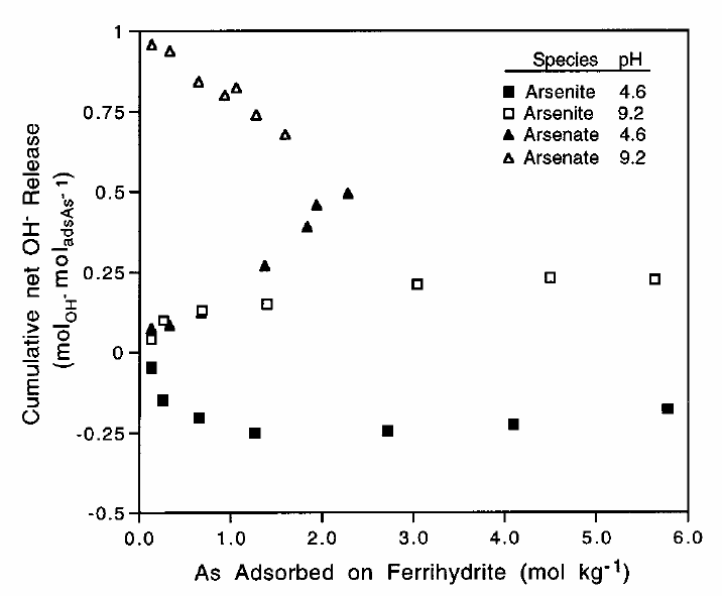

Figure 1.17: Adsorption isotherms and relationship of adsorbed As with net OH^- release during the reaction with arsenite and arsenate with ferrihydrite at pH 4.6 and pH 9.2 (Jain et al., 1999).

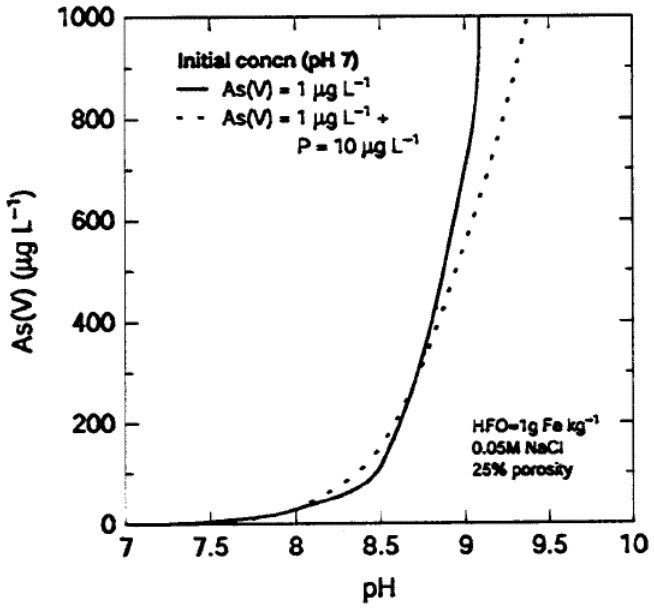

Figure 1.18: Calculated increase in As(V) concentration when the pH of a sediment (containing 1g/kg Fe as HFO) is increased from its initial value of pH 7 under closed-system conditions (Smedley and Kinniburgh, 2002).

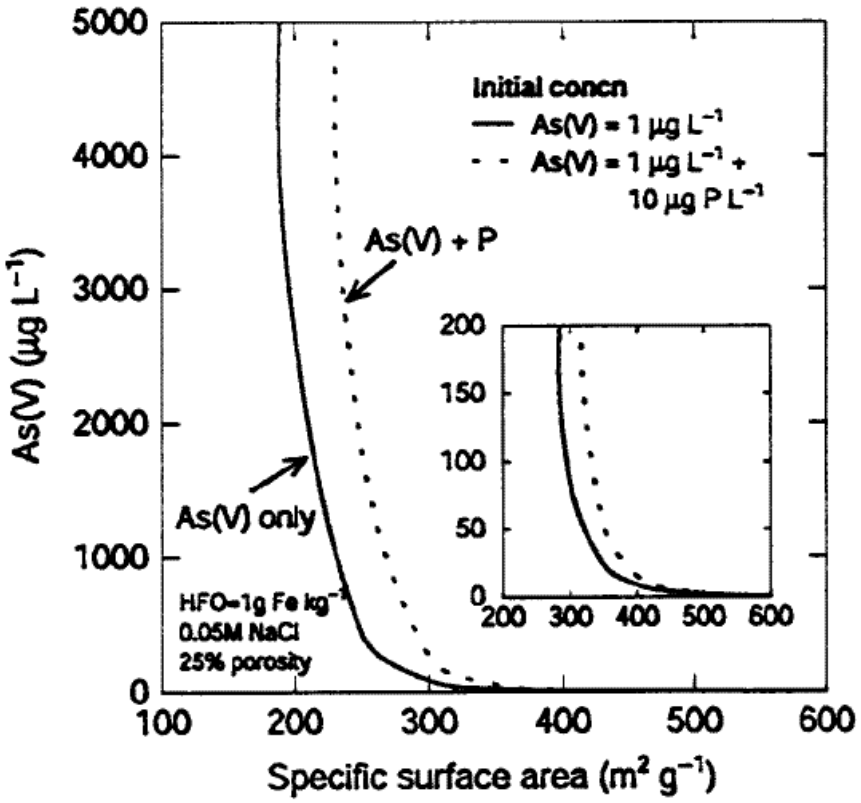

Figure 1.19: Calculated increase in As(V) concentration when the specific surface area of HFO in a sediment (containing 1g/kg Fe as HFO) is reduced from initial value of 600 m^2/g under closed-system condition (Smedley and Kinniburgh, 2002).

Chapter 2: Regional hydrostratigraphy

2.1 Introduction and study area

In this chapter, a hydrostratigraphic model for the arsenic contaminated areas of the western Bengal basin has been proposed with block-scale descriptions of the possible aquifer-aquitard framework.

2.1.1 Extent: The study area represents an interfluvial delta plain, bounded by the main channel of the River Ganges in the North, the River Bhagirathi-Hoogly in the west, the rivers Jalangi, Bhairav, Ichamati, Raimangal and Kalindi in the east, flowing almost along the Indo-Bangladesh border, and the Bay of Bengal in the south (Figure 2.1). In addition, the River Churni bifurcates from the Ichamati and flows toward the Bhagirathi-Hoogly, and the River Matla drains the southern parts of South 24 Parganas (Survey of India, 1971).

2.1.2 Elevation: In general the topography of the area is very flat (maximum elevation of about 35 m above mean sea level (MSL) near Jangipur, Murshidabad, sloping toward the Bay of Bengal in the south), with a gradient of about 0.1 m/km from north to south. In order to obtain detailed elevations, a digital elevation model (DEM) was acquired from the Shuttle Radar Topography Mission (SRTM 90) of NASA (horizontal resolution of 3 arc-sec/90 m; vertical resolution of 1 m) and processed for the study area. The color-coded DEM is shown in Figure 2.2. This DEM was imported into gridding/contouring software (Surfer ® version 8, Golden Software, Golden, CO, USA) and saved in Surfer grid (.grd) format. This resulted in enhanced compatibility of the DEM grid with the other modeling software that has been used in this project.

2.1.3 Coordinate system: The locations of the reference points within the study area were measured in the field by a Trimble® hand-held GPS using a spherical coordinate system of latitude and longitude (datum WGS84). To minimize the distortion for discretization of the grids for the lithologic and groundwater models, the location data were projected to Universal Transverse Mercator (UTM 1983), Zone 45 (central meridian 87, spheroid GRS 80, reference

latitude 0, scale factor of 0.9996, false easting 500,000, false northing 0). The coordinates of origin of the modeled area for both type of modeling were easting 600,000, northing 2,380,000.

2.2 Previous studies

AIP/PHED (1991, 1995), CGWB (1994a, b, c, d, e, 1997), SWID (1998), Acharyya et al. (2000), Goodbred and Kuehl (2000) and Goodbred et al. (2003) are the only detailed publications on the sedimentary framework of the entire study area, although some restricted government reports may also exist. All of these reports tend to provide brief descriptions of the lithology without specifying the relations between the individual aquifers at the local or regional scale.

2.3 Data acquisition and sediment classification

Lithologic data for this study were collected from 143 lithologs of drinking water, irrigation and observation wells drilled in and around the study area as shown in Table 2.1. These lithologs exist in the databases of the PHED and SWID, Government of West Bengal; B.M. Engineering (KrishnaNagar, West Bengal); and the Central Ground Water Board (CGWB), Government of India (CGWB, 1994d; SWID, 1998; PHED, 2003a, b, c, d). The depth of the lithologs ranges from 50 m to 612 m below ground level (bgl) with a mean of 243.4 m. In general the depth of the logs increases from Murshidabad to South 24 Parganas. They are distributed throughout the area except for some areas near the active delta front and near the eastern border of central Nadia district. To fill the data gap in this latter area, five logs were collected from the Bangladesh part of the basin from the Japan International Cooperation Agency (JICA, 2002).

The lithology in the logs has been generally recorded at sub-meter vertical resolution and consists of four major types of unconsolidated sediment: gravel, sand, sandy clay and clay. A number of lithologs from various localities have recorded further subdivision of sands in terms of grain size (very coarse, coarse, medium, fine) and color (white, yellow, gray, dark) along with documentation of the presence of mica, calcareous concretions and fossil fragments (mostly in South 24 Parganas). The clays have also sometimes been described in terms of color (black, gray, yellow/brown etc.) and cohesiveness (sticky, pasty, etc.). However, because in this study,

effort was made only to characterize the regional-scale hydrostratigraphy, only the major types of the sediments were used for conceptualization and modeling. Though this method has excluded more detailed quantitative description of the aquifer materials, it has successfully been able to produce a general regional model without ambitious interpolations. Also, a relatively thin soil horizon with a general thickness of 2 to 4 m covers the study area. The soil varieties are Entisols (Udifluvents) (north of Calcutta), Alfisols (Tropaqualfs) (in most of South 24 Parganas) and Aridisols (in the delta front) (CGWB, 1994e). These soils have not been included in the modeling or the description of the hydrostratigraphy.

From hydrogeologic points of view, these sediments have been categorized as aquifer (sand and gravel) and aquitard (clay). The position of the sandy clay is ambiguous: it can act as either less permeable aquifer or higher permeability aquitard. Its exact category will vary from locality to locality based on the sand/clay ratio and permeability. Although the less permeable sediments like clay transmit some groundwater, they separate the overlying aquifer(s) from lower aquifer(s) by hydraulic conductivity (K) contrast. In the study area, the extent, thickness and K of these clay or aquitard layers are very important as they govern the three-dimensional flow of groundwater at local and regional scales (Tóth, 1963).

2.4 Conceptual interpolation

Four north-south and 25 east-west transects connecting all of the lithologs were laid out on the map of the study area, 11 of which are shown in Figure 2.3. Cross-sections were developed for each of these transects by manual interpolation.

2.5 Lithologic modeling

Based on the acquired lithologs, a lithologic model was developed with RockWorks (RW) version 2004® (RockWare, Golden, CO, USA). RockWorks is multipurpose geologic software that can develop a lithologic solid model in a block-centric finite-difference grid. The gridding was done by eight nearest-neighbor methodology. Initially all the nodes of the solid model were assigned an “undefined” value. Then, based on the presence of the nearest defined nodes, the model can do 3-D interpolation by average minimum distance, and the number of nodes to be included within this distance can be user-defined.

The location (in UTM), elevation (in m), vertical extent (in m) and lithology (above-mentioned sediment types) of each of the lithologs were entered into the RockWorks project database. A solid model was developed to a depth of 300 m below MSL and was assigned an initial land-surface elevation of 30 m above MSL. The resolution of the model was 1000 m (x) × 1000 m (y) × 2 m (z). The resulting discretization consisted of 135 x nodes × 335 y nodes × 165 z nodes, thus having 7,462,125 solid model nodes, each with a voxel volume of 2,000,000 m^3. For interpolation, four nodes were assigned between each defined-undefined node. The SRTM 90-DEM grid was imported into the model to define the topographic elevation.

From the constructed solid model, a number of profile sections and fence diagrams were developed (Figures 2.4 and 2.5), including the transects planned for conceptual interpolation. The output of each of these modeled sections was visually compared with manual interpolation and corrected for any obvious error or noise. It should be remembered that because the modeling has been performed at a regional scale and the interpolations are based on nearest neighbor algorithms, the results are not free of uncertainties and do not represent local-scale variations. Thus the interpretations should be considered as among the most probable scenarios of the lithologic/hydrostratigraphic conditions existing in the study area. It was observed that the modeled transects were closely comparable to the manually interpolated transects, except that the computer-generated ones seemed to demonstrate/simulate the 3-D extent of the lithologic bodies to a greater extent. Some volumetric analyses were also performed for each sediment type at the model resolution in order to understand the volume of aquifer and aquitard sediments within the study area. Several plan-view maps have also been developed for specific depths in order to visualize the nature of the aquifers and aquitards at those depths.

2.6 Discussion

The lithologic modeling suggests the presence of a very complex 3-D hydrostratigraphic framework in the subsurface of the western Bengal basin. A detailed description of the study area at the block scale is provided here to illustrate the general spatial trends in aquifer thickness and spatial variability. This is important because without understanding the subsurface framework in at least the block scale, it is very difficult to ascertain the nature of flow in a particular area and

hence an understanding of the As contaminated areas. The cross-sections in Figures 2.4 and 2.5 and depth-plan maps in Figure 2.6 provide detailed depictions. The names of the localities mentioned henceforth represent the respective blocks (not shown on the map) or towns. These names are followed by numbers in parentheses corresponding to the locations of lithologs listed in Table 2.1. These numbers are also shown in the cross-sections. At a depth of ~300 m from MSL (the base of the model), a thick clay deposit covers the whole area. In the northernmost part of Murshidabad (from west to east, the blocks are Raghunathganj-II, Lalgola, Bhagawangola-I and -II and Raninagar-II), the topmost sand layer extends from near the surface to a depth of about 65 - 75 m (locations 73, 79 in Table 2.1). Below this unconfined aquifer is a basal clay aquitard extending from ~80 m to more than 300 m in the west (73, 74, 75), and dividing into multiple layers toward the east (80, 89). Near Raninagar-II, the upper clay layer is very thin and is mostly replaced by a sandy clay horizon, which lies between thick sand layers. In the west, this thick aquitard extends to near Beldanga (86) and Kaliganj (45), while it diminishes to form a extensive sand layer toward Karimpur-I and -II in the east to a depth of 110 m (58, 59, 60) and gradually increasing to about 190 m (61, 62). The most noteworthy thing about this area is the presence of isolated aquifers at depths of ~200 to 230 m and ~240 to 265 m extending from Bhagawangola (76, 77) to Behrampur (84) through Murshidabad-Jiaganj, with the possibility of southward extension. These isolated aquifers have water chemistry distinct from the shallower aquifer (see Chapter 5). Toward the south, the unconfined sand aquifer thickens to a depth of about 190 m in Nakashipara (near Bethuadahari in the west, 47) and to a depth of about 230 m in Tehatta (67, 70). The basal aquitard exists from ~230 m to more than 300 m depth. There are also some isolated aquifers in Tehatta from a depth of ~120 to 160 m (42, 43).

The unconfined aquifer changes to a confined/semiconfined aquifer south of Shantipur because of thick clay layers from near surface to a maximum depth of 60 m. These layers thin to the east, toward Ranaghat-II (52), and ultimately vanish toward the Bangladesh border (137, 138). In the west, near the town of Kalyani (123), this surficial aquitard extends to about 65 m bgl, extending south to the north-northeast of Calcutta, where it is thin (12 to 25 m bgl) near Dumdum (129) and BidhanNagar (130), and continues toward Diamond Harbour (100, 102). In the east, toward Ranaghat (51, 52) and eastern Chakdah (56), this aquitard thins to about 10-12 m before it disappears near the western border of Bagdah (1). Near the India-Bangladesh border,

two gravel horizons exist at depths of about 110 to 120 m and 160 to 180 m, as observed in Krishnachandrapur (136). These gravel horizons, probably indicating paleo-channels, thin toward the west, and only the top horizon is observable at a depth of about 75 to 100 m at Palashipara, Tehatta (68). The basal aquitard exists at 170 to 200 m depth in south Nadia (51, 52, and 123). In the western part of North 24 Parganas, the extensive basal clay layer splits to form a sandwiched confined aquifer, which continues to the Bay of Bengal. This aquifer starts in the north of Calcutta and is prominently visible in BudgeBudge (111) at a depth of 212 to 280 m. Some gravel horizons are visible near the Bangladesh border of northern North 24 Parganas at a depth of 138 m to 148 m (3) and in Jessore (115 m-120 m, 185 m-190 m, and 260 m-280 m) (137, 138).

Two thick clay lenses occur farther south of Calcutta, toward Budge Budge (111) (52 m to 151 m) in the west and Swarupnagar block (82 m to 204 m) in the east (4, 31), continuing toward south-central South 24 Parganas. The hydrostratigraphy of southern South 24 Parganas is dominated by multiple aquitards (100, 118, 119, 121). Many of these clay layers contain fragments of invertebrate fossils, indicating a marine origin. These clay layers separate a succession of fresh-brackish-fresh aquifers. The brackish aquifers exist at depths of 22 m to 168 m in southern South 24 Parganas (CGWB, 1994d). Around Kariberia, Diamond Harbour (114) area, a gravel horizon is visible at a depth of 98 m to 150 m. This gravel bed is a marker horizon between the overlying brackish aquifer and fresh water below (CGWB, 1994e).

The volumetric analyses of the lithologic model indicate about 2.26×10^{12} m^3 of sand and about 2.85×10^{12} m^3 of clay within the study area. The amount of sandy clay is an order of magnitude lower than these two main lithotypes. Assuming that all the sand layers are saturated and have 20% porosity (n) (Harvey, 2002; JICA, 2002), about 4.52×10^{11} m^3 of water is estimated to reside at steady state in aquifers of the study area.

2.7 Proposition of hydrostratigraphic nomenclature

Hydrostratigraphic units have been defined as bodies of rock with considerable lateral extent that compose a geologic framework for distinct hydrologic systems (Maxey, 1964). Based

on the hydraulic properties of rocks/sediments, they were supposed to be practical mappable fundamental units for describing hydrologic systems in the field (Seaber, 1988).

Several workers have discussed the general nature of the aquifer system in the basin, focusing mostly on Bangladesh (UNDP, 1982; Barker et al., 1989; EPC/MMP, 1991; BGS/DPHE, 2001, Stüben et al., 2003; Ravenscroft et al., 2005). However, for the western Bengal basin there is a scarcity of published regional-scale hydrologic studies. Thus, based on the discussion so far, a hydrostratigraphic nomenclature for our study area is proposed. Seaber (1988) commented that because of the lack of physical material in Maxey's (1964) definition of hydrostratigraphic units (dynamics of hydrologic regime), hydrostratigraphic units have not been formally adopted by North American Commission on Stratigraphic Nomenclature. Hence the proposed nomenclatures in this study are also intended to be informal.

In summary, the study area is dominated by a major single-aquifer system, which is mostly unconfined/semiconfined except in the southernmost part. In several localities, this main aquifer has been locally divided into multiple layers by the presence of discontinuous aquitards, but except in the southernmost part (south portion of North 24 Parganas and South 24 Parganas), the nature of the groundwater flow and chemistry is generally similar throughout (see Chapter 5), supporting our interpretation of a single hydrostratigraphic unit. The deeper, isolated aquifers are differentiable from the semiconfined portions of this main aquifer on the basis of groundwater chemistry (see Chapter 5). The name Golden Bengal or Sonar Bangla (in Bengali) aquifer is proposed for the main aquifer in the study area as shown in Figure 2.7, after the poetic description of Bengal by Tagore (1905). The thick, extensive, basal clay layer that marks a definite division between the Golden Bengal aquifer and any other aquifer present below -300 m MSL is named as the Murshidabad aquitard due to its best development in the Murshidabad area (Figure 2.7). The Golden Bengal aquifer probably formed over the Murshidabad aquitard as a major shift in the delta building process of the Rivers Ganges-Brahmaputra. The Murshidabad aquitard thins toward the east and south, but it can be vertically traced to a depth of at least 300 m. In the southernmost part of the study area, distinct intermediate-depth aquitards extend northward from the active delta front in the south and pinch out northward around the middle of North 24 Parganas. These aquitards have divided the main aquifer into multiple layers, which

have differences in chemistry and flow patterns. While the upper and lower portions of the aquifer in this area contain fresh water, the intermediate portion contains of brackish water (CGWB, 1994e), as a result of seawater intrusion from the Bay of Bengal. These aquitards have confined a part of the Golden Bengal aquifer from near a line between Calcutta and Bashirhat, and thicken toward the south. They are named as the Ichamati-Bhagirathi-Hoogly aquitard system, after the major rivers that drain the area (Figure 2.7).

Table 2.1: Location of lithologs used for this study.

Location No.	Location Name	Block/Town (District[a])	District (Country[b])	Latitude	Longitude	Depth[c] (m)
1	Kurulia	Bagda	NP	23.17	88.88	345
2	Panchita	Bongaon	NP	23.11	88.79	229
3	Ichapur	Gaighata	NP	22.91	88.74	234
4	Barabankra	Swarupnagar	NP	22.76	88.86	371
5	Kankpul	Habra-II	NP	22.87	88.65	209
6	Sadpur	Habra-I	NP	22.86	88.76	278
7	Koyadanga	Habra-I	NP	22.87	88.68	207
8	Madhabpur	Amdanga	NP	22.77	88.53	232
9	Humaipur	Barasat-II	NP	22.68	88.54	177
10	Bamangachi	Barasat-I	NP	22.76	88.57	168
11	Berachampa (Aminpur)	Deganga	NP	22.69	88.67	177
12	Arsula	Baduria	NP	22.75	88.76	168
13	Bansjhari Mullickpur	Bashirhat-I	NP	22.58	88.88	313
14	Champali	Minakhan	NP	22.57	88.80	311
15	Sahebkhali	Hindalganj	NP	22.35	88.93	234
16	Sitaliya	Sandeshkhali-II	NP	22.35	88.90	380
17	Haroa	Haroa	NP	22.60	88.70	371
18	Bishnupur	Rajarhat	NP	22.62	88.56	221
19	Debhog	Bashirhat-I	NP	22.61	88.83	154
20	Sankchura	Bashirhat-I	NP	22.61	88.88	157
21	Rajendrapur	Bashirhat-II	NP	22.63	88.80	207
22	Kalupur	Bongaon	NP	23.01	88.78	198
23	Chandrapara	Gaighata	NP	22.97	88.76	212

Table 2.1 (continued)

Location No.	Location Name	Block/Town (District[a])	District (Country[b])	Latitude	Longitude	Depth[c] (m)
24	Barunhat-Patlikhan	Hasnabad	NP	22.53	88.92	78
25	Murarisha	Hasnabad	NP	22.59	88.81	336
26	Nurpur	Minakhan	NP	22.56	88.78	287
27	Patharghata	Rajarhat	NP	22.59	88.56	124
28	Reckjwani	Rajarhat	NP	22.62	88.53	143
29	Thakdari	Rajarhat	NP	22.60	88.52	147
30	Kalinagar	Sandeshkhali-I	NP	22.44	88.83	169
31	Gobindapur	Swarupnagar	NP	22.87	88.86	240
32	Berachampa (Deulia)	Deganga	NP	22.70	88.68	199
33	Eojhnagar	Bashirhat-II	NP	22.71	88.72	168
34	Dalalpara	Bashirhat Town	NP	22.69	88.85	256
35	Rampur	Gaighata	NP	22.95	88.75	390
36	Banipur	Habra Town	NP	22.83	88.65	250
37	Janapoll	Habra-I	NP	22.87	88.69	253
38	Chikanpara	Gaighata	NP	22.93	88.77	435
39	Andharkoth	Karimpur-I	Nd	24.05	88.72	336
40	Karimpur-Jalangi	Karimpur-II	Nd	23.93	88.58	330
41	Tehatta	Tehatta-I	Nd	23.72	88.53	117
42	Hanspukuria	Tehatta-II	Nd	23.74	88.48	265
43	Iswarchandrapur	Tehatta-II	Nd	23.76	88.50	202
44	Kaliganj	Kaliganj	Nd	23.74	88.27	277
45	Juranpur	Kaliganj	Nd	23.72	88.22	103
46	Jumpukur	Kaliganj	Nd	23.72	88.38	276
47	Birpur	Nakashipara	Nd	23.62	88.48	231
48	Bethuadahari	Nakashipara	Nd	23.61	88.43	106

Table 2.1 (continued)

Location No.	Location Name	Block/Town (District[a])	District (Country[b])	Latitude	Longitude	Depth[c] (m)
49	Bara Andulia	Chapra	Nd	23.64	88.54	320
50	Mamjoani	Hanskhali	Nd	23.81	88.59	140
51	Kamagachi	Ranaghat-I	Nd	23.22	88.56	332
52	Gagnapur	Ranaghat-II	Nd	23.14	88.64	228
53	Shantipur	Shantipur	Nd	23.25	88.43	177
54	Bhaluka	KrishnaNagar-I	Nd	23.35	88.41	288
55	Gobrapota	KrishnaNagar-I	Nd	23.42	88.55	130
56	Ghentugachia	Chakdah	Nd	23.03	88.59	149
57	Debagram	Kaliganj	Nd	23.69	88.33	308
58	Karimpur	Karimpur-I	Nd	23.98	88.65	110
59	Doradaha	Karimpur-II	Nd	24.00	88.61	104
60	Dogachi	Karimpur-II	Nd	24.03	88.58	105
61	Mahisbathan	Karimpur-II	Nd	23.95	88.61	144
62	Narayanpur	Karimpur-II	Nd	23.90	88.53	112
63	Dignagar	KrishnaNagar-I	Nd	23.34	88.44	122
64	Sonatala	KrishnaNagar-II	Nd	23.53	88.51	146
65	Dhubulia	KrishnaNagar-II	Nd	23.52	88.45	136
66	Nazirpur	Tehatta-I	Nd	23.88	88.56	115
67	Betai	Tehatta-I	Nd	23.80	88.59	186
68	Palashipara	Tehatta-II	Nd	23.79	88.45	100
69	Shyamnagar	Tehatta-I	Nd	23.78	88.50	173
70	Bareya	Tehatta-II	Nd	23.75	88.38	191
71	Gopinathpur	Tehatta-II	Nd	23.84	88.46	137
72	Palsunda	Tehatta-II	Nd	23.78	88.40	172
73	Ramakanthapur	Suti-I	Md	24.54	88.06	88
74	Sekendra	Raghunathganj-II	Md	24.50	88.08	330

Table 2.1 (continued)

Location No.	Location Name	Block/Town (District[a])	District (Country[b])	Latitude	Longitude	Depth[c] (m)
75	Mithipur	Raghunathganj-II	Md	24.50	88.05	99
76	Kantanagar	Bhagwangola-I	Md	24.34	88.31	317
77	Habaspur	Bhagwangola-I	Md	24.39	88.37	300
78	Mahishasthali	Bhagwangola-I	Md	24.34	88.32	325
79	Lalgola	Lalgola	Md	24.42	88.25	150
80	Jalangi-Karimpur	Jalangi	Md	24.13	88.72	305
81	Lalbag	Murshidabad-Jiaganj	Md	24.18	88.28	50
82	Jiaganj	Murshidabad-Jiaganj	Md	24.23	88.27	154
83	Behrampur	Behrampur Town	Md	24.09	88.26	91
84	Chaighari	Behrampur	Md	24.16	88.41	330
85	Mahula	Beldanga-I	Md	24.00	88.24	334
86	Takipur	Beldanga-I	Md	23.87	88.25	120
87	Mahimapur	Md	Md	24.21	88.26	96
88	Islampur	RaniNagar-I	Md	24.15	88.47	50
89	Nabipur	RaniNagar-II	Md	24.25	88.60	90
90	Edrakpur	Nawda	Md	23.91	88.46	287
91	Katakopra	Domkal	Md	24.08	88.63	77
92	Shaktipur	Beldanga-II	Md	23.86	88.20	146
93	Ghasiara	Sonarpur	SP	22.44	88.46	254
94	Kalikapore	Sonarpur	SP	22.40	88.48	283
95	Caning Town	Caning-I	SP	22.32	88.65	299
96	Dihikalas	Mograhat-II	SP	22.28	88.37	299
97	Sonakhali	Basanti	SP	22.30	88.74	400
98	Sonaga-Gosaba	Gosaba	SP	22.25	88.80	421
99	Debipur	Mathurapur-I	SP	22.20	88.47	365
100	Diamond Harbour	Diamond Harbour	SP	22.22	88.23	306

Table 2.1 (continued)

Location No.	Location Name	Block/Town (District[a])	District (Country[b])	Latitude	Longitude	Depth[c] (m)
101	Ganga Sagar	Sagar	SP	21.86	88.18	300
102	Sarisha	DH-II	SP	22.28	88.21	301
103	AkhayNagar	Kakdwip	SP	21.98	88.27	309
104	Bhagankhali	Basanti	SP	22.32	88.78	323
105	Baharu	Joynagar-I	SP	22.24	88.46	320
106	Beliaghata	Baruipur	SP	22.30	88.53	300
107	Dakhin Barasat	Joynagar-I	SP	22.26	88.48	295
108	Mograhat	Mograhat-II	SP	22.26	88.42	303
109	South Garia	Baruipur	SP	22.36	88.50	305
110	Bishnupur	Bishnupur	SP	22.36	88.30	304
111	BudgeBudge	BudgeBudge	SP	22.41	88.19	550
112	Falta	Falta	SP	22.30	88.14	304
113	Kakdwip	Kakdwip	SP	21.98	88.25	440
114	Karaibaria	Diamond Harbour-II	SP	22.25	88.14	434
115	Kurulia	Baruipur	SP	22.33	88.56	601
116	Namkhana	Namkhana	SP	21.88	88.27	432
117	Rajpur	Sonarpur	SP	22.45	88.43	612
118	Sitarampur	Kulpi	SP	22.16	88.29	414
119	Jalaberia	Kultali	SP	22.19	88.57	400
120	Anchana	Mandirbazar	SP	22.22	88.35	401
121	JelerHat	Baruipur	SP	22.30	88.56	412
122	Dakhin Durgapur	Pathar Pratima	SP	22.06	88.39	401
123	Kalyani	Kalyani Town	Nd	22.98	88.47	174
124	Naihati	Naihati Town	NP	22.89	88.41	148
125	Panihati	Panihati Town	NP	22.70	88.37	142
126	Barrackpore	Barrackpore Town	NP	22.79	88.36	154

Table 2.1 (continued)

Location No.	Location Name	Block/Town (District[a])	District (Country[b])	Latitude	Longitude	Depth[c] (m)
127	Kamarhati	Kamarhati Town	NP	22.65	88.40	142
128	Rajarhat-Newtown	Rajarhat	NP	22.60	88.44	137
129	South DumDum	Dum Dum Town	CCU	22.58	88.41	200
130	Bidhannagar	Salt Lake Town	CCU	22.56	88.42	152
131	Bhatjangla	KrishnaNagar-I	Nd	23.38	88.50	305
132	Neulia	Ranaghat-II	Nd	23.12	88.63	168
133	Jugpur	Nakashipara	Nd	23.60	88.39	152
134	Chuadanga	(Chuadanga[a])	(Bdesh[b])	23.63	88.85	300
135	Bara Dudhpatalia	(Chuadanga)	(Bdesh[b])	23.55	88.82	300
136	Krishnachandrapur	(Jhenaidah[a])	(Bdesh[b])	23.29	88.91	300
137	Jessore	(Jessore[a])	(Bdesh[b])	23.15	89.22	300
138	Bankabasi	(Jessore[a])	(Bdesh[b])	22.92	89.27	300
139	Bhimpur	KrishnaNagar-I	Nd	23.43	88.62	229
140	Bongaon	Bongaon	NP	23.05	88.82	223
141	Chua	Hariharpara	Md	24.03	88.45	84
142	Kismat-Imadpur	Hariharpara	Md	24.03	88.35	71
143	Surangapur	Nawda	Md	23.93	88.46	96

Md: Murshidabad, Nd: Nadia, NP: North 24 Parganas, SP: South 24 Parganas, CCU: Calcutta Bdesh: Bangladesh

[a] Names of districts in Bangladesh

[b] Name of country other than India

[c] Depth to nearest meter

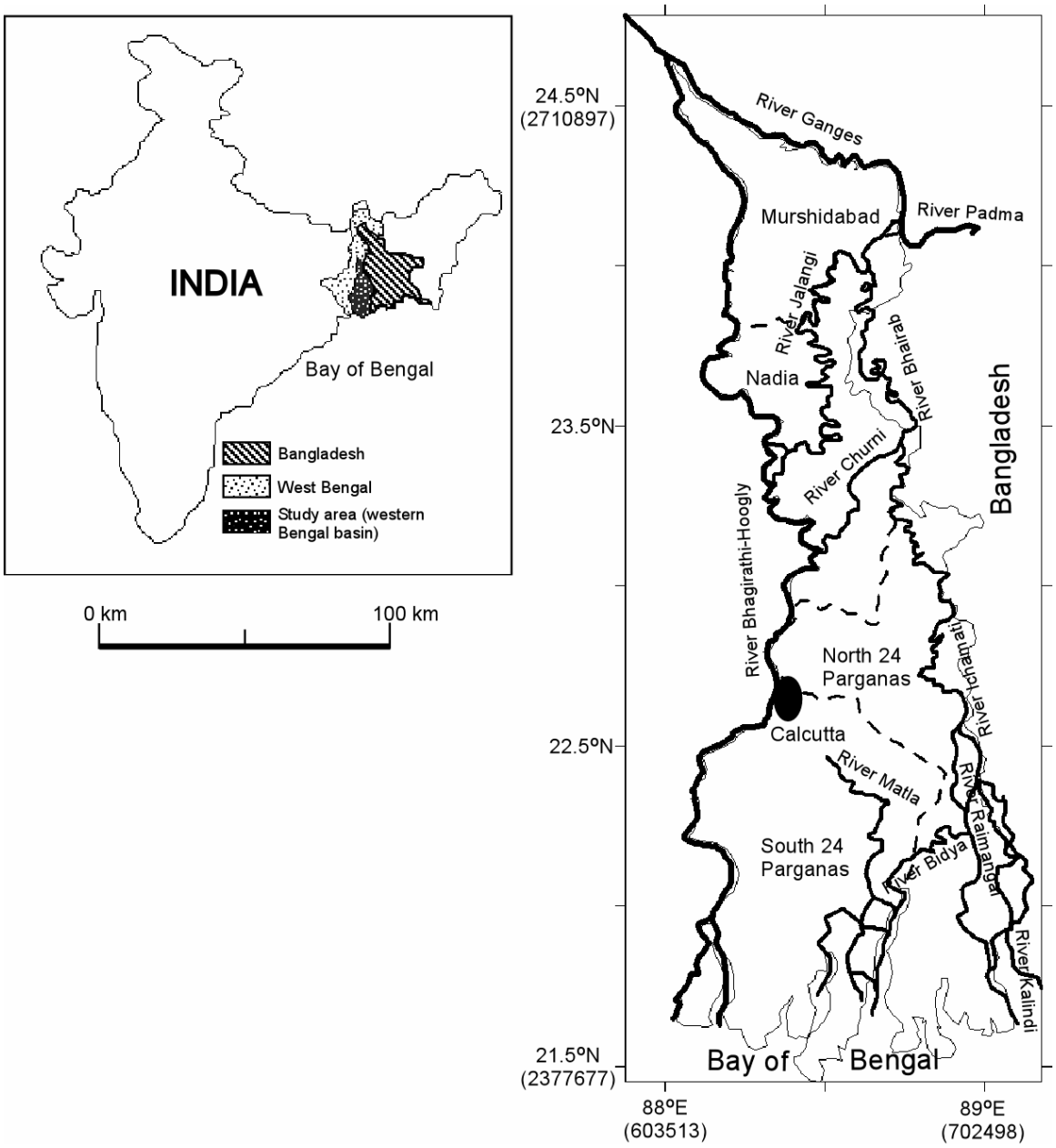

Figure 2.1: Location map of the study area showing the districts and important rivers (district boundaries are in dashed lines). UTM values (in parentheses) are listed beside respective latitude and longitude values.

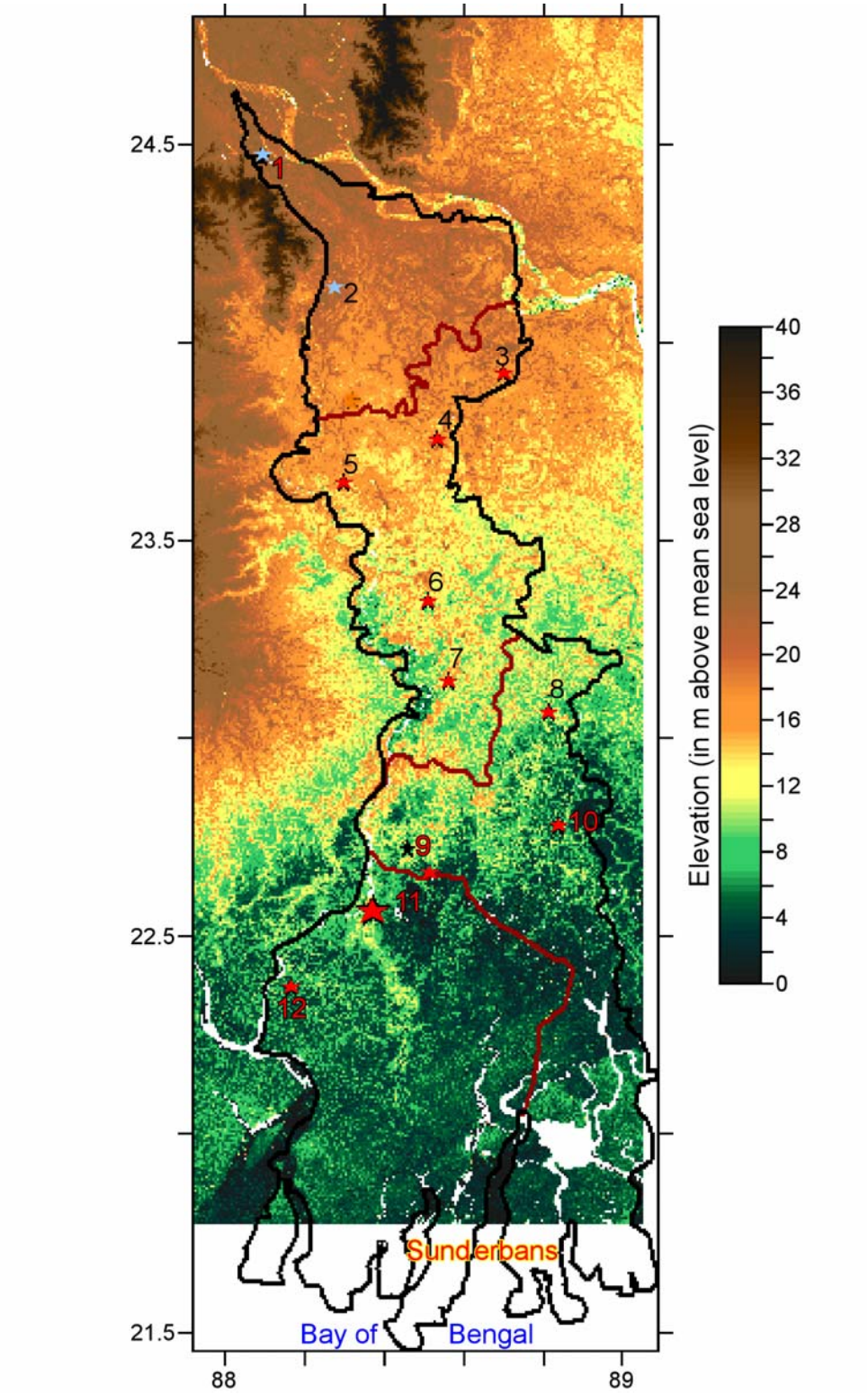

Figure 2.2: Elevation map of the study area prepared from SRTM-90 DEM along with locations of important towns (the stars): #1 Jangipur, #2 Behrampur, #3 Karimpur, #4 Tehatta, #5 Debagram, #6 KrishnaNagar, #7 Ranaghat, #8 Bongaon, #9 Barasat, #10 Bashirhat, #11 Calcutta (Kolkata), #12 Diamond Harbour.

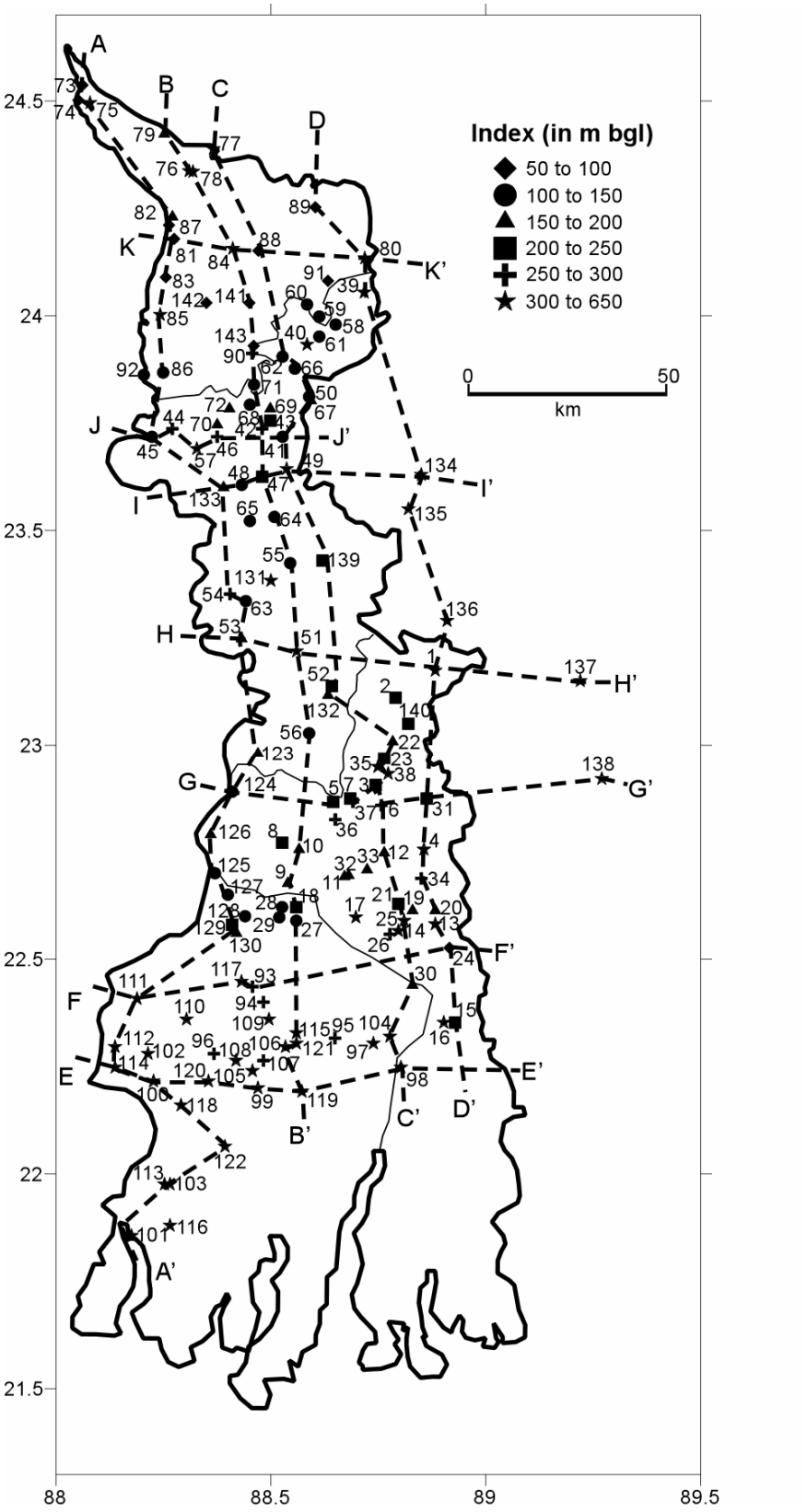

Figure 2.3: Map showing location of the 143 lithologs in Table 2.1 used for lithologic interpolation and orientation of the 11 cross-sections shown in Figures 2.4 and 2.5.

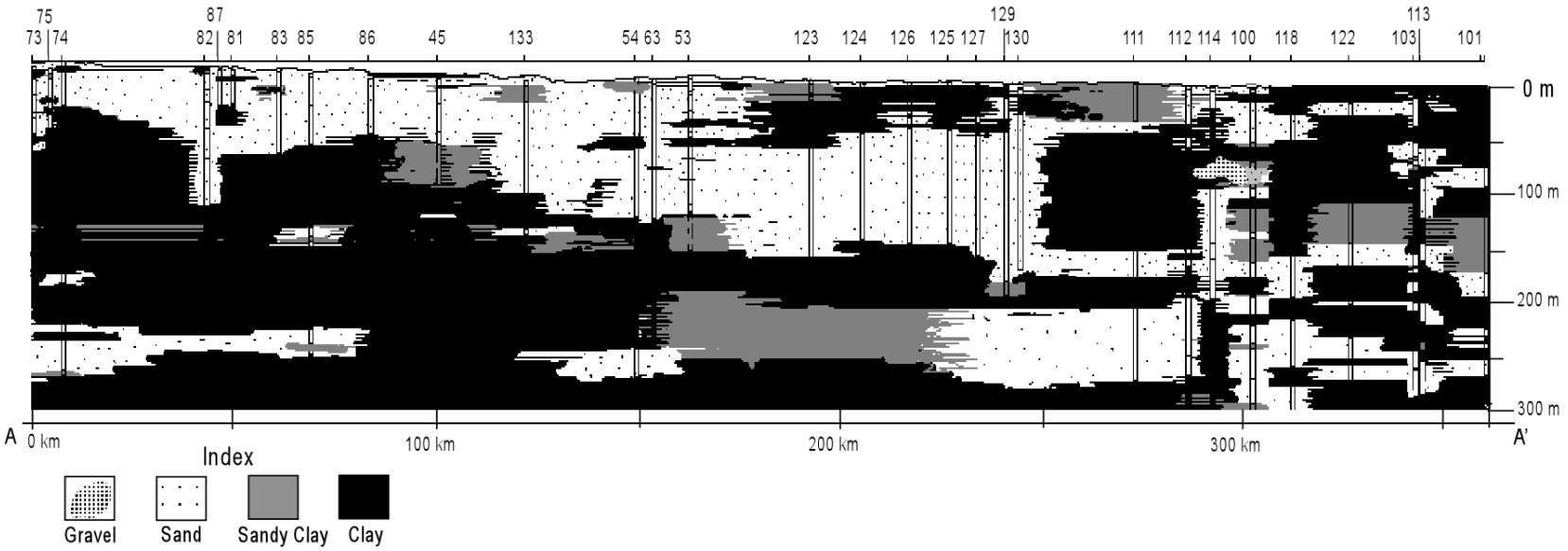

Figure 2.4a: Modeled cross-section along transect AA' in Figure 2.3 (vertical exaggeration = 275×).

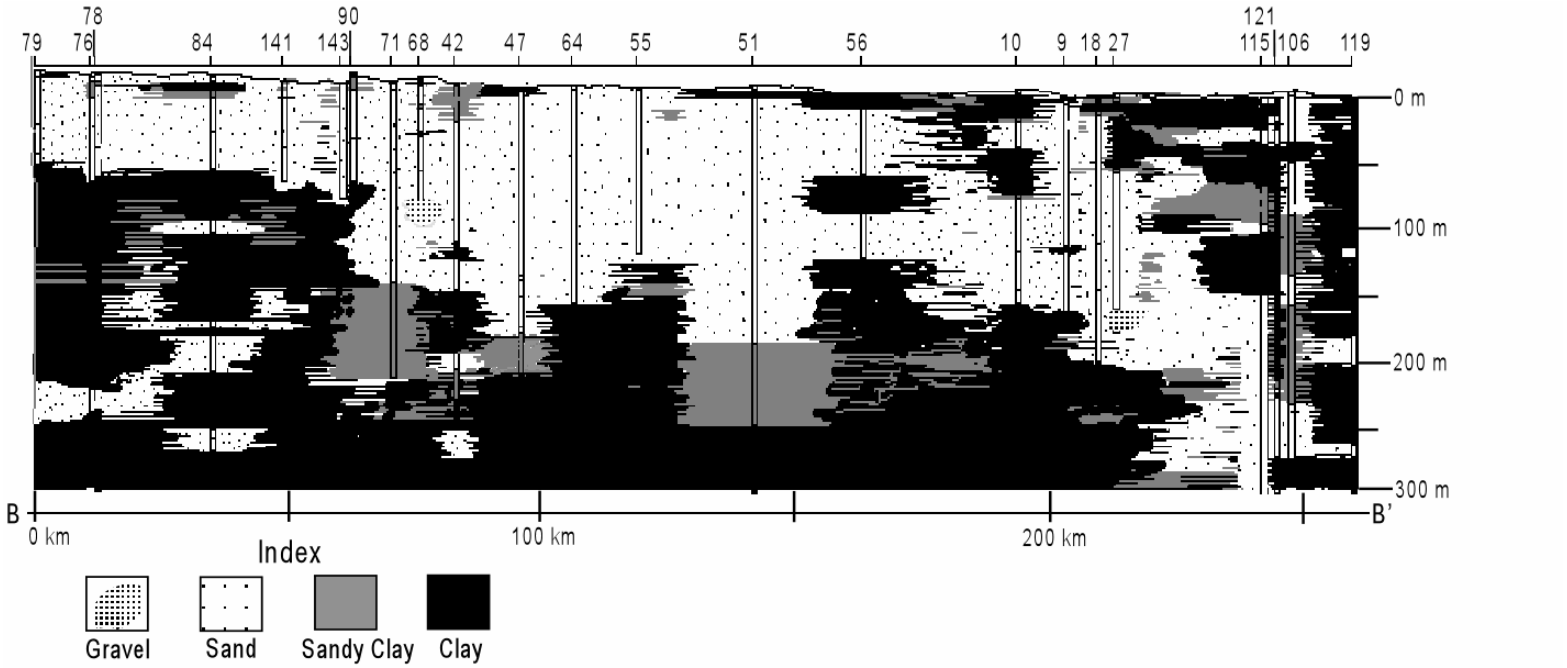

Figure 2.4b: Modeled cross-section along transect BB' in Figure 2.3 (vertical exaggeration = 265×).

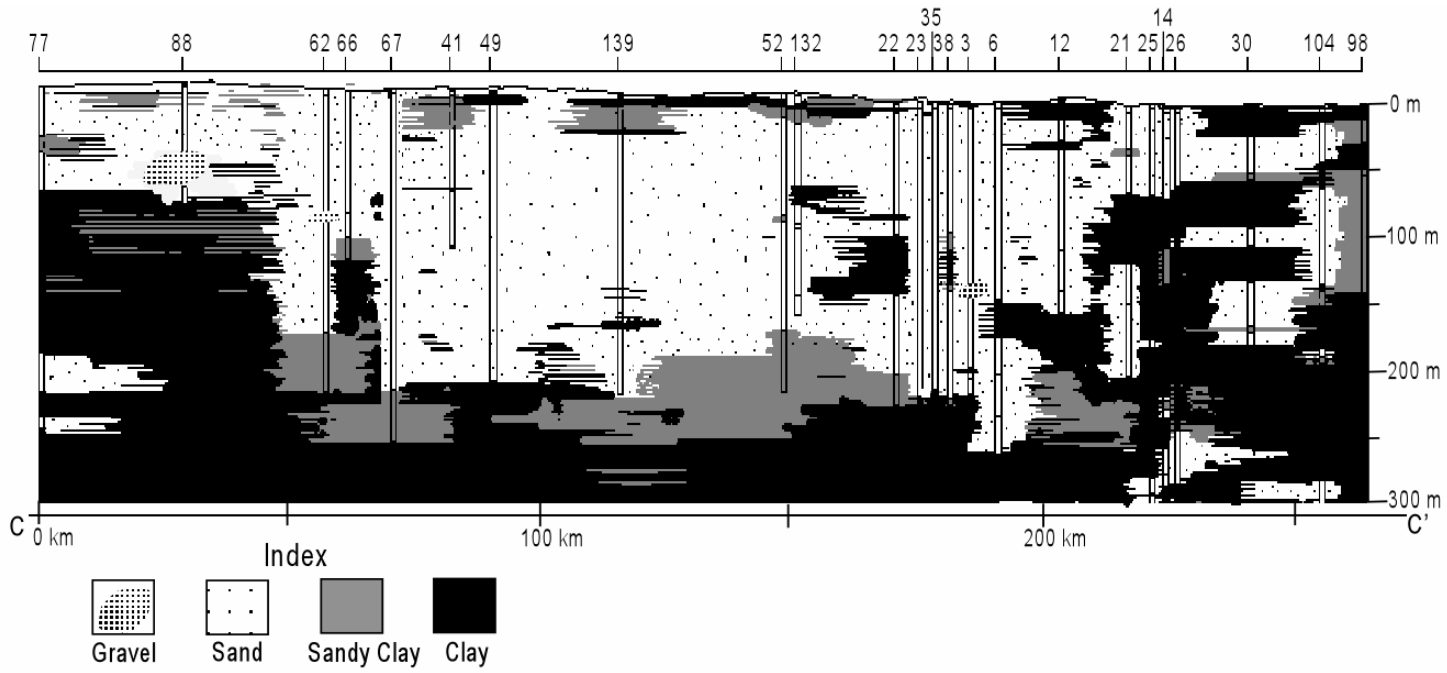

Figure 2.4c: Modeled cross-section along transect CC' in Figure 2.3 (vertical exaggeration = 265×).

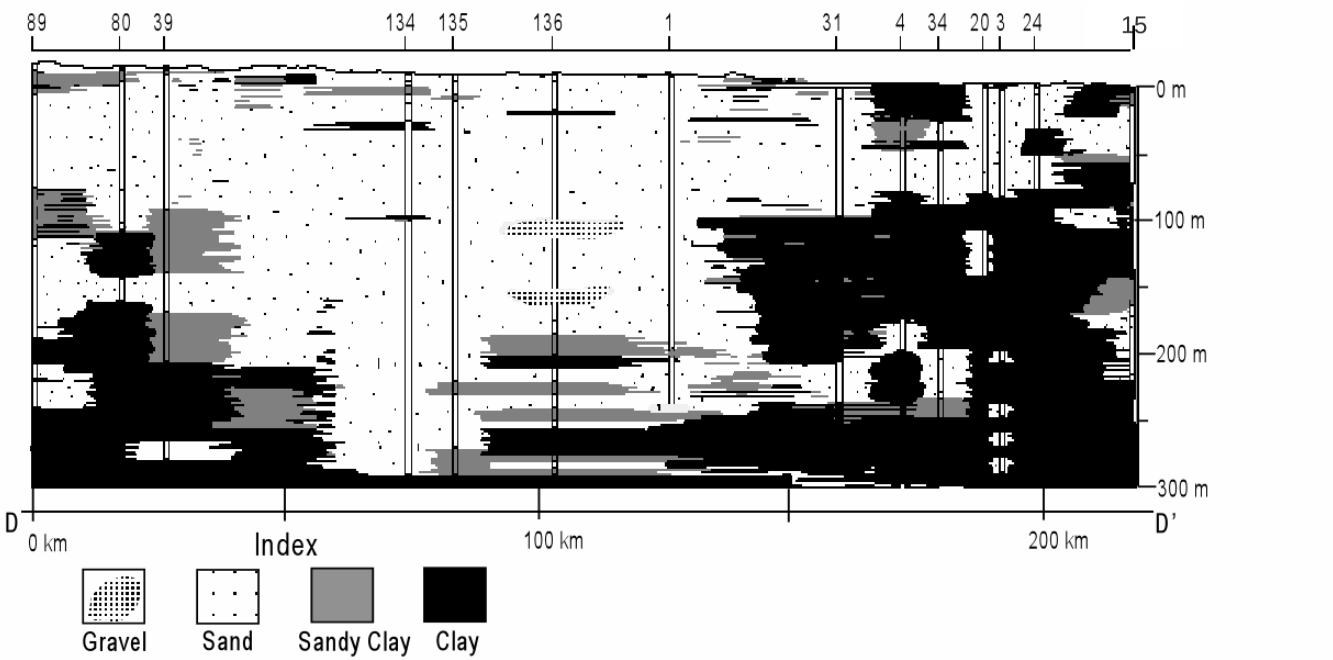

Figure 2.4d: Modeled cross-section along transect DD' in Figure 2.3 (vertical exaggeration = 265×).

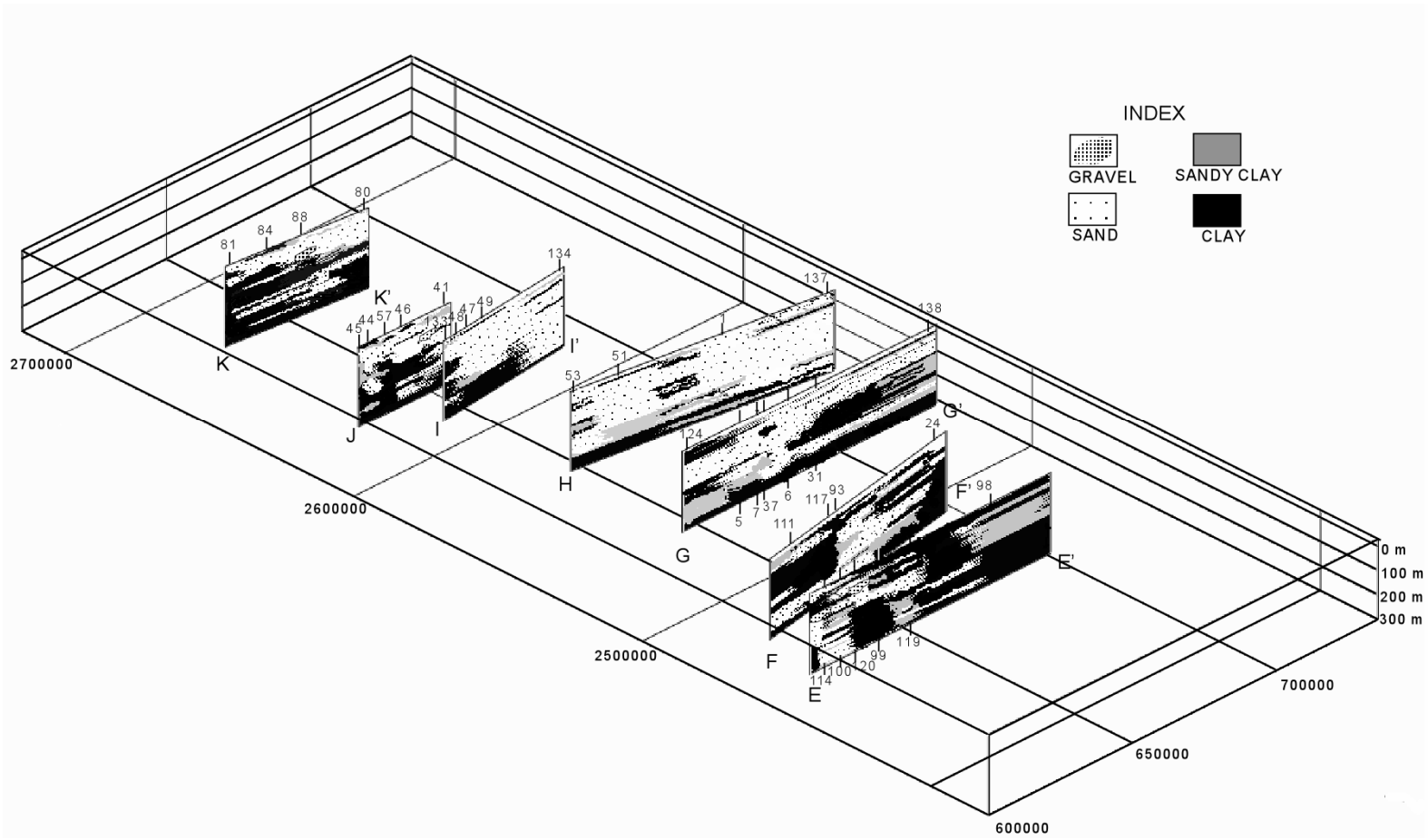

Figure 2.5: Modeled cross-sections along transect EE', FF', GG', HH', II', JJ', KK' in Figure 2.3.

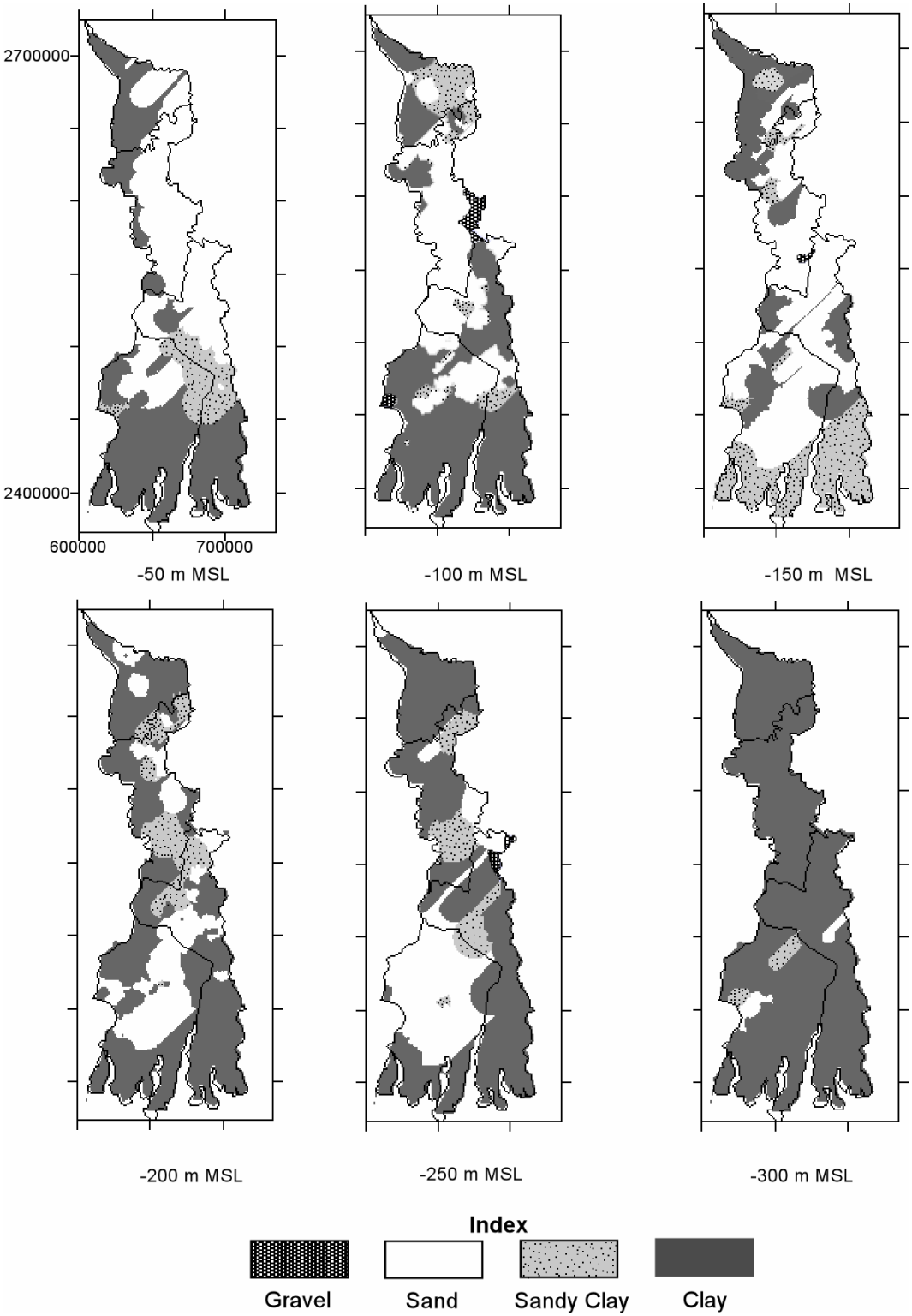

Figure 2.6: Modeled plan maps of the study area showing the subsurface distribution of lithologic units at definite depths.

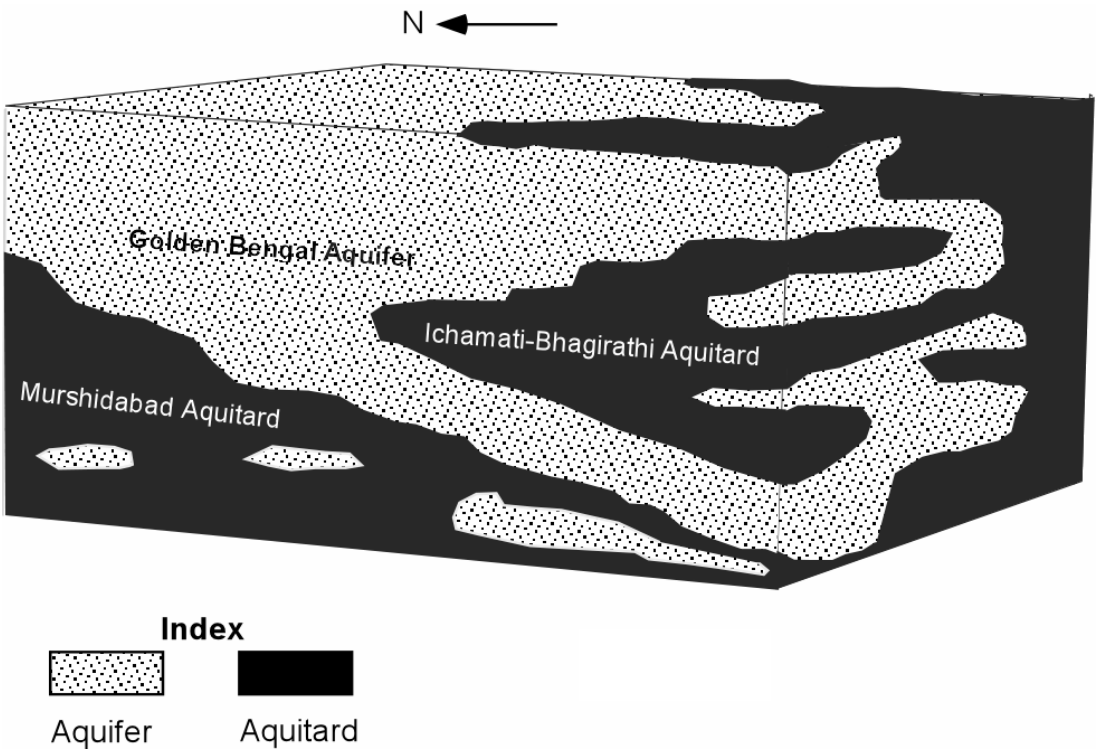

Figure 2.7: Conceptual block model showing the proposed hydrostratigraphic units (not to scale).

Chapter 3: Regional groundwater flow modeling

3.1 Introduction

In this chapter, numerical simulations of regional-scale, seasonal groundwater flows through the proposed hydrostratigraphic framework have been described. The objectives for the groundwater flow modeling were to:

i) understand the groundwater flow pattern at a regional scale in the western Bengal basin;

ii) understand the interactions between shallow and deep groundwater flow and hence the possibility of cross contamination of arsenic across the vertical extent of the aquifers;

iii) calculate the relative magnitude of flow in the shallower and deeper parts of the aquifers;

iv) analyze the effects of pumping at present and projected future rates on the flow patterns and predict the future status of the groundwater resource for the study area.

The rivers (see Figure 2.1) are the most important geomorphic features in the study area. The complete Holocene stratigraphic sequence has been formed by the channel-interchannel-deltaic sedimentation of these rivers. Herein, it is hypothesized that they provide a strong control on the nature of groundwater flow in the area. One rationale for selecting this area is that it can be considered to be a hydrologically closed system for purpose of groundwater flow modeling, considering the major hydrologic boundaries on all four sides.

3.2 Previous modeling efforts

Groundwater flow models for the Bengal basin have been developed for Faridpur and Chapai Nawabganj (BGS/DPHE, 2001) and Jennaidah and Jessore (JICA, 2002) in Bangladesh. These models included 2-D cross-sectional models and a 3-D regional model. No comprehensive modeling study was found to have been done for our study area, although local-scale modeling has been performed for the Yamuna subbasin in North 24 Parganas (Ghosh et al., 1999; Mukherjee, 2004).

3.3 Conceptual model

Before planning the details of the model design, a conceptual model was conceived. Being a tropical fluvio-deltaic system with monsoonal rainfall, groundwater flow in the western Bengal basin is complicated to conceptualize, even without considering extensive anthropogenic impacts. Therefore, in this modeling effort, only the parameters that were thought to have significant control on the groundwater flow were incorporated. The model design is based on the observed hydrostratigraphy, including an upper aquifer and a basal confining unit. Recharge is primarily meteoric, while discharge occurs both through outflow to surface water bodies and pumping for irrigation. The modeled area is bounded in the north, west, and east by the specified-head-boundary Rivers Ganges, Bhagirathi-Hoogly and Jalangi/Ichamati, and to the south by the Bay of Bengal, a constant head boundary.

3.4 Discretization and design

The 3-D groundwater flow in the study area is modeled by MODFLOW (McDonald and Harbaugh, 1988). Groundwater flow in heterogeneous, anisotropic media can be expressed by the following equation:

$$\frac{\partial}{\partial x}(K_{xx}\frac{\partial h}{\partial x})+\frac{\partial}{\partial y}(K_{yy}\frac{\partial h}{\partial y})+\frac{\partial}{\partial z}(K_{zz}\frac{\partial h}{\partial z})-W=Ss\frac{\partial h}{\partial t}$$

where

K_{xx}, K_{yy} and K_{zz} are hydraulic conductivity values in x, y, and z directions, which are assumed to be parallel to the major axes of K (L/T)

h is the hydraulic head (L)

W is volumetric flux per unit volume and represents sources and/or sinks of water (T^{-1})

Ss is the specific storage of the porous material (L^{-1})

t is time (T)

Microsoft Windows® based Groundwater Vistas® (GV) version 4 (Environmental Simulations International, Reinshold, PA, USA) was used as a pre-processor (for design and discretization) and post-processor (for viewing results and mass balance). The modeled study area is 335 km in length and 110 km in width. It coincides almost with the study area except

small areas in the east (east of the River Ichamati) and south (in the active delta front). The description of the model design follows.

3.4.1 Horizontal discretization: The grid is 335 (x) × 110 (y) (36,850 horizontal grid cells) with each grid cell having dimensions of 1000 m × 1000 m.

3.4.2 Vertical discretization and aquifer parameters: The model thickness is 330 m to 300 m, depending on topography, with 21 layers (total of 773,850 3-D grid cells). Except for the top layer, which has variable thickness due to topographic features, each layer is 15 m in thickness. In order to make the model realistic, the hydraulic framework of the different layers was based on the lithologic modeling exercise. A 1000 m × 1000 m × 15 m lithologic model was developed in RockWorks (RW), as discussed earlier. Each of the sediment types was assigned an index value (G) to define the K value for the aquifers and aquitards. Then the lithologic layers from RW were imported to GV via Surfer as grid layers with nodal values of hydraulic conductivity ($K_x = K_y$ and K_z = 1/10 of K_x). Thus the GV model is comprised of hydraulic conductivity values in place of the corresponding lithotypes of the lithologic model, that is, the lithologic model was replicated as a hydrogeologic framework model. The 21st layer (285 m to 300 m below MSL) was defined as the basal no-flow boundary, consistent with the extensive clay layer at about 300 m below MSL.

The initial values of aquifer parameters were taken from the literature. CGWB (1994a, b, c, d) and SWID (1998) estimated that transmissivity (T) values (in m^2/d) vary from 3300 to 7000 in Murshidabad, 5000 to 8800 in North 24 Parganas, and 500 to 3000 in South 24 Parganas, with an average storativity (S) of 0.03. The value of porosity (n) was assumed to be 0.2 (Harvey, 2002; JICA, 2002). BGS/DPHE (2001) suggested that the K values for Gangetic sediments could vary from 10 to 100 m/d. In their site-specific model of Faridpur, they classified the sediment as sandy silt (K= 4 m/d), fine sand (8 m/d), medium sand (25 m/d), and coarse sand (46 m/d). For the present model, we selected uniform initial K_x and K_y (K_z = 1/10 of K_x) values of 4 m/d, 25 m/d and 40 m/d for sandy clay, sand, and gravel, respectively. K_x, K_y, and K_z of 0.01 m/d were selected for clay according to JICA (2002). The final values of the aquifer parameters were ascertained by model response to sensitivity analyses.

3.4.3 Surface topography: The initial thickness of the topmost layer was set as 30 m. The SRTM DEM was imported into GV for the surface elevation/upper bound of the topmost layer.

3.4.4 Specified head boundaries: According to the conceptual model, ArcGIS® (ESRI, Redlands, CA, USA) shape files were developed for each river and then imported into GV as specified-head-boundary river objects. To resemble reality, all of the rivers shown in Figure 2.1 have been included. The rivers were divided into 11 reaches according to geometric similarities along each reach. For each of the stream reaches, the starting and ending cells were specified with attributes like channel width, stream stage, channel bed elevation, and K of the bed sediments. Depending on the reach length and surrounding topography, GV automatically interpolated the attribute values for the cells lying between the starting and ending cells of each reach. The width of each of the reach was specified according to measurements from the base map. In Bangladesh, the stage of the rivers varies from approximately 5 to 13 m above the streambed (Dowling et al., 2003). For this model the stage values for each reach were selected from field experience and the topographic values specified for the cells in the vicinity, assuming that the stage of the river is near the land surface. The other attributes were specified according to estimation, field experience and local information.

3.4.5 Constant head boundaries: Constant head boundaries with a value of 0 m representing the Bay of Bengal were assigned to the southernmost rows of the top four layers of the model. Though not exact, the depth and extent of the constant head boundaries for each layer were guided by the original bathymetric data (Survey of India, 1971). The extreme southern boundary was marked at the southernmost tip of the study area (the active delta front).

3.4.6 Rationale of seasonal models: The study area has distinct wet (monsoon) and dry seasons. On average (1901 to 1970), the seasonal rainfall can be considered as pre-monsoon (January to May) equaling 16.23% of annual rainfall, monsoon (June to October) 82.21% and post-monsoon (November-December) 1.57%. Increased pumping lowers the water level in the dry seasons. The aquifer is mostly full during the monsoon season as an effect of increased precipitation and lower rates of pumping. Hence any excess potential recharge is rejected (BGS/DPHE, 2001), thereby

causing regular, widespread runoff and flooding. The division of seasons for this study was done in the context of irrigation schedules. The seasons have different daily recharge rates and pumping rates for irrigation.

In West Bengal, rice cultivation is dominated by boro (mainly dependent on groundwater irrigation) during the pre-monsoon (January to April/May), followed by kharif (mainly rainwater-fed) during the monsoon (July to October/November). Rabi (post-monsoon) cultivation is also mostly groundwater fed. The high-yielding boro cultivation caught momentum with the onset of groundwater pumping for irrigation in the early 1970s. In Bangladesh, the cultivation increased from less than 0.05% of the total area in the early 1970s to more than 20% (more than 45% of total cultivable area) around 2000 (Hossain et al., 2003; Harvey et al., 2005). Boro requires from about 1 m (Harvey et al., 2005) to about 3 m (AIP/PHED, 1995) of annual irrigation, while kharif requires only about 0.3 m (S.P. SinhaRoy, Arsenic Task Force, Government of West Bengal, personal communication, 2004).

In spite of having some localities with an overdraft problem (where the groundwater is not replenished annually), groundwater levels at the beginning of each irrigation season tend to be similar from year to year, which suggests that the groundwater levels are controlled by local river stages (BGS/DPHE, 2001). This observation and the lack of detailed storativity data for the different hydrologic units led to construction of three separate models for different annual irrigation seasons, instead of a single transient model with three seasons (stress periods). A single transient model would have been preferable, but the disproportionate precipitation (and hence recharge) during the monsoon adversely affects the water levels during other seasons of a transient model, resulting in poorly constrained values of the volume of water in storage. Moreover, calibration of the pre-monsoon model with pumping (at the beginning of the irrigation season) indicates a reasonable fit, as noted below, supporting the rationale of separate seasonal models.

3.4.7 Recharge: The exact recharge values in the study area were not available. Previous studies have estimated 0.3 to 5.5 mm/d (BGS/DPHE, 2001) and 1.6 mm/d (annual average) (Basu et al., 2002; Dowling et al., 2003) for the Bangladesh part of the basin. For the West Bengal part,

SWID (1998) estimated that recharge is up to 15% of total precipitation. Because recharge rate is one of the primary controlling factors for groundwater flow in a low-topographic-gradient study area, a detailed approach for estimating the potential recharge (PR) was developed. The term "potential recharge" is used in place of "recharge" because the rainwater available for recharge will also run off, and there is no record or simple method available for estimating either the recharge or run-off in an area crowded by numerous ponds, ox-bow lakes, small streams and larger rivers. Harvey et al. (2005) noted that the pond/lake bottoms and streambeds can provide significant areas for infiltration of recharge, and irrigation water applied to cultivated fields can also re-infiltrate, resulting in a very complex cycle of recharge and discharge. Actual recharge values can be obtained by the difference in groundwater levels between wet and dry seasons. However, no such data were available except for general values obtained for some small localities. Moreover the daily oscillation of water levels due to irrigation pumping can be more than 0.2 m, thus presenting a very difficult scenario for estimating recharge and groundwater flow directions (Harvey et al., 2005).

Seasonal mean rainfall data, as shown in Table 3.1, were calculated for 25 locations within and near the study area based on multiple years' data obtained from the National Climatic Data Center (http://www.ncdc.noaa.gov/oa/pub/data/ghcn/v2/ghcnftp.html). Table 3.2 shows the monthly mean temperature data for Calcutta from 1811 to 2005. Based on these data, potential evapotranspiration (PET) values were estimated for each location according to Malmstrom (1969):

$$PET(mm/month) = 40.9 \times e^*(T)$$

where

$$e^* = 0.611 \times \exp\left(\frac{17.3 \times T}{T + 237.3}\right)$$

T is average monthly temperature (°C).

Evapotranspiration (ET) values were calculated (Pike, 1964) for each of these 25 locations as:

$$ET(mm/month) = \frac{R}{[1 + (\frac{R}{PET})^2]^{1/2}}$$

where

R = average precipitation (mm/month)

PET = potential evapotranspiration (mm/month)

Potential recharge (PR) was then calculated as:

$$PR\ (mm/month) = R - ET$$

The monthly PR values were aggregated according to the previously described seasons. These values were then used to form 2-D daily PR grids of the study area by kriging in Surfer, where

$$daily\ PR\ (mm/day) = \frac{R_s}{d_s}$$

where

R_s = cumulative mean monthly rainfall for that season (in mm)

d_s = number of days in that season

The daily PR grid files were then imported into GV to form the different zones of recharge in the top layer of each model.

3.4.8 Groundwater abstraction: In the study area, generally four types of pumping wells are used for abstraction of groundwater. Similar to the description of BGS/DPHE (2001) for Bangladesh, they are:

- Low yielding hand-pump tubewells (HTW): These are generally screened at a shallow depth (generally 10 to 50 m depending on their location). They are privately owned or are installed by the PHED and are mostly used for drinking and domestic purposes in villages and towns. They are pumped discontinuously throughout the day and because of their very low yield, they are thought to have minimal stress on groundwater.
- Public-water-supply deep tubewells (PDTW): They are generally owned by PHED or town municipalities. They are operated by electric motorized pumps and have high abstraction rates (50-100 m^3/h). Generally they are used for 6 hours each day. The pumped water is piped to communities for domestic use. Due to their limited numbers and restricted hours of operation, they were not considered in this modeling exercise, except in and around Calcutta, where the main abstraction takes place by a dense network of PDTWs as shown in Table 3.3a.

- Irrigation shallow tubewells (STW): These privately owned tubewells use relatively small diesel-motorized 4.5 h.p. centrifugal or submersible pumps to abstract groundwater from relatively shallow depths (30-75 m). They are generally fitted with 75-mm diameter galvanized iron pipes and have an average yield of 26 m^3/hr (CGWB, 1994e). Because in many instances they are installed privately, their hours and rates of operation are not exactly known, although MID (2001) provided an estimated number of wells for each district (Murshidabad: 66,664, Nadia: 94,789, North 24 Parganas: 63,202, and South 24 Parganas: 9,452). They should have a widespread effect on groundwater flow, at least at shallow depths. However, due to the attached uncertainty, they were not included in the model design, with the understanding that this makes the model incomplete. Thus these provide a possibility of future refinement of the model.
- Irrigation deep tubewells (DTW): These wells are owned by the Government of West Bengal Irrigation Department. Groundwater is withdrawn by 18-20 h.p. electric motors coupled with turbine or submersible pumps, which can yield up to 200 m^3/hr. They are generally 60 to 180 m in depth (average 130 m) with 355- or 305-mm diameter steel pipe for about the upper 30 m and then 216-mm diameter pipe for the rest (CGWB, 1994e). They are one of the main sources of irrigation water in the study area and were included in the model design as pumping nodes. The number of DTWs currently present in the modeled area as shown in Table 3.3a was complied from MID (2001). Their hours of operation vary widely for cultivation seasons, but some generalized estimates of hours of operation and rate (Table 3.3a) were obtained for each district (M.K. Sinha, SWID, Government of West Bengal, personal communication, 2004). These values were used to determine the pumpage for each grid cell following the equation:

$$Q = \left(\frac{N \times r \times t}{A}\right) \times a$$

where

Q = the assigned total pumpage (outflow) value to each grid cell for a specified time [L^3]

A = area of each district within the model boundary [L^2]

N = number of pumps

r = pumpage rate [L^3/T]

t = hours of operation per day [T]

a = area of each grid cell.

The exact depths at which the wells are operating were not available. Hence, the pumping nodes were assigned to model layers closest in depth to the PDTWs (data available from the lithologs) in the area. As it was also not possible to ascertain the lengths of the screened intervals for these pumps, the whole thicknesses of the layers (i.e. 15 m) were used.

Three sets of models were developed:

i) with pumping: pre-monsoon (PREM-p), monsoon (M-p), post-monsoon (POSTM-p), based on numbers of DTWs and PDTWs in 2001;
ii) without pumping: pre-monsoon (PREM), monsoon (M) and post-monsoon (POSTM), assuming no DTWs or PDTWs (pre-1970s conditions);
iii) projected pumping: average population growth of West Bengal for 1991-2001 was 18.15%; rates by district are tabulated in Table 3.3b (Census, 2001). Assuming the same rate of population growth in the next two decades, projected number of pumps and pumping rates for 2011 (2011-p) and 2021 (2021-p) for each district were calculated according to the following equation:

$$N = \eta \times P$$

where

N = projected number of pumps
η = number of pumps per capita in 2001
P = projected population in the year of interest.

Based on these estimated data, two pre-monsoon models (assuming same pumping rates, hours of operation and tapped depths as at present) were simulated.

3.4.9 Calibration and sensitivity analyses: Ideally, the models should have been calibrated for all three seasons for steady-state simulations without any pumping. However, because water-level data were only available for the study area for the pre-monsoon in presence of pumping, the PREM-p model was calibrated at steady state against known head values from 26 locations.

These water-level values for April and May were obtained from various sources (our field measurements, CGWB [1994d, e], and SWID [1998]). Sensitivity analyses were performed on this calibrated model (PREM-p) by sequentially varying the K_{x-y} of sand and clay, S and n values. Model response due to sensitivity analyses are listed in Table 3.4. The model was found to be most sensitive to the K_x values of sand and clay. Using the selected values from the analyses, the final model was recalibrated and found to have good agreement with present water-level contours as shown in Table 3.5. The differences between the observed and computed values were probably a cumulative manifestation of a specified head boundary in the vicinity, discrepancy in topographic elevations, exclusion of STWs, and uncertain aquifer parameters. The finalized values obtained from the sensitivity analyses were then used for defining the aquifer properties of the other seven models (PREM, M, POSTM, M-p, POSTM-p, 2011-p, and 2021-p).

3.5 Simplifications and limitations

As discussed earlier, the complexities of the western Bengal aquifers are so great that it is very difficult to construct a groundwater model that reflects local-scale variations of aquifer properties. Hence, based on the similarity to other data from the study area or previous studies, several generalizations and assumptions were involved in order to construct the model. As a consequence there are several limitations. Thus the modeling exercises for this study should be considered as a guideline or template on which future workers may modify and elaborate, although our results reasonably resemble current conditions. The simplifications are listed below.

i) Values for potential recharge at each cell are based on the interpolated values from the 25 monitoring stations. Calculation of PET was based on the temperature values that were available for Calcutta only. Moreover, as mentioned earlier, there may be differences between the potential recharge and absolute recharge. Hence the amount of water that is actually percolating into the system is not well constrained.

ii) In order to make the numerical flow model executable within the present constraints of time and computational resources, a 15-m vertical resolution was used. This leads to a broad generalization for the hydrostratigraphic layers, so smaller-scale variations in the lithology may be over- or under-emphasized.

iii) Precise aquifer property (K_{x-y-z} and S) values for each locality were not obtained. Hence generalized aquifer property values for the different hydrogeologic units were used

throughout the model and the ranges of observed values obtained from the literature were used for sensitivity analyses.

iv) Most of the specified head values were estimated based on previous literature, field experience, local information and topography, except the stream widths, which were known for each reach.

v) The smaller water bodies (such as small streams, ponds, and lakes), which are present throughout the modeled area, were not built into the model because they were thought to have insignificant effects on the regional flow.

vi) No comprehensive data were found for the DTW pumps (location, rate of pumping, hours of operation or screen depth and length). Hence a number of generalizations were undertaken as explained earlier.

vii) The STWs, which would probably have significant control on the groundwater flow, were not included in the model because of insufficiency of data.

3.6 Results and discussion

Figures 3.1a and 3.1b shows the final simulation results of the eight models as contour maps of groundwater levels in the area. The effects of seasonality due to variable PR rates are distinctly visible in all the models.

The models without pumping (PREM, M and POSTM) suggest that there is a topographically controlled, natural regional flow from the northern boundary of the study area toward the south-southeast. The rivers in the system are in general effluent. The PREM contours indicate lateral flows in the vicinity of the Ganges in the north and northwest and along the Bhagirathi-Hoogly north of Calcutta. Flows also converge in the vicinity of the Jalangi, whereas contours meet the Bhairab and upper part of the Ichamati at high angles. PREM also indicates the development of a few groundwater mounds above the land surface, illustrating aquifer saturation in those localities, with radially outward flow for excess water. Two such prominent localities can be noted near the western part of North 24 Parganas (near Bashirhat) and northern Murshidabad (near Jangipur). These locations match with present-day waterlogged areas (CGWB, 1994e) (Figure 3.2). The reason for this waterlogging is a conjunctive effect of the presence of a shallow aquitard, thickening of clay layers (Figure 2.5) and very flat topography.

The possible result is flow stagnation and groundwater accumulation in these areas. Near the active delta front, contours become more broadly spaced, which is consistent with tidal fluctuations, although the models did not include those. The groundwater flow in M is not conspicuously visible on the map. Because of the large amount of water available for recharge during monsoonal rainfall, aquifer saturation and excess water ponding take place leading to recurrent wide floods and increased runoff to the streams. These are in agreement with Harvey et al. (2005), who observed in Munshiganj (Bangladesh) that groundwater flow ceases as stream stages rise and hydraulic head becomes uniform in flooded areas. BGS/DPHE (2001) reported up to 56.9% of the total area of Bangladesh flooded annually between 1954 and 1988 (based on Miah [1988] and Brammer [1990a, b]). Although no such historical data were available for the study area, a devastating flood in September 2000 affected 18.3 million people (with demise of 1187 people) in 6177 villages of nine districts of West Bengal, including Calcutta (http://www.bapscare.org/services/disaster/2000/2000floods.htm). In Jumpukur (Table 2.1, location 46), Nadia, floodwater marks of 2000 were observed during fieldwork at 1.98 m above land surface (Figure 3.3). Of the 65 blocks within the study area, 75% have flood hazard potential of medium to very high (Sanyal and Lu, 2003). The POSTM model demonstrates north-to-south flow with perpendicular to semi-perpendicular intersection of contour lines with the boundary rivers.

The “with pumping” models (PREM-p, POSTM-p, 2011-p and 2021-p) indicate that in all of the districts, except the southern half of South 24 Parganas, the natural flow paths have been thoroughly disrupted by the formation of cones of depression due to pumping. In vertical sections, local-scale convective flow cells are found to have developed corresponding to these depressions. In southern South 24 Parganas, flow reversal has developed along with increased inflow from the constant-head boundary of the Bay of Bengal. This phenomenon can be easily explained by the large salt-water intrusion that has been documented in these areas (CGWB, 1994d, e; SWID, 1998, Allison et al., 2003). PREM-p demonstrates the effects of abstraction all over the study area, with prominent pumping centers in the blocks of Murshidabad-Jiaganj, Behrampur, Hariharpara and Domkal in central Murshidabad; Kaliganj and Nakashipara in northern Nadia; Shantipur, KrishnaNagar-I and Ranaghat-I in south-central Nadia; Chakdah, Haringhat, Habra-II and Amdanga in southern Nadia; and northern North 24 Parganas and

Calcutta. Of these, the depression around Calcutta (CGWB, 1994e; Sikdar et al., 2001) is most acute due to the huge amount of pumping for municipal water supply through PDTWs. The groundwater mounds near Jangipur and Bashirhat, though still observable, have become substantially reduced in size and extent. In the 2011-p and 2021-p models, the cones have become more pronounced. In 2021-p some dry cells corresponding to deep cones of depression have formed in central Murshidabad, northern North 24 Parganas, and south-southeast Calcutta. These dry cells imply severe overdraft. In the POSTM-p model, in addition to the effects of the PREM-p models, a huge cone of depression has developed in north and central North 24 Parganas with centers at Calcutta, Rajarhat, Barasat-I and II, and Deganga. However, in reality, the cone of depression may not be so large because of the availability of monsoonal water in storage that has not been accounted for in the model design. The effect of pumping is not at all conspicuous in the monsoon model (M-p), indicating that the saturated aquifers are not stressed in spite of pumping.

Table 3.6 and Figure 3.4 show the groundwater mass (inflow-outflow) balance of these models. The mass balance error ranges between 0.02% (PREM-p) and -0.06% (POSTM-p). It indicates that at present the submarine groundwater discharge (SGD) through the delta front of South 24 Parganas seems to have decreased by 6% annually since the onset of pumping, while the annual salt-water intrusion has increased by 98%. The inflow of river water into the system has increased by 92% in the last three decades, but the rivers are still effluent mostly because of the monsoonal groundwater discharge. The model demonstrates that the rivers have changed from slightly effluent to influent for the post-monsoon season. This estimation is probably not viable because of the monsoonal water in storage, as mentioned above.

Dowling et al. (2003) estimated annual SGD as about $1.5 \pm 0.5 \times 10^{11}$ m^3 of water for the entire delta front (500 km wide). Considering that the delta front in the present study area is 110 km, the present estimates for SGD of 5.37×10^6 m^3 are negligible. The probable reason for the difference is that Dowling et al. (2003) considered that all the recharge water reaching below 30 m (first 2 layers of the model) is discharged to the Bay of Bengal. However, the present model shows that a considerable amount of water upwells from the aquifer deeper than 30 m to the rivers. The estimation of abstracted water (only by DTWs and PDTWs) from the modeled area is

about 8×10^8 m^3 annually. On the basis of estimation of resident groundwater (4.52×10^{11} m^3) from the lithologic model, it seems that the total volume of groundwater resource is as yet underutilized. Dowling et al. (2003) suggested an average actual recharge rate of 0.6 m/year. Using that estimation, the total annual recharge in the study area (recharge rate × rechargeable surface area) would be about 9×10^9 m^3, which shows that the groundwater abstraction by DTW and PDTW is only about 9%. This value is similar to Dowling et al.'s estimate of 12 ± 4%. However, the composite cone of depression around Calcutta (as visible in PREM-p and POSTM-p) is perennial and formed by overdraft pumping, which has superseded any recharge in that area. The cause may be exponential metropolitan growth (which is directly proportional to increases in groundwater demand for drinking and industrial use) and the lack of recharge due to impervious urban cover and the near-surface shallow aquitard (Figure 2.4a). The aquifers near Calcutta have not completely dried up probably because of the recharge that takes place in the north (near northern North 24 Parganas and southern Nadia) and subsurface inflow from the Bhagirathi-Hoogly.

Figure 3.5 illustrates the layer-by-layer mass balance calculation for the PREM-p model. The bulk of the groundwater flow in the system takes place between layers 2 and 6 (approximately 15 m to 105 m bgl). This indicates that the local flow systems predominate, which agrees with the conclusion of Harvey et al. (2005) regarding flow in Bangladesh. Although lesser in extent, the medium to regional-scale flow to a depth of about 200 m (layer no. 13) is not insignificant. Below that depth, to the base of the model, there is minimal recharge and groundwater has relatively long residence times. These results indicate that the Golden Bengal aquifer is continuously being recharged and there is substantial flow even in the deeper part of the aquifer, apart from the isolated aquifers mentioned above.

In conclusion, natural groundwater flow in the study area is dependent on the amount and timing of precipitation, and is controlled by the relatively flat topography and locations of major streams, but has been heavily distorted by pumping. This finding is in agreement with the results of 3-D regional modeling in western Bangladesh (JICA, 2002).

Table 3.1: Distribution of rainfall and calculated potential recharge (PR) data from Global Historic Climatology Network (GHCN v. 2 [GHCN, 2005]) stations in and around the study area.

	Data coverage		Pre-monsoon (Jan.-May)		Monsoon (Jun.-Oct.)		Post-monsoon (Nov.-Dec.)	
Location	From	To	Rain (mm/d)	PR (mm/d)	Rain (mm/d)	PR (mm/d)	Rain (mm/d)	PR (mm/d)
Behrampore	1901	1970	1.40	0.14	7.57	3.30	0.31	0.00
Arambagh	1901	1968	1.51	0.13	7.24	3.10	0.39	0.00
Bongaon	1901	1967	2.09	0.31	8.34	3.96	0.35	0.00
KrishnaNagar	1901	1970	1.77	0.21	7.55	3.26	0.38	0.00
Ranaghat	1901	1967	1.73	0.20	6.80	2.73	0.28	0.00
Kalyanganj	1906	1954	1.31	0.12	6.98	2.86	0.30	0.00
Haringhata	1908	1966	1.35	0.10	6.43	2.41	0.30	0.00
Calcutta	1829	2005	1.67	0.19	8.92	4.42	0.47	0.01
BudgeBudge	1901	1970	1.64	0.16	9.27	4.74	0.39	0.00
DumDum	1947	1980	1.47	0.14	8.58	4.13	0.43	0.01
Barrackpore	1901	1965	1.52	0.14	8.01	3.74	0.49	0.01
Barasat	1901	1959	1.62	0.16	8.11	3.75	0.39	0.00
Bashirhat	1901	1970	1.67	0.20	8.54	4.16	0.47	0.01
Diamond Harbour	1901	1967	1.46	0.13	8.93	4.49	0.37	0.00
Gosaba	1921	1956	1.39	0.15	9.41	4.86	0.64	0.02
Sagar Island	1975	1984	1.46	0.11	9.23	4.78	0.31	0.00
Potkabari	1901	1956	1.68	0.24	6.88	2.78	0.39	0.01
Hoogly	1901	1962	1.83	0.22	7.52	3.30	0.40	0.00
Kalna	1901	1963	1.61	0.16	6.78	2.73	0.33	0.00
Howrah	1901	1948	1.59	0.15	8.32	3.95	0.35	0.00
Serampore	1901	1962	1.73	0.20	8.24	3.88	0.39	0.00
Azimganj	1901	1961	1.41	0.14	7.26	3.09	0.25	0.00

Table 3.1 (continued)

Location	From	To	Rain (mm/d)	PR (mm/d)	Rain (mm/d)	PR (mm/d)	Rain (mm/d)	PR (mm/d)
Boinchee	1932	1962	1.63	0.17	7.92	3.63	0.42	0.01
Katwa	1901	1966	1.44	0.13	7.37	3.17	0.32	0.00
Ulubeia	1901	1968	1.83	0.22	8.90	4.47	0.38	0.00

Table 3.2: Monthly temperature (1811 to 2005) and precipitation (1829 to 2005) data for Calcutta along with calculated evapotranspiration (ET) and potential recharge from GHCN v.2 (GHCN, 2005).

Month	Temperature (^{o}C)			Precipitation (mm/month)			ET (mm/month)	PR (mm/month)
	Mean	Max	Min	Mean	Max	Min		
January	19.68	22.70	15.00	11.53	73.70	0.00	11.45	0.08
February	22.65	25.40	18.80	24.25	202.20	0.00	23.70	0.54
March	27.52	30.20	23.60	32.61	159.30	0.00	31.87	0.74
April	30.34	33.10	26.80	52.59	196.20	0.00	50.43	2.17
May	30.80	33.20	28.40	130.64	434.60	2.00	106.19	24.45
June	30.01	32.20	27.70	292.36	946.00	40.60	149.71	142.66
July	29.10	30.80	27.20	333.55	879.00	109.00	148.14	185.41
August	28.98	31.00	27.70	337.26	683.50	122.40	147.69	189.57
September	29.01	30.60	27.70	264.65	944.70	56.10	139.73	124.92
October	27.87	31.20	26.50	136.23	474.00	0.00	102.02	34.21
November	24.00	27.10	21.80	22.37	238.50	0.00	22.01	0.36
December	20.14	23.40	17.80	6.47	146.00	0.00	6.46	0.01

Table 3.3a: Seasonal details of irrigation pumps (DTWs) for each district and PDTWs for Calcutta within the study area.

District	Pump details		Pre-monsoon		Monsoon		Post-monsoon	
	Number	Rate(m^3/hr)[a]	Operation hours(/d)	Pumping ($m^3/m^2/d$)	Operation hours(/d)	Pumping ($m^3/m^2/d$)	Operation hours(/d)	Pumping ($m^3/m^2/d$)
Murshidabad	445	150	18	3.98E-04	8	1.77E-04	10	2.21E-04
Nadia	757	150	18	5.60E-04	8	2.49E-04	10	3.11E-04
North 24 Parganas	324	100	18	1.48E-04	8	6.58E-05	10	8.23E-05
South 24 Parganas	29	75	18	3.88E-06	8	1.72E-06	10	2.16E-06
Calcutta	500[b]	100	6	1.41E-03	6	1.41E-03	6	1.41E-03

Table 3.3b: Projected details of irrigation pumps (DTWs) for each district and PDTWs for Calcutta within the study area.

District	Population	Pre-monsoon 2011		Pre-monsoon 2021	
	Growth rate (1991-2001)	No. of pumps[c]	Pumping ($m^3/m^2/d$)	No. of pumps[c]	Pumping ($m^3/m^2/d$)
Murshidabad	23.76	551	4.92E-04	682	6.09E-04
Nadia	19.54	905	6.70E-04	1082	8.01E-04
North 24 Parganas	22.69	398	1.82E-04	488	2.23E-04
South 24 Parganas	20.85	35	4.69E-06	42	5.67E-06
Calcutta	3.93	520	1.46E-03	540	1.52E-03

[a] M.K. Sinha, State Water Investigation Directorate, Government of West Bengal, personal communication, 2004
[b] number of PDTWs estimated from The Statesman, Calcutta, 6 June 2004, local section, page 6
[c] calculated based on Census (2001)

Table 3.4: Results of sensitivity analyses on PREM-p for uncertain aquifer parameter values.

Sand (K_x) m/d	RSS	Comment
25	78.9	formation of large dry cells
37.5	34.4	used model parameter value
50	21.9	formation of small dry cells in Nd and NP
70	21.7	formation of large dry cells all over the study area
Sand (K_y) m/d		
25	34.4	used model parameter value
37.5	31.2	formation of dry cells near CCU and SP
15	39.5	formation of dry cells near CCU and Md
Clay (K_{x-y}) m/d		
0.1	34.4	used model parameter value
0.5	47.7	not much effect, long time to converge
1	49.1	not much effect, long time to converge
0.01	42.2	distorted contours and flow toward River Ganges
S		
0.03	34.4	used model parameter value
0.015	34.4	no effect
0.06	34.4	no effect
0.3	34.4	no effect
n		
0.2	34.4	used model parameter value
0.1	34.4	no effect
0.4	34.4	no effect

bold: initial values, italicized: used values, RSS = residual sum of squares
Md: Murshidabad, Nd: Nadia, NP: North 24 Parganas, SP: South 24 Parganas, CCU: Calcutta

Table 3.5: Results of model calibration with the best-fitted parameter values from Table 3.4.

Calibration locations	Latitude	Longitude	Layer	Observed (hydraulic head in m above MSL)	Computed (hydraulic head in m above MSL)	Residual
Raghunathganj	24.5	88.08	4	22	21.32	0.68
Lalgola	24.42	88.25	4	20.7	20.40	0.30
Bhagawangola	24.34	88.32	4	19.9	18.38	1.52
Raninagar-II	24.25	88.6	4	16.5	15.27	1.23
Jiaganj	24.23	88.27	4	17.2	18.55	-1.35
Lalbagh	24.18	88.27	4	18.6	17.52	1.08
Raninagar-I	24.15	88.47	4	14.5	11.75	2.75
Behrampur	24.09	88.26	4	17.5	16.34	1.16
Nawda	23.91	88.46	4	14.3	14.09	0.21
Potkabari	23.86	88.52	6	13.5	13.36	0.14
Debagram	23.69	88.33	6	11.3	11.05	0.25
Chapra	23.61	88.56	6	11.9	11.03	0.87
Nakashipara	23.6	88.35	6	12.4	10.98	1.42
Banguin	23.33	88.66	6	8.2	8.24	-0.04
Bongaon	23.05	88.83	7	7.1	6.75	0.35
Amdanga	22.77	88.53	10	4.5	3.64	0.86
Baduria	22.76	88.79	7	7.8	7.19	0.61
DumDum	22.73	88.38	9	3	1.77	1.23
Haroa	22.61	88.68	12	4	6.50	-2.50
East Calcutta	22.56	88.42	9	0	-0.18	0.18
Rajpur-Sonarpur	22.45	88.43	12	5	4.19	0.81
Baruipur	22.4	88.48	12	5	3.43	1.57
Jalerhat	22.3	88.56	12	3.5	2.74	0.76
Sonakhali	22.3	88.74	12	2.8	3.04	-0.24
Kulpi	22.16	88.29	12	2.2	1.38	0.82
Dakhin Durgapur	22.06	88.39	12	2.2	0.89	1.31

residual mean: 0.61
residual standard deviation: 0.97
sum of squares: 34.35
absolute residual mean: 0.93
minimum residual: -2.50
maximum residual: 2.75

Table 3.6: Comparison of annual modeled submarine groundwater discharge (SGD), inflow and pumping volumes between 2001 and pre-1970s.

Attribute	PREM-p	M-p	POSTM-p	Annual (Present)	PREM	M	POSTM	Annual (pre-1970s)	% change with respect to pre-1970s
Annual SGD outflow to Bay of Bengal	1.37E+06	3.41E+06	5.82E+05	5.37E+06	1.61E+06	3.49E+06	6.22E+05	5.72E+06	-6.11
Annual inflow from Bay of Bengal	1.28E+04	1.04E+02	5.57E+03	1.85E+04	0.00E+00	0.00E+00	3.53E+02	3.53E+02	98.09
Annual outflow to rivers	3.89E+08	1.29E+10	3.96E+06	1.33E+10	7.30E+08	1.31E+10	2.04E+07	1.39E+10	-4.21
Annual inflow from river	1.18E+08	3.37E+05	1.09E+08	2.28E+08	1.64E+06	3.33E+05	1.62E+07	1.82E+07	92.03
Annual pumping	4.58E+08	2.27E+08	1.10E+08	7.95E+08	0.00E+00	0.00E+00	0.00E+00	0.00E+00	100.00

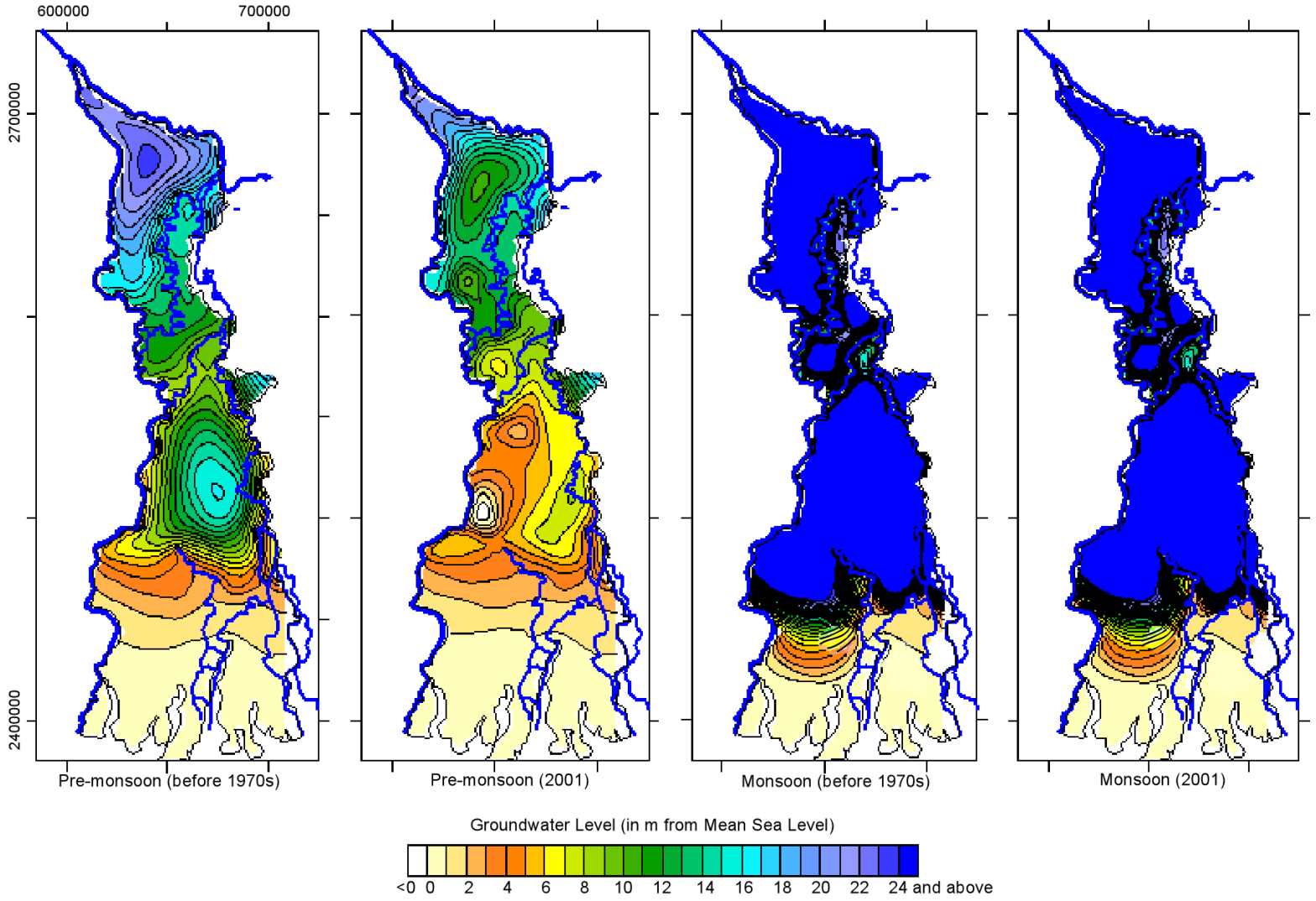

Figure 3.1a: Modeled groundwater level maps obtained from PREM, PREM-p, M, and M-p. The bold blue lines indicated the major rivers in the area. The black areas indicate closely spaced decreasing contour lines.

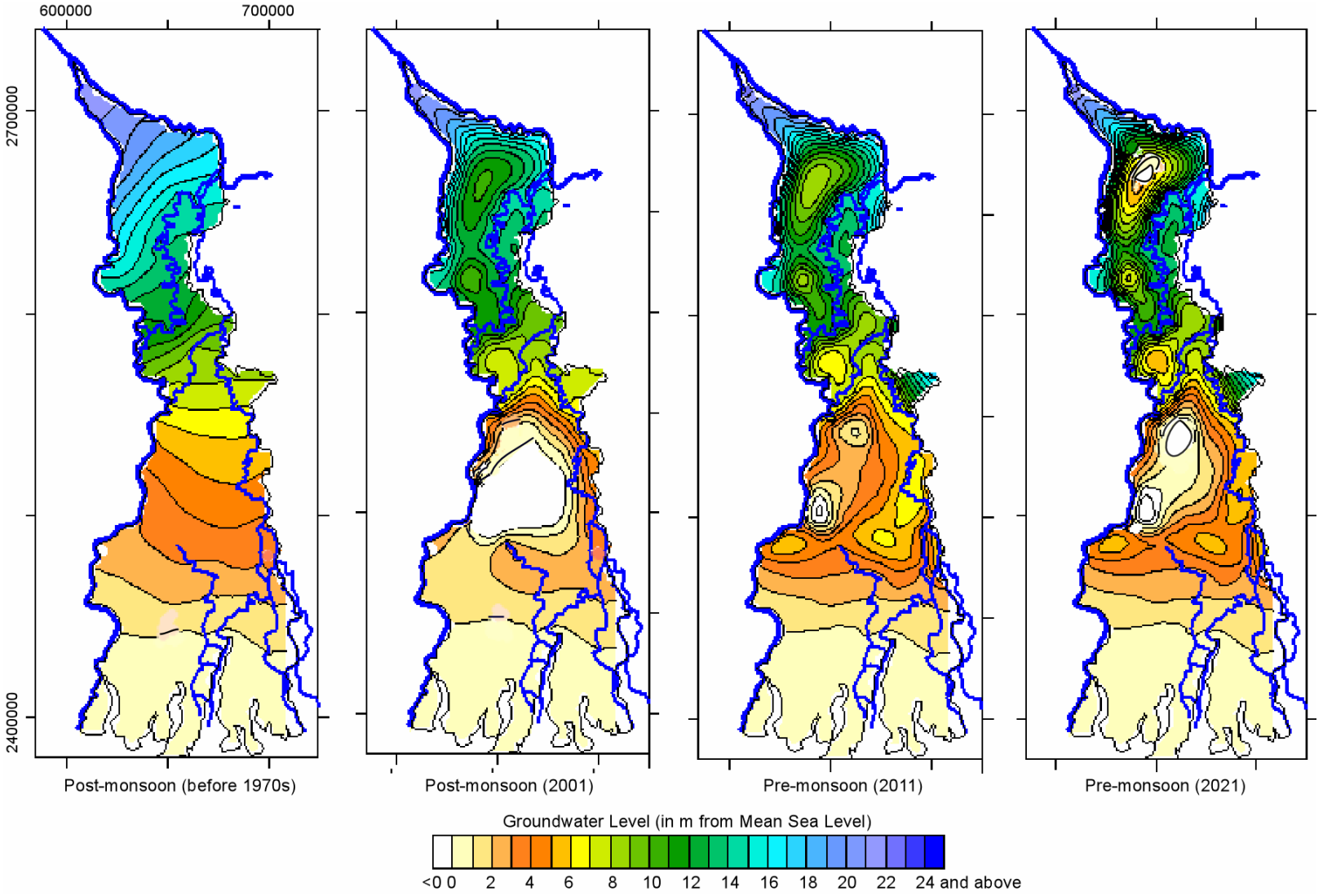

Figure 3.1b: Modeled groundwater level maps obtained from POSTM, POSTM-p, 2011-p, and 2021-p. The bold blue lines indicated the major rivers in the area. The black areas indicate closely spaced decreasing contours lines.

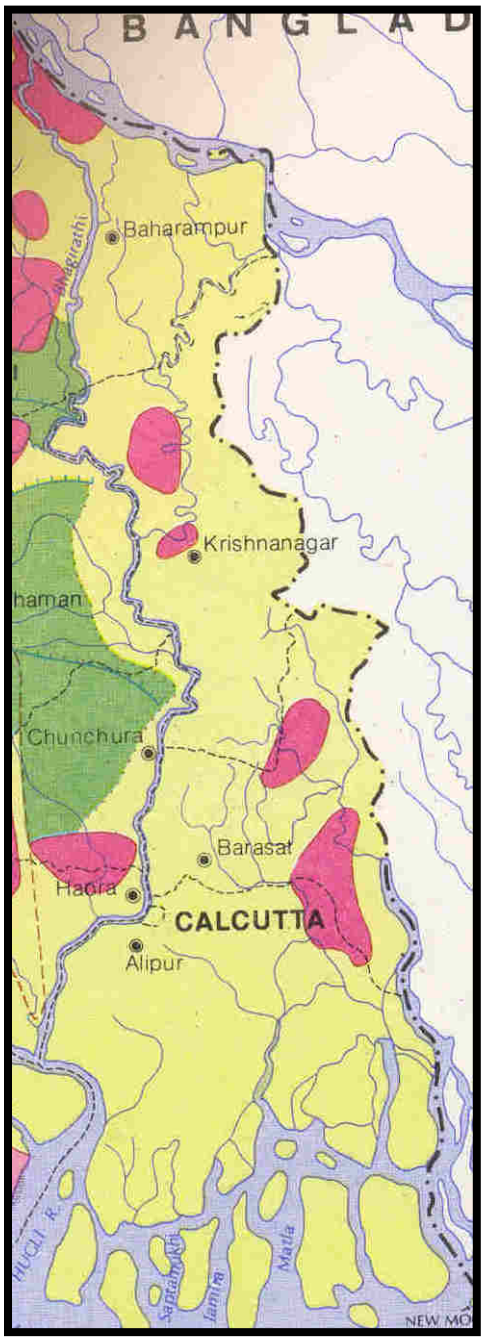

Figure 3.2: Map of water logged areas (marked red) within the study area of western Bengal basin (CGWB, 1994e).

Figure 3.3: Collection of images of monsoon flooding in the study area during 2001-2006 (Source: local newspapers [a-d] and field photo [e]).

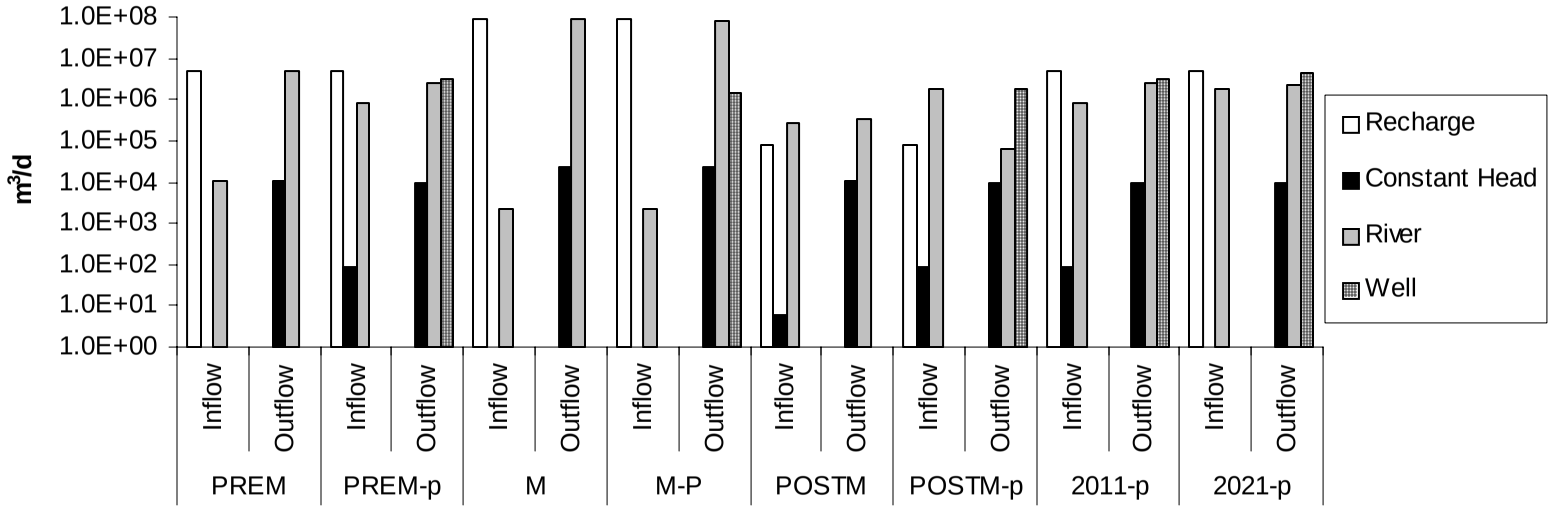

Figure 3.4: Plot of mass balance of the eight flow models shown in Figures 3.1 and 3.2.

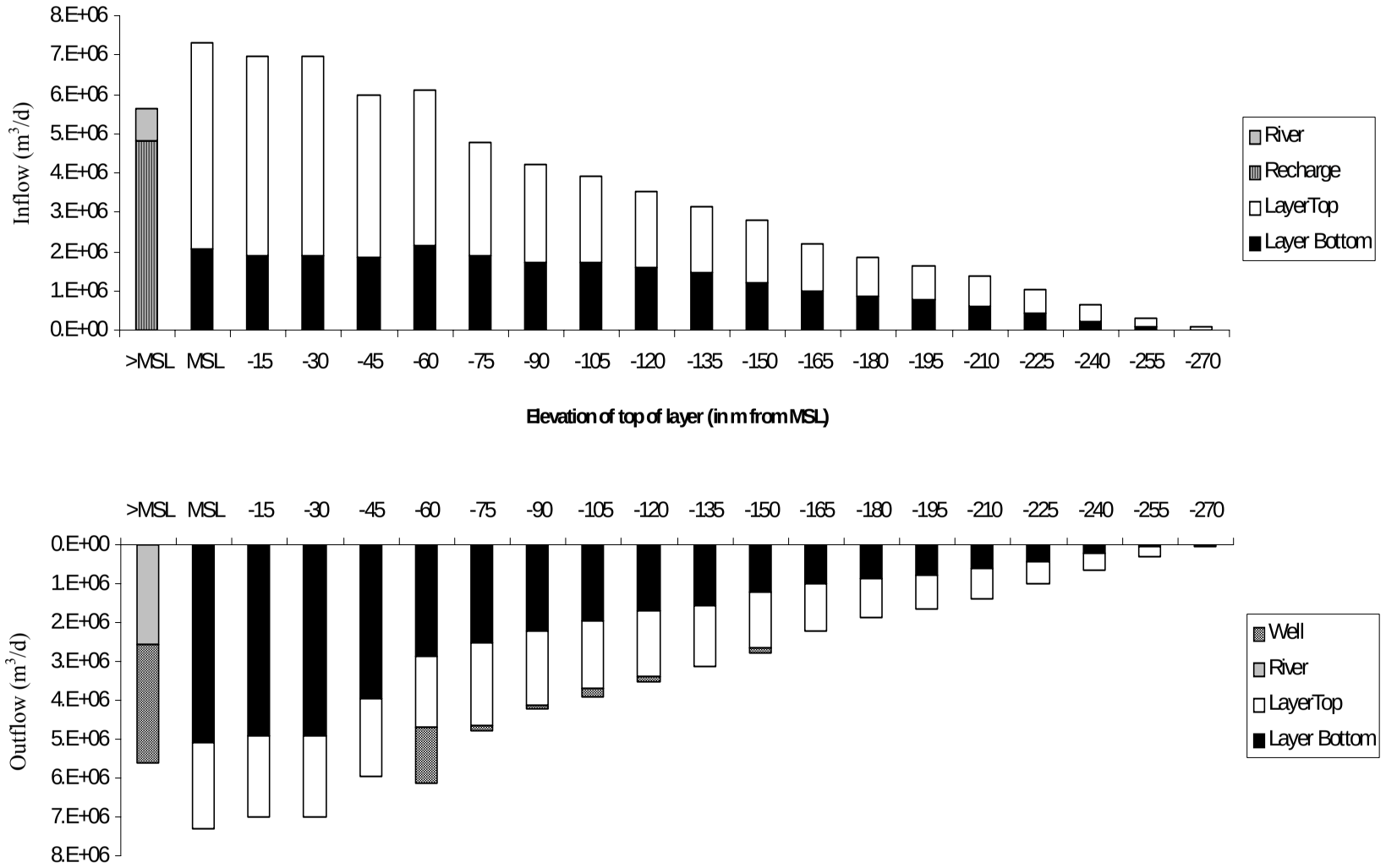

Figure 3.5: Plot of mass balance for each layer for PREM-p (pre-monsoon with pumping [2001]).

Chapter 4: Regional-scale stable isotopic ($\delta^{18}O$-$\delta^{2}H$) signature of recharge and deeper groundwater

4.1 Introduction and background

During the last two decades, several international institutions and organizations have studied the hydrogeochemistry and groundwater dynamics of the Bengal basin by using a variety of hydrogeologic techniques. Previous studies (e.g. Aggarwal et al., 2000; Basu et al., 2002; Stüben et al., 2003; Harvey et al., 2005; Klump et al., 2006) have applied stable isotopic techniques to understand hydrogeochemical processes in the region. This chapter documents and discusses stable isotopic results of the deeper groundwater of the western Bengal basin. The study area is about ~ 22,000 km^2, including the previously described area (eastern Murshidabad, Nadia, North 24 Parganas and northern and central South 24 Parganas) along with the southernmost part of Maldah, (Figure 4.1). The area lies ~ 200 km south of the eastern (Darjeeling) Himalayas. No previous basinal-scale isotopic study has been done in West Bengal. The objective is to delineate the source and recharge of deeper groundwater in Gangetic West Bengal by identifying regional trends in the ^{18}O and ^{2}H compositions of groundwater, surface water and rainwater.

4.1.1 Previous stable isotopic studies of Bengal basin groundwater: Published studies on $\delta^{18}O$ and $\delta^{2}H$ distributions in the Bengal basin have been limited. The earliest work relevant to the present study was done by Dray (1983), who demonstrated that significant isotopic differences exist between groundwater and the River Ganges in Bangladesh, indicating a lack of rapid interaction between the two.

Krishnamurthy and Bhattacharya (1991) collected 55 shallow groundwater samples (<10 m below ground) along a ~1400 km transect between Calcutta and Delhi. Of these, only three of the samples were collected from or near the present study area. The samples from Calcutta and North 24 Parganas had $\delta^{18}O$ values of ~ -4.3 and ~ -4‰ (VSMOW) respectively (values estimated from figure), while a sample about 20 km west of Calcutta was found to have $\delta^{18}O$ of ~ -4.5‰. The authors showed that as the Indian southwestern monsoon wind moves from the Bay of Bengal west-northwest toward central India (Ananthakrishnan, 1977; Rao, 1981), there is

a clear continental effect (Dansgaard, 1964), so that the $\delta^{18}O$ of groundwater becomes more depleted.

Ramesh and Sarin (1992) documented that the Ganges headwaters, which originate at >3500 m in northern India, are isotopically highly depleted ($\delta^{18}O$: -7.8‰ to -14.4‰ and $\delta^{2}H$: -51‰ to -103‰), defining a slope that is similar to the global meteoric water line (GMWL). The Ganges mainstream was found to be enriched downstream by evaporation.

Shivanna et al. (1999) reported stable isotopic results for water samples collected from various depths in selected areas of Murshidabad and South 24 Parganas districts of West Bengal. They inferred that the aquifers in Murshidabad are connected, while there is limited connectivity between deeper and shallower groundwater in South 24 Parganas. They also showed that isotopic compositions of both the shallow groundwater and rivers are seasonally dependent, with maximum depletion occurring in December (Murshidabad groundwater $\delta^{18}O$: -3.00‰ to -8.00‰; River Bhagirathi: -8.50‰; River Bhairavi: -5.50‰) and maximum enrichment in May (-3.00‰ to -7.50‰; -6.78‰; and -3.53‰, respectively), probably because of enrichment by enhanced evaporation. Furthermore, they suggested that the depleted stable isotope values of some shallow groundwater compared to local precipitation in Murshidabad is an artifact of interaction with the depleted Ganges water, while most of the other localities have recharge from precipitation.

Aggarwal et al. (2000) provided a detailed and systematic basin-scale study of Bangladesh, in which they attempted to delineate As-contaminated and uncontaminated aquifers and discussed the mechanisms of As mobilization based on stable isotopic signatures. They also evaluated the effect of geomorphic and sea level changes on atmospheric isotope composition and hence recharge. They grouped waters based on isotopic composition and depth and assigned them to different climatic regimes. They concluded that the older, deeper groundwaters are generally uncontaminated.

Stüben et al. (2003) concluded that the shallow groundwater of their study area (in the vicinity of Behrampur, Murshidabad district) is of meteoric origin, whereas more depleted River

Bhagirathi water ($\delta^{18}O$: -7.91‰ to -8.01‰) indicates a contribution of snowmelt water from the Himalayas and precipitation further up in the Ganges valley.

Harvey et al. (2005) and Klump et al. (2006) concluded from their study site in Bangladesh (Munshiganj) that there is a difference in $\delta^{18}O$ values between groundwaters above and below ~ 30 m from ground surface, suggesting mixing of chemically and isotopically distinct groundwater bodies at that depth. Values of $\delta^{18}O$ are relatively depleted (< -3‰) above ~ 30 m depth, become abruptly enriched (~ -1‰) at ~ 30 m depth, and then decrease slightly downward to a depth of ~ 100 m.

Zheng et al. (2005a) studied the annual variation in stable isotopic compositions of rainwater, surface water and shallow groundwater at Araihazar, Bangladesh. They concluded that the composition of precipitation falls on the GMWL and that the surface water bodies are significantly evaporated, resulting in a $\delta^{18}O$ enrichment of up to 10‰ in the dry season. The groundwater suggests recharge both from direct precipitation and from moderately evaporated surface water during the wet season and at the beginning of the dry season. The authors did not find evidence of recharge from strongly evaporated irrigational water in paddy fields. Figure 4.2 combines results from some of the previous stable isotopic studies in the Bengal basin.

Literature on the isotopic composition of precipitation in the study area is scarce. The nearest monitoring points of the International Atomic Energy Agency and World Meteorological Organization (Global Network of Isotopes in Precipitation) are located in New Delhi, Allahabad, Shillong and Yangon (Myanmar). The average $\delta^{18}O$ compositions for rainfall in these locations are: New Delhi (dry season [ds]: -1.53‰; monsoon [m]: -5.85‰), Yangon (ds: -3.92‰; m: -4.54‰), Allahabad (annual mean [am]: -7.36‰) and Shillong (am: -3.67‰) (Araguas-Aruguas et al., 1998). Considering these values, Aggarwal et al. (2000) suggested the isotopic composition of recharge in their Bangladesh study area to be ~ -4.5‰ for $\delta^{18}O$ and ~ -30‰ for $\delta^{2}H$. They also suggested an average $\delta^{18}O$ value of -4.5‰ for rains in Calcutta based on shallow groundwater results from Krishnamurthy and Bhattacharya (1991).

4.1.2 Climate: Due to its proximity to the Bay of Bengal and its low latitude position (the Tropic of Cancer passes through the study area), Gangetic West Bengal experiences a warm and humid climate with distinct dry and wet seasons. These may be termed as pre-monsoon (January to May), monsoon (June to October) and post-monsoon (November-December). The bulk of the precipitation takes place as a result of moisture-laden monsoon winds from the Bay of Bengal. Local convectional storms contribute to some pre-monsoonal rainfall. On average (based on Global Historic Climatology Network [GHCN] version 2 data from 1901 to 1970 [GHCN, 2005]), pre-monsoon rainfall contributes 16.23% of the annual rainfall, monsoon 82.21% and post-monsoon 1.57%. It is hypothesized that most of the groundwater in the study area is recharged from monsoonal precipitation. Aggarwal et al. (2000) concluded from their study in Bangladesh that the stable isotopic signature of deeper water (at depths of 100-150 m and ~ 300 m) is different from that of the shallower aquifers, suggesting that recharge of the deeper water took place following rainfall 3 to 30 ka ago.

Monthly precipitation results from 35 monitoring stations in and around the study area have been acquired. Figure 4.3 shows the contour plots of the annual rainfall in these stations (computed from GHCN version 2 data) along with average daily summer temperature to illustrate the present climatic regime of Gangetic West Bengal.

4.1.3 Hydrostratigraphic framework: The hydrostratigraphic characterization of the study area (up to a depth of 300 m below mean sea level [MSL], and excluding the part of the study area in Maldah) has resulted in the delineation of several types of aquifers (Figure 4.4) (Chapter 2). The first is a continuous, semiconfined sand aquifer (termed hereafter as the main aquifer) underlain by a thick clay aquitard. The names “Sonar Bangla aquifer” for this main aquifer and “Murshidabad aquitard” for the basal clay aquitard have been proposed in Chapter 2. The main aquifer deepens from a maximum of ~ 50-80 m below land surface in the north to ~ 180 to >200 m in the south. In the southern half of the study area, discontinuous clay layers locally divide the near-surface aquifer to form several deeper, confined aquifers. Several smaller, isolated aquifers at greater depths than the main aquifers (~200-300 m) contain groundwater with considerably different solute compositions (Chapter 5). Finally, some deep parts of the main aquifer are not isolated but appear to demonstrate restricted conditions (intermediate between the main and

isolated aquifers). The hydrostratigraphic positions of the two sampled wells that are screened below 300 m and of the four sampled wells in Maldah are not known.

4.2 Methods

4.2.1 Sampling: Sixty-four groundwater, seven river-water and fourteen rain-water samples were collected from Gangetic West Bengal during the months of May to August of 2003–2005 (Figure 4.1, Table 4.1). The latitude and longitude of each of the sampling points were recorded in the field using a handheld Global Positioning System (datum WGS84).

A number of deep, community water supply wells with single intake zones (single strainers) were selected. These wells (except the ones in Calcutta) are owned and operated by the Public Health Engineering Directorate (PHED), Government of West Bengal. Detailed information about the well completion and tapped aquifer was obtained from the PHED database and a local drilling agency (B.M. Engineering, KrishnaNagar). Similar information was not available for the four wells in the district of Maldah, but they were ascertained to have single strainers (personal communication with PHED officers). Groundwater is withdrawn from all of these wells by 15-20 h.p. electric motors powering turbine or submersible pumps with general yields of 50 to 100 m^3/hr, which can go up to 200 m^3/hr. They are typically operated for 6 hours (2–3 hours at a time) each day. The wells are generally screened at depths of 50 to 409 m, with the overall trend of increasing well depth toward the south and east of the study area.

During 2004 and 2005, groundwater samples were collected according to standard sampling protocols (Wood, 1981). The wells were purged for 40 to 75 minutes until the E_H, pH, temperature (T) and electrical conductivity (EC) of the out-flowing water were stable, thereby indicating that the sampled water was representative of the aquifer. Each sample was then collected by pumping water through a disposable 0.45-μm plastic capsule filter. River water samples were collected using a hand-filtration unit with the same kind of filter. All of the samples for $\delta^{18}O$ and $\delta^{2}H$ were collected in 40-mL amber glass vials with solid caps. Care was taken to exclude air bubbles. During 2003, the samples were not filtered and were collected after ~20-30 minutes of purging. The field parameters (E_H, pH, T and EC) were also not measured for these samples**.** One-liter HDPE bottles were used to collect rainwater samples for $\delta^{18}O$ and $\delta^{2}H$.

As much as possible, each rain sample was collected during an entire storm to capture an average composition. Later, some of these waters were sub-sampled and transferred to 10-mL glass vials with solid caps.

4.2.2 Laboratory methods: Isotope analyses of 2003 and 2004 samples were performed at the University of Kentucky Environmental Research and Training Laboratory (UK ERTL) on a ThermoFinnigan Delta Plus XP isotope ratio mass spectrometer (IRMS) using a Gas Bench II peripheral unit equipped with a GC-autosampler. The analyses were standardized against the international references Vienna-Standard Mean Ocean Water (VSMOW), Greenland Ice Sheet Project (GISP), and Standard Light Antarctic Precipitation (SLAP), as well as internal standards, with three standard gas injections followed by seven sample gas measurements. Precision was determined with duplicate and triplicate samples. For $\delta^{18}O$ analyses, 0.5 mL of each standard and sample were transferred into individual exetainers and then flushed for one minute with 0.5% CO_2 in He at 40 mL/min. They were then left to equilibrate at room temperature on a Gas Bench II for 48 hours before being analyzed. For $\delta^{2}H$, 0.5 mL of each standard and sample were transferred into individual exetainers containing platinum rods and flushed for three minutes with 2% H_2 in He at 90 mL/min. The samples were then left to equilibrate in a hot block in the gas bench for 16 hours at 22^{o} C before analysis. Precision was ± 0.1‰ for $\delta^{18}O$ and ± 1.0‰ for $\delta^{2}H$.

Analyses of 2005 isotope samples were performed at the University of Arizona Isotope Geochemistry Laboratory on a gas-source IRMS (Finnigan Delta S) standardized with VSMOW, SLAP, and internal standards. The $\delta^{18}O$ samples were equilibrated with CO_2 at ~15^{o}C in an automated equilibration device coupled to the IRMS. For $\delta^{2}H$, samples were reacted with Cr at 750^{o}C using a Finnigan H device coupled to the spectrometer. Precision was ± 0.08‰ for $\delta^{18}O$ and ± 0.9‰ for $\delta^{2}H$.

4.2.3 Data grouping and statistical clustering: The stable isotopic compositions of the sample locations with known well-completion details were grouped hydrostratigraphically into main (containing all the locations that were thought to be pumping water from the main aquifer) and isolated (consisting of the wells drawing water from the isolated aquifers and from depths >300

m). The rationale for grouping >300-m and isolated aquifer samples together is that a clay aquitard underlies the study area south of Maldah at a depth of ~300 m (Chapter 2).

For all the wells, $\delta^{18}O$ and $\delta^{2}H$ values were evaluated by hierarchical cluster analysis (HCA) to investigate statistical relationships between hydrochemical and spatial parameters (Drever, 1997). Statistical associations do not necessarily demonstrate a causal relationship but do represent data in a condensed version for better visualization. Cluster analysis was used to determine if the samples could be grouped into distinct hydrochemical populations (Güler et al., 2002). The HCA was done on the original data set (without any weighting or standardization) following Davis (1986), Güler et al. (2002), and Dreher (2003). The clustering was done by importing the $r \times c$ data matrix (r samples with c variables) into the statistical software package SPSS version 14 (SPSS Inc., Chicago, IL). For best grouping, the dendogram was constructed by Ward's method of linkage (Ward, 1963) with squared Euclidean distance (Güler et al., 2002). Ward's method uses an analysis of variance (ANOVA) approach to evaluate the distances between clusters. See Table 4.1 for the cluster number corresponding to each location.

4.3 Results

4.3.1 Rainwater: Because of the small number of samples (n = 14), rainwater samples were not used for statistical analyses or calculating mean weighted annual composition, but were used to generate a local meteoric water line (LMWL) for Gangetic West Bengal. As noted in Table 4.1, 11 of the 14 samples were collected during 2004; the remaining three were collected in 2005. The samples represent May to August; 10 samples were from the monsoon season and four from the pre-monsoon. In 2004, the monsoon season in West Bengal began on 12 June (news release from Regional Meteorological Office, Alipur, Calcutta; Anandabazar Patrika, Calcutta, 12 June 2004, page 1). Calcutta received 156 mm of rainfall (9.39% of total 1661 mm for 2004) during the pre-monsoon (January to May) and 1505 mm (90.61%) during the monsoon (June to October) (Figure 4.5). No rainfall occurred in November and December. Thus assuming that the rest of the study area had similar pattern and proportion of precipitation (as evident from the seasonal means stated in section 4.1.2), it can be assumed that our rainfall dataset fairly represents the isotopic composition of the precipitation available for groundwater recharge in Gangetic West Bengal.

The LMWL plotted from our data in Figure 4.6 compares well to the global meteoric water line (GMWL) (Craig, 1961). The LMWL with a relation of

$$\delta^2H = 7.24\ \delta^{18}O + 7.73\ (r^2 = 0.93)$$

is quite similar to the line developed by Bhattacharya et al. (1985) for a limited number of precipitation samples from New Delhi, Ahmedabad and Shillong:

$$\delta^2H = (7.2 \pm 0.1)\ \delta^{18}O + (5.1 \pm 0.1).$$

Krishnamurthy and Bhattacharya (1991) suggested a δ^2H-$\delta^{18}O$ slope of ~7.2 for average Indian monsoonal precipitation. Our data agree well with this suggestion. Figure 4.6 also distinguishes between the monsoon and pre-monsoon rains. Except for samples rain-water R1 and R8, the monsoon samples have $\delta^{18}O$ values (-4.74‰ to -9.34‰) that are more isotopically depleted than those of the pre-monsoon rains (1.45‰ to 0.32‰). This suggests that the pre-monsoon rains may originate from isotopically enriched local moisture sources (such as evaporated surface water bodies), whereas the monsoon rain clouds have traveled a greater distance and had multiple fractionations before precipitation. An explanation for the higher $\delta^{18}O$ and δ^2H values of samples R1 and R8 is that they represent moisture sources that are relatively close to the sampling locations. The six samples for Calcutta plotted against month (June to August) do not demonstrate any seasonal trend (Figure 4.5).

4.3.2 River water: All of the river water samples plot below the LMWL (Figure 4.7), suggesting evaporation. The Bhagirathi-Hoogly samples (river sample numbers 1, 2 and 3), with $\delta^{18}O$ values of -5.57‰ to -5.74‰, are more depleted than the Jalangi and Ichamati samples, with $\delta^{18}O$ of -3.15‰ to -0.37‰. The Bhagirathi-Hoogly values are more enriched than other reported values for that river (Shivanna et al., 1999; Stüben et al., 2003). No data from other studies appear to exist for the Jalangi and Ichamati. One of the Ichamati samples (river water location [RW] # 7 [see Table 4.1 for location details]) was significantly more enriched than the other samples from this group and represents the composition of the tidally influenced southern rivers.

4.3.3 Groundwater: Figure 4.7 differentiates the isotopic composition of samples between the main and the isolated aquifers. With the exception of one sample (groundwater location # 64 [see Table 4.1 for location details]), the $\delta^{18}O$ values of the samples range from -3.12‰ to -6.12‰. Of the 64 samples, 40 have $\delta^{18}O$ values more depleted than the mean (-4.80‰) of all samples. Five

of six isolated aquifer samples and 19 of the 54 main aquifer samples were more enriched than the mean, which indicates that the isolated groundwaters are relatively isotopically heavier than the main aquifer samples. Kalinagar (#64) ($\delta^{18}O$ of -0.48‰) is located in the southernmost part of the study area (near the delta front [Sunderbans]) and is suspected of being influenced by seawater intrusion from the Bay of Bengal or brackish water intrusion from one of the numerous tidal channels in the vicinity

.

Statistical grouping of the data by HCA suggests three distinct groups (Table 4.1, Figure 4.7). Most samples fall in *group 1* (n = 49), while 7 samples fall in *group 2* and 8 fall in *group 3*. All of the groups contain samples from both main and isolated aquifers.

4.4 Factors influencing $\delta^{18}O$ and $\delta^{2}H$ composition of recharge and groundwater:

In general, the isotopic composition of groundwater is similar to the mean weighted annual precipitation composition, although variations may result depending on types of soils and vegetation, unsaturated flow through heterogeneous porous media, evapotranspiration, seasonal variations, long-term climatic variations, and residence time in the recharge zone (Clark and Fritz, 1997). For the study area, the effect of evaporation before or during infiltration, seawater influence toward the south, and seasonal variability may be important. As noted earlier, Bengal basin recharge is dominated by monsoonal precipitation, although in certain areas and years there might be a significant contribution from the pre-monsoonal rainfall. The effect of seasonal variation would be most dominant in the shallow groundwaters. Clark and Fritz (1997) noted that in a system lacking preferential flow, the seasonal effects generally disappear below a critical depth. Hence, considering the depth from which groundwater samples were collected for this study, the isotopic composition of the groundwater should be similar to the weighted annual mean composition of precipitation after accounting for evaporation. However, it should be noted that because all the groundwater and river water samples were collected at the same time of the year, no study of seasonal trends was undertaken.

4.4.1 Precipitation: Most of the groundwater samples plot slightly below the LMWL (Figure 4.7). A linear fit relation of all groundwater samples

$$\delta^{2}H = 5.8\ \delta^{18}O - 2.96\ (n = 64,\ r^{2} = 0.82)$$

has a lower slope than both the LMWL and GMWL, indicating that the isotopic composition of the study area is influenced by some additional factors (e.g. evaporation, sea water intrusion) besides precipitation. This relationship is similar to the one determined by Krishnamurthy and Bhattacharya (1991) for shallow groundwater for their study area from Calcutta to Delhi:

$$\delta^2H = 6.4\ \delta^{18}O - 1.0\ (n = 55,\ r^2 = 0.95),$$

but somewhat different from Bhattacharya et al. (1985):

$$\delta^2H = (6.8 \pm 0.1)\ \delta^{18}O + (2.2 \pm 0.4)$$

for groundwater samples from several other stations in addition to those of Krishnamurthy and Bhattacharya (1991). Our relationship is also different from that of Aggarwal et al. (2000) for Bangladesh (reconstructed from reported values for both <100 and >100 m samples):

$$\delta^2H = 6.9\ \delta^{18}O + 1.0\ (n = 53,\ r^2 = 0.91)$$

However, when only the main aquifer samples are considered (excluding the tidal/sea-water influenced #64), the relationship

$$\delta^2H = 6.7\ \delta^{18}O + 1.44\ (n = 53,\ r^2 = 0.84)$$

is very similar to those of Bhattacharya et al. (1985) and Aggarwal et al. (2000). The groundwater $\delta^{18}O$ range (except for #64) is within the range of monsoon precipitation composition during 2004-2005. This indicates that groundwater of the study area is probably recharged primarily from precipitation with similar isotopic composition to the present. The slight deviation of the samples from the LMWL suggests that some evaporation of rainfall occurs prior to or during infiltration, or there might be some mixing of the infiltrating water with preexisting soil moisture that has undergone several cycles of evaporation and wetting (Allison, 1982). Harvey et al. (2005) concluded that the recharge in their study area in Bangladesh is very complex: in addition to direct infiltration from precipitation, recharge may also take place from the bottom of ponds, ox-bow lakes, rivers, and re-infiltration of groundwater withdrawn for irrigation. Such a scenario is probably also true for our study area.

4.4.2 Distance from sea (continental effect): Comparison of the $\delta^{18}O$ and δ^2H compositions of groundwater with distance from the Bay of Bengal (monsoonal moisture source) (Figure 4.8) shows a prominent continental effect. Because of the north-south orientation of the study area, latitude was used as a proxy for distance from the sea. The $\delta^{18}O$ value decreased from about -3.2‰ (excluding #64) from near the southernmost part of the study area to about -6‰ in the

northernmost part (r^2 = 0.31 and P = 0.01). This pattern is consistent with recharge from the southwest monsoon, which moves from the Bay of Bengal toward the north with a Rayleigh-type distillation, where the air moisture becomes progressively depleted with successive phases of precipitation (Dansgaard, 1964). Krishnamurthy and Bhattacharya (1991) and Bhattacharya et al. (2003) documented similar subcontinent-scale depletion from the southwest monsoon. Krishnamurthy and Bhattacharya (1991) also concluded that the continental effect from Calcutta to Delhi cannot be solely explained by Rayleigh distillation, but must also account for re-entry of enriched vapor into the air from evapotranspiration (with an efficiency of ~40%). The inland gradient of $\delta^{18}O$ depletion for our samples (~ -0.84‰ per 100 km) is much higher than the reported gradients of -2‰ per 1,000 km by Krishnamurthy and Bhattacharya (1991) for Calcutta to Delhi and -6‰ per 1,000 km by Bhattacharya et al. (1985) for Ahmedabad (western India) to Delhi. A decrease in the inland gradient can be caused by significant recycling of water vapor within the basin by evapotranspiration, as noted by Salati et al. (1979) for the Amazon basin and by Krishnamurthy and Bhattacharya (1991). However, estimation for Calcutta (see Chapter 3) indicates up to 50% evapotranspiration occurs during the summer, suggesting sufficient vapor mass recycling. Therefore, the cause of the high gradient in our study area is unresolved. It should also be noted that the calculations and conclusions by Krishnamurthy and Bhattacharya (1991) were based on the assumption of insignificant isotopic variation normal to the west-northwest movement of the monsoon (i.e. along the long axis of our study area). In our study, plotting the $\delta^{18}O$ values with longitude, a prominent trend of depletion (from ~ -3‰ to ~ -6‰) parallel to the westward component of the southwest monsoon (similar to the observation of Krishnamurthy and Bhattacharya [1991]) can also be seen. Thus the isotopic composition of monsoon precipitation in Gangetic West Bengal appears to show a continental effect both northward and westward. This hypothesis could have been confirmed more robustly with a more detailed precipitation data set across the study area, but except for Behrampur (n = 3) and Calcutta (n = 6), our sample set lacks multiple samples from individual locations. The measured $\delta^{18}O$ ranges for monsoon rainfall in Behrampur (-6.72‰ to -9.34‰) and Calcutta (-0.46‰ to -8.15‰) fail to show any trend (Figure 4.9).

4.4.3 River water: In order to understand the influences of the individual major streams within the study area on the isotopic composition of recharge, the groundwater samples are grouped by

proximity to the rivers and plotted against distance from the sea (latitude). These sample sets are (a) River Ganges-Bhagirathi-Hoogly (n = 32), (b) River Jalangi (n = 14), and (c) River Ichamati (n = 11). Some of the samples co-exist in both the Ganges and Jalangi groups. Distinct spatial trends are observed between these three groups, which might indicate some causal relationship.

(a) River Ganges-Bhagirathi-Hoogly (Figure 4.10a): The composition of the river water samples from the Bhagirathi-Hoogly is almost the same over a distance of about 300 km, indicating a minimal latitudinal effect on the river water composition. The river water is generally more depleted than the groundwater, perhaps because of the highly depleted snow melt from the Himalayas (source of the Ganges) (Ramesh and Sarin, 1992; Stüben et al., 2003). The groundwater isotope values trend more positive toward the south, in contrast to the river water. In the northern to central portion of the study area (up to central Nadia), the river water and groundwater values are similar, indicating the possibility of recharge from the inflow of the river. Some of the samples deviating from the Ganges-Bhagirathi-Hoogly river water can also be grouped with the River Jalangi, indicating the possibility of influence from both the rivers. The maximum deviation from the linear trend in this area is Jumpukur (#24), which is suspected to have restricted recharge because of hydrostratigraphic heterogeneity. In the south, the groundwater-river water dissimilarity increases. The two most dissimilar groundwater samples, from Ghasiara (#34) and Canning (#36), are thought to have influences of restricted recharge (due to depth) and sea-water intrusion, respectively. The value from Calcutta (#4) is very similar to river water of Belur (RW #3), suggesting that recharge of groundwater in Calcutta is influenced by the Bhagirathi-Hoogly. This also agrees with the prediction of a groundwater model developed for the area (see Chapter 3) that high urban pumpage of groundwater attracts inflow of water from the river.

(b) Jalangi (Figure 4.10b): The river is highly meandering (in contrast to the Ganges-Bhagirathi-Hoogly and the Ichamati) and covers relatively little latitudinal distance. The two isotopic values of the river water are similar to each other, but they are far more enriched than groundwater in this group. The enrichment can be attributed to high evaporation from the relatively narrow stream channel and surface runoff influences. The groundwater locations in this group do not show any spatial trend. The greatest deviation from the linear trend was shown by the isolated aquifer sample from Iswarchandrapur (#45) and restricted main aquifer in Bhaluka (#49). Thus the Jalangi may not have much influence on groundwater recharge.

(c) Ichamati (Figure 4.10c): Both the groundwater and the river water become highly enriched toward the south. The trends of groundwater and river water are sub-parallel to each other. The isotopic values of the river water are enriched than the groundwater. While the reason for enrichment of the Ichamati at Bongaon (RW #6) is probably evaporation and surface runoff influence, at Taki (RW #7), where the stream channel is very wide, the enrichment is consistent with tidal inflow from the Bay of Bengal. The maximum deviation of groundwater from the linear trend is demonstrated by Kalinagar (#64) near the delta front, reflecting seawater intrusion.

4.4.4 Spatial distribution and depth: It is evident from the discussion so far that the isotopic composition of Gangetic West Bengal groundwater shows a prominent spatial pattern. A plot of the statistical groups on a map of the study area helps to better visualize this pattern (Figure 4.11). The reason for this pattern, while not definitive, can be a composite or cumulative influence of precipitation, latitudinal effect, temperature, river inflow, seawater intrusion, hydrostratigraphy and (or) depth. Many of these points have already been individually discussed. Figure 4.11 shows that most of the areas except south-central North 24 Parganas and eastern South 24 Parganas are represented by HCA group 1, succeeded southeastward by groups 2 and 3. Of the two outliers in the north, the one in Murshidabad is represented by the isolated aquifer at Chaighari (#17). The outlier in Nadia has two points: group 3 is represented by the restricted main aquifer at Jumpukur (#24), and group 2 represents Debagram (#20). The reasons for these outliers are not certain.

The influences of depth and seawater intrusion for the observed pattern require evaluation. A $\delta^{18}O$-depth plot (Figure 4.12) illustrates that no apparent relation exists, and the distributions of the statistical groups are not dependent on the absolute depth. However, most of the isolated aquifer samples have been assigned in the higher order HCA groups, suggesting some hydrostratigraphic control. A lack of correlation between $\delta^{18}O$ and Cl^- concentration (see Chapter 5) negates the idea that the southward existence of the higher-order groups reflects a seawater influence from the Bay of Bengal.

4.5 Implications for groundwater recharge

The isotopic compositions of deep groundwater (both in the main aquifer and isolated aquifers) are similar to modern-day precipitation values from the study area. This observation indicates that the deeper parts of the aquifers of Gangetic West Bengal have been recharged by rainfall under a climatic regime similar to the present, with a moisture source in the south (Bay of Bengal) and progressive depletion of monsoonal rainfall as it moves toward the north. Aggarwal et al. (2000) concluded that the samples with $\delta^{18}O$ values heavier than -3‰ or lighter than -6‰ probably indicate recharge from older rainwater from a different climatic regime, although this water plots on the present day meteoric water line. In our study area, only a few samples had $\delta^{18}O$ values close to older water range of Aggarwal et al. (2000). The samples with $\delta^{18}O$ values close to or < -6‰ are from Sujapur (#7), Islampur (#3), Nabipur (#2), Habaspur (#37) and Kamagachi (#54). All of these samples (except Sujapur, which is undefined) are from the main aquifer. Four of the six isolated aquifers (Chaighari [#17], Chikanpara [#29], Bansjhari Mullickpur [#31], and Murarisha [#63]) and a few main aquifer samples (Berachampa [#27], Dalapara [#30], and Kalinagar [#64]) have $\delta^{18}O$ values close to -3‰, which do not vary systematically with depth. It can be noted that the northernmost wells #2, #3, #7, and #37 (as mentioned above) are more depleted and the southwestern wells #27, #30, and #64 are less depleted, probably as a result of the continental effect as described in section 4.4.2. Hence simply being enriched or depleted relative to a critical value may not solely indicate climatic differences, and several other factors need to be carefully evaluated. It is possible that because of hydrostratigraphic heterogeneities, the deeper samples of Aggarwal et al. (2000) are older than ours, but in the absence of radioisotope data for our samples, we were not able to evaluate this possibility.

Based on similarities in isotope data from 1979 and 1999 from Bangladesh, Basu et al. (2002) concluded that extensive irrigational pumping has not disturbed regional groundwater flow in the Bengal basin. The authors inferred that such pumping would have resulted in mixing of groundwater from various depths, assuming that isotopic composition with depth would reflect a difference between 1979 (pre-pumping era) and 1999 (present pumping conditions). Our data show no significant difference in isotopic composition between the shallower water (Shivanna et al., 1999; Stüben et al., 2003) and the deeper water of the main aquifer system.

Moreover, no direct relation was observed between depth and isotopic composition for our groundwater samples from the main aquifer. There are several possible reasons for this homogeneous distribution, including similarities in hydrostratigraphy, climate and land use within the study area.

Flow-model simulations of the study area (see Chapter 3) indicate that pumping could have caused vertical mixing of groundwater in the main aquifer, thus homogenizing the chemical and isotopic compositions locally. Therefore, the lack of a significant vertical trend in isotopic compositions with depth in the study area could in part be an artifact of pumping. However, the persistence of a lateral isotopic trend consistent with depletion of rainfall with distance from the Bay of Bengal and similarity in isotopic compositions between water from the isolated aquifers and the main aquifer indicate that pumping has not completely homogenized groundwater. Hence, there should not be a notable difference between regional-scale isotope distributions in 1979 (before extensive pumping) and 1999 as suggested by Basu et al. (2002). Therefore conclusions regarding groundwater mixing cannot be solely based on isotopic signatures.

4.6 Conclusion

Stable oxygen and hydrogen isotopic compositions of rainwater samples collected during this study show that the monsoonal precipitation is generally more isotopically depleted than the pre-monsoon rainfall in Gangetic West Bengal, India. The isotopic composition of deeper water from the main aquifer of the study area suggests recharge under current climatic conditions with the prevailing southwest monsoon originating from the Bay of Bengal in the south and moving to the north (toward the eastern Himalayas) and west-northwest (toward north-central India), indicating a continental effect caused by precipitation with a Rayleigh-type distillation. Effects of evaporation are observable in the recharged water. The depletion gradient determined in the present study is more than any previous values documented from India. Depletion or enrichment with depth, as proposed by some previous workers, was not observed. Comparison with previous studies suggests that the isotopic compositions of the deeper and shallower parts of the main aquifer are similar, and inferences about groundwater mixing from various depths cannot be drawn based exclusively upon stable isotopic data at the regional scale. Moreover, the lack of prominent differences between the isolated and main aquifer samples

makes it impossible to distinguish between the climatic regimes during which they were recharged. The sample from the active delta front indicates seawater or brackish water intrusion, while those from locations near the north-central part of the study area and from Calcutta indicate recharge influenced by the River Ganges-Bhagirathi-Hoogly. The snow-fed Ganges-Bhagirathi-Hoogly river samples are distinctly more depleted than those of the other major rivers of the area (Jalangi and Ichamati), which are affected by evaporation, surface runoff and tidal influences.

Table 4.1: Stable isotopic sample locations for groundwater, river water and rainwater from Gangetic West Bengal.

Loc. No.	Collection Date	Location	Administrative Block/Town	District[1]	Latitude	Longitude	Depth[2]	Aquifer[3]	$\delta^{18}O$ (‰)	$\delta^{2}H$ (‰)	HCA Cluster[4]
1	17/5/03	Banipur	Habra town	NP	22.82	88.69	150	M	-4.54	-23.92	2
2	27/5/03	Nabipur	RaniNagar-II	MD	24.25	88.60	243	M	-6.00	-36.48	1
3	27/5/03	Islampur	RaniNagar-I	MD	24.15	88.47	88	M	-5.87	-36.65	1
4	18/6/03	Kalighat	Calcutta	SP	22.52	88.34	120	M	-5.55	-35.56	1
5	3/7/03	Dattapara	Shantipur town	ND	23.25	88.43	128	M	-5.23	-34.56	1
6	16/5/03	Berachampa (Deulia)	Deganga	NP	22.70	88.68		M	-5.01	-30.70	1
7	23/5/03	Sujapur (Bakharpur)	Kaliachak-I	MA	24.92	88.09		U	-6.12	-38.13	1
8	23/5/03	Baishnabnagar (Dariapur)	Kaliachak-III	MA	24.82	87.99		U	-5.73	-34.45	1
9	23/5/03	Mothabari	Kaliachak-II	MA	24.94	88.06		U	-5.84	-36.64	1
10	23/5/03	Sahapur	Old Maldah town	MA	25.01	88.15		U	-5.63	-33.38	1
11	24/5/03	Aurangabad	Suti-II	MD	24.62	88.03		M	-5.56	-33.81	1
12	20/5/04	Lalgola	Lalgola	MD	24.42	88.25	66	M	-5.68	-36.55	1
13	21/5/04	Lalbag Morgue	Murshidabad town	MD	24.23	88.27	32	M	-4.60	-29.61	1
14	21/5/04	Kantanagar	Bhagwangola-I	MD	24.34	88.31	66	M	-5.73	-36.53	1
15	22/5/04	Edrakpur	Nawda	MD	23.91	88.46	82	M	-5.18	-30.73	1
16	22/5/04	Takipur	Beldanga-I	MD	23.87	88.25	55	M	-5.11	-31.27	1
17	23/5/04	Chaighari	Behrampur	MD	24.16	88.41	228	I	-3.97	-24.35	2
18	24/5/04	Sekendra	Raghunathganj-I	MD	24.50	88.08	37	M	-5.22	-36.27	1
19	25/5/04	Behrampur Girls' College	Behrampur town	MD	24.09	88.26	74	M	-5.13	-32.10	1

Table 4.1 (continued)

Loc. No.	Collection Date	Location	Administrative Block/Town	District[1]	Latitude	Longitude	Depth[2]	Aquifer[3]	$\delta^{18}O$ (‰)	$\delta^{2}H$ (‰)	HCA Cluster[4]
20	25/5/04	Debagram	Kaliganj	ND	23.69	88.33	78	M	-4.15	-27.04	2
21	26/5/04	Juranpur	Kaliganj	ND	23.72	88.22	155	M	-5.37	-35.10	1
22	26/5/04	Birpur	Nakashipara	ND	23.63	88.48	185	M	-5.84	-36.80	1
23	27/5/04	Bethuadahari	Nakashipara	ND	23.61	88.43	89	M	-5.62	-33.16	1
24	27/5/04	Jumpukur	Kaliganj	ND	23.72	88.38	269	M	-3.61	-20.51	3
25	28/5/04	Hanspukuria	Tehatta-II	ND	23.74	88.48	230	I	-5.11	-32.50	1
26	29/5/04	Gagnapur	Ranaghat-II	ND	23.14	88.64	176	M	-5.01	-31.54	1
27	1/6/04	Berachampa (Aminpur)	Deganga	NP	22.69	88.67	298	M	-3.35	-19.77	3
28	2/6/04	Janapoll	Habra-I	NP	22.87	88.69	151	M	-3.83	-26.15	2
29	2/6/04	Chikanpara	Gaighata	NP	22.93	88.77	409	>300	-3.65	-21.53	2
30	3/6/04	Dalalpara	Bashirhat town	NP	22.69	88.85	230	M	-3.36	-18.89	3
31	3/6/04	Bansjhari Mullickpur	Bashirhat-I	NP	22.58	88.88	273	I	-3.12	-17.13	3
32	4/6/04	Berachampa	Deganga	NP	22.70	88.68	155	M	-5.18	-32.62	1
33	4/6/04	Eojhnagar	Bashirhat-II	NP	22.71	88.72	151	M	-4.50	-27.77	2
34	5/6/04	Ghasiara	Sonarpur	SP	22.44	88.46	240	M	-3.53	-19.17	3
35	5/6/04	Kalikapore	Sonarpur	SP	22.40	88.48	240	M	-4.79	-29.39	1
36	7/6/04	Canning	Canning-I	SP	22.32	88.65	189	M	-3.56	-18.70	3
37	16/5/05	Habaspur	Bhagawangola-I	MD	24.32	88.34	76	M	-6.07	-40.53	1
38	17/5/05	Chua	Hariharpara	MD	24.03	88.45	84	M	-4.68	-35.63	1
39	17/5/05	Surangapur	Nawda	MD	23.93	88.46	96	M	-5.16	-32.78	1
40	18/5/05	Mahimapur Palace	Murshidabad	MD	24.21	88.26	32	M	-4.95	-31.39	1
41	18/5/05	Kismat-Imadpur	Hariharpara	MD	24.03	88.35	71	M	-4.68	-30.58	1
42	19/5/05	Nazirpur	Tehatta-I	ND	23.86	88.54	110	M	-5.06	-33.60	1
43	19/5/05	Narayanpur	Karimpur-II	ND	23.92	88.55	108	M	-5.14	-33.80	1

Table 4.1 (continued)

Loc. No.	Collection Date	Location	Administrative Block/Town	District[1]	Latitude	Longitude	Depth[2]	Aquifer[3]	$\delta^{18}O$ (‰)	$\delta^{2}H$ (‰)	HCA Cluster[4]
44	20/5/05	Palashipara	Tehatta-II	ND	23.79	88.46	95	M	-5.05	-35.32	1
45	20/5/05	Iswarchandra pur	Tehatta-I	ND	23.76	88.46	217	I	-4.46	-30.22	1
46	21/5/05	Dhubulia	KrishnaNagar-II	ND	23.50	88.45	132	M	-5.41	-35.88	1
47	21/5/05	Sonatala	KrishnaNagar-II	ND	23.52	88.51	140	M	-5.11	-34.42	1
48	22/5/05	Gobrapota	KrishnaNagar-I	ND	23.42	88.55	120	M	-5.17	-30.14	1
49	22/5/05	Bhaluka	KrishnaNagar-I	ND	23.35	88.41	279	M	-4.34	-29.55	1
50	23/5/05	Bhimpur	Krishnanaga-I	ND	23.43	88.62	211	M	-5.36	-36.00	1
51	26/5/05	Newtown	Rajarhat	NP	22.58	88.45	132	M	-5.10	-33.52	1
52	26/5/05	Patharghata	Rajarhat	NP	22.58	88.51	120	M	-4.44	-30.06	1
53	27/5/05	Ghentugachia	Chakdah	ND	23.03	88.59	129	M	-3.57	-29.52	1
54	27/5/05	Kamagachi	Ranaghat-I	ND	23.22	88.56	152	M	-5.83	-42.81	1
55	28/5/05	Panchita	Bongaon	NP	23.11	88.80	193	M	-5.35	-34.10	1
56	28/5/05	Bongaon Hospital	Bongaon town	NP	23.05	88.82	202	M	-4.92	-30.55	1
57	29/5/05	Rampur	Gaighata	NP	22.95	88.75	200	M	-4.91	-31.30	1
58	29/5/05	Kankphul	Habra-II	NP	22.86	88.62	190	M	-3.64	-22.81	2
59	30/5/05	Bamangachi	Barasat-I	NP	22.75	88.51	158	M	-5.00	-32.34	1
60	30/5/05	Humaipur	Barasat-II	NP	22.68	88.47	159	M	-4.49	-29.56	1
61	31/5/05	Haroa	Haroa	NP	22.60	88.68	167	M	-4.88	-32.01	1
62	31/5/05	Arsula	Baduria	NP	22.74	88.77	148	M	-5.08	-33.50	1
63	1/6/05	Murarisha	Hasnabad	NP	22.59	88.84	362	>300	-3.57	-19.72	3
64	1/6/05	Kalinagar	Sandeshkhali-I	NP	22.45	88.87	165	M	-0.48	-14.80	3
Rivers			**River**								
1	28/5/04	Mayapur	Bhagirathi-Hoogly	ND	23.42	88.39			-5.74	-38.75	

Table 4.1 (continued)

Loc. No.	Collection Date	Location	River	District[1]	Latitude	Longitude	Depth[2]	Aquifer[3]	$\delta^{18}O$ (‰)	$\delta^{2}H$ (‰)	HCA Cluster[4]
2	23/5/04	Behrampur town	Bhagirathi-Hoogly	MD	24.09	88.26			-5.67	-39.88	
3	11/6/04	Belur town	Bhagirathi-Hoogly	HW	22.63	88.36			-5.57	-36.36	
4	17/5/05	Amtala	Jalangi	ND	23.93	88.46			-2.95	-29.60	
5	21/5/05	Sonatala	Jalangi	ND	23.52	88.51			-3.15	-24.22	
6	28/5/05	Bongaon town	Ichamati	NP	23.05	88.83			-3.00	-21.32	
7	31/5/05	Taki	Ichamati	NP	22.59	88.94			-0.37	-6.67	
Rains			**Season**								
1	21/5/04	Behrampur town	Pre-monsoon	MD	24.09	88.26			4.39	23.95	
2	25/5/04	Debagram	Pre-monsoon	ND	23.69	88.33			1.45	22.27	
3	6/6/04	Barasat town	Pre-monsoon	NP	22.76	88.59			0.32	14.31	
4	12/6/04	Calcutta	Monsoon	SP	22.52	88.34			-7.34	-48.96	
5	15/6/04	Behrampur town	Monsoon	MD	24.09	88.26			-9.34	-64.54	
6	19/6/04	Calcutta	Monsoon	SP	22.52	88.34			-8.15	-52.23	
7	4/7/04	Behrampur town	Monsoon	MD	24.09	88.26			-6.72	-45.61	
8	12/7/04	Calcutta	Monsoon	SP	22.52	88.34			-0.46	8.34	
9	15/7/04	Shantipur town	Monsoon	ND	23.25	88.43			-6.38	-37.06	
10	14/7/04	Barasat town	Monsoon	NP	22.76	88.59			-4.74	-13.81	
11	2/8/04	Calcutta	Monsoon	SP	22.52	88.34			-5.49	-40.55	
12	19/5/05	Betai	Pre-monsoon	ND	23.75	88.38			1.23	18.83	
13	1/7/05	Calcutta	Monsoon	SP	22.52	88.34			-4.93	-9.41	
14	2/8/05	Calcutta	Monsoon	SP	22.52	88.34			-7.08	-52.54	

[1] District name: MD: Murshidabad, ND: Nadia, NP: North 24 Parganas, SP: South 24 Parganas, HW: Howrah
[2] Depth of bottom of strainer
[3] Aquifer type: M: main, I: isolated, U: undefined, >300: greater than 30
[4] Hierarchical Cluster Analyses (HCA) results

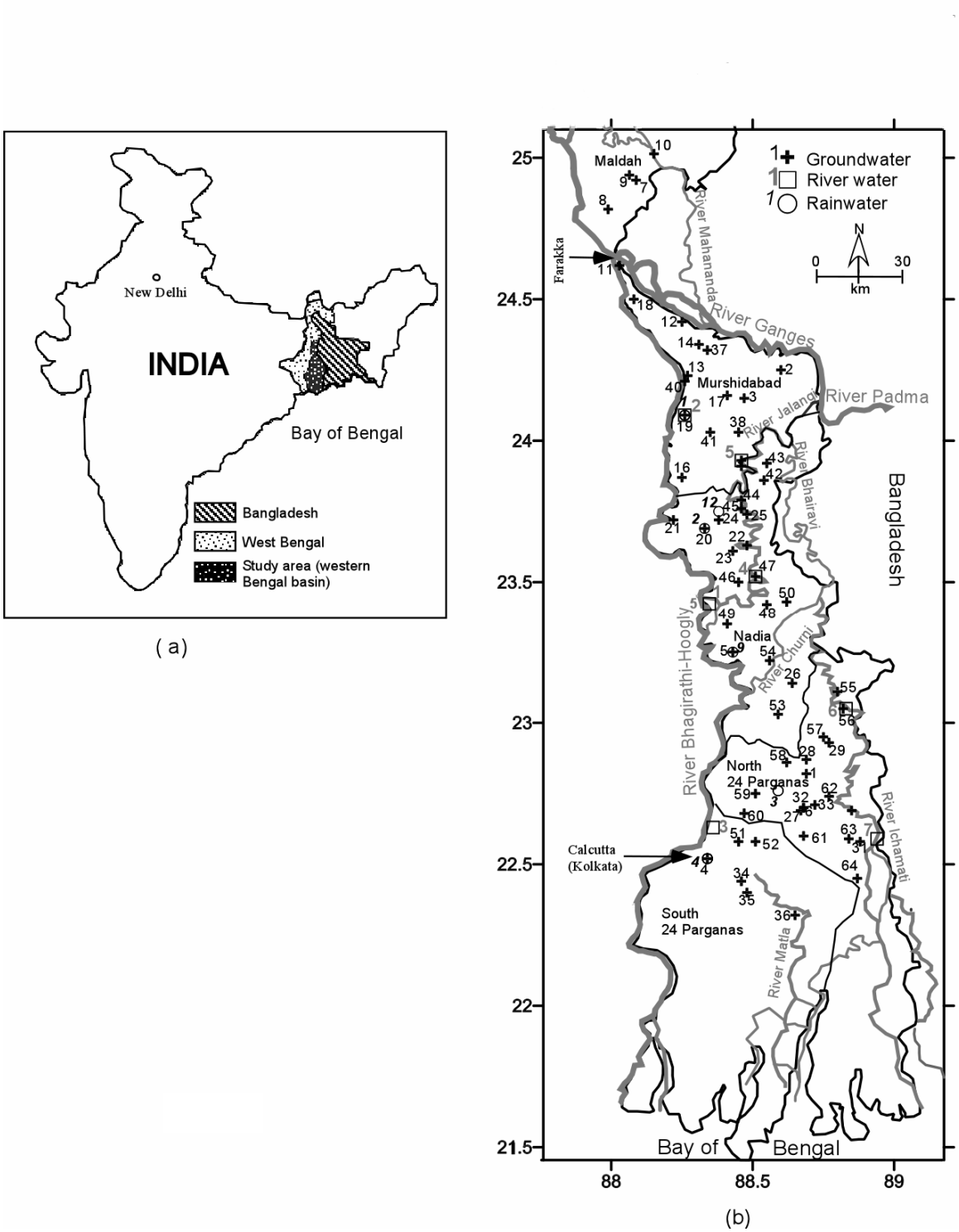

Figure 4.1: Map of the study area showing the sampling locations for groundwater, river water and rainwater.

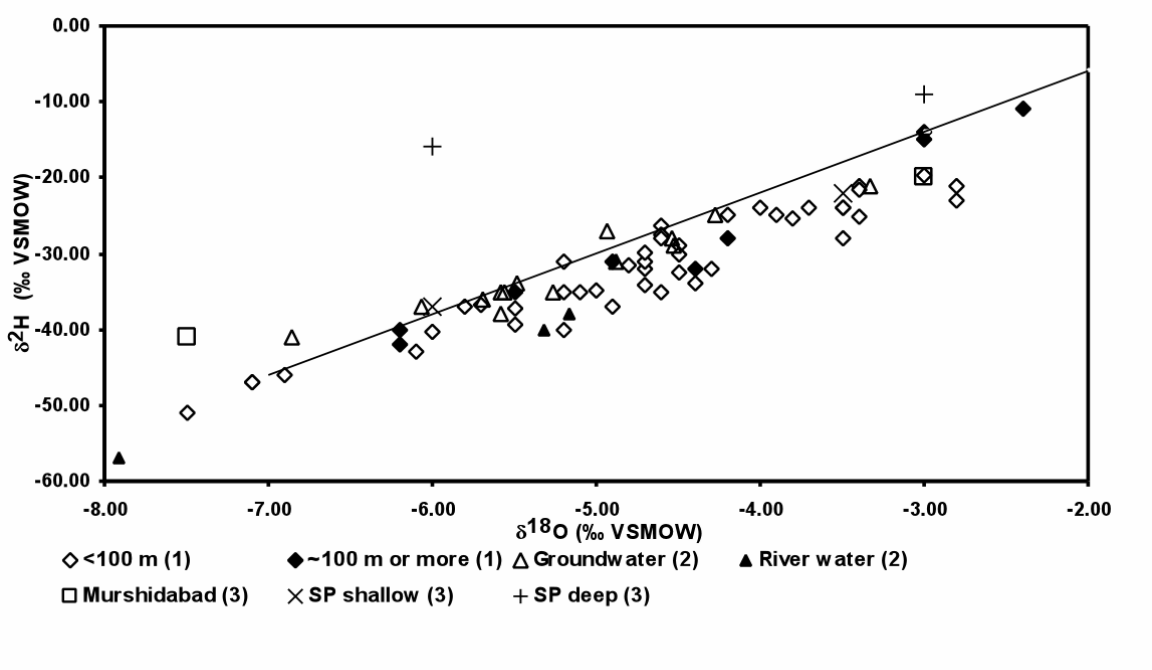

Figure 4.2: Composite $\delta^{18}O$–$\delta^{2}H$ bivariate plot showing the findings of previous workers in Bengal basin. 1: Aggarwal et al. (2000); 2: Stüben et al. (2003); 3: Shivanna et al. (1999). Note that the values from Shivanna et al. (1999) are only the maximum and minimum ranges; detailed values were not available. SP denotes South 24 Parganas.

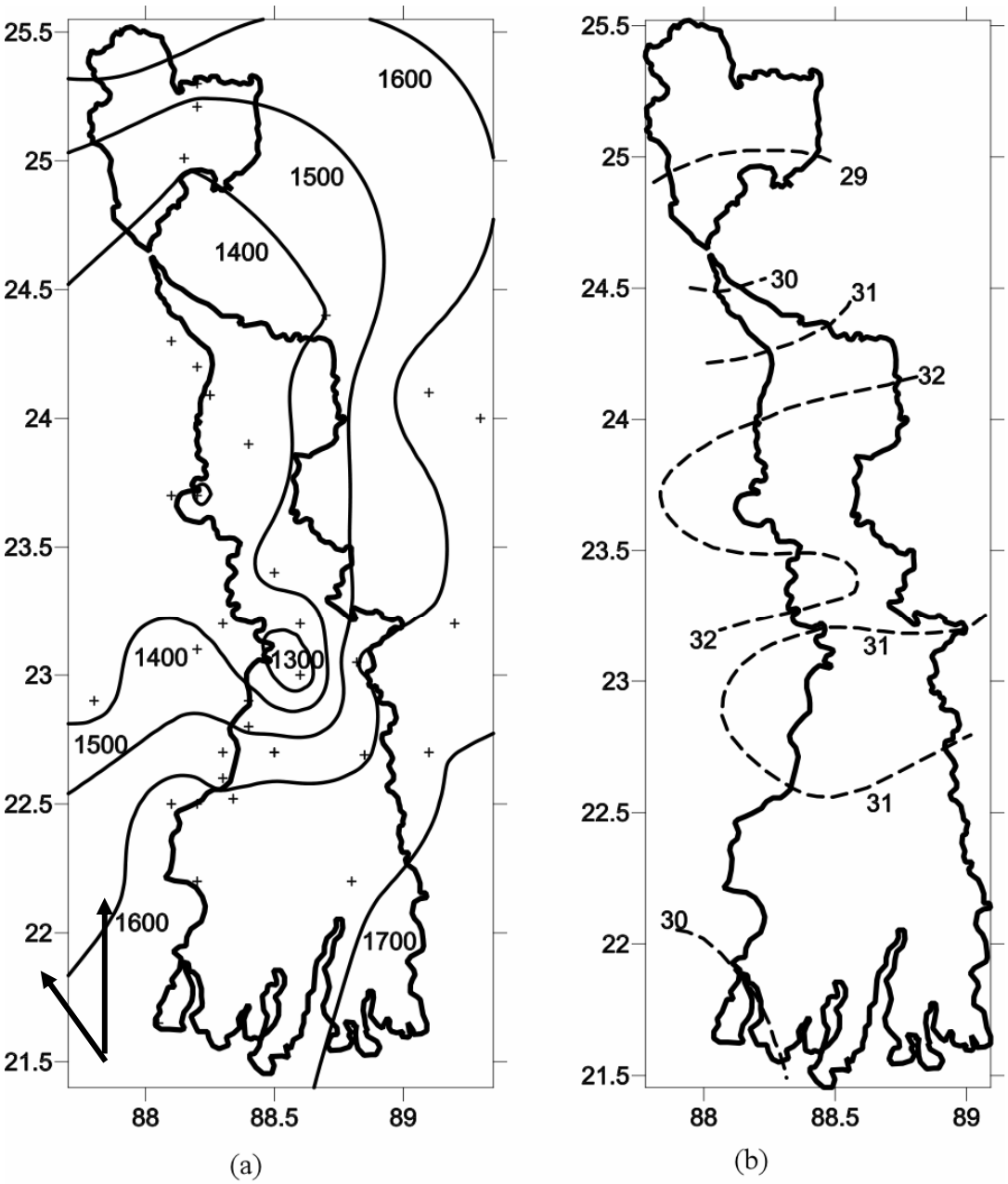

Figure 4.3: Map of the study area showing (a) contour plot of mean annual rainfall (in mm). The + symbol indicates the location of the monitoring stations whose data were used for drawing the contours. Maximum data range: 1821 to 2005, although most of the stations have data ranging from 1901–1970. The arrows show the approximate direction of movement of the southwest monsoon wind from the Bay of Bengal; (b) contours of average daily summer air temperature (in ^{o}C) redrawn after CGWB (1994e).

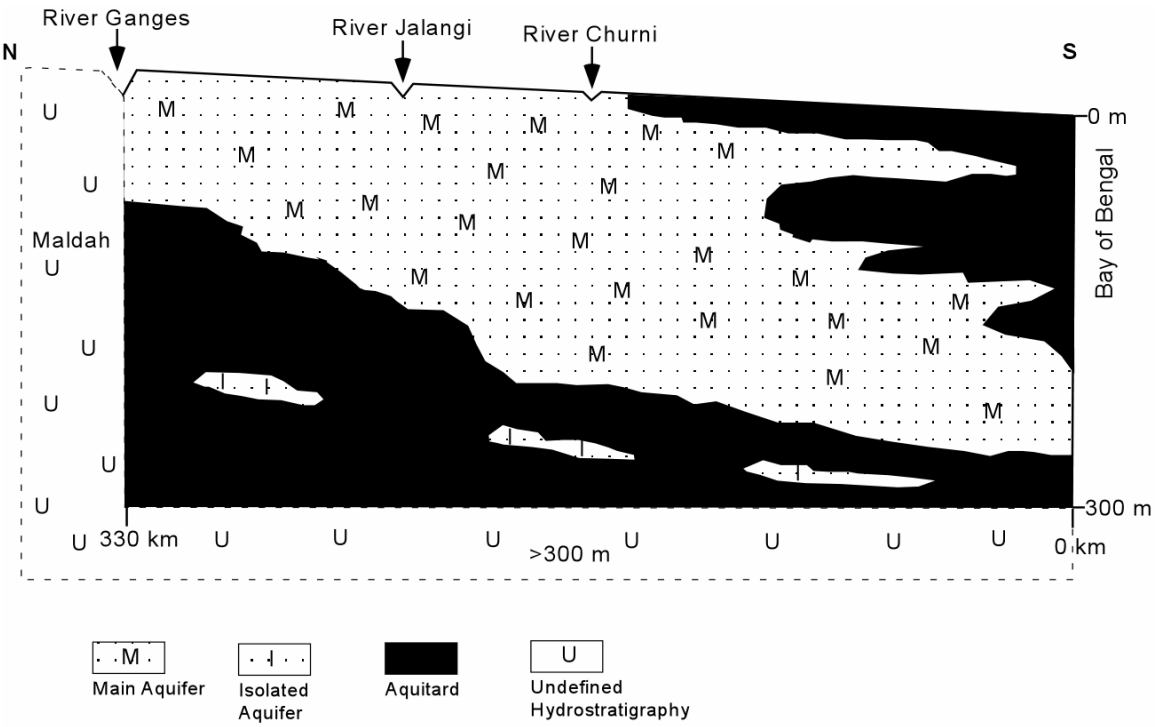

Figure 4.4: Simplified hydrostratigraphic diagram of the study area (not to scale) showing the different type of aquifers discussed in this article (see Chapter 2 for details). Note that no data were available for the part of the study area in Maldah and below 300 m from mean sea level, so those areas have been marked as undefined (U).

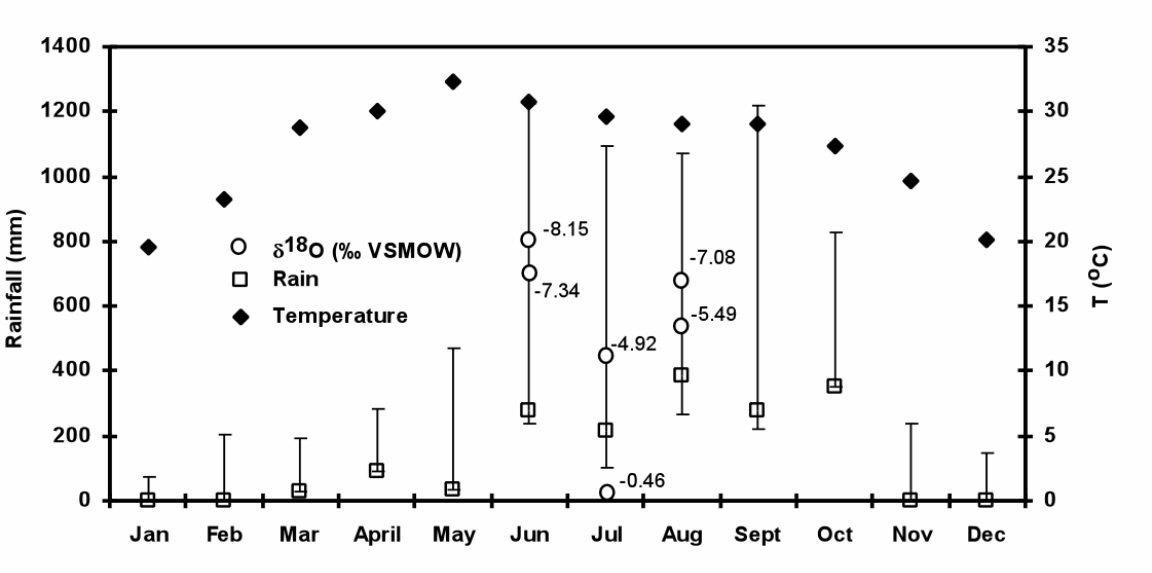

Figure 4.5: Double-axis plot of monthly rainfall (in mm) and air temperature (in ^{o}C) for Calcutta in 2004. The bars indicate the maximum and minimum rainfall in each month between 1821 and 2005 (based on GHCN v. 2). The higher values of rain from June to October indicate the monsoon in 2004. The $\delta^{18}O$ compositions of the six samples collected from Calcutta during the 2004 and 2005 monsoons are also plotted.

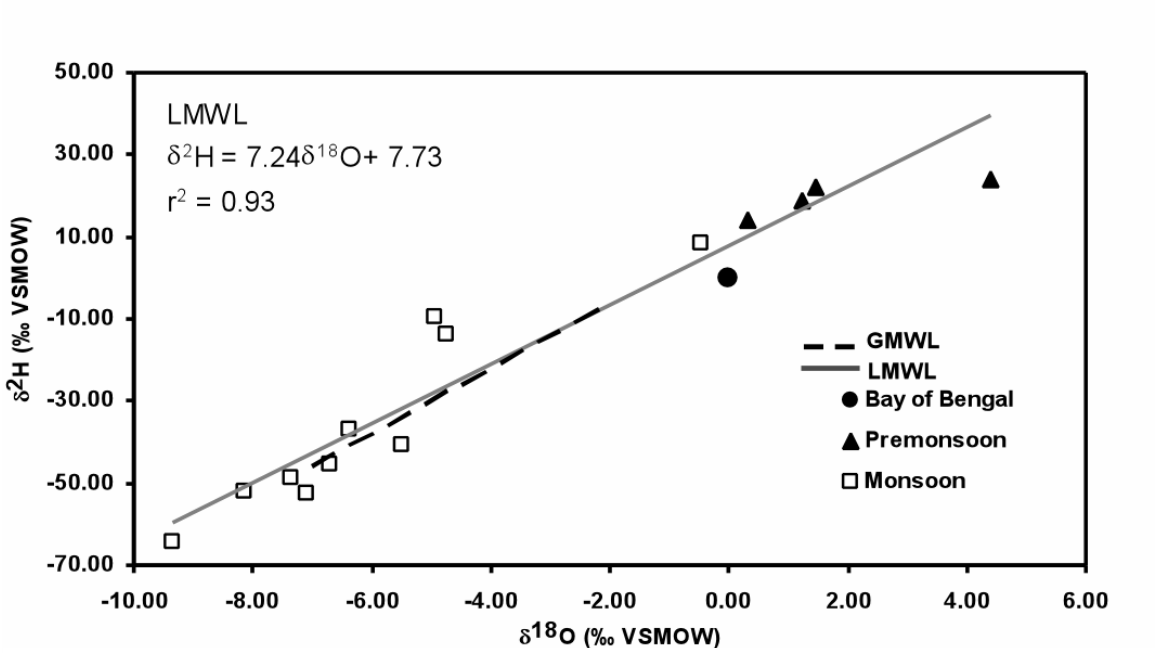

Figure 4.6: $\delta^{18}O$–$\delta^{2}H$ bivariate plot of the rainwater samples collected during the present study. The linear regression fit for these data indicates the local meteoric water line (LMWL) for the study area. The global meteoric water line (GMWL) of Craig (1961) and the expected isotope composition of the Bay of Bengal (0, 0) are also plotted for reference.

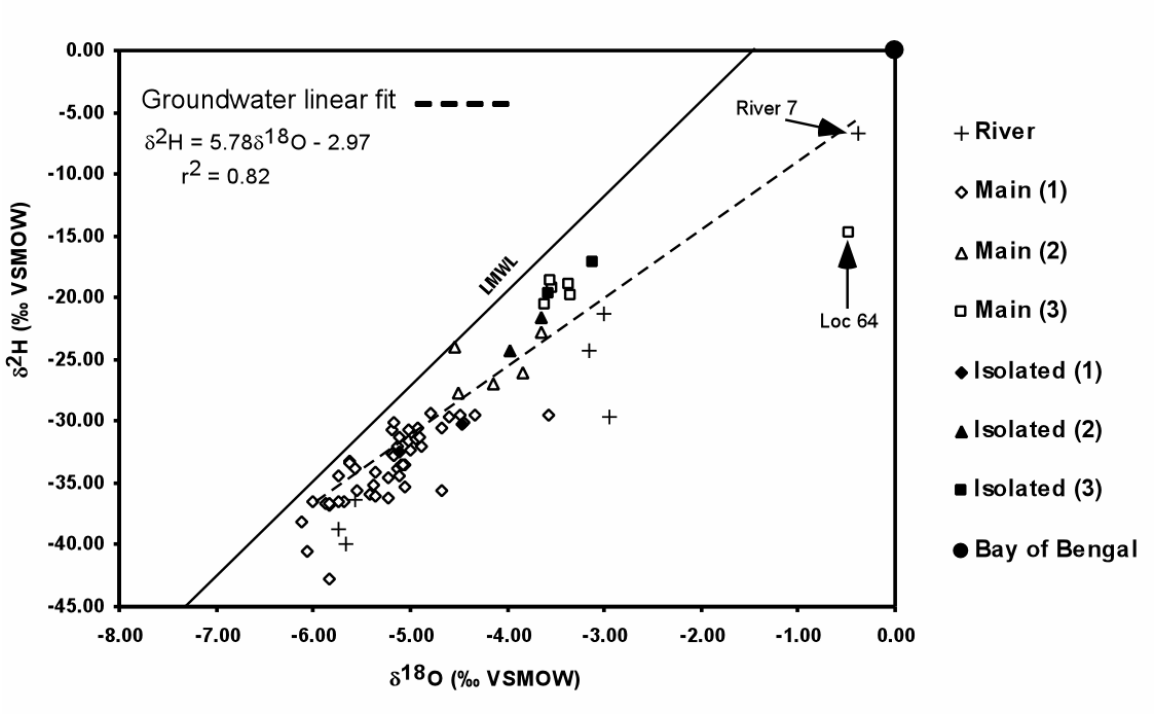

Figure 4.7: $\delta^{18}O$–$\delta^{2}H$ bivariate plot of deeper groundwater and river water from the study area. The groundwater samples have been grouped by (a) aquifer types (main and isolated) and (b) statistical groups (1, 2 and 3, see Table 4.1). The LMWL represents the linear fit line defined in figure 4.6. The dashed line represents the linear fit of all the groundwater samples. The location no. 64 represents the marine influence on the groundwater in the southern part of the study area. The expected value of the isotopic composition of the Bay of Bengal (0, 0) is also plotted for reference.

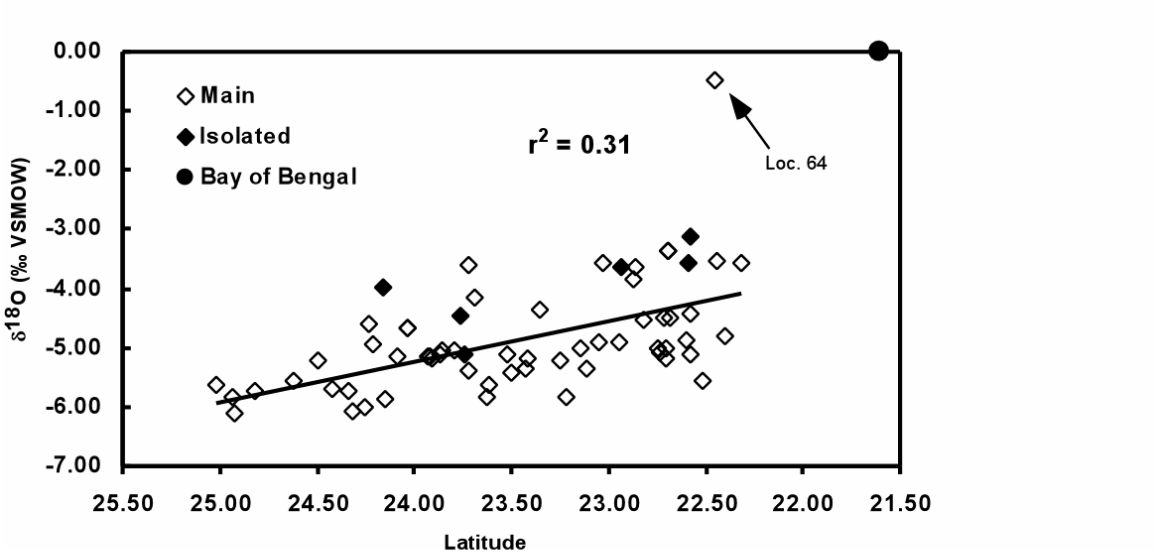

Figure 4.8: Bivariate plots of latitudinal locations and $\delta^{18}O$. The solid lines represent the trend lines obtained from linear regression fit of the data. The location no. 64 represents the marine influence on the groundwater in the southern part of the study area. The expected value of the isotopic composition of the Bay of Bengal (0, 0) is also plotted for reference.

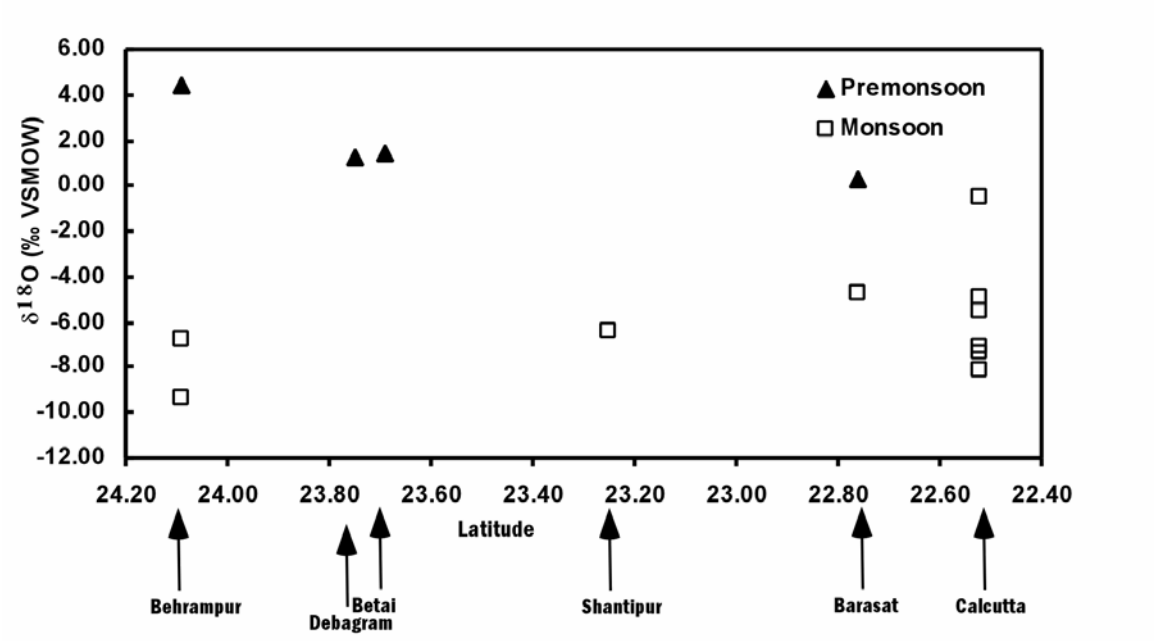

Figure 4.9: Plot of $\delta^{18}O$ of the rainwater samples along latitude.

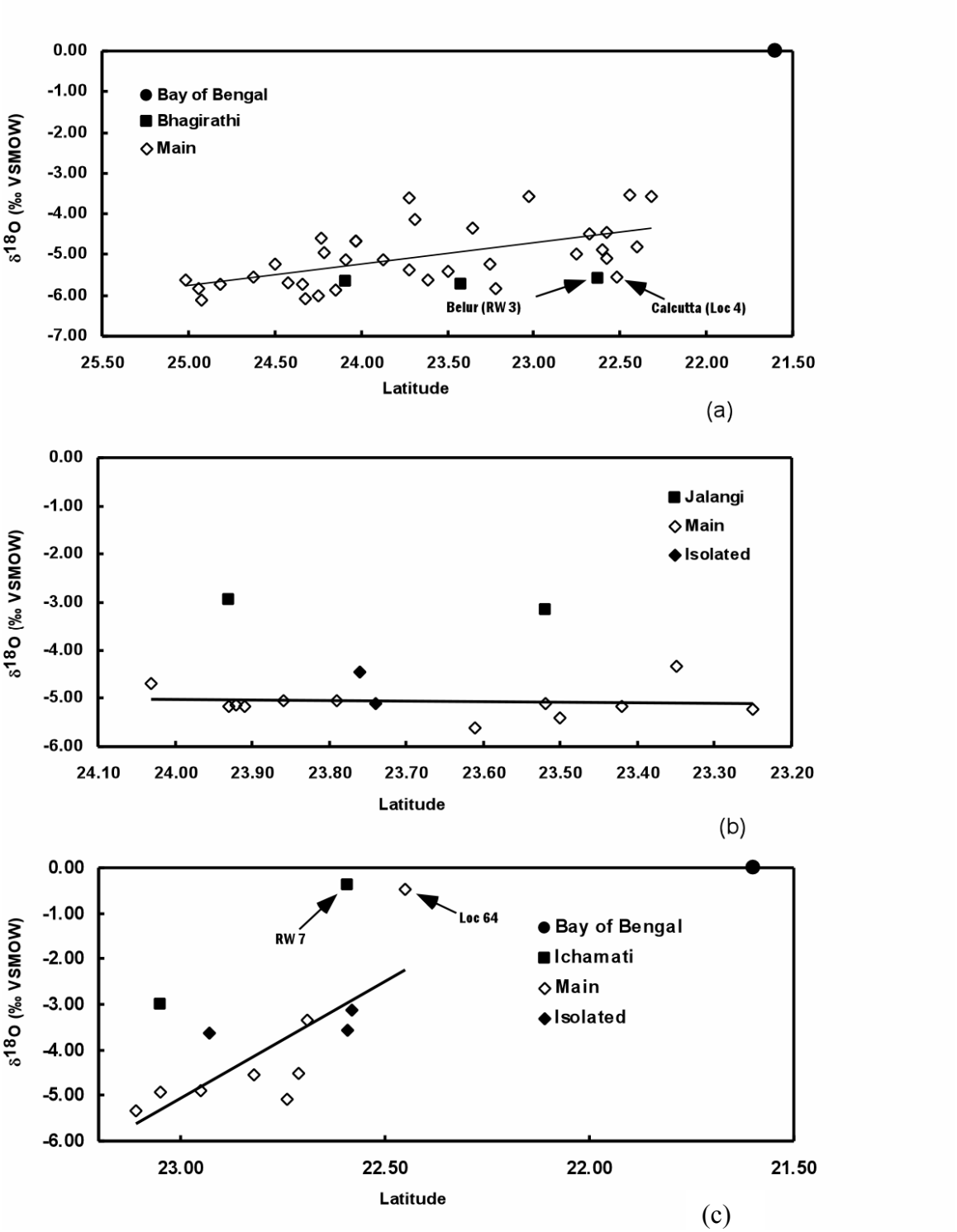

Figure 4.10: $\delta^{18}O$ composition of river water and groundwater plotted versus latitude. The groundwater data have been grouped based on proximity to the rivers (a) Ganges-Bhagirathi-Hoogly, (b) Jalangi, and (c) Ichamati. The solid line represents the trend-line obtained from the linear regression fit of the data. The approximate latitude and $\delta^{18}O$ value of the Bay of Bengal (21.4^{o}N, 0) are also plotted for reference.

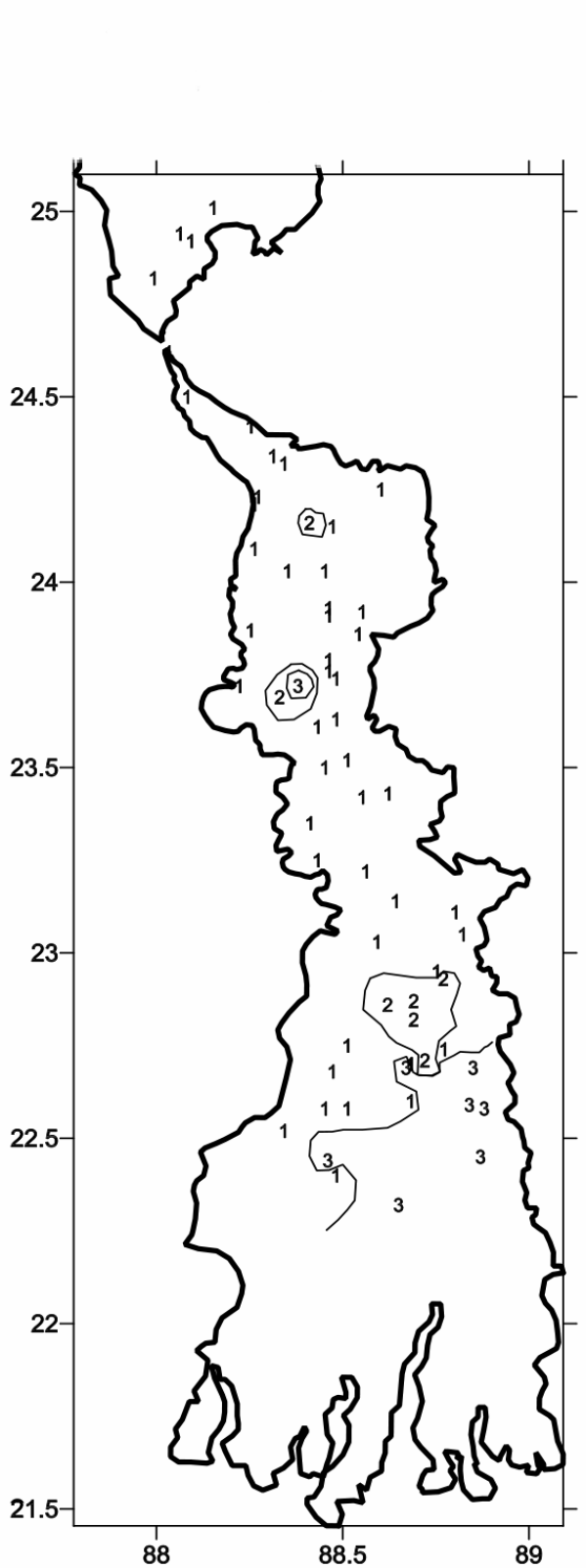

Figure 4.11: Map of the distribution of the groundwater data points classified on the basis of the statistical (HCA) groups 1, 2 and 3.

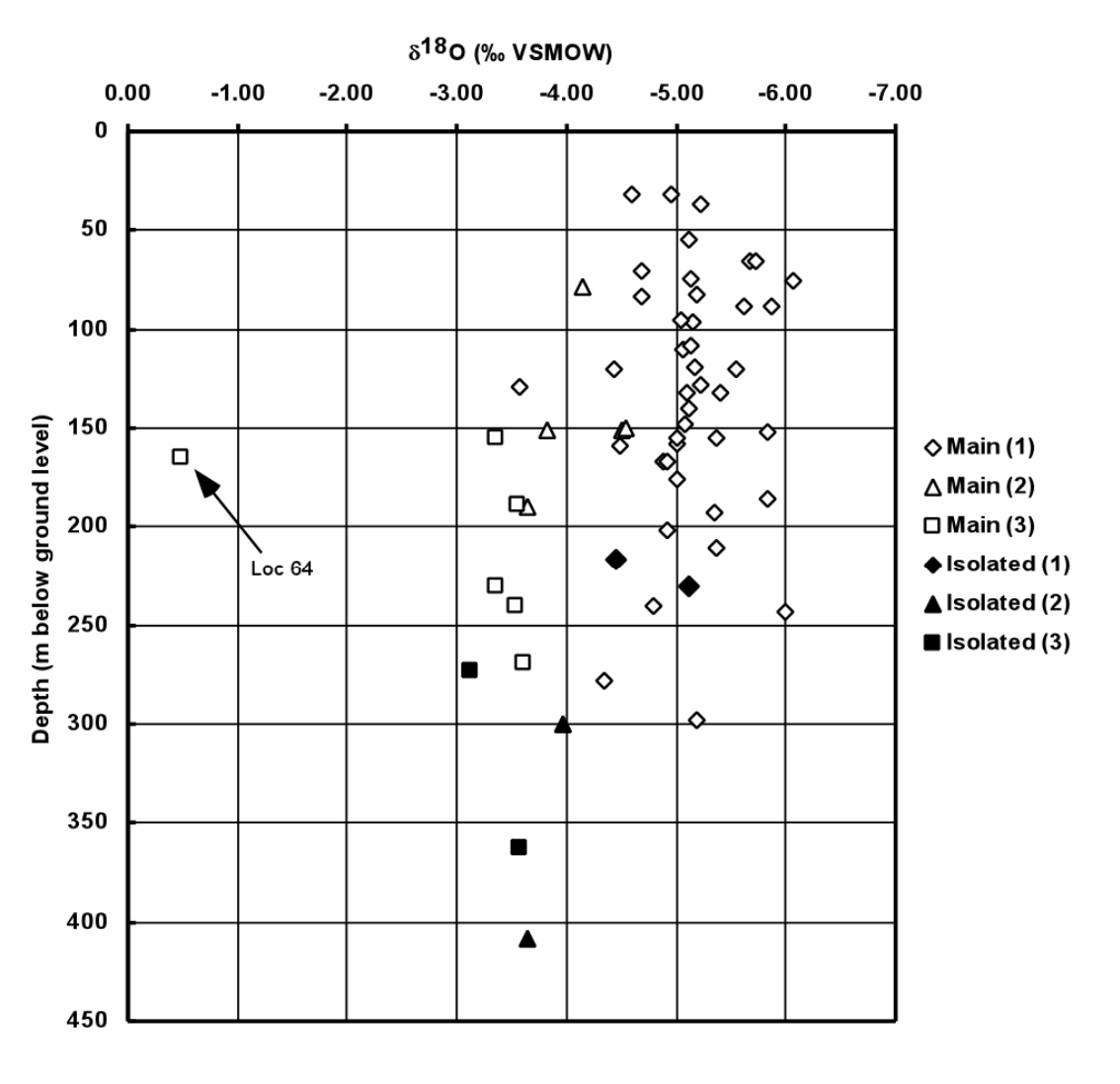

Figure 4.12: Depth profile of the $\delta^{18}O$ of groundwater samples in the study area classified based on aquifer type and statistical groups. The location no. 64 represents the marine influence on the groundwater in the southern part of the study area.

Chapter 5: Deeper groundwater chemistry and geochemical modeling

5.1 Introduction and background

This chapter documents the first detailed characterization and geochemical modeling of the deeper water chemistry of the study area in the western Bengal basin (Figure 5.1).

5.1.1 Hydrostratigraphic framework: The hydrostratigraphic characterization of the study area (up to a depth of 300 m below mean sea level [MSL]) has resulted in delineation of two major types of aquifers (Figure 5.2) (see Chapter 2). The first is a continuous, semiconfined sand aquifer (termed henceforth as the main aquifer) underlain by a thick clay aquitard. This main aquifer or Golden Bengal aquifer (as proposed in Chapter 2), deepens from a maximum of ~ 50-80 m below ground level [bgl] in the north to ~180 to >200 m bgl in the south. In the southern half of the study area, discontinuous clay layers locally divide the near-surface aquifer to form several deeper, confined aquifers. Second, in some localities there are several smaller, isolated aquifers present at greater depths (~200-300 m) containing groundwater with considerably different chemistry from the main aquifer (termed henceforth as isolated aquifers). For this study, the term "deeper" is used to connote either the deeper portions of the main aquifer or the isolated aquifers, and the absolute depth varies spatially depending on the local hydrostratigraphy. There are also some deep parts of the main aquifer that are partially isolated and have chemical characters between those of the upper main and the isolated aquifers. A study-area wide aquitard has been observed at a depth of ~300 m MSL (which also forms the base of the hydrostratigraphic model [Figure 5.2]).

5.1.2 Controls on hydrogeochemistry of the Bengal basin: Galy and France-Lanord (1999) concluded that the water chemistry of the Ganges-Brahmaputra drainage system is controlled by the presence of carbonates, the composition of silicates and the oxidation of sulfides, and, despite heavy monsoonal rainfall, chemical weathering is limited in the Ganges flood plains and lower elevations than in the Himalayas. The authors suggested that weathering in the basins is dominated by H_2CO_3 liberated by degradation of organic matter in the soil, with an estimated 6-9% of the weathering of the Ganges caused by H_2SO_4 action derived from the oxidation of sulfides. About 60% of the Gangetic clay has been inferred to be smectite + kaolinite (Galy and

France-Lanord, 1999). Dowling et al. (2003) suggested that Ganges-Brahmaputra floodplains have been dominated by carbonate weathering, according to the following generalized reaction: carbonates + H^+ → cations (Ca^{2+} or Mg^{2+}) + HCO_3^-.

However, some authors have argued that the development of the foreland basin, in front of the Himalayas (Burbank, 1992), has resulted in deposition of silt-dominated sediments in the Ganges-Brahmaputra flood plain, favoring silicate weathering (Derry and France-Lanord, 1996; Galy and France-Lanord, 1999). Following Appelo and Postma (1994) and Faure (1998), this can be generalized as:

feldspars (orthoclase and plagioclase) + CO_2 + H_2O → clay minerals (e.g., kaolinite) + cations (Na^+ or K^+) + HCO_3^- + SiO_2;

mica/pyroxene + CO_2 + O_2 + H_2O → clay minerals (e.g. kaolinite) + Fe-hydroxides + cations (Ca^{2+}, K^+ or Mg^{2+}) + HCO_3^- + SiO_2.

Hence, Na^+ and K^+ may enter the Bengal basin groundwater from incongruent dissolution of feldspars, micas and pyroxenes, whereas Ca^{2+} and Mg^{2+} can be derived both from silicate and carbonate weathering. Other than carbonate and silicate weathering, HCO_3^- in groundwater can originate from the vadose zone or biogenic CO_2 gas dissolution (Garrels, 1967).

Galy and France-Lanord (1999) suggested that Na^+ and K^+ are the dominant cations released by the weathering of the alkaline Himalayan silicates because of lower abundance of Ca-plagioclase in the Himalayas. Mg^{2+} may be introduced from weathering of biotite, and to a lesser extent from pyroxenes, chlorites and garnets (Galy and France-Lanord, 1999), to form hydrobiotite, vermiculite or smectite, which are found in the Himalaya-derived sediments (Baumler and Zech, 1994; Grout, 1995). Thus Ca^{2+} in the Bengal basin groundwater will most probably be introduced from carbonate dissolution, while Mg^{2+} will probably have mixed contributions.

It should also be noted that the sediments in the study area may not have been derived solely from the Himalayas. Alam et al. (2003) suggested that during different stages of the development of the Bengal basin, sediments were derived from two major depocenters: the Himalayas in the north and cratonic India in the west. Hence mineralogy and sediment chemistry of the western Bengal basin may have been influenced by erosion of the Precambrian

gneiss, schist and Chotonagpur basalts from the Indian craton by the west-bank tributary systems of the River Bhagirathi-Hoogly (e.g. River Damodar). This contribution would be more subdued moving toward the central part of the basin in Bangladesh.

Most of the recent studies of groundwater chemistry in the Bengal basin have strongly advocated that the redox processes in the aquifer at various depths are largely controlled by FeOOH reduction as an effect of microbially mediated oxidation of natural organic matter (Bhattacharya et al., 1997; Nickson et al., 1998, 2000; McArthur et al., 2001, 2004; Harvey et al., 2002, 2005; Zheng et al., 2004), which may occur as dissolved organic carbon or peat layers (McArthur et al., 2001; 2004, Ravenscroft et al., 2001, 2005) leading to production of high concentrations of HCO_3^-. The groundwater has been found to be anoxic (Harvey et al., 2002; Swartz et al., 2004, Mehta and Bhattacharya, c. 2000), with frequent presence of sulfide and CH_4 (e.g. Ahmed et al., 1998; Gavrieli et al., 2000; Nickson et al., 2000; McArthur et al., 2001, 2004) and very little dissolved O_2.

5.2 Methodology

5.2.1 Sampling and field analyses: Fifty-three deep groundwater and seven river-water samples (three from the River Bhagirathi-Hoogly and two each from the River Jalangi and River Ichamati) were collected from the study area (Table 5.1, Figure 5.1) during the summers (May to early July) of 2004 and 2005. The groundwater samples were located approximately along the original (pre-1970s) regional groundwater flow path (see Chapter 3). The sample locations were recorded by a hand-held GPS unit using a spherical coordinate system of latitude and longitude (datum WGS84). The groundwater samples were collected from single-strainer, public supply wells installed and maintained by the Public Health Engineering Directorate (PHED), Government of West Bengal. Water is withdrawn from these wells by 15-20 h.p. electric motors coupled with a turbine or submersible pumps with general yield of 50 to 200 m^3/hr. They are generally pumped daily for 6 hours in two or three shifts. Well completion data were obtained from PHED archives and a local driller (B.M. Engineering, KrishnaNagar, Nadia). Generally, the tapped depth deepens from the north (Murshidabad) toward the south and east. Among the 53 groundwater samples, 47 samples have been collected from the main aquifer and four from isolated aquifers. The remaining two sampled wells are screened below the regional basal

aquitard, so their hydrostratigraphic position is uncertain. They are termed as >300 m. For hydrochemical discussion, the isolated aquifer samples and the >300-m samples are grouped together as "isolated", because both of these types of samples are hydrostratigraphically separated from the main aquifer.

The groundwater samples were collected according to standard methods (Wood, 1981). An in-line flow cell was fitted with an Orion® pH electrode (model no. 8165BN), platinum redox electrode (model no. 9678BN) and temperature probe (model no. 917005) such that the outflowing water had minimal contact with the atmosphere. Specific conductance (EC) was also measured simultaneously by an Orion® conductivity meter (model no. 130). Before sampling at each location, the pH electrode was calibrated using standard pH 4, 7 and 10 buffer solutions (Wood, 1981) and the redox electrode was referenced to ZoBell's solution (ZoBell, 1946). Before sample collection, the wells were extensively purged (40 minutes to more than an hour) in order to obtain stable E_H, pH and temperature (T) values, which were considered to be representative of in-situ conditions. After the starting of the pump, E_H and pH were recorded every 10 minutes, whereas T and EC were noted every 5 minutes until stabilization (EC was not measured for some 2005 samples due to instrument malfunction). Groundwater samples were collected through high capacity in-line 0.45-μm filters after purging. Redox-sensitive parameters were measured by CHEMets® (Chemetrics, Calverton, VA, USA) medium-to-low range field kits: NO_3-N (Cd reduction/azo dye formation method [APHA, 1995a]), NO_2^--N (azo dye formation method [APHA, 1995b]), NH_4^+-N (nesslerization method [APHA, 1992]), total Fe and Fe(II) (1.10-phenanthroline method [Tetlow and Wilson, 1958]) and S^{2-} (only 2005) (methylene blue method [EPA, 1979; APHA, 1995c]). Sulfide was also qualitatively determined by odor and taste (both years) (Ross et al., 1999; Varner et al., 2004). Dissolved oxygen (O_2) samples were collected in 300-mL biological oxygen demand (BOD) bottles (Wheaton) and were measured immediately with a Orion® electrode (model no. 970899). Samples for cations (except NH_4^+) were collected in separate 125-mL white high-density polyethylene (HDPE) bottles and were acidified in the field with 1.5 mL 6N HNO_3 to buffer the sample to pH ~ 2. Samples for As(III) were collected in amber HDPE bottles after adding 1 mL of 0.250 M EDTA to ~30 mL sample and subsequently extracted through a disposable Supelco® (Supelco/Sigma-Aldrich, Bellefonte, PA, USA) anion-exchange resin cartridge (model LC-SAX). EDTA was added to preserve the

As species distribution by chelating metal cations, buffering the sample pH, and reducing microbial activity (Gallagher et al., 2001; Bednar et al., 2002). Samples for analyses of N species (NH_4^+, NO_3^+ and NO_3^-) and other anions were collected in separate 125-mL white HDPE bottles. Nitrogen species were preserved by adding 1.5 mL $CHCl_3$ in the field (Böttcher et al., 1990). Dissolved organic carbon (DOC) samples were collected in 40-mL amber glass vials with solid caps to which 1.5 mL of 50% H_2SO_4 were added in order to eliminate inorganic carbon. CH_4 samples were collected without air bubbles in separate 40-mL amber glass vials with septa to exclude headspace. Carbon-13 samples were collected in solid-capped 40-mL amber glass vials poisoned in the field with five drops of $HgCl_2$. Samples for sulfur-34 were collected in 1-L HDPE bottles to which ~15 g of $BaCl_2$ were added in order to precipitate $BaSO_4$. The samples were allowed to sit overnight and the supernatant was siphoned off, after which the precipitates were transferred and stored in 125-mL white HDPE bottles. Samples for alkalinity were collected in BOD bottles without headspace and analyzed within 2 days by a digital titrator (Hach Company, Loveland, CO, USA) and magnetic stirrer by titrating a 100-mL sample with 1.600 N H_2SO_4 to pH < 4.5 (Wood, 1981). The titration data were used to obtain HCO_3^- and CO_2 concentrations via the U.S. Geological Survey (USGS) alkalinity calculator (http://or.water.usgs.gov/alk).

River-water samples were generally collected in the same fashion as groundwater samples. However, E_H, pH, and T were not measured in a flow cell, and samples were collected using a hand-filtration unit. Analyses were limited to major and minor solutes.

5.2.2 Laboratory analyses: The samples (except for ^{13}C and ^{34}S) were analyzed in the laboratories of the University of Kentucky (UK). Analyses of cations and anions were done in the Environmental Research and Teaching Laboratory at UK (ERTL). Total As and As(III) were measured using an atomic absorption spectrophotometer with a graphite furnace (Varian AAS 880 with Zeeman GF). Other major cations (except NH_4^+) and trace metals were measured by multi-element scans using an inductively coupled plasma-optical emission spectrometer (VarianVista Pro ICP-OES). Accuracy of analyses was assessed by method blanks, laboratory controlled standards and spiked samples, and precision was determined by duplicate and

triplicate analyses. For 2005 samples, Y was used as an internal standard to account for instrumental error. The precision of analyses was generally better than 5%.

Anions (preserved and unpreserved) and N species were measured at ERTL using an ion chromatograph (IC) (Dionex ICS-2500) with AS18 column for 2004 samples and by an IC (Dionex ICS-2000) and an autoanalyzer (Bran-Luebbe AAIII) (for N species) for 2005 samples at the UK Department of Forestry. The error was generally <6 % for the IC and <3% for the autoanalyzer. The CH_4 samples were analyzed using a gas chromatograph with flame ionization detector (Shimadzu GC-14A with Chromatopac C-R5A) at the UK Department of Agronomy. DOC was measured using a Phoenix 8000 UV-Persulfate TOC Analyzer at the Kentucky Geological Survey. Stable isotope analyses were performed at the Isotope Geochemistry Laboratory at the University of Arizona using a continuous-flow isotope-ratio mass spectrometer (IRMS) (ThermoQuest Finnigan Delta*Plus*XL). Before analyses of ^{34}S, the $BaSO_4$ precipitates of the samples were filtered with a vacuum filter. Only samples with sufficient precipitate (~ 2 mg) were able to be analyzed. The IRMS was standardized against international standards OGS-1 and NBS123 as well as several other sulfide and sulfate materials. Precision (1σ) of the analyses was ± 0.15‰. Samples for ^{13}C of dissolved inorganic carbon (DIC) were reacted for >1 hour with H_3PO_4 at room temperature in exetainer vials previously flushed with He gas. Standardization was done using NBS-19 and NBS-18, and precision (1σ) was ±0.25‰.

5.2.3 Statistical analyses: Multivariate statistics (hierarchical cluster analyses [HCA] and principal component analyses [PCA]) were used to investigate relationships among the samples (Drever, 1997). Both HCA and PCA were performed on the concentrations of As(total), B, Ba, Ca, Fe(total), K, Mg, Mn, Na, NH_4^+, Sr, Cl^-, SO_4^{2-}, HCO_3^-, and CO_3^- for each location. Below-detection-level (bdl) concentrations were replaced by bdl × 0.55 (Sanford et al., 1993). While cluster analyses were used to determine if the samples could be grouped into distinct hydrochemical populations, PCA was used to reduce the dimension of the data (Güler et al., 2002) in order to understand relations among different chemical parameters. The multivariate statistical analyses were done on the original data set (without any weighting or standardization) following theories and methodologies stated in Davis (1986), Güler et al. (2002) and Dreher (2003), by importing the $r \times c$ data matrix (r samples with c variables) into the statistical software

package SPSS version 14 (SPSS Inc., Chicago, IL). For best grouping in HCA, the dendogram was constructed by Ward's method of linkage (Ward, 1963) with squared Euclidean distance (Güler et al., 2002). PCA was done without restricting the component numbers, but it was found that the first six components were able to account for 90% of the variance of all variables. The component axes were rotated using a varimax algorithm for simplified visualization.

5.2.4 Geochemical modeling: Saturation indices (SI = log[IAP K_T^{-1}], where IAP is the ion activity product and K_T is the equilibrium solubility constant of a phase at ambient temperature) were calculated for groundwater and river water samples using PHREEQC version 2.8 (Parkhurst and Appelo, 1999) with thermodynamic values of phases from the MINTEQ database (Allison et al., 1990) except for CH_4, for which the PHREEQC database was used. Concentrations of As and Fe were entered according to their redox states. The Fe(II)/Fe(III) couple was assigned for calculation of pe for groundwaters and O(-II)/O(0) was assigned for river waters. However, as the dissolved oxygen values of river waters were not measured, a value of O_2 = 7 mg/L was assigned for all of the river locations. Natural surface waters generally have an O_2 concentration of ~ 8 mg/L (Langmuir, 1997). SI > 0 (supersaturation) indicates precipitation of phases is thermodynamically favorable (although slow rates of reactions can inhibit precipitation), while SI <0 (undersaturation) suggests dissolution (Drever, 1997).

Minimal reaction-path models (in inverse mode) were developed using PHREEQC for pairs of wells located along 60 possible flowpaths as predicted by a regional groundwater flow model with pumping at quasi-current (2001) rates (see Chapter 3). The mass-balance models were developed for reactions with and without mixing. However, because of a lack of thermodynamic constraints in the program algorithm, these models can lead to thermodynamically impossible results (Sracek et al., 2004b). The models were designed to evaluate the amounts of exchangeable cations (CaX_2, KX, MgX_2, and NaX, where X is an anion), carbonates (calcite, dolomite, siderite), other carbon phases (CO_2, CH_2O, CH_4) and pyrite that could react along each flow path in order to explain the gross hydrochemistry of the western Bengal aquifers. Trace elements (e.g. As, Mn, and V) were not included in the mass balance calculations because of lack of information about the solid phases in which they reside. Halite was used as a proxy for mixing with connate seawater along flowpaths, as suspected from an

increase in Cl^- concentration in a down-gradient well relative to the up-gradient well. The other models were balanced on Cl^- concentrations (assuming Cl^- as a conservative solute). The sea-water composition from Nordstrom et al. (1979) was used for Bay of Bengal water in the mixing models.

The inaccuracy in the choices of end-member waters and in analytical data is handled by PHREEQC by including uncertainty in the inverse modeling. Fryar et al. (2001) used up to 20% uncertainty for inverse modeling. A similar approach was undertaken and the uncertainty was initially set at 5% (the default value for PHREEQC) and was increased incrementally by 1% up to a maximum of 20%, until a model was obtained. Because of the possible existence of a large number of alumino-silicate mineral phases leading to numerous model solutions, silicate weathering was not directly included in the modeling; instead, Si was assumed to be conservative within the specified level of uncertainty.

5.3 Groundwater quality

5.3.1 Hydrochemical facies: Table 5.2 lists the results of field observations and analyses of all the groundwater and river water samples collected in this study. Most previous studies of the Bengal basin have not distinguished between the regional settings of the aquifers (e.g. Dowling et al., 2002, 2003; Stüben et al., 2003, McArthur et al., 2004). The general description of Bengal basin groundwater is Ca^{2+}-HCO_3^- dominated water with some Na^+-Cl^- waters, high As, Fe, and Mn, and very low or undetectable SO_4^{2-} and NO_3^- (e.g. Ahmed et al., 1998; BGS/DPHE/MML, 1999; Nickson et al., 1998, 2000; McArthur et al., 2001; Dowling et al., 2003). This general description can be further typified when the water chemistry is considered in a hydrostratigraphic context. Ca^{2+} and HCO_3^- are the predominant ions for most of the main aquifer waters (mean values Ca^{2+} 106.45 mg/L, HCO_3^- 457.24 mg/L, Na^+ 58.76 mg/L, and Cl^- 63.93 mg/L), while Na^+ and Cl^- are more common in the isolated aquifer waters (mean values Na^+ 1132.07 mg/L, Cl^- 1619.58 mg/L, Ca^{2+} 33.92 mg/L, and HCO_3^- 573.36 mg/L) except Chaighari (location #6, see Table 5.1), which has HCO_3^- 1474 mg/L and Cl^- 1620 mg/L. Some of the main aquifer wells deeper than ~ 200 m, such as Jumpukur (#13), Dalalpara (#19), Ghasiara (#23) and Kalikapore (#24), which are suspected to have semi-isolated conditions, have higher Na^+ than Ca^{2+}.

The charge-balance computation shows that the main aquifer samples have higher error (below +10%, except #1 and #26) than the isolated aquifer samples (-3.22 to +0.65%, except #34). These errors are within the ranges of some of the previous studies in the Bengal basin (e.g. Aggarwal et al., 2000; Dowling et al., 2003; Stüben et al., 2003). The positive errors for the main aquifer indicate that there are more anions in the waters than have been accounted for. A possible explanation is that some of the Cl^- has co-precipitated with Fe (oxidized to Fe(III) during sampling) in the anion samples (D. Chakraborty, Jadavpur University, Calcutta, personal communication, 2003). No reason was found for the higher errors for #1 and #26, which were confirmed even after running duplicate analyses of the samples in different laboratories. However, it should be noted that #1 and #26 were the first samples collected for 2004 and 2005, respectively, which may indicate a sluggish response of the pH electrode during alkalinity titrations.

A Piper plot (Piper, 1944) (Figure 5.3) suggests that deeper groundwater in the western Bengal basin can be broadly divided into seven hydrochemical facies (following Morgan and Winner, 1962, and Back, 1966): 1) Ca^{2+}-HCO_3^-; 2) Ca^{2+}-Na^+-HCO_3^-; 3) Na^+-Ca^{2+}-HCO_3^-; 4) Ca^{2+}-Na^+-HCO_3^--Cl^-; 5) Na^+-Cl^--HCO_3^-; 6) Na^+-Cl^-; and 7) Ca^{2+}-Cl^-. Thirty-eight of the 47 main aquifer samples and the river water samples (except the tidally influenced Ichamati [RW #7]) fall in facies 1, while the isolated aquifer samples are divided into facies 5 and 6. The plot also illustrates that when the locations are grouped by districts (which is similar to grouping according to distance from the Bay of Bengal because of the north-south orientation of the study area), all of the main aquifer samples from Murshidabad (n = 12) and 14 of 16 Nadia samples belong to facies 1. A Piper plot of shallow groundwaters from the Behrampur area of Murshidabad constructed by Stüben et al. (2003) agrees with this observation. For 24 Parganas (North and South combined), only 12 of 19 samples belong to facies 1, indicating the presence of chemically distinctive water bodies nearer to the Bay of Bengal. The presence of these brackish waters can be attributed to cation exchange and/or mixing with more saline water bodies; their evolution is discussed in more detail in the geochemical modeling section (5.7). Sikdar et al. (2001) and Chatterjee et al. (2004) identified hydrochemical facies similar to our samples for North and South 24 Parganas in and around Calcutta.

The hierarchical cluster analysis (HCA) of the groundwater data by locations illustrates the presence of three distinct clusters. All of the main aquifer samples aggregate within Group 1, while Group 2 contains the isolated aquifer (<300-m) samples and Group 3 contains >300-m samples (Table 5.1). The plot of the HCA groups corresponding to the 1st (PC1, 36.46% of total variance, Table 5.3) and 2nd (PC2, 20.41% of total variance) principal component axes (Figure 5.4) illustrates this finding in more detail. All the main aquifer locations except Kalikapore (#24) have much lower PC1 values than the other two groups. The isolated aquifers (<300-m) except Chaighari (#6) have higher PC2 than the >300-m wells. While Kalikapore (#24) has PC2 values similar to isolated aquifer wells, Chaighari (#6) is distinct from all other wells in terms of its PC1 composition. HCA by chemical constituents does not show any prominent clustering, although Stüben et al. (2003) and Sracek et al. (2004a) observed such clusters in their local-scale study areas.

5.3.2 Processes controlling major solute distributions in groundwater: Minerals that have been documented by previous authors from Bengal basin sediments are listed in Table 5.4. A Na-normalized Ca versus HCO_3^- plot (Figure 5.5a, following Gaillardet et al., 1999) shows that the main aquifer samples range from being influenced by silicate weathering to carbonate dissolution. The molar Ca/Na ratio for average crustal continental source rock is 0.6 (Taylor and McLennan, 1985). The other wells show mixed contributions of both silicate and carbonate reactions. A Ca versus Mg bivariate plot (not shown) shows a somewhat linear relationship for the main aquifer ($r^2 = 0.38$) and more so for the isolated aquifers ($r^2 = 0.69$). The same plot normalized by Na (Figure 5.5b) shows some samples in the range of silicate weathering, indicating that although most of the Mg may have been derived from carbonate dissolution, some has a silicate source. A bivariate plot (Figure 5.5c) of Ca+Mg versus HCO_3^- shows some scatter. Dowling et al. (2003) noted that average $(Ca+Mg)/HCO_3^-$ is ~0.9 for their study area, with depths of 10 to 400 m. However, the results from the present study have an average value of only 0.53 for the main aquifer. Stallard and Edmond (1983, 1987) suggested that a molar ratio of (Na + K)/Cl > 1 may indicate silicate weathering. Only four of the 47 main aquifer samples of this study have (Na+K)/Cl < 1. Dowling et al. (2003) also showed that Sr was correlated well with HCO_3^- and inversely related to $(Na+K)_{excess}$ (= [Na+K]-Cl). For the main aquifer samples for the present study, a Sr versus HCO_3^- plot (not shown) yielded $r^2 = 0.02$, and no relation is apparent

between $(Na+K)_{excess}$ and Sr, although a Na- normalized Ca versus Sr plot yielded $r^2 = 0.77$ and 0.95 for main and isolated aquifers, respectively. Although Sr and Ca have probably been contributed by carbonate dissolution, not all HCO_3^- has originated from carbonate dissolution, and it is not the predominant chemical reaction influencing deeper groundwater in the western Bengal basin, as suggested by Dowling et al. (2003) for Bangladesh.

Al^{3+} tends to be conserved in the solid phase (Freeze and Cherry, 1979). Because of its low solubility and tendency to occur as a colloidal hydroxide (Stumm and Morgan, 1996), measured Al concentrations are viewed as semi-quantitative and are not reported and discussed here. Stability diagrams (Figure 5.6) illustrate the relationship between feldspars, mica (muscovite) and clay minerals. The diagrams were generated assuming end-member compositions using the equilibrium relationships of Tardy (1971) and Drever (1997) for standard temperature (25 ^oC) and pressure (1 atm) and by plotting log $([Ca^{2+}]/[H^+]^2)$ or log $([Na^{2+}]/[H^+])$, log $([K^{2+}]/[H^+])$, versus log $[H_4SiO_4^0]$, where [ ] denotes solute activity calculated by PHREEQC using the MINTEQ database. The plots indicate that the groundwater of the study area is in equilibrium with kaolinite, with some samples close to Na-smectite and muscovite, and feldspars (anorthite, albite and orthoclase) are unstable, suggesting weathering. These observations match very well with the observed mineralogy of the Bengal basin. The plots show that most of the samples are close to equilibrium with quartz than with amorphous silica, discussed in section 5.7. This observation agrees well with Hem (1992), who mentioned that natural waters are typically supersaturated with respect to quartz but undersaturated with respect to amorphous silica.

Some interesting patterns are notable when pH, Ca+Mg, Na+K and Si are plotted against depth and along distance from the Bay of Bengal (latitude) (Figures 5.7 and 5.8). The values of pH are circumneutral, but at depths >200 m, the waters become more alkaline. The concentration of Ca+Mg decreases with increasing depth and with nearness to the sea. Na+K is higher in the deeper wells (generally more than 200 m bgl) and the isolated aquifer wells than the shallower and northern wells. Ahmed et al. (2004) mentioned without any elaboration that Ca, Mg, Na and K vary significantly with depth and region in Bangladesh. Si increases to a depth of ~150 m, when it starts to scatter and decrease. Si increases toward the south and then starts decreasing, probably as a function of depth. The isolated aquifer wells have relatively low Si concentrations.

The decrease of Ca+Mg in comparison to Na+K along the regional hydraulic gradient in the North and South 24 Parganas suggests cation exchange according to the following general reaction (after Schwartz and Zhang, 2002):
bivalent cation (Ca^{2+} or Mg^{2+}) + Na-clay → Na+ + Bivalent cation (Ca^{2+} and/or Mg^{2+})-clay.
A (Na+K)/Cl versus Si bivariate plot (Figure 5.5d) suggests that (Na+K)/Cl increases as Si becomes more than ~500 μmole/L, suggesting some threshold value as an indicator of significant silicate weathering. The Cl^- ratio helps to normalize the samples affected by saltwater intrusion or mixing with connate water. HCO_3^- does not vary regionally either with distance (Figure 5.8c) or depth in the main aquifer, indicating that the processes consuming and liberating the anion are approximately in overall equilibrium.

The brackish groundwaters encountered in the isolated aquifers and some deeper portions of the main aquifer (e.g. locations #16, #23, #24, #38) differ considerably from those in the main aquifer, suggesting different pathways of chemical evolution. Brackish water (e.g. #40, #53) in the main aquifer in the southernmost part of the study area probably results from mixing with intruded seawater in this region, as documented by CGWB (1994d, e). A plot of Cl-normalized Br^- concentrations (Figure 5.9) following Whittemore (2004) shows a definite trend of mixing of fresh groundwater with water with present-day seawater composition.

The existence of brackish water and brines in sedimentary basins can be caused by a) dissolution of evaporites, b) retention of formation waters buried with the sediments and c) membrane filtration (Schwartz and Zhang, 2002). Fresh groundwater becoming more saline with flow downdip from the recharge area has been documented in the Williston Basin, USA (Downey, 1984; Butler, 1984), the Dakota Sandstone in South Dakota, USA (Peter, 1984), and the Milk River aquifer in the USA and Canada (Hendry et al., 1991). Ranganathan and Hanor (1987) showed that diffusion can cause salinization of fresh water overlying formational brines at depth. In the present study area, some parts of the deeper main aquifer are relatively fresh in contrast to adjoining areas with higher Cl^- concentrations (e.g. location #39). This fresh water "nose" (Schwartz and Zhang, 2002), reflecting insufficient mixing and flushing, is similar to that seen in Ohio, USA (Lahm et al., 1998).

The isolated aquifers probably contain formation water trapped within lower permeability sediments and may be similar to modified-connate water pockets reported from South 24 Parganas (Handa, 1972; Sikdar et al., 2001) and several places in Bangladesh (Ahmed, 1994; Bhattacharya et al., 2002). This is consistent with the isolated aquifers falling close to the evaporite range in the Ca/Na versus HCO_3^-/Na plot (Figure 5.5a; note that three isolated samples are not shown in the plot because of very low values [Ca/Na < 0.01]). The depth of these isolated aquifers generally increases toward the south, probably in congruence with the delta-building process and recession of the proto-Bay of Bengal. The marine origin is further supported by the fact that, except for Chaighari (#6), the isolated aquifer wells are dominated by Na^+ and Cl^-. Moreover, they contain lower concentrations of Si and much higher B (Si mean [except #34, which has a relatively higher concentration]: 8.12 mg/L, B mean: 3.14 mg/L) than the main aquifer wells (Si: 16.21 mg/L; B: 0.10 mg/L). Seawater contains 0.02 to 4 mg/L Si and 4.5 mg/L B on average (Mance et al., 1988). Nordstrom et al. (1979) documented a Si value of 4.28 mg/L for seawater.

Formation waters can be modified by meteoric diagenesis prior to burial. Land and Prezbindowski (1981) showed that connate water of the Edwards Formation (Texas, USA) was altered by mixing with several pore volumes of meteoric recharge. This might explain the similarity between $\delta^{18}O$ of the main aquifer waters of this study (~ -3 to -6‰ VSMOW) and that of isolated aquifer waters and restricted main aquifer waters (~ -3 to -5‰) (see Chapter 4). Alternatively, as suggested by Sikdar et al. (2001), there may still be some mixing between the main aquifer and isolated aquifers through higher permeability "windows" within the confining beds.

The Na^+-Cl^--HCO_3^- type water at Chaighari (#6) is distinct from any other well sampled in the study area. Schwartz and Zhang (2002) noted Na^+-HCO_3^- type water can evolve along with relatively high F^- concentrations as a result of continuous availability of CO_2 in the system. The major source of CO_2 in deeper aquifers may be bacterially-mediated oxidation of organic matter (Chapelle, 1993). Exchange of Ca^{2+} in the evolving water for Na^+ on marine-originated clays in the aquifer can also enhance carbonate dissolution and introduction of more Na^+ and

HCO_3^- into solution (Plummer et al., 1994). A combination of these processes has produced sodium-bicarbonate water in the Atlantic Coastal Plain, USA (Foster, 1950), Eocene aquifers of the east Texas basin, USA (Fogg and Kreitler, 1982), and the Milk River aquifer, USA and Canada (Hendry and Schwartz, 1990). Interestingly, Chaighari has the highest F^- and B concentrations in the study area (F^- of Chaighari is ~10 times of the mean of all other wells [0.14 mg/L] and B is ~3 times the mean of other isolated aquifers).

5.4 Redox conditions in groundwater

5.4.1 Results: Sampling of existing public supply wells can result in aeration of water through the pump-head or plumbing (Parkhurst et al., 1996; Nickson et al., 2000). McArthur et al. (2004) did not tabulate O_2 data from their study site in North 24 Parganas because they suspected sample aeration. It is possible that samples in this present study were aerated during collection. Notwithstanding these concerns, samples in the present study had very little O_2, with a mean of 1.04 mg/L. Only six of 53 samples had O_2 of more than 1.5 mg/L, and 17 samples had 1 to 1.5 mg/L. The E_H measurements by platinum electrodes fell mostly in a range of +15 mV to +120 mV with a mean of +80.8 mV. A few samples had much higher (n = 5, maximum +311.4 mV) or lower (n = 4, minimum -40.2 mV) values. The general range also agrees with observations of Swartz et al. (2004) of +20 to +100 mV. Excluding the two isolated aquifer wells in Nadia (locations #14 and #34), in general the deeper wells have lower E_H along with higher pH values.

Consistent with the low O_2 and E_H values, only two samples had NO_3^--N greater than the detection level (DL) of 0.12 mg/L. NO_2^- and PO_4^{3-} were not detected at any location (DL: 0.1 and 0.12 mg/L, respectively). NH_4^+ was detected at 36 locations (mean: 0.36 mg/L, maximum: 1.59 mg/L). SO_4^{2-} was detected in a number of wells in both the main and isolated aquifers, mostly in the northern part of the study area, with a mean of 7.1 mg/L and maximum of 39.6 mg/L. H_2S was not detected either by smell or taste in any sample (DL: 0.05 to 0.5 mg/L [Ross et al., 1999; Varner et al., 2004]) or by CHEMets in 2005 samples (DL: 0.05 mg/L). CH_4 concentrations were greater than room-air concentration (measured during analyses: ~250 μM) in 15 samples; 13 of these 15 samples had concentrations more than 1000 μM. The maximum was 68×10^3 μM at Iswarchandrapur (#34), followed by 32×10^3 μM at Hanspukuria (#14). It should be noted that due to the volatility of CH_4, and relatively long lead time between sampling

and analyses due to travel and shipping, these reported values might underestimate actual concentrations. Fe(II) and As(III) were the predominant Fe and As species in all sampled waters with detectable concentrations. Dissolved Fe(II) was almost indistinguishable from total dissolved Fe (Fe[II]/Fe mean: 97%), while As(III) averaged 72% of the total dissolved As measured from locations with concentrations above detection level (0.005 mg/L).

5.4.2 Environment: Oxidation-reduction processes, as defined by the activities of aqueous redox couples, generally tend to segregate into discrete zones in the aquifer following a predictable pattern (Chapelle, 1993). Berner (1981) classified the redox environments of sedimentary aquifers as oxic and anoxic (postoxic, sulfidic, and methanic) (Parkhurst et al., 1996). The oxic system is defined by the presence of measurable O_2. Parkhurst et al. (1996) used 1 mg/L as the arbitrary boundary between oxic and anoxic environments, while Chapelle et al. (1995) suggested 0.5 mg/L as the boundary. Systematic geochemical trends of redox zones depend on the nature of metabolic pathways of bacterial decomposition and the nature of organic matter (Martens and Goldhaber, 1978). Some trace elements (e.g. As, Cr) may change their redox state in the postoxic zone (Parkhurst et al., 1996). The redox zones can be demarcated by calculating the negative log of activity of electrons (p_e) in aqueous solutions, where

$$p_e = 16.9E_H \text{ at } 25^oC.$$

The p_e values of the various redox couples were calculated for the sample waters using PHREEQC with the MINTEQ thermodynamic database (Allison et al., 1990) for As, Fe, O and N species and the PHREEQC database (Parkhurst and Appelo, 1999) for C species. Following Parkhurst et al. (1996), a distribution plot of the observed platinum electrode potential (E_H) to calculated E_H of redox couples (computed from p_e) shows that the waters from both the main and isolated aquifers (Figure 5.10) lie in the postoxic environment of Berner (1981), while the river waters exist near the oxic-postoxic boundary. The observed values cluster mostly in the data range of Fe(II)/Fe(III) with some values in the range of As(III)/As(V) and approaching sulfidic. This suggests that in the western Bengal basin, notwithstanding the presence of several redox-sensitive couples, Fe(II)/Fe(III) is the dominant redox couple in deep groundwater. This observation agrees well with the finding of Barcelona et al. (1989) that average observed E_H agreed with values calculated using the Fe(II)/Fe(III) couple in a suboxic system and suggestions

of previous workers that Fe(III) reduction may be controlling the redox state of Bengal basin sediments (e.g. Bhattacharya et al., 1997; McArthur et al., 2004; Zheng et al., 2004). Sracek et al. (2004a) found that for Bangladesh water, E_H values calculated using As(III)/As(V) were lower than field measurements and suggested that this may be attributed to dominance of another redox couple.

Vanadium exists mostly in its oxidized state (V[V]) in hydrologic systems because of the low solubility of the reduced form (V[III]) (Parkhurst et al., 1996). V was detectable in all samples, with a mean of 0.09 mg/L. The highest V concentrations were detected in some of the deepest wells of the main aquifer (e.g. Kalikapore [#24]: 0.34 mg/L). V(V) is generally reduced to V(III) in the postoxic to sulfidic range at circumneutral pH, which suggests that deeper water of the western Bengal basin is not sufficiently reduced to immobilize V.

5.4.3 Governing processes: Similar to other regional studies in the Bengal basin (e.g. Aggarwal et al., 2000; Dowling et al., 2002, 2003), this study is limited by the number of sample locations and may not be sufficient to understand the processes operating at the local scale (centimeters to meters vertically and tens to hundreds of meters laterally). However, in spite of these constraints, redox-sensitive parameters show broad patterns with depth and distance from the Bay of Bengal (Figures 5.11 and 5.12). A depth versus E_H plot (Figure 5.11a) demonstrates a weak inverse relation ($r^2 = 0.28$), with relatively lower values from >200 m depth. Similar spatial trends of E_H and pH have been reported by Jackson and Peterson (1982). Mn, Fe (total and Fe[II]), As (total and As[III]), and SO_4^{2-} generally decrease with depth, while CH_4 and As(III)% seem to increase with depth (with some scatter). Similarly, when plotted against distance, Mn and SO_4^{2-} are higher in the northern part of the study area and tend to decrease southward (SO_4^{2-} outliers in South 24 Parganas may have been caused by modern or unflushed paleo-seawater [evident from a Cl^--normalized SO_4^{2-} plot to account for marine influence]). Fe and As may decrease southward, but the trends are not very prominent. These observations indicate that the redox processes operating in the western Bengal basin are depth-dependent.

5.4.3.1 Iron dissolution: Fe is ubiquitous in Bengal basin groundwater, and has been found to be correlatable with HCO_3^-. This correlation is suggested to have been caused by reductive

dissolution of Fe (oxyhydr)oxides by oxidation of organic matter (e.g. Nickson et al., 1998, 2000; McArthur et al., 2001; Ahmed et al., 2004). However, no such correlation was observed between Fe and HCO_3^- in samples of this study ($r^2 < 0.001$ for main aquifer), probably because other processes besides organic matter oxidation (e.g. weathering) also produce HCO_3^-. Some of the samples have Fe concentrations correlatable with Mn (Figure 5.13a), but the other locations have wide scatter, suggesting that some but not all of the Fe and Mn dissolution is causally related with overlapping redox zones. Fe and Mn should be more concentrated in the shallower depths (Farmer and Lovell, 1986; Stumm and Morgan, 1996) in response to post-depositional diagenetic remobilization, with peak Fe concentrations at shallower depths than Mn (Anwar et al., 2002). McArthur et al. (2004) noted that reduction of FeOOH is more dominant than reduction of Mn oxides toward the top and base of the aquifer at their study site. These observations do not hold well for samples in the present study, as Mn concentrations decrease strongly with depth.

5.4.3.2 Sulfur cycling: The decrease of SO_4^{2-} southward from Murshidabad indicates that 1) either the aquifer water becomes sulfidic as depth increases and results in deposition of authigenic sulfide or 2) the input of SO_4^{2-} in deeper groundwater of Nadia and North 24 Parganas was originally low. Zheng et al. (2004) opined that the very low SO_4^{2-}/Cl^- ratios in their study area suggest SO_4^{2-} reduction rather than low original SO_4^{2-} concentrations. H_2S was not detected in any of the samples in the present study and thus there is no direct proof of SO_4^{2-} reduction. However, H_2S has been reported from shallow groundwater from some locations of Murshidabad and South 24 Parganas of West Bengal (Mehta and Bhattacharya, c. 2000) and some areas in Bangladesh (Ahmed et al., 2004). It is possible that the high level of Fe(II) in most locations scavenged all of the reduced S species present in the water. High levels of authigenic sulfide deposition can take place even in a low-SO_4^{2-} system with high organic carbon content (Neumann et al., 2005). Pyrite and other authigenic sulfides have been documented from sediments in various locations within the Bengal basin (e.g. Das et al., 1996; Chowdhury et al., 1999; Chakraborti et al., 2001; Pal et al., 2002). McArthur et al. (2004) commented that diagenetic Fe sulfides in the sands of North 24 Parganas may have formed during the onset of anoxia as a result of SO_4^2 -reduction in connate water.

The $\delta^{34}S_{SO4}$ elucidates the S redox cycling in more detail. Incomplete SO_4^{2-} reduction causes ^{34}S to be depleted in the precipitating pyrite and progressively enriched in the residual SO_4^{2-}. Conversely, oxidation of this authigenic pyrite could introduce SO_4^{2-} depleted in ^{34}S (Faure, 1998). Hence, in a SO_4^{2-}-reducing system, the concentration of SO_4^{2-} should be inversely related to $\delta^{34}S_{SO4}$. Jacks et al. (1994) documented a $\delta^{34}S$ composition of ~10 ‰ for the monsoonal rainwater. Groundwater in a closed system without mixing and having $\delta^{34}S_{SO4}$ composition >10 ‰ can thus be suspected to have undergone extensive reduction (Zheng et al., 2004), while lower values may indicate oxidation. Results from this study show that $\delta^{34}S_{SO4}$ ranges from 5.7 to 45.8‰ VCDT, which suggests, given the predominance of monsoonal recharge (Stüben et al., 2003; see also Chapter 4), that both oxidation and reduction of sulfur have taken place. A plot of SO_4^{2-}/Cl^- versus $\delta^{34}S_{SO4}$ (Figure 5.14) shows an inverse trend in agreement with SO_4^{2-} reduction, but this trend bifurcates, which suggests that some of the SO_4^{2-} might have gone through repeated phases of reduction and reoxidation, as hypothesized by Zheng et al. (2004).

5.4.3.3 Carbon cycling: Zheng et al. (2004) showed that their few deeper groundwater samples from Araihazar in Bangladesh are generally low in HCO_3^- (<4000 μM), suggesting that this water is less evolved (McArthur et al., 2001). Zheng et al. (2004) also argued that deeper groundwater has relatively high O_2 concentrations due to lack of oxygen demand or limited availability of labile organic matter. However, in the present study, HCO_3^- concentrations in the deeper water of the main aquifer were relatively uniform, with a mean of 457 mg/L (7131 μM). A distance-O_2 plot (Figure 5.12f) qualitatively shows (relative to a concentration of 0.8 mg/L [50 μM], between the threshold concentrations of Chapelle et al. [1995] and Parkhurst et al. [1996]) that the oxygen content may decrease southward (equivalent to increasing depth), suggesting the progressive consumption of oxygen along the flow path. Dissolved organic carbon (DOC) concentrations were low but detectable at most locations. Chatterjee et al. (2004) reported values of DOC up to 12.9 mg/L from the Baruipur area of South 24 Parganas (depth not specified). The mean DOC concentration of the main aquifer (0.92 mg/L) from this study was lower than that of the isolated aquifers (1.65 mg/L). The persistence of DOC can reflect limited microbial activity or the presence of relatively refractory organic matter (Chapelle, 1993). The chemical nature and

source of the organic carbon can limit the amount of reductive bacterial activity (Beck et al., 1974; Martens and Goldhaber, 1978).

CH_4 concentrations >250 μM (room-air concentration during sample analyses) indicate highly reducing conditions (Berner, 1981; Zheng et al., 2004). Very high CH_4 concentrations (>2500 μM) were generally found in southern Nadia and North 24 Parganas. CH_4 in Bengal basin groundwater has also been documented by Ahmed et al. (1998), Harvey et al. (2002), and McArthur et al. (2004). CH_4 is a common product of decomposition of natural organic matter (NOM) in aquifer systems (Barker and Fritz, 1981; Coleman et al., 1988; Leuchs, 1988, Grossman et al., 1989; Simpkins and Parkin, 1993; Aravena et al., 1995b; Zhang et al., 1998) by pathways of acetate fermentation and CO_2 reduction by H_2 (Oremland, 1988). In the Bengal basin, possible sources of NOM include human wastes (Harvey et al., 2002, 2005; McArthur et al., 2004) and peat. Peat fragments in southern Bengal basin sediments are expected because of the geomorphic evolution of the delta (Umitsu, 1987, 1993; Islam and Tooley, 1999; Allison et al., 2003). Peat was formed as waterlogged back-channel deposits of the paleo-rivers in this area at about 5,000 years before present during late Quaternary sea-level change (Umitsu, 1993) when the erosional base levels of the paleo-rivers were much lower than present (Ravenscroft et al., 2001). Peat fragments have been recovered from Calcutta (Barui and Chanda, 1992; A. Mukherjee, University of Kentucky, unpublished data), North and South 24 Parganas (Umitsu, 1987, 1993; Banerjee and Sen, 1987; CGWB, 1994d; Pal et al., 2002; McArthur et al., 2004), and at various locations in Bangladesh (e.g. Reimann, 1993; Brammer, 1996; Ahmed et al., 1998; Safiullah, 1998; BGS/DPHE/MML, 1999; Islam and Tooley, 1999; AAN, 2000; Ishiga et al., 2000; Tareq et al., 2003; Swartz et al., 2004). Elevated CH_4 concentrations in the study area may be related to the existence of peat layers in the vicinity, although no peat was identified in the lithologic logs of the wells. However, CH_4 concentrations >500 μM were also observed at shallower depths in several locations in Murshidabad and Nadia. The detection of CH_4 and other reduced solutes in these wells probably cannot be explained by the presence of peat, as the author is not aware of any report of peat occurrence in these areas. Harvey et al. (2002) documented a similar situation in their study area in Munshiganj, Bangladesh, and commented that CH_4 in the shallow waters was derived from the dissolved inorganic carbon (DIC) pool and was probably formed by carbonate reduction. However, McArthur et al. (2004) argued that peat

could have been missed during drilling. Methanogenesis at shallow depths (2-3 m below the water table) has been reported (≥ 400 μM) in the sandy aquifer of Rømø, Denmark and has been attributed primarily to CO_2 reduction along with subordinate acetate fermentation, occurring predominantly in microenvironments with higher H_2 concentrations (Hansen et al., 2001).

Understanding the $\delta^{13}C$ composition of dissolved inorganic carbon (DIC), which is mostly HCO_3^-, might give some insight to C cycling within the system. Zheng et al. (2004) commented that depleted values of $\delta^{13}C_{DIC}$ probably confirm that CO_2 from oxidation of organic matter contributes a portion of DIC in Bengal basin groundwater. BGS/DPHE/MML (1999) recorded $\delta^{13}C_{DIC}$ up to +10‰, which is common for methanogenic CO_2 (Whiticar, 1999; McArthur et al., 2001). McArthur et al. (2004) showed that the $\delta^{13}C_{DIC}$ content at two of three locations studied in North 24 Parganas becomes enriched with depth (range 0 to -10 ‰ VPDB). At one of these locations, peat fragments were identified in the aquifer, which may have supported methanogenesis. The location where an opposite trend was observed had a peat layer embedded in an overlying thick aquitard, which may have limited the CH_4 mixing. McArthur et al. (2001) mentioned that at their study location in Bangladesh (Faridpur), $\delta^{13}C$ became depleted with increasing Ca, suggesting the dissolution and equilibration of depleted calcite (0 to -6‰ [Quade et al., 1997; Singh et al., 1998]) or pedogenic carbonates (lower Himalayan carbonates: ~-12 ‰ [Quade et al., 1997]) by enriched methanogenic CO_2 (+5 to +10‰). The depleted DIC in groundwater can form from oxidation of CH_4 (McArthur et al., 2001; Zheng et al., 2004).

In the present study, the $\delta^{13}C_{DIC}$ in the shallower part of the main aquifer (~ -8 ‰ VPDB) is generally more depleted than the deeper part (~ 0‰ VPDB), but this trend has a number of outliers, suggesting that multiple processes are involved (Figure 5.15). No trend was observed between $\delta^{13}C_{DIC}$ and Ca or HCO_3^-. Enrichment of $\delta^{13}C_{DIC}$ with depth may take place as a result of lessened biological activity in the deeper part of the main aquifer; incomplete CO_2 reduction to form highly ^{13}C-depleted CH_4, thereby progressively enriching the residual CO_2 (consistent with Harvey et al. [2002] and the existence of higher concentration of CH_4 at depth [Figure 5.11i]); lessened dissolution of depleted carbonates at depth; and/or mixing with $\delta^{13}C$-enriched connate water ($\delta^{13}C_{DIC}$ ~ 0 ‰ for seawater). Alternatively, depleted DIC (at shallower depths as

well as in some of the deep water) could have formed from some CH_4 oxidation. Most of the wells appear to reflect one or more of these trends, but Chaighari (#6) was probably influenced more by organic matter oxidation, as evident from the most depleted $\delta^{13}C_{DIC}$ (-8.2‰ VPDB).

5.4.4 Summary: The finding from this study that Fe(III) reduction is the dominant redox process in deeper groundwater of the western Bengal basin is consistent with other studies of groundwater in the Bengal basin. However, the co-existence of O_2, NH_4^+, Fe(II), As(III), V, SO_4^{2-}, and CH_4 in various wells indicates that the aquifer volumes sampled by these wells are not in redox equilibrium. Similar partial equilibrium systems have been observed in other studies, e.g. Fe(III) reduction and methanogenesis (Berner, 1981), SO_4^{2-}-reduction and methanogenesis (Kuivila et al., 1989; Parkes et al., 1990), SO_4^{2-} and Fe(III) reduction (Canfield et al., 1993; Wersin et al., 1993; Postma and Jakobsen, 1996), and Fe(III) reduction, SO_4^{2-}-reduction and methanogenesis (Jakobsen and Postma, 1999).

5.5 Arsenic in deeper groundwater

Elevated arsenic (>10 µg/L) has been observed in a majority of the deep groundwater samples from this study, with concentrations reaching > 137 µg/L. Arsenic concentrations in Bengal basin sediments are close to the average crustal concentration (Swartz et al., 2004). Most of the recent studies from the Bengal basin have hypothesized the release of sorbed As phases by reductive dissolution of FeOOH (e.g. Bhattacharya et al., 1997; Nickson et al., 2000; McArthur et al., 2001, 2004; Harvey et al., 2002, 2005; Dowling et al., 2002; Stüben et al., 2003), although some authors have also suggested As liberation by oxidation of As-enriched pyrite (e.g. Mallick et al., 1995; Das et al., 1996; Mandal et al., 1998).

Reductive dissolution and mobilization of As(III) can happen in less reducing environments (Seyler and Martin, 1989; Eary and Scramke, 1990; Kuhn and Sigg, 1993) or even oxidizing environments (Abdullah et al., 1995). Van Geen et al. (2004) showed that reductive dissolution of As can take place even in mildly oxic conditions. Anaerobic metal-reducing bacteria could play a catalytic role in mobilization of As from Bengal basin sediments (Islam et al., 2004). Such dissimilatory microbial reduction may be stimulated by addition of a substrate

(van Geen et al., 2004) and may be performed by SO_4^{2-}-reducing bacteria (Inskeep et al., 2002; Oremland et al., 2002).

Several studies of Bengal basin groundwater have observed a moderate to strong correlation between As and Fe, as expected from reductive dissolution of FeOOH onto which As is adsorbed (e.g. Nickson et al., 1998, 2000; McArthur et al., 2001; Dowling et al., 2002 [locally up to $r^2 = 0.8$ to 0.9]; Stüben et al., 2003). In the samples of this study, Fe correlates weakly with As ($r^2 = 0.26$, $p = 0.01$, Figure 5.13b), although Fe(II) yields a better correlation with As(III) ($r^2 = 0.32$, Figure 5.13c). Swartz et al. (2004) showed that As in sediments of the deeper aquifer in Munshiganj, Bangladesh (~165 m), does not co-vary well with Fe. Such weak correlations suggest that reduction of As and Fe may not be simultaneous. Islam et al. (2004) showed that As is released from sediments after Fe(III) reduction. McArthur et al. (2004) suggested that some of the As released by reductive dissolution can be re-sorbed to the residual or partially reduced FeOOH. Complex cycles of oxidation and reoxidation of Fe and S species can cause preferential immobilization of As (Zheng et al., 2004). At a regional scale, the As concentrations in our samples do not have significant correlations with Mn ($r^2 = 0.12$), NH_4^+ ($r^2 = 0.02$), CH_4 ($r^2 = 0.03$), DOC ($r^2 < 0.01$), O_2 ($r^2 < 0.01$), HCO_3^-($r^2 = 0.03$), or chalcophile elements (e.g. Zn [$r^2 < 0.01$]), as have been suggested by previous workers (e.g. Mn [Stüben et al., 2003], NH_4^+ [Dowling et al., 2002; Ahmed et al., 2004], CH_4 [Ravenscroft et al., 2001; McArthur et al., 2001, 2004; Dowling et al., 2002], DOC [Ahmed et al., 2004], and Zn [Stüben et al., 2003]). The lack of these correlations suggests that As is mobilized by multiple processes, perhaps by reactions having occurred in the shallow subsurface, above the sampling depths of this study. Moreover, the lack of correlation of As with pH ($r^2 = 0.12$) indicates that pH-dependent sorption reactions probably do not play a significant role in regulating As mobility in deeper groundwater of the western Bengal Basin.

Although the presence of peat layers in certain areas can act as the redox driver for mobilization of As, as argued by McArthur et al. (2004), this explanation does not appear to apply to areas such as Murshidabad and northern Nadia, where the existence of peat in the aquifer framework up to 300 m depth is highly improbable in light of the Ganges-Brahmaputra delta-building history. Harvey et al. (2002, 2005, 2006) proposed that anthropogenic organic

matter (human waste) or natural organic matter (NOM) can infiltrate through the bottoms of rivers, lakes and ponds, and thus influence groundwater redox chemistry. Although this explanation is plausible in light of the large population of the study area, infiltration of dissolved organic matter (DOM) cannot solely explain the existence of the As in deeper groundwater, as most of the DOM should be oxidized at shallower depths under normal vertical hydraulic gradients.

The authors envision a scenario whereby As liberated by metal (oxyhydr)oxide reduction remains mobile except to the extent that it is sequestered in authigenic sulfides. McArthur et al. (2004) commented that As desorbed during reduction of Mn oxides can be re-sorbed onto residual FeOOH phases. Results from the present study indicate that Mn is reduced at a shallower depth than Fe, so As that is resorbed onto residual FeOOH phases will be remobilized by subsequent Fe(III)-reduction. Although McArthur et al. (2004) commented that SO_4^{2-} reduction is improbable at present because of the dominance of Fe(III) reducing bacteria over SO_4^{2-} reducing bacteria (Chapelle and Lovely, 1992), the $\delta^{34}S_{SO4}$ results from this study suggest that SO_4^{2-}-reduction is occurring but probably overlapping with other redox zones. This process might result in deposition of authigenic Fe sulfides, which could partially scavenge the As, depending on the initial SO_4^{2-} concentrations. The reason that As still exists in solution in sulfidic and even methanogenic zones is because of the partial redox equilibrium and the possibility of limited SO_4^{2-} availability in deeper groundwater. Zheng et al. (2004) mentioned that the introduction of small amounts of oxygen into a SO_4^{2-}-reducing environment with high As/Fe ratios can result in re-oxidation of Fe(II). This process may also contribute to remobilization of some previously immobilized As in sulfides. Furthermore, the recirculation of water by extensive pumping (Chapter 3) may cause homogenization of the aquifer and availability of more aerated water from shallower depths. Although such reoxidation is highly unlikely at the regional scale in a large, reduced aquifer like the main aquifer of the study area, it could happen at smaller scales, as suggested by the occurrence of lower As(III)% values at depth (Figure 5.11f). Moreover, oxidation of As(III) to As(V) can take place even in anoxic environments by activity of autotrophic microorganisms (Rhine et al., 2006).

5.6 River water-groundwater interaction

5.6.1 River water chemistry: The rivers in the study area and their possible interactions with the main aquifer can be classified into three groups: the Ganges (G), Jalangi-upper Ichamati (JI), and the tidal rivers (T). Group G consists of the three samples from the Bhagirathi-Hoogly (R1, R2, and R3). As the main Indian distributary of the Ganges, the Bhagirathi-Hoogly reflects the weathering of upstream terrains, including the Himalayas. The JI are relatively smaller rivers and probably reflect more local recharge (R4, R5, R6), while T (R7), the sample from the lower reach of the Ichamati, represents the chemistry of southern tidal rivers.

The hydrochemical facies distribution (Figure 5.3) shows that while T is of Na-Cl type, consistent with diluted sea water, G and JI are of Ca^{2+}-HCO_3^- type, and almost indistinguishable from the main aquifer samples in this facies. All the river samples were slightly alkaline (pH 7.5 to 8.3) and had high E_H (266 to 408 mV), suggesting oxidizing conditions. Of these, the pH ranges of the samples from the Bhagirathi-Hoogly and Jalangi (which discharges to the Bhagirathi-Hoogly and has a tributary from the Ganges main channel) are higher than the Ichamati samples. G and JI generally have major ion concentrations in the lower range of main aquifer groundwater and relatively low Si and HCO_3^-. The carbonate units in the provenance of the Gangetic sediments dominate the ionic distribution of the river water from north to south in the basin (Galy and France-Lanord, 1999). The G and JI samples fall on the carbonate dissolution trend of the Na-normalized Ca versus HCO_3^- plot (not shown), in agreement with this idea. The JI samples generally are more dominated by carbonate dissolution and more enriched with other major ions than the G samples, probably as a result of enhanced evaporation. This idea is further reinforced by the higher SO_4^{2-}/Cl^- ratio (G: 3.8 to 2.9; JI: 1.1 to 0.4) and more depleted $\delta^{18}O$ (-5.6 to -5.7 ‰ versus -2.9 to -3.1 ‰) of G relative to JI (see Chapter 4). Galy and France-Lanord (1999) concluded that river water originating in the Himalayas has depleted $\delta^{34}S_{SO4}$ values in response to the higher input of SO_4^{2-} by oxidation of pyrite. G samples have higher concentrations of SO_4^{2-} than JI, but the $\delta^{34}S_{SO4}$ of those samples were not determined.

Based on the similarity in $\delta^{18}O$ data (see Chapter 4), there may be some inflow of the G water to the thinner portions of the main aquifer in the vicinity of Murshidabad and near Calcutta. Conversely, there is probably groundwater discharge to JI. These claims are also

supported by the regional groundwater flow model developed in Chapter 3, showing that during present-day summers (the sampling season), there should be natural groundwater inflow from the Bhagirathi-Hoogly in northern Murshidabad and outflow to the Jalangi and upper reaches of the Ichamati. Irrigational/urban overdraft pumping can cause inflow from the Bhagirathi-Hoogly in west-central Murshidabad and near Calcutta. If this is true, then the chemical differences between the river water and groundwater in these localities may reflect groundwater evolution by reactions within the aquifer sediments and the hyporheic zones. Groundwater discharge along the Jalangi and upper Ichamati probably explains the higher concentrations of solutes in those streams relative to the Bhagirathi-Hoogly. The interaction of group T with groundwater could not be evaluated because of strong seawater influence.

5.6.2 Arsenic in river water: One very interesting observation was the occurrence of elevated As concentrations for all three samples of the JI group. The samples were re-analyzed three times from splits to validate this observation. Elevated As has not been reported in most studies of surface water in the Bengal basin, although Stüben et al. (2003) noted As in water of a small stream (River Gobra) in Murshidabad. They suggested that the As in this stream has been mobilized by reduction of Mn in the alluvial sediments because of the low oxygen content of the stream water relative to the Bhagirathi-Hoogly. However, given the observed E_H values of the present study, groundwater discharge is a more plausible explanation for occurrence of As in stream water. Elevated As was detected in groundwater samples (locations #27, #28, #30, #31, #32, #36, #44, and #45) near the JI sample locations. The differences in As concentrations between the river water and deeper groundwater could be caused by enrichment by evaporation, outflow from shallower, more As-enriched groundwater (not analyzed in this study), and (or) oxidation of As-bearing pyrite in river bank and bed sediments. Although the valence state of the As was not determined, it was probably As(V) because of the elevated E_H values and lack of Fe and Mn.

5.7 Geochemical modeling

5.7.1 Saturation indices: Table 5.5 lists the ranges of SI values for some of the important phases that are thought to affect the chemistry of the deeper groundwater and major rivers in the study area. SI values for phosphate and sulfide phases were not calculated because those solutes were

below detection level. Previous literature on SI values for Bengal basin groundwater is very limited (e.g. Ahmed et al., 2004; Sracek et al., 2004a; Swartz et al., 2004). Groundwater is highly undersaturated with respect to oxygen but has higher-than-atmospheric P_{CO2}, consistent with DIC inputs from organic matter oxidation and carbonate dissolution. Sracek et al. (2004a) reported similar values of P_{CO2} for Bangladesh. SI for methane for most wells is slightly undersaturated or near equilibrium. Groundwater is undersaturated with respect to the major As phases (e.g. arsenolite, As_2O_5, and $FeAsO_4 \cdot 2H_2O$) and Mn oxide phases (e.g. birnessite, bixbyite, manganite, nsutite, and pyrolusite), indicating that once As and Mn enter into solution, they do not precipitate. Groundwater is highly to moderately supersaturated with respect to Fe(III) (oxyhydr)oxide phases like magnetite, hematite, goethite, lepidocrosite, maghemite, Mg-ferrite, and ferrihydrite, but near equilibrium or undersaturated with respect to Fe(II) minerals like siderite and mixed Fe oxides like $Fe_3(OH)_8$. Swartz et al. (2004) commented that the Fe(II) in pore water of the Bengal basin may have been derived from Fe(II) minerals like siderite, vivianite ($Fe_3(PO_4)_2$), and mixed Fe (oxyhydr)oxides (e.g. green rust), which form from biogenic reduction of FeOOH (Zachara et al., 1998; Nickson et al., 2000). Groundwater is supersaturated with respect to carbonate phases except for rhodochrosite. Ahmed et al. (2004) suggested that the near-equilibrium SI values for carbonates indicate that the high HCO_3^- values in Bengal basin groundwater cannot be totally attributed to carbonate dissolution and may have a significant input from organic carbon oxidation. Sracek et al. (2004a) calculated siderite supersaturation for Bangladesh groundwater. Groundwater and river water are supersaturated with respect to quartz and undersaturated with respect to amorphous SiO_2, in agreement with the stability diagrams (Figure 5.6).

5.7.2 Inverse modeling of groundwater evolution along flow paths: Reaction-path models have been used in various studies worldwide to elucidate hydrochemical evolution along regional (tens to hundreds of kilometers) flow paths, as reviewed by Nordstrom (2004) and Glynn and Plummer (2005). However, no reaction-path modeling has been reported for the western Bengal basin. The Piper plot (Figure 5.3) indicates some major-ion evolution along groundwater flow paths. Intense irrigational pumping beginning around 1970 may have disrupted the regional groundwater flow path in the western Bengal basin, resulting in local flow paths towards centers of pumping (see Chapter 3). However, the earlier discussion of groundwater quality (Section 5.3)

indicated that some major solute trends along depth and distance can still be discerned, and hence chemical evolution of groundwater at the regional scale can still be evaluated.

Sixty reaction-path (inverse) models, converging within the specified maximum uncertainty range, were developed for the study area (Table 5.6). Six models developed for evolution of Chaighari groundwater (#6) by mixing with Bay of Bengal water failed to converge and are not included in Table 5.6. Of the 60 models, 37 models involved flow with both mixing and reactions, and 23 involved flow with reactions but not mixing. The models were broadly used to investigate:

i) evolution of isolated aquifer water (locations #6, #14, #18, #20, #34, #52) by mixing with connate water (paleo-Bay of Bengal) or modern Bay of Bengal seawater;

ii) evolution of the main aquifer water with relatively high Cl^- concentrations in the northern part of the study area (Murshidabad and Nadia, e.g. #38) by mixing with connate water or diffusion from isolated aquifers at depth (models 30 and 31) (following Ranganathan and Hanor, 1987);

iii) evolution of the main aquifer water with relatively high Cl^- concentrations in the southern part of the study area (North and South 24 Parganas, e.g. #16, #19, #23, #24) by mixing with connate water via diffusion from isolated aquifers (models 32 and 38), or by seawater intrusion or tidal water infiltration (e.g. #25, #53);

iv) river water-groundwater interaction: mixing of infiltrating river water (whether through natural inflow or induced infiltration by pumping) with up-gradient groundwater to evolve down-gradient groundwater (e.g. #2, #11, #35, #37); mixing of discharging groundwater with upstream river water to evolve downstream river water (R2, R4); and tidal influence on river water chemistry (R7).

Because of the similarities of major solute chemistry for most parts of the individual aquifers, mass balance models were only developed for pair of wells/river locations that were thought to represent two distinct end-member waters or for mixing of two waters followed by reactions to produce a third water. For many locations (particularly the isolated wells), present-day hydraulic connections between the respective wells have not been established by physical means; the flow paths are intended to test hypotheses of the possible hydrochemical evolution processes from similar up-gradient water in the recent geologic past, during delta progradation.

Similarly, the mixing with Bay of Bengal water for the isolated aquifers and deeper main aquifer water (e.g. #16, #23, #24) was meant to be a proxy of the past seawater intrusion from the proto-Bay of Bengal and interaction with the paleo-groundwater. Mixing with Bay of Bengal water for shallower main aquifer wells (e.g. #25, #53) in North and South 24 Parganas was used to evaluate present-day seawater intrusion.

The mass balance processes in the models included carbonate weathering (calcite, dolomite, and siderite dissolution and precipitation), cation exchange (Ca^{2+}/Mg^{2+}, Ca^{2+}/Na^{+}, Ca^{2+}/K^{+}, Na^{+}/Mg^{2+}, $Mg^{2+}/K^{+}$and Na^{+}/K^{+}), carbon cycling (CO_2 and CH_4 dissolution and exsolution; CH_2O [organic carbon] oxidation), and sulfur cycling (pyrite dissolution and precipitation). Halite dissolution was used for 23 models as a proxy for mixing with connate water from the proto-Bay of Bengal. All but six models (models 51-55) relating to the mixing of river water with groundwater were balanced for Cl^- (Cl^- balance is not shown in Table 5.6). The unbalanced, questionable models depict very high (up to 100%) mixing of river water with groundwater, which is probably an unrealistic scenario. Si balance was used to evaluate the role of silicate weathering processes. While the balance would indicate minimal Si influx from weathering within the specified uncertainty, a failure suggests the presence of processes that have not been accounted by the mechanisms included in the models. Models for isolated aquifers (locations #6 [except model 3], #18, #20, and #52) and the deeper main aquifer (locations #16, #19 [except model 38], and #38) indicated some Si cycling. All of these wells are suspected to have water with long residence times (as suggested in Chapter 3), which favors silicate weathering because of the slow dissolution kinetics (Langmuir, 1997). The reason for the imbalance of location #53 (models 47-48) is unclear, but it could have been caused by inaccuracy in the choice of the up-gradient water.

In general, the convergence of the reaction-path models (except evolution of location #6 from Bay of Bengal water and the mixing models of groundwater-river water interaction) indicates that various processes could control chemical evolution of groundwater in the western Bengal basin. Within the constraints of the present study, no definite reaction pathways can be identified. Conservative stable isotopes ($\delta^{18}O$ and $\delta^{2}H$), which can indicate distinct sources of water, are relatively homogeneous with depth and between different aquifers, and dependent on

distance from the sea (see Chapter 4). In addition, the selection of acceptable mass-balance models is difficult in light of the simplifications undertaken for model design, particularly the selection of end members, the program's requirement that mixing precede reactions, and the assumption of one-dimensional flow without dispersion.

All of the models (except models 57 and 58 for evolution of R4, which did not include cation exchange) involved a combination of cation exchange and carbonate weathering. Siderite dissolution was observed for all flow paths involving groundwater and sea water mixing. Pyrite was found to precipitate along all groundwater flow paths (except models 41, 43, 44, 45), supporting our previous inference about the redox environment. Models 43 and 44, which involve pyrite dissolution as water of location #23 evolves to #24, are suspect because $\delta^{34}S$ for #23 is much more enriched than for #24. Many of the models also indicate exsolution of CO_2 along flow paths. While this seems to be possible in light of the higher-than-atmospheric P_{CO2} values, such CO_2 outgassing is not expected to happen within deeper groundwater, which is isolated from the atmosphere. However, gas bubbles were observed while collecting many of groundwater samples in this study, which may indicate CO_2 exsolution as a result of aeration and depressurization during pumping.

All of the isolated aquifers except Chaighari (#6) could have evolved as a result of mixing of main aquifer water with paleo-seawater. Chaighari may evolved from a groundwater similar to any of the selected upgradient wells that underwent cation exchange ($+K^+$, $+Na^+$, $-Ca^{2+}$, $-Mg^{2+}$), carbonate dissolution (mostly dolomite and siderite), consumption of CH_4 and CH_2O, and precipitation of pyrite. The evolution of the brackish main aquifer waters through diffusion from more saline isolated aquifers seems to be possible for locations #16 and #38, but is improbable for #19, because mixing of >75% of isolated aquifer water (with composition of #52) would be required.

River sample R2, representing the Bhagirathi-Hoogly water, though spatially separated from R4 (the northernmost River Jalangi location), was assigned as the upstream end-member for models 57 and 58 with the rationale that both rivers are distributaries of the Ganges, and R2 should more closely resemble the Ganges. Those models suggest that R4 and R5 (the two As-

contaminated river locations) have significant inflow from groundwater with composition of #28 and #32 (up to 24% for R4) and #36 (up to 12% for R5). Locations #28, #32, and #36 all have elevated As concentrations, thus reinforcing the inference in section 5.6.2 about discharge of As-contaminated groundwater to smaller rivers in summer. The composition of upstream Ichamati water (R6) can evolve to the downstream composition (R7) by mixing with a large amount (up to 47%) of Bay of Bengal water (model 60).

5.8 Conclusion

This study has delineated patterns of, and inferred the controls on, deeper groundwater and stream-water quality in the western Bengal basin. The importance of the study lies in assessing the groundwater quality of the deeper, semiconfined regional aquifer, whose shallower parts have been reported to be contaminated by As. Like studies of regional aquifers elsewhere, this study entailed sampling from public water-supply wells, which are screened over depths of a few meters to tens of meters. While sampling from such wells results in depth-integrated data, it can also mask smaller-scale geochemical heterogeneities (Ronen et al., 1987; Parkhurst et al., 1996; Fryar et al., 2001). However, for most of the wells (except a few in Murshidabad), the thickness of the screened intervals is probably small relative to the total depth of the aquifer considered at those locations. Notwithstanding this constraint of large screened intervals, groundwater analyses show distinct spatial (along depth and distance) and chemical trends indicative of various hydrochemical processes. The depths of the sampled wells for the main aquifers generally increase towards the south, consistent with the hydrostratigraphy.

In general, the groundwater of the main aquifer is chemically distinctive from that of the isolated aquifers, indicating different recharge sources and (or) pathways of evolution. The major-ion composition of water in the main aquifer in the northern part of the basin is a Ca^{2+}-HCO_3^- type, which evolves to six other facies toward the south in response to mixing with intruded seawater from the Bay of Bengal or connate waters as well as reactions. Carbonate dissolution and cation exchange may be the dominant processes influencing the major-ion composition, but silicate weathering also plays an important role. The predominant anion (HCO_3^-) in the main aquifer appears to be introduced as a combination of oxidation of NOM and mineral weathering. The Na^+-Cl^- waters of the isolated aquifers are believed to be connate water

from the proto-Bay of Bengal, which has been significantly modified by diagenetic processes and recharge from the overlying aquifer.

Multiple mechanisms control the redox chemistry of the aquifers. Average E_H of the sub-oxic water is mostly similar to the values calculated using the Fe(II)/Fe(III) redox couple and extends into the As(III)/As(V) range. The redox processes are depth-dependent and hydrostratigraphically variable. The water contains little or no NO_3^-, with no detectable PO_4^{3-} and H_2S. A partial redox equilibrium model with overlapping redox zones is proposed. Concentrations of SO_4^{2-} and Mn decrease with increasing depth below the surface and with distance from north to south. Highest concentrations of total and reduced species of Fe and As generally occur at depths ~100 m bgl, with an increase in the $As(III)/As_{total}$ ratio and in CH_4 concentrations with depth.

Arsenic mobilization may be controlled by microbially mediated Fe(III) reduction, but such mobilization probably involves multiple processes, as indicated by the weak correlation between Fe and As and by the lack of correlation with several other parameters suggested by previous workers. Once mobilized from the sediments, As is likely to persist unless sequestered by authigenic pyrite. However, $\delta^{34}S$ data suggest that such pyrite can be reoxidized, probably in micro-environments.

The chemistry of the River Bhagirathi-Hoogly is somewhat different from that of the other, smaller streams in the area (e.g. the River Jalangi and upper reaches of the Ichamati). The northern parts of the deeper main aquifer may receive some recharge from the Bhagirathi-Hoogly, but subsequently undergo moderate to extensive chemical evolution. Groundwater discharge into the Jalangi and Ichamati in summer (supported by groundwater modeling by [Chapter 3] and geochemical modeling) appears to cause elevated concentrations of As in these streams.

Table 5.1: Location and details of the groundwater and river water samples from the western Bengal basin.

No.	Well location	Block/Town	District [a]	Latitude	Longitude	Screen top (m bgl) [b]	Screen bottom (m bgl) [b]	Aquifer Type [c]	Sampling date (d/m/y)	HCA Group [d]
1	Lalgola	Lalgola	MD	24.42	88.25	42	66	Main	20/5/04	1
2	Lalbag Morgue	Murshidabad	MD	24.23	88.27	20	32	Main	21/5/04	1
3	Kantanagar	Bhagwangola-I	MD	24.34	88.31	48	66	Main	21/5/04	1
4	Edrakpur	Nawda	MD	23.91	88.46	52	82	Main	22/5/04	1
5	Takipur	Beldanga-I	MD	23.87	88.25	31	55	Main	22/5/04	1
6	Chaighari	Behrampur	MD	24.16	88.41	209	228	Isolated (<300 m)	23/5/04	2
7	Sekendra	Raghunathganj-I	MD	24.50	88.08	21	37	Main	24/5/04	1
8	Behrampur	Behrampur town	MD	24.09	88.26	47	74	Main	25/5/04	1
9	Debagram	Kaliganj	ND	23.69	88.33	48	78	Main	25/5/04	1
10	Juranpur	Kaliganj	ND	23.72	88.22	43	64	Main	26/5/04	1
11	Birpur	Nakashipara	ND	23.63	88.48	164	185	Main	26/5/04	1
12	Bethuadahari	Nakashipara	ND	23.61	88.43	72	89	Main	27/5/04	1
13	Jumpukur	Kaliganj	ND	23.72	88.38	246	269	Main	27/5/04	1
14	Hanspukuria	Tehatta-II	ND	23.74	88.48	215	230	Isolated (<300 m)	28/5/04	2
15	Gagnapur	Ranaghat-II	ND	23.14	88.64	145	176	Main	29/5/04	1
16	Berachampa (Aminpur)	Deganga	NP	22.69	88.67	274	293	Main	1/6/04	1
17	Janapoll	Habra-I	NP	22.87	88.69	122	151	Main	2/6/04	1
18	Chikanpara	Gaighata	NP	22.93	88.77	400	409	Isolated (>300 m)	2/6/04	3
19	Dalalpara	Bashirhat town	NP	22.69	88.85	206	230	Main	3/6/04	1
20	Bansjhari Mullickpur	Bashirhat-I	NP	22.58	88.88	262	273	Isolated (<300 m)	3/6/04	2
21	Berachampa	Deganga	NP	22.70	88.68	140	155	Main	4/6/04	1
22	Eojhnagar	Bashirhat-II	NP	22.71	88.72	121	151	Main	4/6/04	1
23	Ghasiara	Sonarpur	SP	22.44	88.46	216	240	Main	5/6/04	1

Table 5.1 (continued)

No.	Well location	Block/Town	District [a]	Latitude	Longitude	Top	Bottom	Aquifer	date	HCA
24	Kalikapore	Sonarpur	SP	22.40	88.48	220	240	Main	5/6/04	1
25	Canning Town	Canning-I	SP	22.32	88.65	170	189	Main	7/6/04	1
26	Habaspur	Bhagawangola-I	MD	24.32	88.34	61	76	Main	16/5/05	1
27	Chua	Hariharpara	MD	24.03	88.45	70	84	Main	17/5/05	1
28	Surangapur	Nawda	MD	23.93	88.46	81	96	Main	17/5/05	1
29	Mahimapur Palace	Murshidabad	MD	24.21	88.26	20	32	Main	18/5/05	1
30	Kismat-Imadpur	Hariharpara	MD	24.03	88.35	56	71	Main	18/5/05	1
31	Nazirpur	Tehatta-1	ND	23.86	88.54	85	110	Main	19/5/05	1
32	Narayanpur	Karimpur-II	ND	23.92	88.55	79	108	Main	19/5/05	1
33	Palashipara	Tehatta-II	ND	23.79	88.46	71	95	Main	20/5/05	1
34	Iswarchandrapur	Tehatta-I	ND	23.76	88.46	211	217	Isolated (<300 m)	20/5/05	2
35	Dhubulia	KrishnaNagar-II	ND	23.50	88.45	103	132	Main	21/5/05	1
36	Sonatala	KrishnaNagar-II	ND	23.52	88.51	110	140	Main	21/5/05	1
37	Gobrapota	KrishnaNagar-I	ND	23.42	88.55	101	120	Main	22/5/05	1
38	Bhaluka	KrishnaNagar-I	ND	23.35	88.41	261	279	Main	22/5/05	1
39	Bhimpur	Krishnanaga-I	ND	23.43	88.62	182	211	Main	23/5/05	1
40	Newtown	Rajarhat	NP	22.58	88.45	91	120	Main	26/5/05	1
41	Patharghata	Rajarhat	NP	22.58	88.51	96	120	Main	26/5/05	1
42	Ghentugachia	Chakdah	ND	23.03	88.59	100	129	Main	27/5/05	1
43	Kamagachi	Ranaghat-I	ND	23.22	88.56	122	152	Main	27/5/05	1
44	Panchita	Bongaon	NP	23.11	88.80	162	193	Main	28/5/05	1
45	Bongaon Hospital	Bongaon town	NP	23.05	88.82	177	202	Main	28/5/05	1
46	Rampur	Gaighata	NP	22.95	88.75	181	199	Main	29/5/05	1
47	Kankphul	Habra-II	NP	22.86	88.62	159	190	Main	29/5/05	1
48	Bamangachi	Barasat-I	NP	22.75	88.51	127	158	Main	30/5/05	1
49	Humaipur	Barasat-II	NP	22.68	88.47	128	159	Main	30/5/05	1
50	Haroa	Haroa	NP	22.60	88.68	137	167	Main	31/5/05	1
51	Arsula	Baduria	NP	22.74	88.77	117	148	Main	31/5/05	1

Table 5.1 (continued)

No.	Well location	Block/Town	District [a]	Latitude	Longitude	Top	Bottom	Aquifer	date	HCA
52	Murarisha	Hasnabad	NP	22.59	88.84	330	362	Isolated (>300 m)	1/6/05	3
53	Kalinagar	Sandeshkhali-I	NP	22.45	88.87	142	165	Main	1/6/05	1
	River location	**River name**						**River group[e]**		
R1	Mayapur	Bhagirathi-Hoogly	ND	23.42	88.39			G	28/5/04	
R2	Behrampur	Bhagirathi-Hoogly	MD	24.09	88.26			G	23/5/04	
R3	Belur	Bhagirathi-Hoogly	HW	22.63	88.36			G	11/6/04	
R4	Amtala	Jalangi	MD	23.93	88.46			JI	17/5/05	
R5	Sonatala	Jalangi	ND	23.52	88.51			JI	21/5/05	
R6	Bongaon	Ichamati	NP	23.05	88.83			JI	28/5/05	
R7	Taki	Ichamati	NP	22.59	88.94			T	31/5/05	

[a] MD: Murshidabad, ND: Nadia, NP: North 24 Parganas, SP: South 24 Parganas, HW: Howrah (opposite Calcutta)
[b] bgl: below ground level
[c] See Section 5.1.1 (Hydrostratigraphic framework) for details about aquifer types
[d] See Sections 5.2.3 and 5.3 for HCA
[e] G: River Ganges (River Bhagirathi-Hoogli); JI: Rivers Jalangi and Ichamati; T: tidal rivers (lower reach of River Ichamati)

Table 5.2a: Field measurements and major solute composition of the water samples. Loc. corresponds to no. in table 5.1. All units are in mg/L except where mentioned. Blank fields indicate no measurement.

Loc.	T (^{o}C)	pH	Eh (mV)	SC (µS)	O_2	Ca[a]	K	Mg	Na	Si	Cl	SO_4^{2-} [b]	HCO_3^-
1	29.1	7.10	15.08	894	0.94	136.67	4.08	36.85	38.16	13.46	50.10	13.45	368.00
2	28.4	6.92	311.42	1061	1.50	154.06	7.78	44.87	53.13	12.73	56.75	31.00	590.70
3	28.1	7.02	79.84	643	1.10	117.35	2.95	26.13	13.22	15.24	3.07	bdl	436.00
4	28.0	6.91	120.72	736	0.83	132.50	2.59	30.19	18.74	17.08	3.19	11.40	490.00
5	28.3	6.92	83.79	768	0.86	130.76	2.65	34.22	23.26	16.18	10.37	3.44	481.80
6	32.8	8.09	17.87	6490	1.29	bdl	8.28	1.23	1557.54	7.80	1620.00	bdl	1474.20
7	27.8	6.94	81.57	873	1.23	152.73	3.17	36.80	20.43	14.12	35.50	21.45	502.50
8	28.5	6.91	118.34	705	0.49	110.21	2.42	27.65	23.83	16.44	37.95	13.95	395.30
9	28.2	6.88	70.07	751	1.08	132.22	6.25	33.96	24.10	14.03	35.20	2.70	488.90
10	28.5	7.11	126.94	619	0.96	115.49	2.71	29.44	15.75	14.69	23.05	9.41	414.30
11	28.3	6.83	106.69	760	1.30	136.03	3.43	34.13	16.10	18.53	4.62	0.25	525.50
12	31.8	7.12	163.33	943	1.51	155.49	3.64	32.82	35.72	12.60	73.70	36.20	481.30
13	31.4	7.48	83.34	714	1.25	41.20	2.83	21.58	97.38	14.58	41.70	1.17	472.40
14	29.9	7.44	99.38	5280	0.75	36.16	6.73	37.71	1096.02	10.66	1610.00	bdl	482.40
15	28.5	7.00	100.64	689	1.40	113.55	2.63	28.28	18.23	16.45	6.78	bdl	452.10
16	33.0	7.67	30.12	1032	0.65	16.73	4.15	26.95	180.20	9.73	133.50	bdl	440.80
17	28.3	6.87	87.69	632	0.82	103.59	2.15	27.39	14.40	18.88	3.55	bdl	409.20
18	34.5	7.73	-16.32	3960	1.31	16.19	4.90	21.69	844.07	7.57	1085.00	bdl	597.60
19	32.4	7.91	18.08	1807	0.79	13.20	2.99	13.34	373.83	7.02	401.00	bdl	446.70
20	32.2	7.69	19.73	6100	1.44	20.40	11.19	53.90	1347.85	7.38	1870.00	bdl	643.80
21	29.8	7.14	66.85	802	2.32	107.34	3.22	39.37	44.12	20.51	12.95	bdl	544.80
22	29.2	7.06	108.31	775	1.37	111.32	3.09	38.81	33.71	20.90	8.20	bdl	502.40
23	32.5	7.05	64.60	1510	0.89	88.36	4.79	47.15	190.78	16.03	286.00	24.30	440.70
24	32.7	6.98	109.75	2230	0.72	200.04	6.99	79.75	200.20	17.73	665.50	22.80	400.90
25	30.2	7.45	44.75	1115	0.92	73.11	4.15	47.83	107.97	12.76	162.00	18.35	406.00

Table 5.2a (continued)

Loc.	T (^{o}C)	pH	Eh (mV)	SC (µS)	O_2	Ca[a]	K	Mg	Na	Si	Cl	SO_4^{2-} [b]	HCO_3^-
26	29.1	7.09	74.28	618	1.30	121.99	4.54	26.61	24.20	12.90	29.74	11.84	330.30
27	29.3	7.16	44.43	750	1.21	113.39	3.00	26.20	27.55	14.34	27.84	18.23	410.10
28	28.2	6.78	81.97	850	1.51	145.01	3.09	31.55	25.68	17.23	5.29	5.14	542.20
29	27.8	7.07	144.37	1059	2.50	129.41	7.40	37.30	48.20	11.13	53.40	39.64	527.30
30	28.6	7.13	117.26	786	1.82	104.55	2.81	25.85	23.83	15.12	24.23	15.71	446.30
31	30.8	7.09	91.99	566	0.63	86.26	2.42	17.55	12.23	15.49	2.49	2.20	356.30
32	29.1	7.04	75.18	745	1.67	105.48	2.80	24.44	17.57	15.36	7.26	4.32	466.90
33	29.1	6.76	77.18	876	1.62	133.10	4.41	28.95	24.78	15.46	35.61	30.57	456.50
34	27.9	7.23	47.90	7860	0.29	124.14	12.18	72.21	1298.20	14.33	0.00	bdl	385.30
35	28.1	6.84	201.44	695	1.19	110.44	2.48	23.33	16.88	17.47	2.32	bdl	447.40
36	28.0	7.01	77.82	787	0.67	130.11	3.27	31.80	31.93	18.21	23.55	17.98	510.90
37	29.4	7.01	69.06	612	0.89	92.90	2.52	20.78	12.36	16.13	1.99	bdl	380.90
38	30.5	7.51	6.42	892	0.76	19.81	2.12	12.77	187.83	9.41	110.25	bdl	417.20
39	28.3	6.99	96.89	627	0.13	103.01	2.57	23.30	12.48	19.11	0.82	bdl	421.00
40	32.2	7.06	103.73	747	1.36	117.92	4.10	41.99	149.16	17.58	260.25	12.98	477.50
41	28.4	6.85	99.62		0.71	120.37	2.67	27.68	59.96	18.49	82.36	4.55	466.30
42	31.4	7.07	79.74		0.90	100.99	2.45	26.39	17.60	19.07	3.24	bdl	444.00
43	29.2	7.03	71.41		0.37	97.79	2.64	22.24	15.44	18.99	1.48	bdl	401.90
44	30.8	7.28	51.29		0.53	77.92	3.23	27.61	104.39	16.37	48.68	bdl2	553.30
45	28.8	6.92	45.01		0.25	110.77	1.96	25.81	24.93	16.56	26.60	3.41	437.60
46	30.0	7.04	60.90		0.17	101.94	2.97	24.04	17.89	20.28	6.10	bdl	443.80
47	30.4	6.98	101.50		0.85	112.94	2.42	31.62	21.77	20.83	3.77	bdl	493.80
48	29.9	7.08	119.08		0.49	108.47	2.80	32.30	31.16	20.47	17.32	bdl	480.50
49	29.2	6.73	110.51		0.48	107.69	3.70	29.20	25.41	26.32	9.22	bdl	479.40
50	31.2	7.19	112.39		0.54	83.98	3.33	32.03	62.90	19.93	32.97	bdl	482.90
51	29.4	7.24	77.56		3.50	93.85	3.04	30.55	52.56	19.74	24.64	bdl	490.50
52	34.6	8.19	-29.70	4370	0.35	6.65	3.50	9.47	648.75	7.18	673.91	bdl	757.70
53	29.3	7.67	-40.17		0.55	31.00	4.42	19.05	169.62	10.18	108.72	bdl	435.10

Table 5.2a (continued)

Rivers													
Loc.	**T (°C)**	**pH**	**Eh (mV)**	**SC (µS)**	**O_2**	**Ca[a]**	**K**	**Mg**	**Na**	**Si**	**Cl**	**SO_4^{2-} [b]**	**HCO_3^-**
R1	38.1	8.20	407.55	266		26.49	3.06	10.90	14.22	5.27	8.62	13.00	137.10
R2	28.8	8.30	269.81	322		29.37	3.14	14.42	17.42	6.03	11.45	15.00	145.20
R3	29.5	7.92	368.08	281		27.50	2.85	9.42	13.45	4.49	12.70	14.50	149.20
R4	34.4	8.01	297.96	561		80.66	3.10	23.06	18.35	9.63	15.67	2.89	344.30
R5	32.8	8.30	266.37	392		43.36	5.36	21.66	18.95	12.59	19.51	3.98	260.60
R6	32.9	7.56	309.20			69.77	1.93	21.75	23.69	12.23	15.94	6.85	313.30
R7	31.5	7.70	322.06			237.35	29.41	667.78	4986.36	1.99	6969.70	bdl	128.60

bdl = below detection level

[a] Detection level (DL) = 10 mg/L

[b] DL = 0.12 mg/L

Table 5.2b: Minor solute, dissolved gas and stable isotopic compositions of the water samples. Loc. corresponds to no. in table 5.1. All units are in mg/L except where mentioned. Blank fields indicate no measurement. DL: detection level, bdl: below detection level. Concentrations of Al, Be, Co, Cr, Cu, Ni, Pb, Sb, Se, Tl, U, NO_2^--N, and PO_4^{3-} for all samples were below detection level.

Loc.	As(tot.)	As(III)	B	Ba	Fe(tot.)	Fe(II)	Mn	NH_4^+	Sr	V	Zn	Br	F	NO_3-N	CO_3^{2-}	CH_4 (μM)	DOC	$\delta^{13}C$ (‰)	$\delta^{34}S$ (‰)
DL	*0.005*	*0.005*	*0.01*	*0.10*	*0.02*	*0.10*	*0.01*	*0.05*	*0.10*	*0.01*	*0.01*	*0.10*	*0.12*	*0.12*			*0.50*		
1	0.060	0.042	0.09	0.21	2.62	2.00	0.48	0.44	0.34	0.13	bdl	bdl	0.27	bdl	0.80	4.187E+00	1.30		
2	0.016	0.013	0.06	0.27	bdl	bdl	0.57	bdl	0.34	0.17	0.03	bdl	0.50	0.54	0.80	6.316E+00	1.20		12.10
3	0.092	0.064	0.03	0.13	2.09	2.00	0.41	0.93	0.23	0.09	0.01	bdl	bdl	bdl	0.70	1.241E+03	1.10		
4	0.020	0.018	0.01	0.17	3.24	3.00	0.17	0.18	0.20	0.10	0.03	bdl	0.13	bdl	0.60	6.698E+00	1.10		8.20
5	0.137	0.082	0.01	0.13	0.92	0.90	0.54	0.73	0.31	0.12	0.10	bdl	0.12	bdl	0.40	4.689E+00	1.20		
6	bdl	bdl	10.28	bdl	0.41	0.20	bdl	bdl	0.61	bdl	0.03	5.56	1.07	bdl	20.50	2.960E+00	1.90	-8.16	
7	0.074	0.057	0.17	0.15	3.79	3.80	0.62	0.31	0.31	0.14	0.08	bdl	0.17	bdl	0.50	8.390E+00	1.00		18.40
8	0.044	0.040	0.18	bdl	0.75	0.70	0.06	0.27	0.31	0.10	0.03	bdl	0.29	bdl	0.30	6.407E+00	1.20		14.30
9	0.123	0.071	0.08	0.20	5.23	5.20	0.27	1.59	0.25	0.12	0.03	bdl	0.36	bdl	0.50	7.901E+02	1.80		
10	0.008	0.005	0.06	0.36	0.40	0.40	0.47	0.39	0.24	0.10	0.02	bdl	0.33	bdl	0.50	6.422E+00	1.20		7.40
11	0.039	0.013	0.05	0.21	0.33	0.30	0.06	0.53	0.40	0.12	bdl	bdl	bdl	bdl	0.50	5.228E+01	1.00		
12	0.052	0.035	0.05	0.14	0.44	0.40	0.59	bdl	0.19	0.11	bdl	bdl	0.56	bdl	0.60	7.992E+00	0.90		21.60
13	bdl	bdl	0.17	bdl	0.33	0.30	bdl	0.34	0.28	0.07	0.02	bdl	0.43	bdl	1.30	1.071E+01	0.70		
14	bdl	bdl	2.09	bdl	0.20	0.20	bdl	bdl	0.80	0.10	0.02	5.30	bdl	bdl	1.90	3.227E+04	0.70	-2.17	
15	0.080	0.054	0.06	0.12	1.26	1.20	0.09	0.66	0.23	0.10	bdl	bdl	bdl	bdl	0.40	1.589E+03	1.00		
16	bdl	bdl	0.20	bdl	0.15	0.10	bdl	0.47	0.22	0.08	0.03	bdl	0.77	bdl	2.00	3.276E+03	0.80		
17	0.088	0.057	0.04	0.16	1.61	1.60	0.07	0.91	0.25	0.09	0.01	bdl	bdl	bdl	0.30	8.947E+00	1.30		
18	0.028	0.021	2.68	bdl	0.11	0.20	0.02	bdl	0.35	0.06	bdl	3.95	bdl	bdl	4.60	8.229E+00	2.60	-2.57	
19	bdl	bdl	0.46	bdl	0.04	bdl	0.01	0.76	0.18	0.04	bdl	1.23	bdl	bdl	2.70	1.397E+04	3.70	-5.27	
20	0.008	0.003	1.33	bdl	0.14	0.10	bdl	bdl	0.33	0.15	0.03	6.16	bdl	bdl	7.60	2.026E+01	4.70	-0.53	
21	bdl	bdl	0.06	0.21	0.66	0.60	0.08	0.49	0.39	0.13	bdl	bdl	0.23	bdl	0.80	5.205E+00	1.20		
22	bdl	bdl	0.05	0.22	0.84	0.80	0.11	0.38	0.38	0.14	bdl	bdl	0.22	bdl	0.90	7.166E+00	0.90		
23	bdl	bdl	0.14	0.28	0.53	0.50	0.04	bdl	0.44	0.15	bdl	0.84	bdl	bdl	0.80	1.385E+01	0.90		45.80

Table 5.2b (continued)

Loc.	As(tot.)	As(III)	B	Ba	Fe(tot.)	Fe(II)	Mn	NH_4^+	Sr	V	Zn	Br	F	NO_3-N	CO_3^{2-}	CH_4 (µM)	DOC	$\delta^{13}C$ (‰)	$\delta^{34}S$ (‰)
24	bdl	bdl	0.08	0.31	0.65	0.60	0.19	bdl	0.86	0.34	0.04	1.94	bdl	bdl	0.50	2.604E+01	0.50		11.50
25	bdl	bdl	0.09	0.10	0.24	0.20	0.03	0.60	0.49	0.16	0.02	0.52	bdl	bdl	1.00	1.493E+01	0.80		
26	0.032	0.021	0.29	0.22	1.47	1.00	0.29	bdl	0.45	0.04	0.02	bdl	bdl	bdl	0.30	8.172E+01	1.00	-8.29	
27	0.055	0.054	0.18	0.23	2.10	2.10	0.52	bdl	0.34	0.07	bdl	0.54	bdl	bdl	0.40	9.840E+01	1.00	-7.36	16.40
28	0.015	0.013	0.13	0.30	3.56	3.56	0.08	bdl	0.30	0.08	bdl	bdl	bdl	bdl	0.40	8.554E+01	1.30	-2.00	
29	bdl	bdl	0.15	0.22	0.40	0.40	0.68	0.17	0.39	0.10	0.03	1.33	bdl	0.14	0.40	1.073E+02	0.90	-6.10	11.10
30	0.024	0.020	0.09	0.14	1.03	1.00	0.31	0.63	0.27	0.08	0.01	0.58	bdl	bdl	0.20	2.010E+03	1.00	-4.82	11.70
31	0.027	0.027	0.06	0.12	0.61	0.60	0.11	bdl	0.21	0.04	0.05	bdl	bdl	bdl	0.30	2.716E+02	0.70	-3.73	
32	0.099	0.049	0.06	0.17	1.80	1.80	0.10	bdl	0.25	0.07	bdl	bdl	bdl	bdl	0.40	8.278E+01	0.80	-4.73	
33	0.011	0.011	0.06	0.31	2.29	2.00	0.22	bdl	0.31	0.08	0.01	1.04	bdl	bdl	0.40	1.149E+02	0.80	-3.51	5.70
34	bdl	bdl	4.05	0.21	1.26	1.20	0.03	3.29	3.78	0.18	0.05	7.36	bdl	bdl	0.80	6.822E+04	0.70	-2.38	
35	bdl	bdl	0.11	0.10	bdl	bdl	0.51	0.16	0.33	0.06	bdl	0.69	0.12	bdl	0.60	1.236E+02	0.70	-3.10	15.80
36	0.020	0.020	0.11	0.78	1.12	1.00	0.11	0.12	0.37	0.09	0.01	1.33	0.13	bdl	0.60	8.584E+01	0.80	-2.10	
37	0.049	0.049	0.06	0.21	1.65	1.65	0.16	0.17	0.23	0.05	0.05	bdl	bdl	bdl	0.30	4.549E+02	0.80	-3.94	
38	bdl	bdl	0.39	bdl	0.04	bdl	0.02	0.26	0.37	0.03	0.03	1.20	bdl	bdl	1.50	1.255E+04	1.40	-5.07	
39	0.018	0.011	0.03	0.12	0.70	0.70	0.03	0.29	0.31	0.06	0.02	bdl	bdl	bdl	0.30	1.282E+02	0.70	-1.12	
40	bdl	bdl	0.09	0.26	0.94	0.90	0.23	bdl	0.75	0.12	0.04	1.90	0.24	bdl	0.30	1.069E+02	0.50	-4.16	
41	0.029	0.029	0.06	0.18	1.38	1.30	0.19	0.13	0.42	0.07	0.01	0.80	bdl	bdl	0.30	9.725E+01	bdl	-6.09	
42	0.055	0.055	0.02	0.15	1.31	1.30	0.09	0.87	0.42	0.07	0.01	bdl	0.12	bdl	0.50	1.880E+04	bdl	-2.55	
43	0.049	0.048	0.01	0.11	1.21	1.20	0.06	0.21	0.35	0.05	0.01	bdl	bdl	bdl	0.30	4.179E+03	bdl	-1.28	
44	0.010	0.010	0.35	bdl	0.50	0.50	0.07	1.12	0.82	0.06	0.11	1.75	bdl	bdl	0.60	9.611E+01	1.3		
45	0.028	0.027	0.01	0.30	5.10	5.00	0.07	0.94	0.28	0.06	bdl	1.33	0.14	bdl	0.30	7.859E+01	0.50	-5.09	
46	0.054	0.053	0.01	0.28	3.53	3.50	0.09	bdl	0.30	0.08	bdl	bdl	bdl	bdl	0.20	1.000E+02	bdl	-0.76	
47	bdl	bdl	0.01	0.20	0.51	0.50	0.09	0.17	0.51	0.09	bdl	bdl	bdl	bdl	0.50	1.447E+04	1.2	-5.15	
48	bdl	bdl	0.01	0.16	1.02	1.00	0.06	0.10	0.60	0.08	0.12	1.29	0.23	bdl	0.40	1.634E+04	1.4	-2.03	
49	0.019	0.019	0.01	0.22	1.25	1.20	0.26	bdl	0.36	0.10	0.04	1.52	0.14	bdl	0.30	8.221E+01	1.0	-2.46	
50	bdl	bdl	0.05	0.13	0.43	0.40	0.08	0.69	0.45	0.08	bdl	0.98	bdl	bdl	0.70	4.811E+01	1.70	-4.20	

Table 5.2b (continued)

Loc.	As(tot.)	As(III)	B	Ba	Fe(tot.)	Fe(II)	Mn	NH_4^+	Sr	V	Zn	Br	F	NO_3-N	CO_3^{2-}	CH_4 (µM)	DOC	$\delta^{13}C$ (‰)	$\delta^{34}S$ (‰)
51	bdl	bdl	0.04	0.13	0.82	0.80	0.13	0.19	0.45	0.07	bdl	1.70	0.20	bdl	1.40	2.975E+03	0.50	-5.60	
52	bdl	bdl	1.37	bdl	bdl	bdl	0.01	1.24	0.13	0.03	0.07	3.69	0.49	bdl	12.50	1.351E+02	0.50	-2.08	
53	bdl	bdl	0.18	0.10	bdl	bdl	0.01	0.53	0.31	0.03	0.01	0.15	0.12	bdl	1.80	6.598E+01	0.50	-5.53	
Rivers																			
R1	bdl		0.01	bdl	bdl		0.00	bdl	0.12	0.05	0.04	bdl	0.20	0.20	0.70				
R2	bdl		0.02	0.10	0.23		0.00	bdl	0.13	0.06	0.04	bdl	0.17	bdl	0.65				
R3	bdl		bdl	bdl	0.03		0.02	bdl	0.10	0.05	0.02	bdl	0.20	0.22	0.60				
R4	0.055		0.01	0.18	bdl		0.03	bdl	0.28	0.04	0.00	0.46	bdl	bdl	2.40				
R5	0.101		0.00	bdl	bdl		0.01	bdl	0.20	0.05	0.01	1.35	0.16	bdl	2.70				
R6	0.037		0.01	0.15	bdl		0.03	0.05	0.24	0.04	0.00	0.40	bdl	bdl	1.40				
R7	bdl		2.33	0.18	bdl		0.00	bdl	3.67	1.86	0.04	26.97	bdl	bdl	0.70				

Table 5.3: Details of the first six components (showing 90% of the variance) obtained from the principal component analyses (PCA) for 15 parameters. Rotation method: Varimax with Kaiser normalization. Rotation converged in six iterations.

Principal Component	**1**	**2**	**3**	**4**	**5**	**6**
% Variance	***36.461***	***20.405***	***12.466***	***10.508***	***6.291***	***3.770***
HCO_3^-	0.951	-0.001	-0.008	-0.055	-0.088	-0.017
CO_3^{2-}	0.925	0.067	-0.150	-0.109	-0.069	-0.186
B	0.894	0.265	-0.107	-0.055	0.176	-0.086
Na	0.664	0.616	-0.263	-0.135	0.110	-0.214
K	0.373	0.850	0.132	-0.091	0.136	-0.009
Mg	-0.366	0.783	0.233	-0.046	0.128	0.265
Cl	0.464	0.767	-0.211	-0.115	0.276	-0.132
Mn	-0.101	-0.085	0.907	0.214	-0.020	-0.017
SO_4^{2-}	-0.075	0.167	0.804	-0.124	-0.241	0.259
Ca	-0.428	0.066	0.571	0.322	0.085	0.485
As(tot.)	-0.131	-0.142	0.190	0.867	0.048	-0.231
Fe(tot.)	-0.072	-0.079	-0.018	0.815	0.057	0.417
NH_4^+	-0.018	0.162	-0.136	0.164	0.910	-0.083
Sr	0.039	0.603	-0.053	-0.144	0.717	0.120
Ba	-0.165	0.037	0.175	0.019	-0.048	0.899

Table 5.4: List of selected minerals (in no definite order) documented in the sediments of the Bengal basin by previous workers. Name of the individual member of group minerals is mentioned wherever available, otherwise mentioned as group name.

Author	Site	Mineral phases
FAO (1971)	Across Bangladesh	Clays, quartz, calcite, dolomite, mica
Das et al. (1995)	Maldah, North 24 Parganas (West Bengal)	$FeSO_4$, hematite, magnetite, quartz, pyrite
Datta et al. (1997)	Across Bangladesh	Quartz, feldspar, carbonate (unspecified, very low), illite, kaolinite, amphibole
Chowdhury et al. (1999)	Bangladesh and West Bengal	Pyrite, rozenite ($FeSO_4 \cdot H_2O$), FeOOH, hematite, magnetite, quartz, calcite
Nickson et al. (2000)	Tungipara, Gopalganj (Bangladesh)	Fe-oxyhydroxide, authigenic pyrite
Breit et al. (2001)	Brahmanberia (Bangladesh)	Biotite, siderite, vivianite
Chakraborti et al. (2001)	Murshidabad, Nadia, North and South 24 Parganas (West Bengal)	Pyrite, Fe-oxide, Fe-oxyhydroxide, gypsum, calcite, quartz, goethite, mica, feldspar, $Ca_3(PO_4)_2$, rozenite
BGS/DPHE (2001)	Chapai Nawabganj, Laxmipur, Faridpur (Bangladesh)	Quartz, mica (including altered biotite), feldspars, pyroxene, Fe_2O_3, apatite, smectite, illite, kaolinite, chlorite, authigenic pyrite, calcite
Anwar et al. (2002)	Narayanganj (Bangladesh)	Kaolinite, illite, montmorillonite, goethite, amorphous Fe-oxide, mica, feldspar, amphibole
Dowling et al. (2002)	Laxmipur (Bangladesh)	Quartz, biotite, altered vermiculite, Fe-oxyhydroxide
Pal et al. (2002)	Nadia, South 24 Parganas (West Bengal)	Quartz, feldspar, calcareous concretion, Fe-oxide, Fe-oxyhydroxide, siderite, hornblende, muscovite, biotite, kaolinite, illite, montmorillonite
Allison et al. (2003)	Gangetic delta front (Bangladesh)	Smectite, kaolinite
Heroy et al. (2003)	Gangetic flood plain (Bangladesh)	Dolomite, calcareous concretion, smectite, kaolinite
Ahmed et al. (2004)	14 locations across Bangladesh	Quartz, muscovite, biotite, feldspar (fresh and altered), chlorite, hornblende
McArthur et al. (2004)	North 24 Parganas (West Bengal)	Fe-oxyhydroxide, calcite
Swartz et al. (2004)	Munshiganj (Bangladesh)	Quartz, plagioclase, orthoclase, muscovite, biotite, magnetite, hornblende, chlorite, apatite, pyrite

Table 5.5: Summary of saturation indices (SI) calculated by PHREEQC for some phases possibly in contact with western Bengal groundwater and river water samples. Blank fields indicate values not available. SI < 0: undersaturation; SI > 0: supersaturation.

Phases		**Main aquifer (n = 47)**			**Isolated aquifers (n = 6)**			**River (G group, n = 3)**			**River (JI group, n = 3)**			**River (T)**
Name	**Formula**	**Mean**	**Max**	**Min**	**Mean**	**Max**	**Min**	**Mean**	**Max**	**Min**	**Mean**	**Max**	**Min**	**(n = 1)**
Arsenolite	As_4O_6	-22.13	-20.26	-25.22	-24.39	-22.91	-25.87				-134.3	-132.2	-136.2	
	As_2O_5	-31.31	-28.70	-34.05	-33.84	-33.60	-34.08				-32.74	-31.18	-33.81	
Birnessite	MnO_2	-16.14	-11.57	-18.27	-16.82	-15.63	-17.66	5.72	5.72	5.72	4.79	4.97	4.44	
Bixbyite	Mn_2O_3	-14.84	-9.88	-17.56	-15.64	-13.68	-16.85	7.93	7.93	7.93	6.81	7.33	6.03	
	$Ca_3(AsO_4)_2{\cdot}6H_2O$	-13.33	-11.01	-15.78	-14.38	-14.12	-14.64				-9.92	-9.17	-11.03	
Calcite	$CaCO_3$	0.27	0.54	-0.01	0.21	0.37	0.07	0.41	0.54	0.18	0.87	1.08	0.54	0.31
	Log P_{CO2}	-1.41	-1.03	-2.23	-1.92	-1.69	-2.30	-2.94	-2.71	-3.12	-2.44	-2.02	-2.85	-2.74
Dolomite	$CaMg(CO_3)_2$	0.32	1.04	-0.28	0.83	1.20	0.47	0.75	1.07	0.20	1.60	1.98	0.88	1.40
	$Fe(OH)2.7ClO_3$	5.66	7.75	0.65	6.48	7.83	6.06	6.98	7.50	6.46				
	$Fe_3(OH)_8$	0.48	4.74	-3.00	1.62	5.44	0.52	-5.81	-4.61	-7.01				
	$FeAsO_4{\cdot}2H_2O$	-6.84	-4.55	-8.35	-8.04	-7.91	-8.16							
Ferrihydrite	$Fe(OH)_3$	0.95	2.82	0.39	1.30	2.76	0.78	2.36	2.76	1.95				
Goethite	FeOOH	5.50	7.35	4.93	5.94	7.42	5.28	6.90	7.29	6.50				
Greenalite	$Fe_3Si_2O_5(OH)_4$	-1.32	0.93	-8.93	-0.52	2.09	-1.98	-29.62	-28.34	-30.90				
Hematite	Fe_2O_3	16.03	19.73	14.88	16.92	19.89	15.58	18.82	19.60	18.03				
Lepidocrosite	FeOOH	4.47	6.34	3.91	4.83	6.28	4.31	5.88	6.28	5.47				
Maghemite	Fe_2O_3	5.29	9.03	4.17	6.01	8.92	4.97	8.11	8.92	7.30				
Magnetite	Fe_3O_4	17.52	21.73	13.86	18.96	22.88	17.44	11.18	12.34	10.02				
Manganite	MnOOH	-7.56	-5.07	-8.96	-8.01	-7.08	-8.55	3.82	3.82	3.82	3.18	3.43	2.80	
Methane	CH_4	-1.02	1.19	-2.48	-0.72	1.73	-2.60							
Mg-Ferrite	$MgFe_2O_4$	6.68	10.48	4.81	8.73	11.26	6.62	11.17	12.39	9.94				
	$Mn_3(AsO_4)_2{\cdot}8H_2O$	-12.51	-8.84	-15.41	-13.86	-13.86	-13.86				-11.75	-10.88	-12.42	
Nsutite	MnO_2	-15.55	-10.98	-17.68	-16.23	-15.04	-17.07	6.31	6.31	6.31	5.37	5.56	5.03	
	O_2	-42.68	-34.56	-46.73	-42.45	-40.07	-45.31	-0.72	-0.71	-0.73	-0.72	-0.72	-0.72	-0.68
Pyrolusite	MnO_2	-13.59	-9.10	-15.68	-14.11	-12.73	-15.22	8.27	8.27	8.27	7.60	7.83	7.22	
Quartz	SiO_2	0.15	0.38	-0.24	-0.13	0.15	-0.27	-0.38	-0.27	-0.46	-0.05	-0.01	-0.14	-0.74
Rhodochrosite	$MnCO_3$	-0.80	0.94	-2.00	-1.49	-0.99	-2.15	-1.30	-1.30	-1.30	-1.10	-0.71	-1.45	

Table 5.5 (continued)

Phases	**Formula**	**Mean**	**Max**	**Min**	**Mean**	**Max**	**Min**	**Mean**	**Max**	**Min**	**Mean**	**Max**	**Min**	
Siderite	$FeCO_3$	0.08	0.79	-2.29	0.02	0.93	-0.74	-10.56	-10.38	-10.73	-1.38	-1.38	-1.38	
	SiO_2 (amorph.)	-1.12	-0.89	-1.50	-1.39	-1.13	-1.52	-1.63	-1.54	-1.69	-1.26	-1.26	-1.26	-2.00

Table 5.6: Details of the reaction path models. Results indicate: cation exchange (a: CaX_2, b: KX, c: MgX_2, d: NaX), sulfur cycling (m: pyrite), carbon cycling (n: CO_2, o: CH_4, p: organic carbon [CH_2O]) and carbonate weathering (x = calcite, y = dolomite, z = siderite).

Model No.	Flowpath (wells/river)		Mixing with [1]	Mixing (range %)	No. of minimal models	Uncertainty % (5 to 20)	Halite Dissolution [2]	Si balance [3]	Result (phases)	
	To	From							Dissolution (+) [4]	Precipitation (-) [5]
	Evolution of isolated groundwater									
1	6	26			9	11	used	failed	b,d,y,o,p,x	a,c,m,o
2	6	8			9	6	used	failed	b,d,z,y,n,o,p,x	x/a,c,m
3	6	29			9	18	used	worked	d,z,y,n,o,p,x	a,c,m,o,x
4	6	30			6	8	used	failed	b,d,z,y,n/p,x	a,c,m,o
5	6	2			9	6	used	failed	d,z,y,n,o,p,x	a,c,m
6	6	27			9	8	used	failed	b,d,z,y,n,o/p,x	a,c,m
7	14	33			6	19	used	worked	b,d,y,z,o/p	a,m,n
8	14	33	BoB	9.3	2	15	not used	worked	d,z,o/p	x,b,c,m,n
9	14	13			13	17	used	worked	b,c,d,z,o/p,y,n	d,m,a,x
10	14	13	BoB	6.3	5	15	not used	worked	d,z,o,n/p	a,m,b,c,n
11	34	33			4	13	used	worked	a,b,c,z,o/p,y	x,d,m,n
12	34	33	BoB	15	2	13	not used	worked	a,z,o/p	x,b,c,m,n
13	34	13			6	15	used	worked	a,b,c,z,o/p,n,y	d,m,x,n
14	34	13	BoB	11.0-12.0	2	16	not used	worked	a,z,o/p	x,b,c,m,n
15	20	19			10	6	used	worked	b,c,x/y,z,n/p	x/a,o,d
16	20	19	BoB	7.6-8.1	4	6	not used	worked	d,z,n/p,y	x/a,b,c,m,o
17	20	51			6	5	used	failed	b,d,y/x,n/p,c	x/a,z,o,c
18	20	51	BoB	8.4-9.7	4	6	not used	failed	d,z,n/p,y	a,b,c,m,o,x
19	20	19	R7	19	6	19	not used	worked	d,y/x,z,n/p	a/x,c,o
20	18	17			3	6	used	failed	d,b,y/x	a/x,c,z,o
21	18	17	BoB	5.1-5.2	6	5	not used	failed	d,z,y/x,o/p	a/x,b,c,m
22	18	46			6	6	used	failed	b,d,y/x,n	a,c,z,o,x
23	18	46	BoB	4.7-5.8	6	7	not used	failed	d,z,o/p,y/x	a,b,c,,m,n,x

Table 5.6 (continued)

No.	To	From	Mixing	%	Minimal no.	Uncertainty	Halite	Si	Dissolution (+) [4]	Precipitation (-) [5]
24	52	51			6	8	used	failed	d,y,x,n/p	a,z,c,o,x
25	52	51	BoB	3	6	8	not used	failed	d,z,y/x,p,n	a,b,c,m,o,x
26	52	22			6	8	used	failed	d,y/x,o/p	a,c,z
27	52	22	BoB	2.8-3.1	6	8	not used	failed	d,z,y/x,p/o	a,b,c,m
	Evolution of main aquifer brackish water in northern study area (Nadia)									
28	38	35			4	6	used	failed	d,z,o/p,y	x,a,b,c,n
29	38	36			4	6	used	failed	d,z,o/p,,y	x,a,b,c,m,n
30	38	35	14	6.6	4	6	not used	failed	d,z,o/p,y	x,a,c,n,b
31	38	35	34	3.6	4	14	not used	failed	d,o/p,y	a,b,c,n
	Evolution of main aquifer brackish water in southern study area (24 Parganas)									
32	16	21	20	6	4	7	not used	failed	b,d,o/p,y	x,c,a,z,n
33	16	21			4	7	used	failed	b,d,o/p,y	x,a,c,z
34	16	21	BoB	0.5	4	7	not used	failed	d,z,o/p,y	x,a,c,b,m,n
35	16	22			4	7	used	failed	d,o/p,b,y	x,a,c,n,b
36	16	22	BoB	0.6	4	7	not used	failed	d,z,o/p,b,y	x,c,a,m,n
37	19	51	BoB	1.7-1.8	4	6	not used	failed	d,y,o/p	x,a,c,b,n,m
38	19	51	52	77	2	18	not used	worked	a,o/p	x,d,z,n
39	19	51			4	6	used	failed	d,y,o/p	x,a,c,z,n
40	23	41	BoB	0.9-1	13	8	not used	worked	c,d,z,y	a,m,n,b,x,o
41	23	41			4	8	used	worked	b,m,y/c	d,x,a,o,n,z
42	24	23	BoB	1.8-1.9	2	6	not used	worked	a,z,o/p	x,b,d,m
43	24	23	R7	3.4-4.7	3	18	not used	worked	a,o/p,m	d,n
44	24	23			10	6	used	worked	a,b,y,m,o/p,c	x,d
45	25	41	R7	1.2-1	3	18	not used	worked	c/d,m	a/x,z,n,o
46	25	41	BoB	0.4-0.6	9	19	not used	worked	d/c,z	a,m,o,n,z,x
47	53	50	BoB	0.3	4	6	not used	failed	d,z,o/p,y	x,a,c,m,n
48	53	50	R7	0.8-0.9	5	18	not used	failed	d,y,x,	a,c,z,x

Table 5.6 (continued)

No.	To	From	Mixing	%	Minimal no.	Uncertainty	Halite	Si	Dissolution (+)	Precipitation (-)
	Mixing of groundwater with infiltrating river water									
49	2	29	R2	0	4	7	not used	worked	y/x,z,c,n/p	a,m
50	11	12	R4	0	10	20	not used	worked	a/c,z	d,m
51	11	12	R5	1	34	20	not used	worked	*too many solutions*	
52	35	12	R1	0	2	17	not used	worked	a,z,o/p	b,d,x,m,o
53	35	36	R5	0-38	5	5	not used	worked	a,z,n,p,o	b,c,d,m,x,o
54	35	36	R1	0	2	5	not used	worked	a,z,o/p	b,c,d,m,x
55	37	36	R5	46-62	3	5	not used	worked	a,z,x,p	b,c,d,m
	Mixing of river water with discharging groundwater									
56	R1	R2	35	5.5	2	12	not used	worked	a	x,c,z/m,n
57	R4	R2	28	16.2	2	20	not used	worked	x,y,z	m
58	R4	R2	32	23.9	2	20	not used	worked	x,y,z	m
59	R5	R4	36	7.8-11.5	6	10	not used	worked	b	x,a/c/d,z/m,n
60	R7	R6	BoB	47.3	3	12	not used	worked	a	x,b,c,d,n,m

[1] BoB: Bay of Bengal.
[2] Halite dissolution used as a proxy for mixing with marine connate water
[3] Si balance indicates insignificant silicate weathering along the flow path
[4] +: dissolution or desorption
[5] -: precipitation or adsorption or exsolution (of gases)

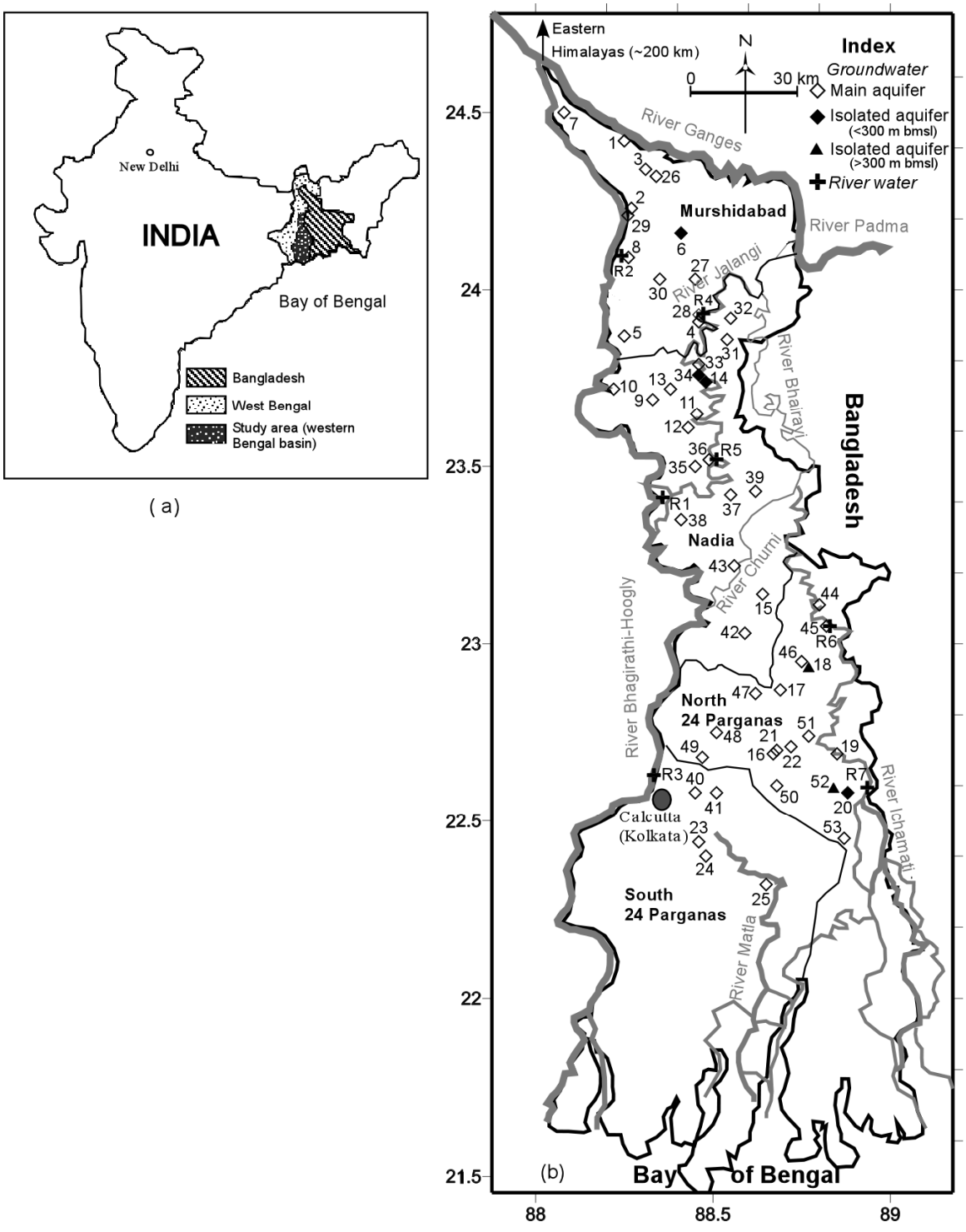

Figure 5.1: Map of the study area showing the 53 groundwater (hydrostratigraphically classified) and 7 river water-sampling locations; bmsl: below mean sea level. The thin black solid lines within the map (b) indicate the district boundaries.

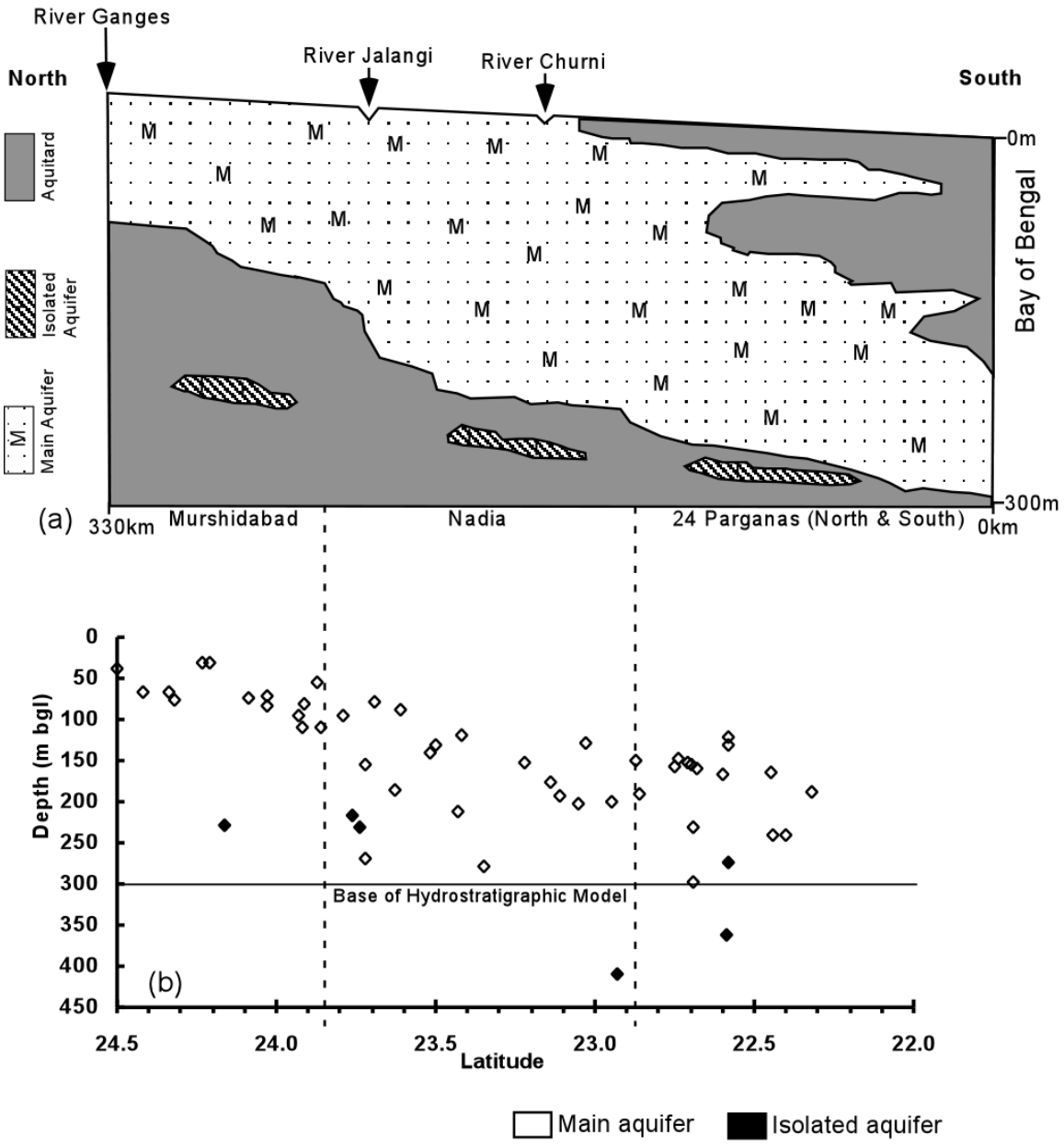

Figure 5.2: (a) Generalized hydrostratigraphic framework along a north-south transect, parallel to the River Bhagirathi-Hoogly, redrawn for each district (not to scale). (b) Plot of the maximum tapped depth (bgl: below ground level) of the sampled wells.

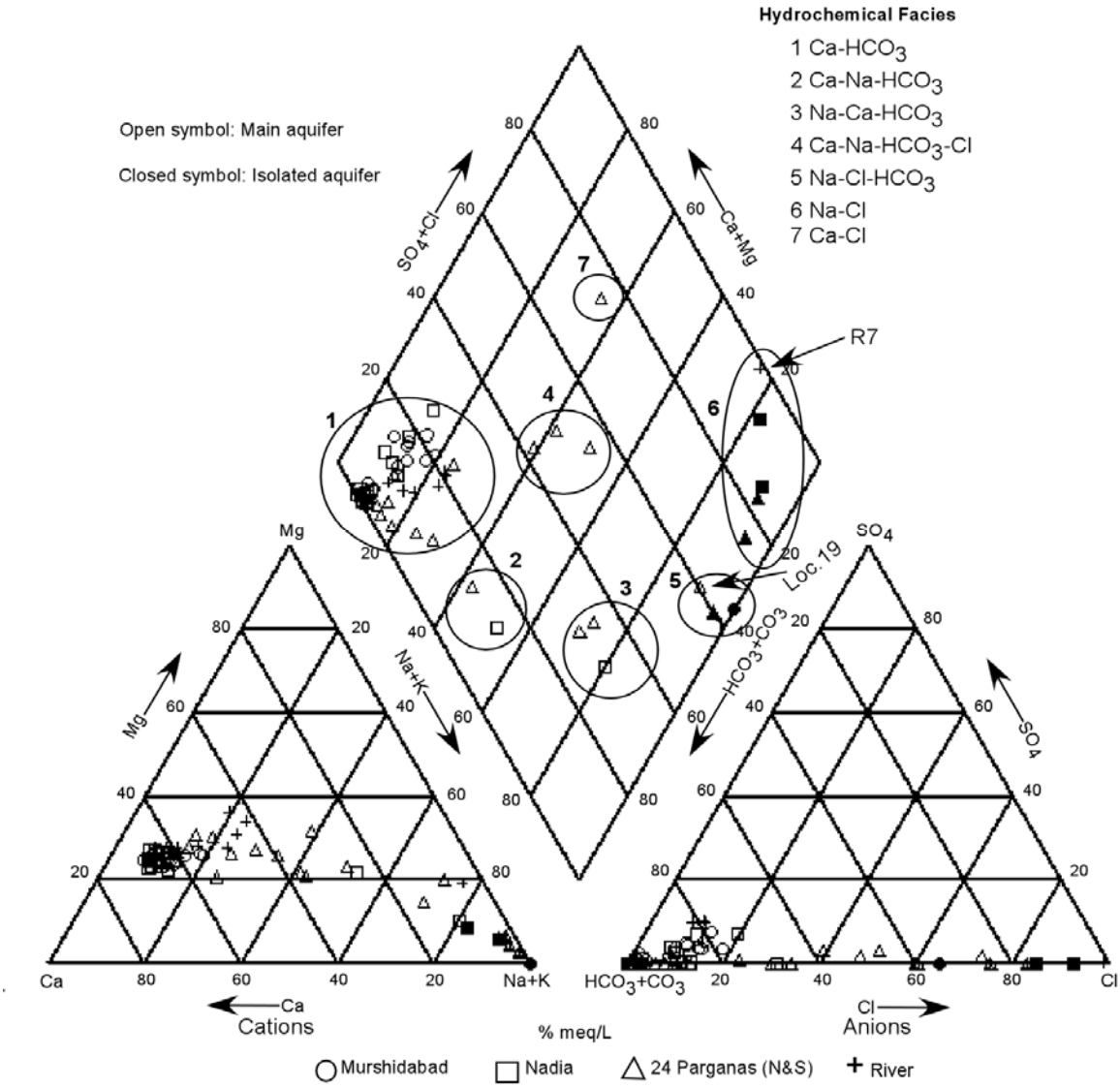

Figure 5.3: Piper plot of the hydrochemical facies distribution of groundwater and river water samples by aquifer type and district.

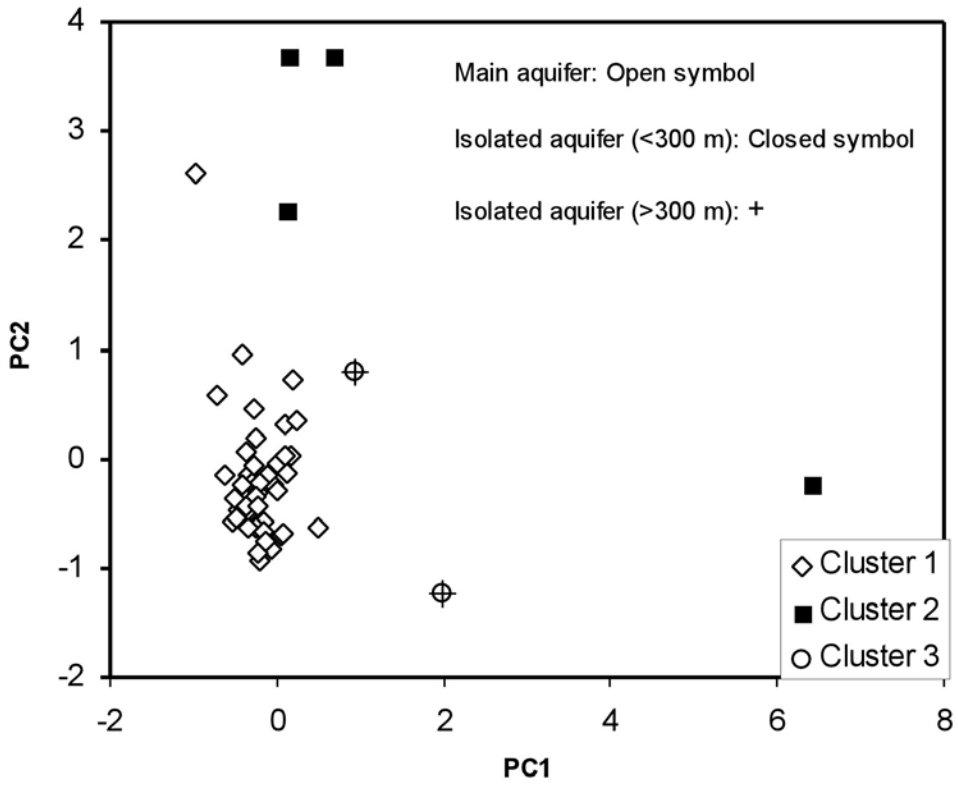

Figure 5.4: Bivariate plot of the three clusters obtained from hierarchical cluster analyses (HCA) with the first and second principal component (PC) axes. The data points are further classified according to aquifer type.

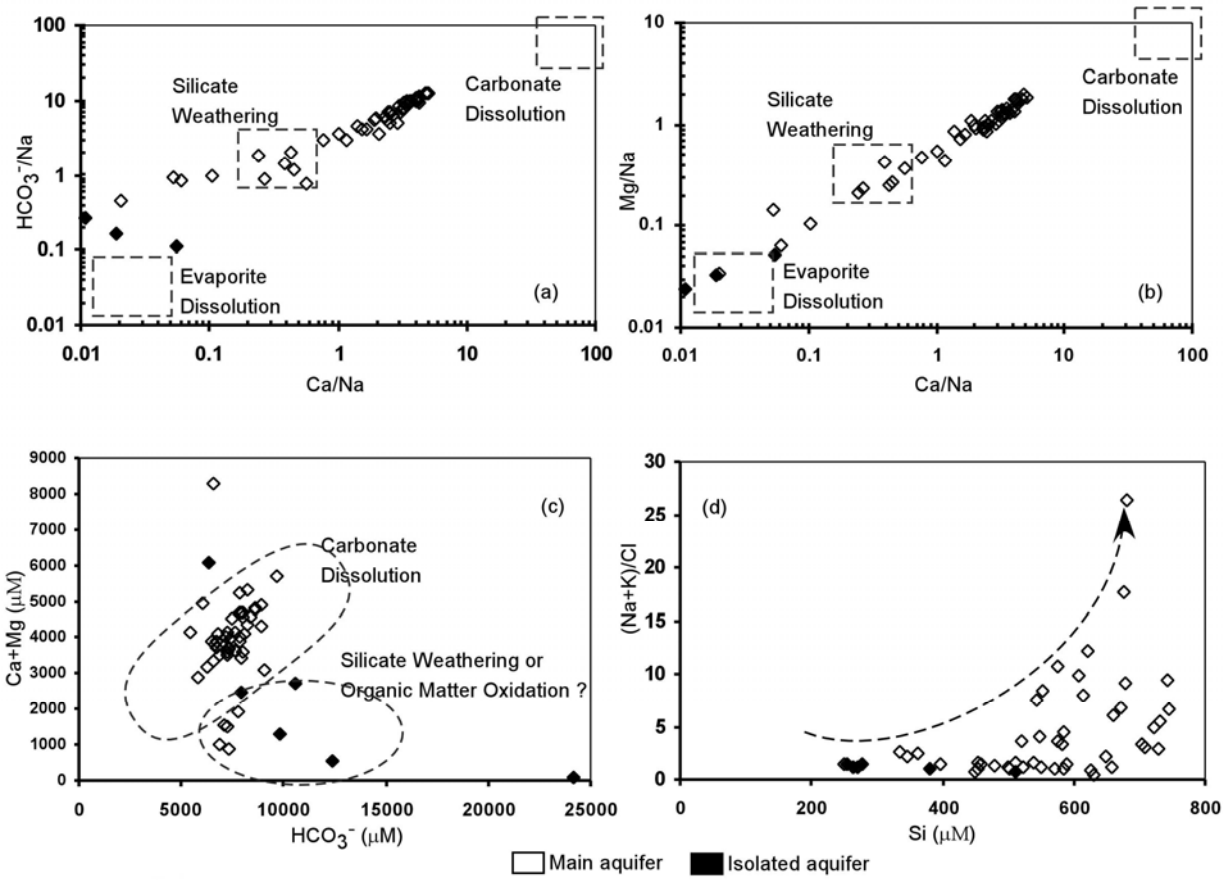

Figure 5.5: Molar ratio bivariate plots (plotted after Gaillardet et al. [1999]) of a) Na-normalized Ca and HCO_3^-, b) Na-normalized Ca and Mg, c) Ca+Mg versus HCO_3^-, and d) Si and Cl-normalized (Na+K). The dashed boxes in plots (a) and (b) represent the ranges of approximate compositions of the three main source end members (evaporites, silicates, and carbonates) without any mixing. Only three isolated aquifer samples can be seen in (a) and (b), as the other three have very low molar Ca/Na ratios. Bivariate plots between.

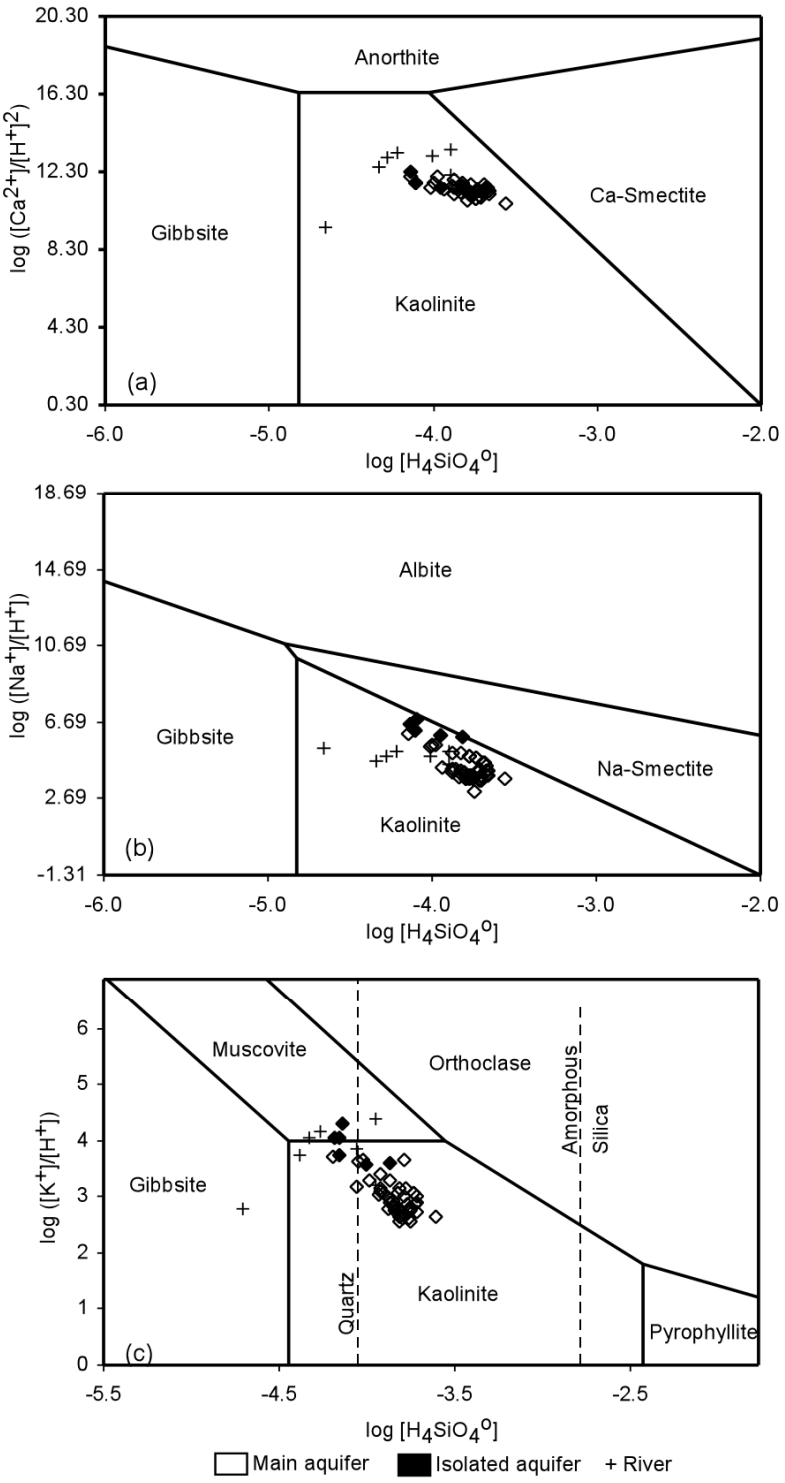

Figure 5.6: Stability field of a) Ca-Al silicate phases, b) Na-Al silicate phases, and c) K-Al silicate phases relative to groundwater and river water samples from the western Bengal basin. The phase boundaries are plotted using thermodynamic data of Tardy (1971) for (a) and (b), and Drever (1997) for (c).

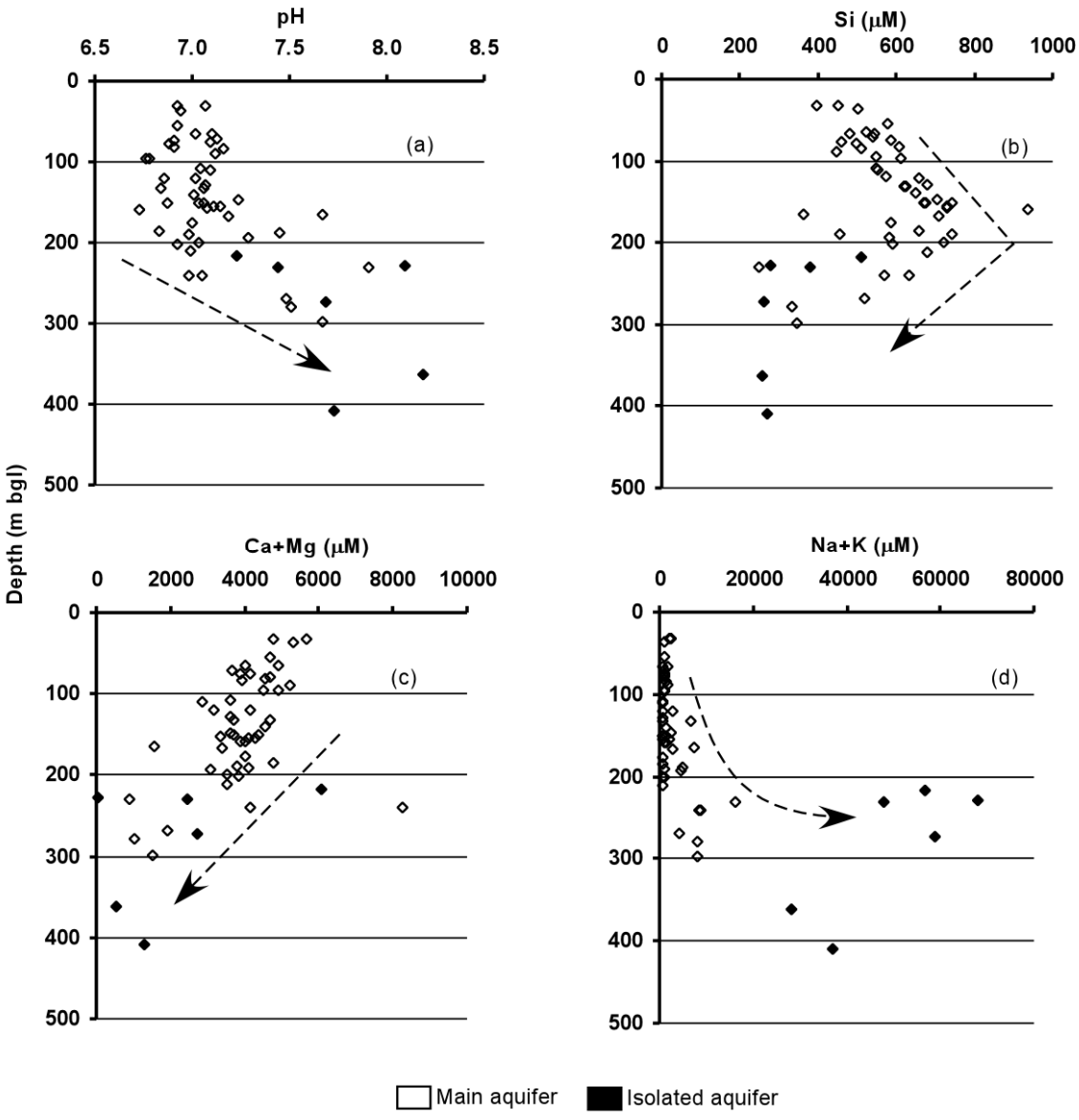

Figure 5.7: Depth-profiles of water quality parameters: a) pH, b) Si, c) Ca+Mg, and d) Na+K; bgl: below ground level.

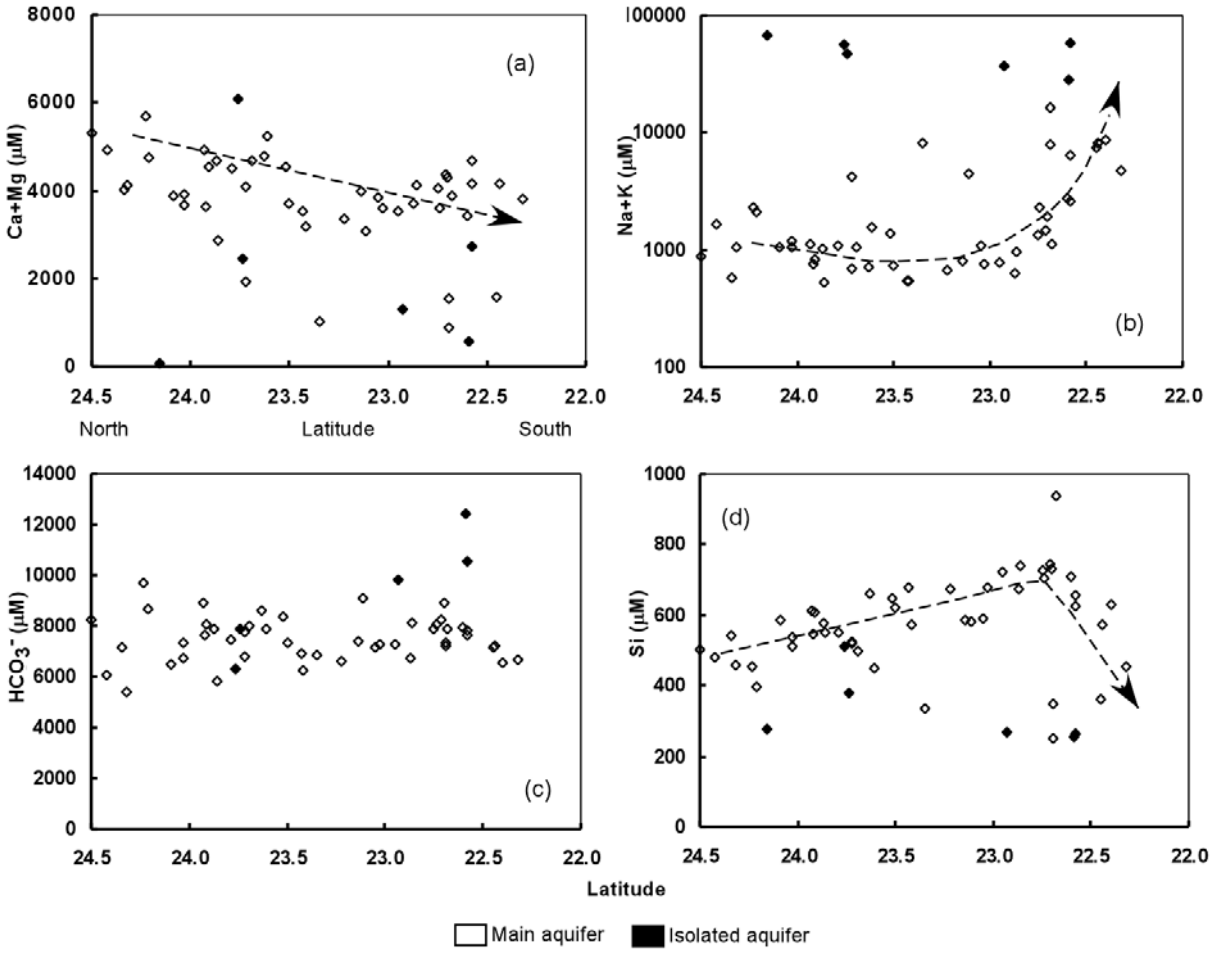

Figure 5.8: Distance (with latitude) plots of water quality parameters: a) Ca+Mg, b) Na+K, c) HCO_3^-, and d) Si.

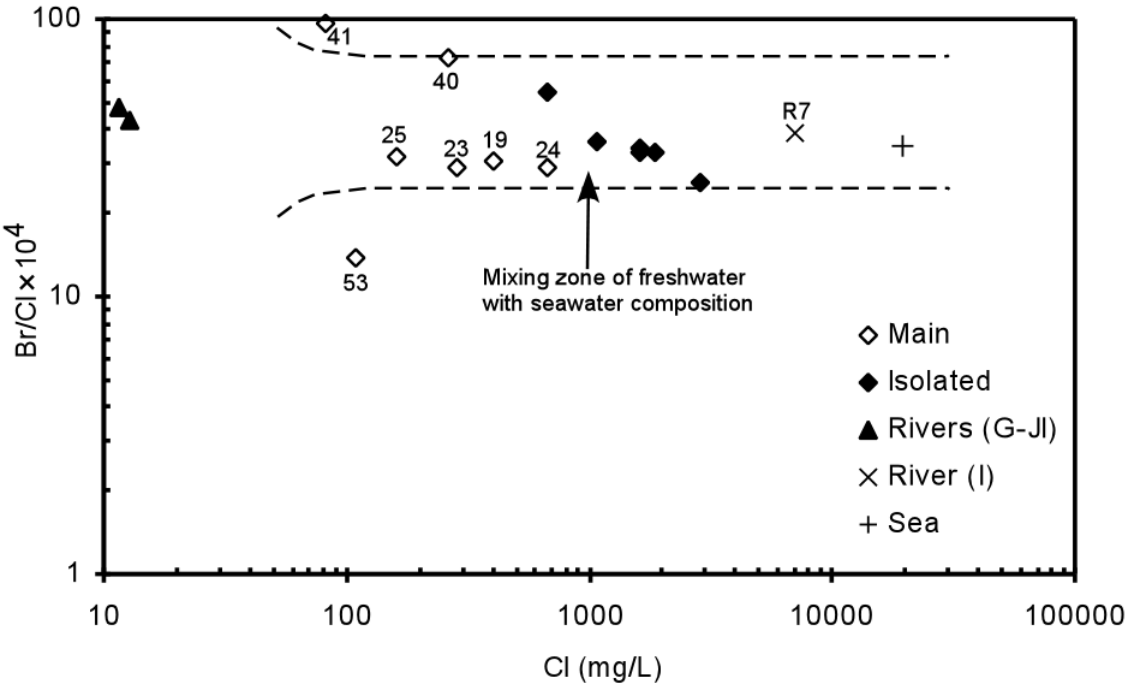

Figure 5.9: Plot of Br^-/Cl^- mass ratio versus Cl^- concentration (following Whittemore [2004]) for groundwater, river water, and seawater (from Drever [1997]). Only the main aquifer and river water samples with Cl^- concentrations > 10 mg/L and detectable Br concentrations are shown in the plot. The area between the dashed lines indicates the mixing zone of freshwater with seawater composition. The numbers beside the data points represent sample locations.

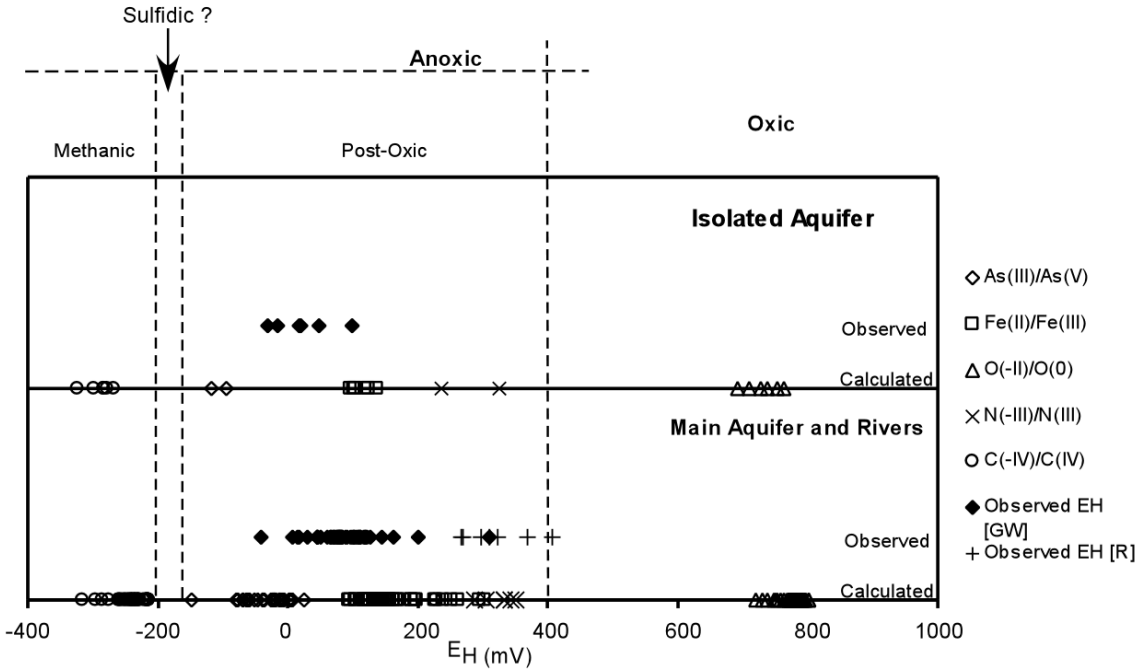

Figure 5.10: Comparison of observed E_H of the groundwater and river water samples with calculated E_H (converted from pe) of redox couples present in the waters. The plot has been classified into the redox system of oxic and anoxic (postoxic, sulfidic, and methanic) after Berner (1981). The sulfidic zone has been marked with (?) because of lack of S^{2-} detection. GW: groundwater, R: river.

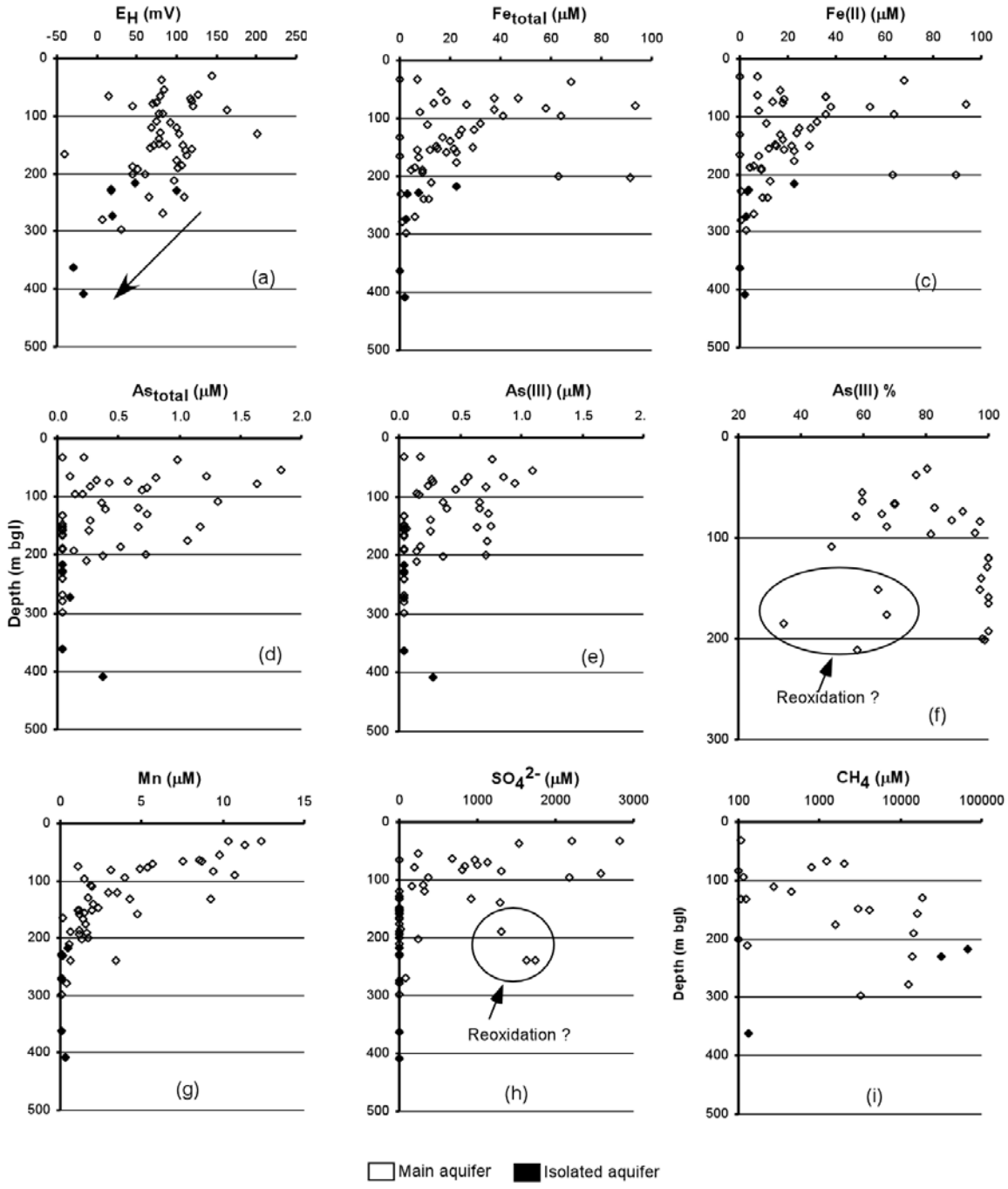

Figure 5.11: Depth-profiles of redox-sensitive parameters: a) E_H, b) Fe(total), c) Fe(II), d) As(total), e) As(III), f) percentage of As(III) in the main aquifer samples with detectable (≥ 0.005 mg/L) As(III), g) Mn, h) SO_4^{2-}, and i) CH_4; bgl: below ground level.

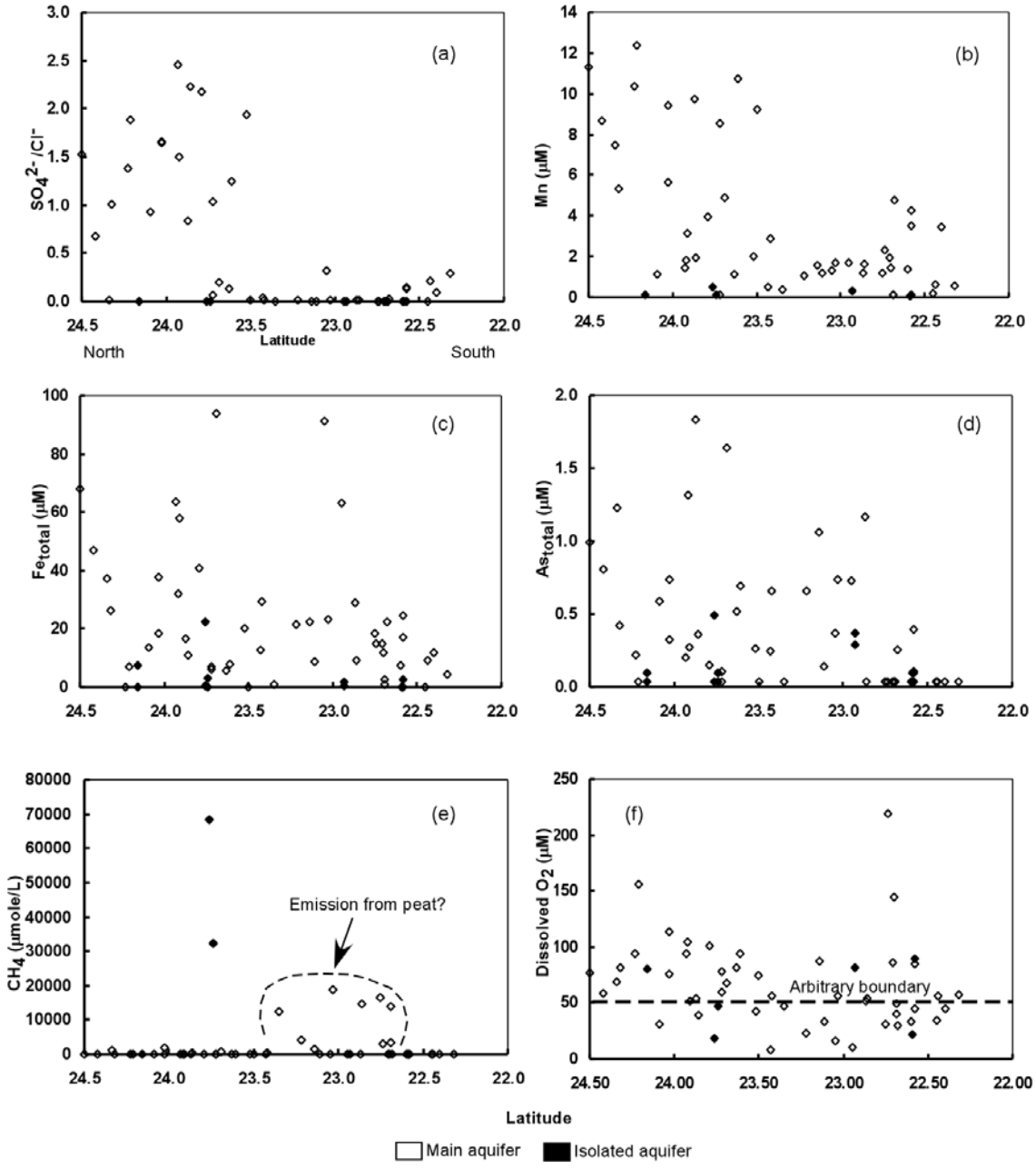

Figure 5.12: Distance (with latitude) plots of redox-sensitive parameters: a) Cl^--normalized SO_4^{2-}, b) Mn, c) Fe (total), d) As (total), e) CH_4. The very high CH_4 concentrations are present in southern Nadia and northern North 24 Parganas. (f) shows the number of samples with O_2 concentrations higher than 50 μmole/L (0.8 mg/L) is generally higher in the northern part of the flow path (north of ~23.5°N latitude).

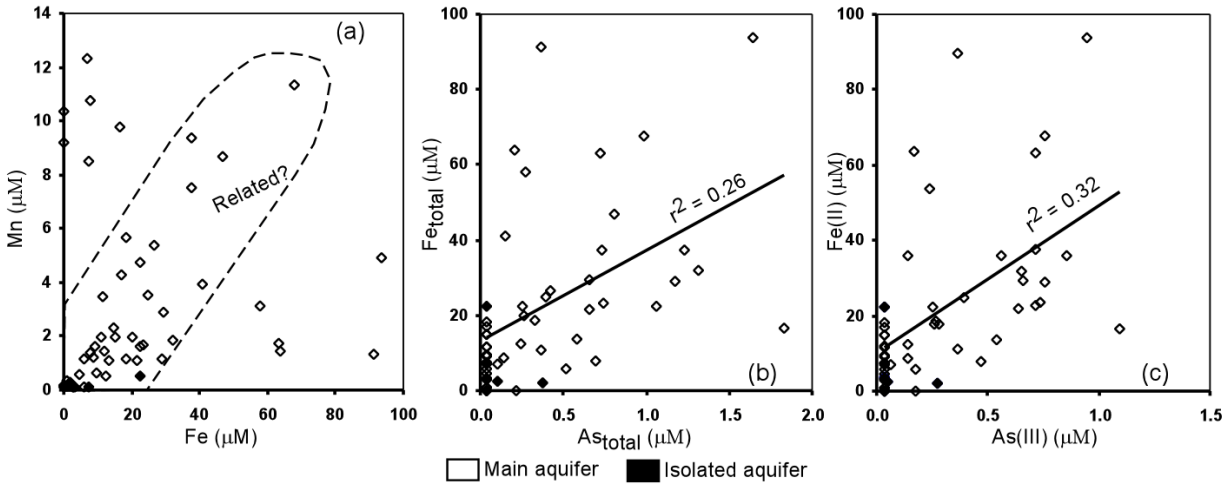

Figure 5.13: Bivariate plots showing relations between a) Fe(total) and Mn, b) As(total) and Fe(total), and c) As(III) and Fe(II).

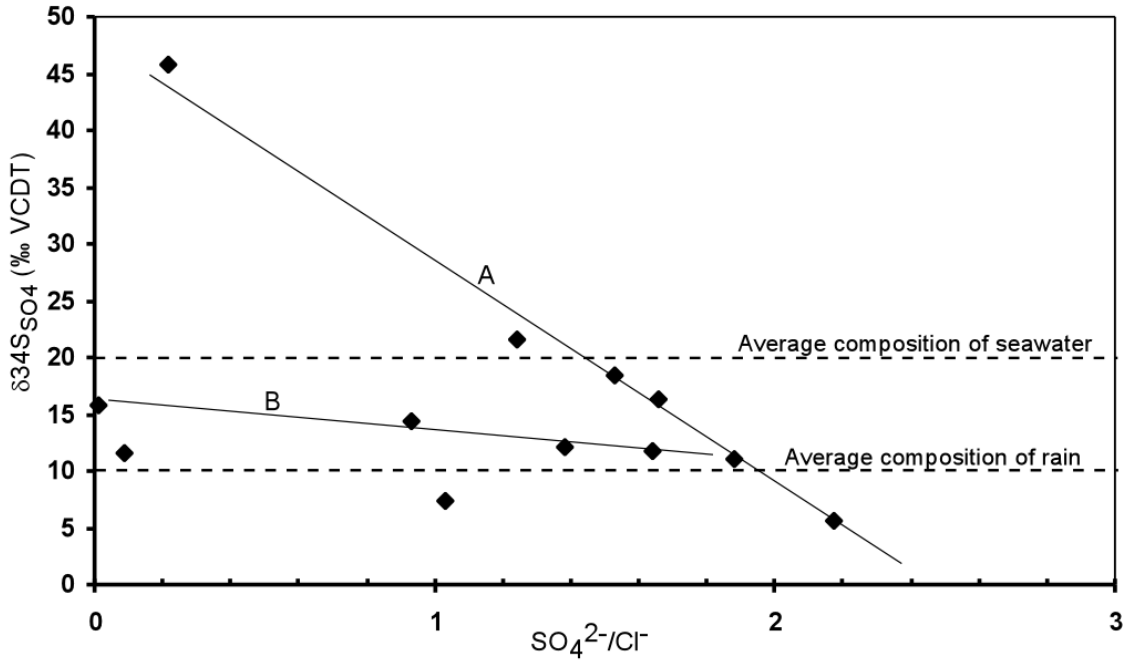

Figure 5.14: Plots of $\delta^{34}S_{SO4}$ versus Cl-normalized SO_4^{2-} concentrations. Location 4 with very high SO_4^{2-}/Cl^- is not shown. The solid lines represent visual trend lines; line (A) has a much higher gradient than (B), suggesting (B) possibly has undergone some reoxidation.

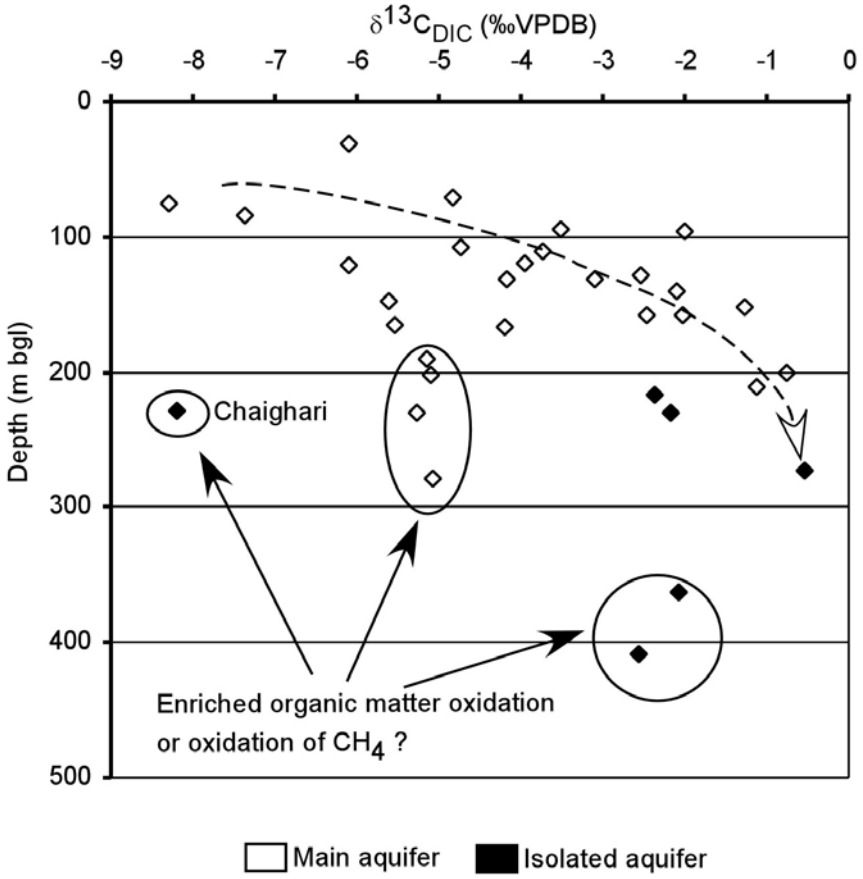

Figure 5.15: Plot of $\delta^{13}C_{DIC}$ with depth (bgl: below ground level).

Chapter 6: Suitability of deeper groundwater as an alternate drinking water source

6.1 Introduction and findings

Natural, non-point source, elevated concentrations of arsenic (As) in groundwater of the Bengal basin (Bangladesh and West Bengal, India) have put an estimated 50 million people at risk. This pollution has been regarded as the greatest mass poisoning in human history (Smith et al., 2000). Polluted groundwater is believed to reside mostly at depths <100 m, and the deeper groundwater has been considered a safe alternate water source in Bangladesh by various workers (BGS/DPHE, 2001; van Geen et al., 2003; Ravenscroft et al., 2005).

In order to provide safer water, the decision-making authorities of West Bengal began drilling deep community water-supply wells around the mid-1970s. As of 2004 about 35% of the total West Bengal population of 80 million is being supplied water from such wells (Figure 1.3a). The main objective of the present study has been to evaluate the suitability of the deep water-supply wells in the study area with acutely As-contaminated shallow groundwater. In this area, an estimated 13.5 million people are at risk (Table 1.1). The number of reported malignancies from this area has grown to an estimated 300 at the turn of the century (Figure 1.2c). This study has shown that deeper groundwater commonly has As concentrations exceeding the World Health Organization safe limit of 10 μg/L (WHO, 1993, 2001) and has explored the possible causes of such contamination. Figure 6.1 provides a flow chart of such causes (described afterward) that could have lead to the deeper water contamination.

Unfiltered arsenic concentration data collected during this study and compiled from PHED (as of 2004) (Table 6.1) show that ~60% of the sampled community water-supply wells (well depths 31 m to 400 m below ground level [bgl]), supplying water to ~ 5 million people, have As concentrations >10 μg/L, while ~20% of sampled wells have As concentrations > 50 μg/L (Government of West Bengal safety standard) (Figure 6.2). Samples collected during this study have a higher percentage of wells having As >50 μg/L than the PHED data (Figure 6.3). Some of the reasons for this may include spatial variation between sampling locations and analytical protocols. Comparison of results of this study with previously reported As results from adjoining, relatively deep (>50 m bgl) Bangladesh groundwater (BGS/DPHE, 2001) suggests

that the study area may have a greater proportion of contaminated deep wells (except areas south of ~23.5^{o}N latitude) than in Bangladesh (Figures 6.4 and 6.5).

6.2 Probable causes

To investigate the finding of elevated As in deeper groundwater in this study, which contravenes existing hypotheses (BGS/DPHE, 2001; van Geen et al., 2003; Ravenscroft et al., 2005), aquifers in the study area were delineated (see Chapter 2), realizing that the presence of extensive confining layers (aquitards) between shallower and deeper aquifers would limit groundwater mixing. Construction of regional aquifer-aquitard models, based on 143 drillers' logs at a 2-m vertical resolution and up to 300 m depth below MSL, indicate the presence of a single (main) aquifer devoid of significant confining layers from the north of the study area down to ~23.7^{o}N latitude. This absence suggests the possibility of mixing of contaminated and uncontaminated waters at various depths along natural groundwater flow paths by advection and dispersion, as well as mixing by flow induced by pumping. The aquifer deepens southward (toward the Bay of Bengal) and eastward (toward the basin center in Bangladesh) from about ~50 m depth in northern Murshidabad, in correspondence with the delta-building architecture of the River Ganges and its distributaries.

Potable deeper groundwater is available to a maximum depth of ~200 m in most central and southern parts of the study area, while such water is available only to ~80 m depth in most parts of Murshidabad and northern Nadia because of the existence of thick basal aquitards. Isolated aquifers at greater depths have high chloride and boron (a potential contaminant) concentrations (Cl^{-} mean: 1619.6 mg/L, B mean: 3.6 mg/L), rendering them undrinkable. The presence of intermediate-depth confining layers in the southern portions of the study area and locally present elsewhere have not resulted in distinct differences in overlying and underlying groundwater chemistry, although these aquitards have limited groundwater mixing *via* local-scale (10^2 to 10^3 m laterally) cross-formational flow. Lower As concentrations in the southern parts of the Bengal basin (Figure 6.4) may be an artifact of the presence of these intermediate-depth aquitards. Some studies from Bangladesh (Aggarwal et al., 2000; Basu et al., 2001) have proposed a distinction between As-contaminated and uncontaminated water by depth, as illustrated by ^{18}O composition. However, compositions of major solutes (n = 53, Chapter 5) and

stable isotopes (^{2}H and ^{18}O) (n = 64, $\delta^{18}O$ range: -3 to -6 ‰ VSMOW, depending on distance from the Bay of Bengal; Chapter 4) in groundwater are similar at various depths in the main aquifer (except seawater-intruded southern parts [CGWB, 1994d, e]), suggesting similarity in sources of recharge, pathways of geochemical evolution and the presence of interconnected aquifers.

To understand groundwater flow patterns in the study area, regional-scale numerical flow models were developed for various seasons with and without pumping. The models suggested the occurrence of pre-pumping flow cells extending laterally ~2 to 10 km and vertically across almost the entire depth of the main aquifer. With the introduction of deep irrigational pumping, the models developed widespread, deep centers of depression with radial inflows from shallower depths.

Recent studies in Bangladesh (Harvey et al., 2002; Zheng et al., 2005b have suggested that land use (e.g. irrigational pumping from deeper water) may have an important control on the As distribution with depth. Deeper irrigational pumping (>100 m) is much more common in West Bengal (MID, 2001; see Chapter 3) than in Bangladesh (BGS/DPHE, 2001), which could explain greater As concentrations in deeper groundwater of the study area.

To investigate this in more detail, groundwater flow was modeled in a 12-km^2 area around a contaminated well at Kamagachi (23.22^{o}N, 88.56^{o}E, block Ranaghat-I, Nadia, maximum tapped depth 150.5, As: 0.049 mg/L, Figure 6.6). Within this area, a <10-m thick layer of clayey surficial sediment is underlain by the main aquifer sand (medium to fine), which extends continuously to 201 m bgl and is underlain by sandy clay (64 m) and clay to at least 300 m bgl. Particle-tracking simulations based on flow modeling without (Figure 6.7a) and with pumping (Figure 6.7b) showed that dissolved As at shallow depths (50 m bgl) and up to ~75 m horizontal distance, as well as As at depths ≥ 60 m and located 100 m away horizontally, could have reached the target well (150 m bgl) within 30 years (deep irrigational pumping started in the 1970s). The results suggest that deeper irrigational and drinking water pumping could have caused As movement to deep wells.

Recent studies from the Bengal basin (e.g. Horneman et al., 2004; McArthur et al., 2004; Bhattacharya et al., 2005) have suggested that the gray color of aquifer sediments can be an indicator of chemically reduced conditions leading to the existence of As in solution, rather adsorbed onto orange/yellow (oxidized) iron-rich sediments. Such orange sediments have been reported to exist at depths of ~150 m in Bangladesh and have been attributed as one of the major causes for As contamination of groundwater there (Zheng et al., 2004). Compilation and manual extrapolation of sediment color data (Figure 6.8) from lithologs in the hydrostratigraphic model shows that with few exceptions (mostly at shallower depths), the sands are mostly grey up to a depth of 300 m, suggesting that reduction is the dominant chemical process with depth. This observation was supported by the general decrease of SO_4^{2-} and Mn and increase of CH_4 and As(III)% with depth (Chapter 5). $\delta^{13}C_{DIC}$ enrichment with depth suggests that some CH_4 has probably been derived from CO_2 reduction than totally originating from peat, a suggested redox driver for arsenic mobilization in the Bengal basin (McArthur et al., 2001, 2004; Ravenscroft et al., 2001). Peat has been encountered in many places in the paleo-delta front in the southern part of the study area, but not in the north. Although Fe(III) reduction is likely the dominant redox process (e.g. Bhattacharya et al., 1997; Harvey et al., 2002; McArthur et al., 2001, 2004; Ravenscroft et al., 2001), outliers in SO_4^{2-} and As(III)% trends with depth and distance suggest localized re-oxidation at scales less than the lateral spacing of deep wells (10 to 10^2 m). $\delta^{34}S_{SO4}$ results (Zheng et al, 2004; Chapter 5, this study) support this observation, as does the presence of yellow/orange sediment lenses in Figure 6.8. These observations lead to the inference infer that As fate depends on the interplay among Fe, S, and C cycles: As is mobilized from host sediment under reducing conditions, but can also be partially scavenged by precipitation of pyrite (limited by the availability of S), which in turn may be locally re-oxidized to re-liberate As. The oxidation may be caused by circulation of more oxygenated water from the shallow subsurface during intensive deeper groundwater abstraction or by complex interaction among redox-sensitive solutes.

The occurrence of elevated As concentrations in deeper groundwater of the western Bengal basin is not solely dependent on any one of the above-mentioned causes, but is probably a cumulative effect of sediment architecture, deep pumping and subsurface redox conditions. Arsenic can be liberated from deeper sediments (depending on the original solid-phase

concentration) by Fe(III) reduction, and is being retained in solution except as sequestered by authigenic pyrite. The contaminated water is then circulated, with acceleration via pumping, to previously uncontaminated depths through interconnected sand bodies.

6.3 Implications for future water-resource development and management

This study concludes that extensive deeper water exploitation may not be a sustainable alternative for drinking water supply for most of the study area (at least from Murshidabad to central North 24 Parganas). Switching to treated surface water could be an alternative (as has been done in parts of Maldah, North and South 24 Parganas, and Calcutta), but the associated costs and logistical difficulties of supplying to distant locations have limited its applicability. Thus pragmatically, deep drinking water wells would probably have to be installed, but would need very careful pre-installation site characterization, including local hydrostratigraphy (~10 km^2). Also, the newly installed wells need to be regularly monitored, realizing that safe wells can become contaminated with time. Arsenic treatment technologies are widely available, but when such technologies are used (e.g. pump and treat), their performance also needs to be monitored regularly.

Deeper irrigational pumping should be strongly discouraged, as it appears to spread As to previously uncontaminated zones of the main aquifer. The reason that deeper water of Bangladesh is still relatively As-free is probably because of less extensive deep pumping. Development of such pumping in future poses a serious threat and should be a focus of future studies. It is also important to understand the vertical and lateral extent and rate of contaminant transport at the local scale between contaminated and as-yet uncontaminated areas.

Table 6.1: Details of unfiltered arsenic concentrations detected in the public water supply wells used in the present study. **Bold text for As concentration**: sampled during this study; plain text: data collected from PHED database.

Location[a]	Block (Town)	District[b]	Latitude	Longitude	Depth (m)[c]	As (mg/L)[d]	Population[e]
Kalighat	Calcutta	CCU	22.52	88.34	~120	**<0.005**	na
Ramakanthapur	Suti-I	MD	24.54	88.06	39.4	<0.005	15,553
Mithipur	Raghunathganj-II	MD	24.50	88.05	37.8	0.040	10,885
Mahishasthali	Bhagwangola-I	MD	24.34	88.32	76.1	0.080	na
Jalangi-Karimpur	Jalangi	MD	24.13	88.72	115.9	<0.005	31,169
Jiaganj	Murshidabad	MD	24.23	88.27	84.9	<0.005	na
Mahula	Beldanga-I	MD	24.00	88.24	266.8	0.010	10,869
Katakopra	Domkal	MD	24.08	88.63	73.5	<0.005	23,803
Shaktipur	Beldanga-II	MD	23.86	88.20	143.3	0.010	26,650
Lalgola	Lalgola	MD	24.42	88.25	66.0	**0.060**	38,267
Lalbag	Murshidabad	MD	24.23	88.27	31.65	**0.016**	na
Kantanagar	Bhagwangola-I	MD	24.34	88.31	65.9	**0.092**	12,775
Edrakpur	Nawda	MD	23.91	88.46	82.1	**0.020**	10,951
Takipur	Beldanga-I	MD	23.87	88.25	54.8	**0.137**	37,881
Chaighari	Behrampur	MD	24.16	88.41	228.0	**<0.005**	10,479
Sekendra	Raghunathganj-I	MD	24.50	88.08	37.1	**0.074**	16,348
Girl's College	Behrampur Town	MD	24.09	88.26	74.2	**0.044**	na
Habaspur	Bhagawangola-I	MD	24.32	88.34	75.8	**0.032**	14,379
Chua	Hariharpara	MD	24.03	88.45	83.8	**0.055**	15,496
Surangapur	Nawda	MD	23.93	88.46	96.0	**0.015**	37,936
Mahimapur Palace	Murshidabad	MD	24.21	88.26	31.6	**<0.005**	na
Kismat-Imadpur	Hariharpara	MD	24.03	88.35	70.6	**0.024**	35,977
Nazirpur	Tehatta-1	MD	23.86	88.54	110.6	**0.027**	10,303
Narayanpur	Karimpur-II	MD	23.92	88.55	108.4	**0.099**	12,091
Nabipur	RaniNagar-II	MD	24.25	88.60	243.0	**<0.005**	11,420
Islampur	RaniNagar-I	MD	24.15	88.47	88.0	**0.041**	26,981
Andharkoth	Karimpur-I	ND	24.05	88.72	183.4	<0.005	12,780
Tehatta	Tehatta-I	ND	23.72	88.53	111.0	0.019	18,031

Table 6.1 (continued)

Location[a]	Block (Town)	District[b]	Latitude	Longitude	Depth (m)[c]	As (mg/L)[d]	Population[e]
Kaliganj	Kaliganj	ND	23.74	88.27	105.7	0.030	16,152
Bara Andulia	Chapra	ND	23.64	88.54	145.3	0.021	36,174
Karimpur	Karimpur-I	ND	23.98	88.65	106.7	0.030	29,634
Doradaha	Karimpur-II	ND	24.00	88.61	100.4	0.025	12,506
Dogachi	Karimpur-II	ND	24.03	88.58	100.4	<0.005	18,313
Mahisbathan	Karimpur-II	ND	23.95	88.61	140.2	0.017	14,616
Dignagar	KrishnaNagar-I	ND	23.34	88.44	118.1	0.030	24,193
Shyamnagar	Tehatta-I	ND	23.78	88.50	167.8	0.030	na
Bareya	Tehatta-II	ND	23.75	88.38	187.7	0.010	12,876
Gopinathpur	Tehatta-II	ND	23.84	88.46	134.0	0.060	14,093
Palsunda	Tehatta-II	ND	23.78	88.40	167.3	0.030	na
Debagram	Kaliganj	ND	23.69	88.33	78.3	**0.123**	27,477
Juranpur	Kaliganj	ND	23.72	88.22	154.7	**0.008**	12,896
Birpur	Nakashipara	ND	23.63	88.48	185.4	**0.039**	12,719
Bethuadahari	Nakashipara	ND	23.61	88.43	88.9	**0.052**	4,451
Jumpukur	Kaliganj	ND	23.72	88.38	268.9	**<0.005**	31,000
Hanspukuria	Tehatta-II	ND	23.74	88.48	230.0	**<0.005**	13,591
Gagnapur	Ranaghat-II	ND	23.14	88.64	176.0	**0.080**	13,562
Palashipara	Tehatta-II	ND	23.79	88.46	95.0	**0.011**	15,884
Iswarchandrapur	Tehatta-I	ND	23.76	88.46	217.0	**<0.005**	2,463
Dhubulia	KrishnaNagar-II	ND	23.50	88.45	132.0	**<0.005**	37,175
Sonatala	KrishnaNagar-II	ND	23.52	88.51	140.0	**0.020**	15,322
Gobrapota	KrishnaNagar-I	ND	23.42	88.55	119.6	**0.049**	2,880
Bhaluka	KrishnaNagar-I	ND	23.35	88.41	278.6	**<0.005**	18,202
Bhimpur	Krishnanaga-I	ND	23.43	88.62	211.0	**0.018**	19,982
Ghentugachia	Chakdah	ND	23.03	88.59	129.0	**0.055**	8,683
Kamagachi	Ranaghat-I	ND	23.22	88.56	151.6	**0.049**	34,245
Datta Para	Shantipur Town	ND	23.25	88.43	128.2	**0.212**	na
Kurulia	Bagda	NP	23.17	88.88	240.0	0.044	20,963
Ichapur	Gaighata	NP	22.91	88.74	222.0	0.033	14,009
Barabankra	Swarupnagar	NP	22.76	88.86	319.0	<0.005	22,378

Table 6.1 (continued)

Location[a]	Block (Town)	District[b]	Latitude	Longitude	Depth (m)[c]	As (mg/L)[d]	Population[e]
Sadpur	Habra-I	NP	22.86	88.76	238.0	<0.005	7,146
Koyadanga	Habra-I	NP	22.87	88.68	198.0	0.054	6,812
Champali	Minakhan	NP	22.57	88.80	289.9	<0.005	4,643
Sahebkhali	Hindalganj	NP	22.35	88.93	208.0	<0.005	10,550
Bishnupur	Rajarhat	NP	22.62	88.56	151.0	0.060	18,214
Debhog	Bashirhat-I	NP	22.61	88.83	269.0	0.010	7,738
Sankchura	Bashirhat-I	NP	22.61	88.88	150.0	<0.005	12,925
Rajendrapur	Bashirhat-II	NP	22.63	88.80	205.0	0.028	9,926
Kalupur	Bongaon	NP	23.01	88.78	196.1	0.020	9,210
Chandrapara	Gaighata	NP	22.97	88.76	207.8	0.022	16,347
Barunhat-Patlikhan	Hasnabad	NP	22.53	88.92	73.0	<0.005	19,992
Nurpur	Minakhan	NP	22.56	88.78	283.5	<0.005	6,238
Reckjwani	Rajarhat	NP	22.62	88.53	137.1	0.036	27,378
Thakdari	Rajarhat	NP	22.60	88.52	141.0	0.010	9,724
Gobindapur	Swarupnagar	NP	22.87	88.86	234.7	<0.005	13,993
Kalyani	Kalyani Town	NP	22.98	88.47	145.70	0.010	na
Naihati	Naihati Town	NP	22.89	88.41	144.9	0.050	na
Panihati	Panihati Town	NP	22.70	88.37	139.0	0.010	na
Barrackpore	Barrackpore Town	NP	22.79	88.36	150.7	0.010	na
Kamarhati	Kamarhati Town	NP	22.65	88.40	139.2	0.010	na
South DumDum	Dum Dum	NP	22.58	88.41	152.0	<0.005	na
Bidhannagar	Salt Lake	NP	22.56	88.42	146.1	0.010	na
Janapoll	Habra-I	NP	22.87	88.69	151.0	**0.088**	8,683
Chikanpara	Gaighata	NP	22.93	88.77	408.7	**0.028**	19,821
Dalalpara	Bashirhat Town	NP	22.69	88.85	230.2	**<0.005**	na
Bansjhari Mullickpur	Bashirhat-I	NP	22.58	88.88	272.9	**0.008**	6,974
Berachampa	Deganga	NP	22.70	88.68	298.0	**<0.005**	33,203
Berachampa (Aminpur)	Deganga	NP	22.69	88.67	155.0	**<0.005**	same
Berachampa (Deulia)	Deganga	NP	22.70	88.68	293.0	**<0.005**	same
Eojhnagar	Bashirhat-II	NP	22.71	88.72	151.2	**<0.005**	11,804

Table 6.1 (continued)

Location[a]	Block (Town)	District[b]	Latitude	Longitude	Depth (m)[c]	As (mg/L)[d]	Population[e]
Newtown	Rajarhat	NP	22.58	88.45	132.0	**<0.005**	na
Patharghata	Rajarhat	NP	22.58	88.51	120.3	**0.029**	10,668
Panchita	Bongaon	NP	23.11	88.80	192.9	**0.010**	10,223
Bongaon Hospital	Bongaon Town	NP	23.05	88.82	201.6	**0.028**	na
Rampur	Gaighata	NP	22.95	88.75	200.0	**0.054**	14,634
Kankphul	Habra-II	NP	22.86	88.62	190.1	**<0.005**	9,111
Bamangachi	Barasat-I	NP	22.75	88.51	157.7	**<0.005**	8,700
Humaipur	Barasat-II	NP	22.68	88.47	158.5	**0.019**	19,192
Haroa	Haroa	NP	22.60	88.68	167.6	**<0.005**	16,861
Arsula	Baduria	NP	22.74	88.77	147.6	**<0.005**	19,768
Murarisha	Hasnabad	NP	22.59	88.84	362.3	**<0.005**	9,854
Kalinagar	Sandeshkhali-I	NP	22.45	88.87	165.0	**<0.005**	15,265
Banipur	Habra Town	NP	22.82	88.69	150.0	**0.320**	na
Dihikalas	Mograhat-II	SP	22.28	88.37	267.0	<0.005	na
Baharu	Joynagar-I	SP	22.24	88.46	272.9	<0.005	15,657
Beliaghata	Baruipur	SP	22.30	88.53	278.0	<0.005	22,696
Dakhin Barasat	Joynagar-I	SP	22.26	88.48	278.0	<0.005	15803
Mograhat	Mograhat-II	SP	22.26	88.42	252.0	<0.005	32,604
South Garia	Baruipur	SP	22.36	88.50	256.8	<0.005	18,202
Ghasiara	Sonarpur	SP	22.44	88.46	240.0	**<0.005**	27816
Kalikapore	Sonarpur	SP	22.40	88.48	240.0	**<0.005**	32,719
Caning	Caning Town	SP	22.32	88.65	188.7	**<0.005**	11,719

[a]Location: Two or more public supply wells present in each location (also called scheme)
[b]District: CCU: Calcutta, MD: Murshidabad, ND: Nadia, NP: North 24 Parganas, SP: South 24 Parganas
[c]Depth: Maximum tapped depth from ground level
[d]As: Unfiltered As concentrations measured from one well of each location (scheme)
[e]Population: Population (based on Census, 2001) served by all the wells in each location (scheme)

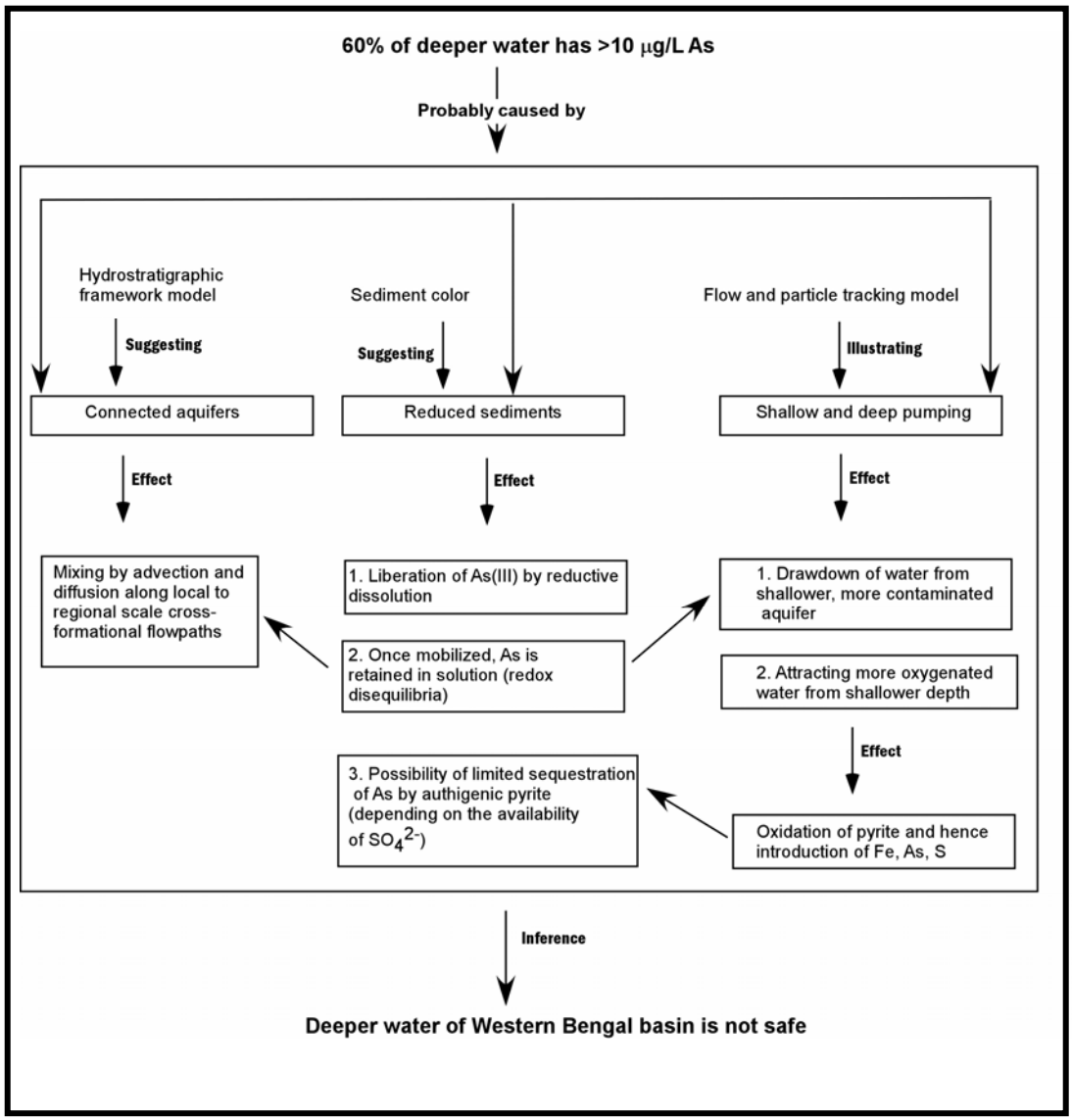

Figure 6.1: Flow chart showing the probable causal factors and processes that could have led to pollution of the deeper groundwater of the western Bengal basin.

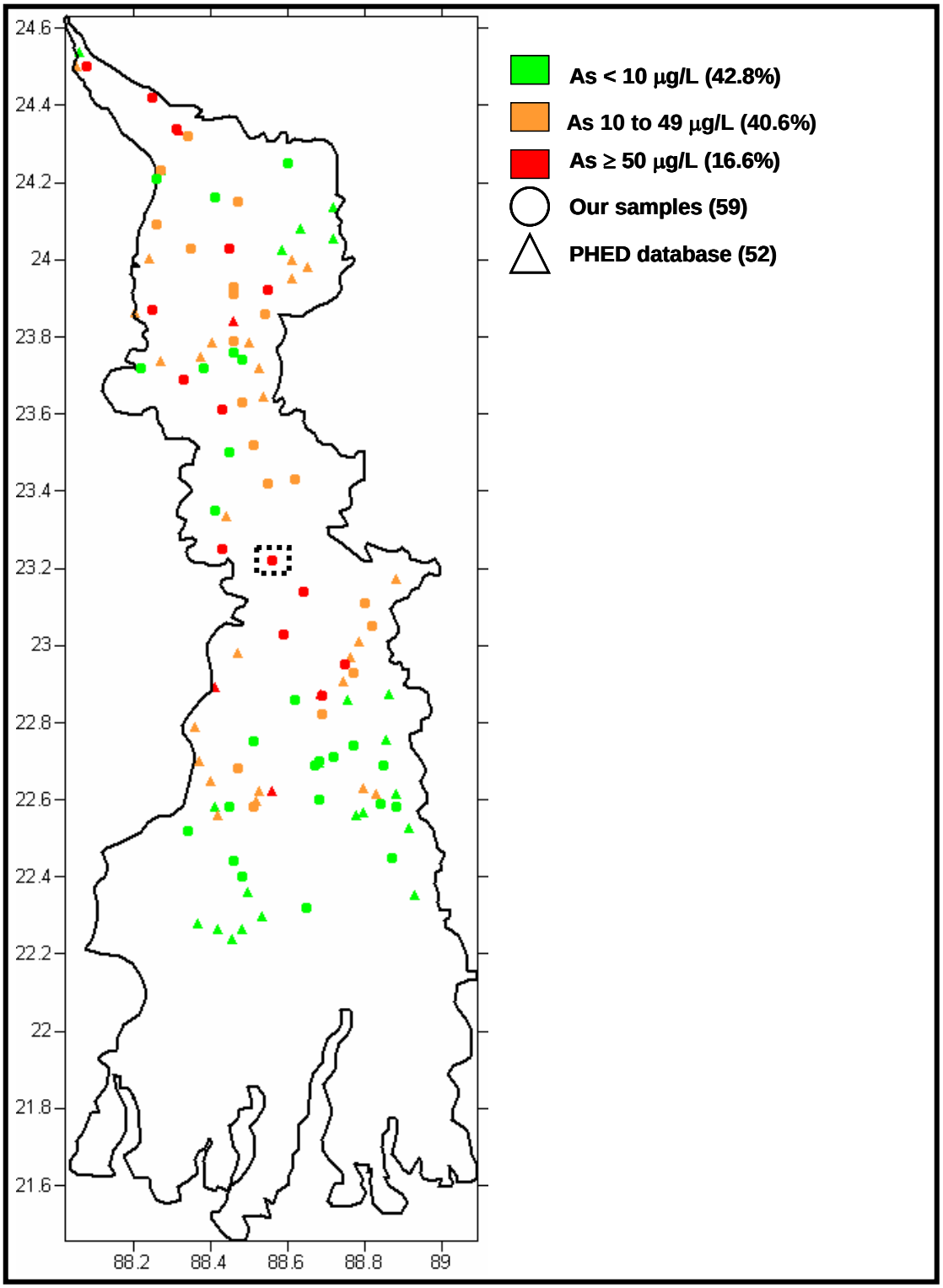

Figure 6.2: Map of unfiltered arsenic concentrations of deeper water within the study area. The dashed box indicates the area used for particle tracking modeling (Figure 6.7)

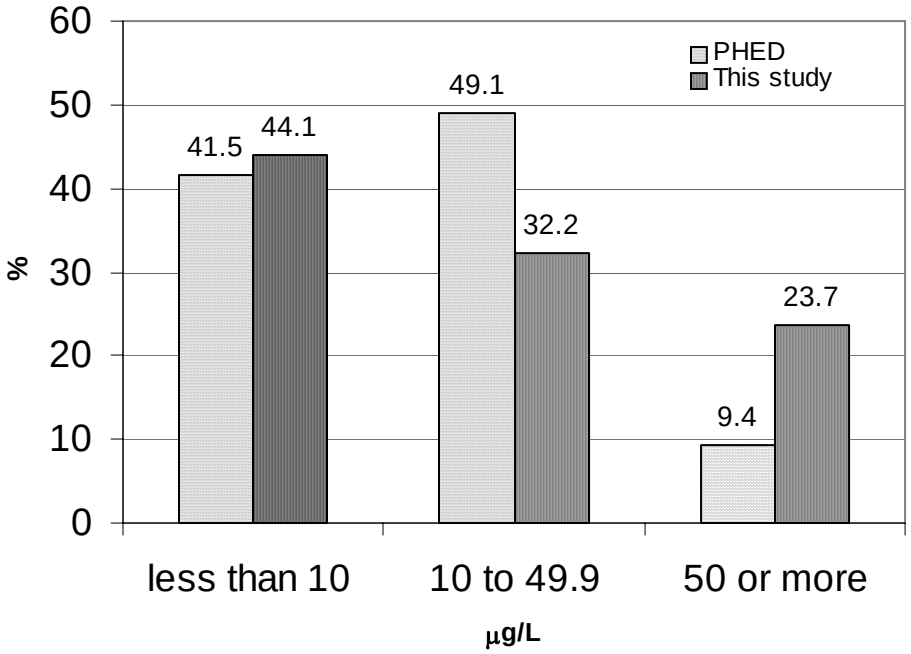

Figure 6.3: Comparison of percentage of arsenic concentrations between unfiltered samples collected during this study and data collected from PHED.

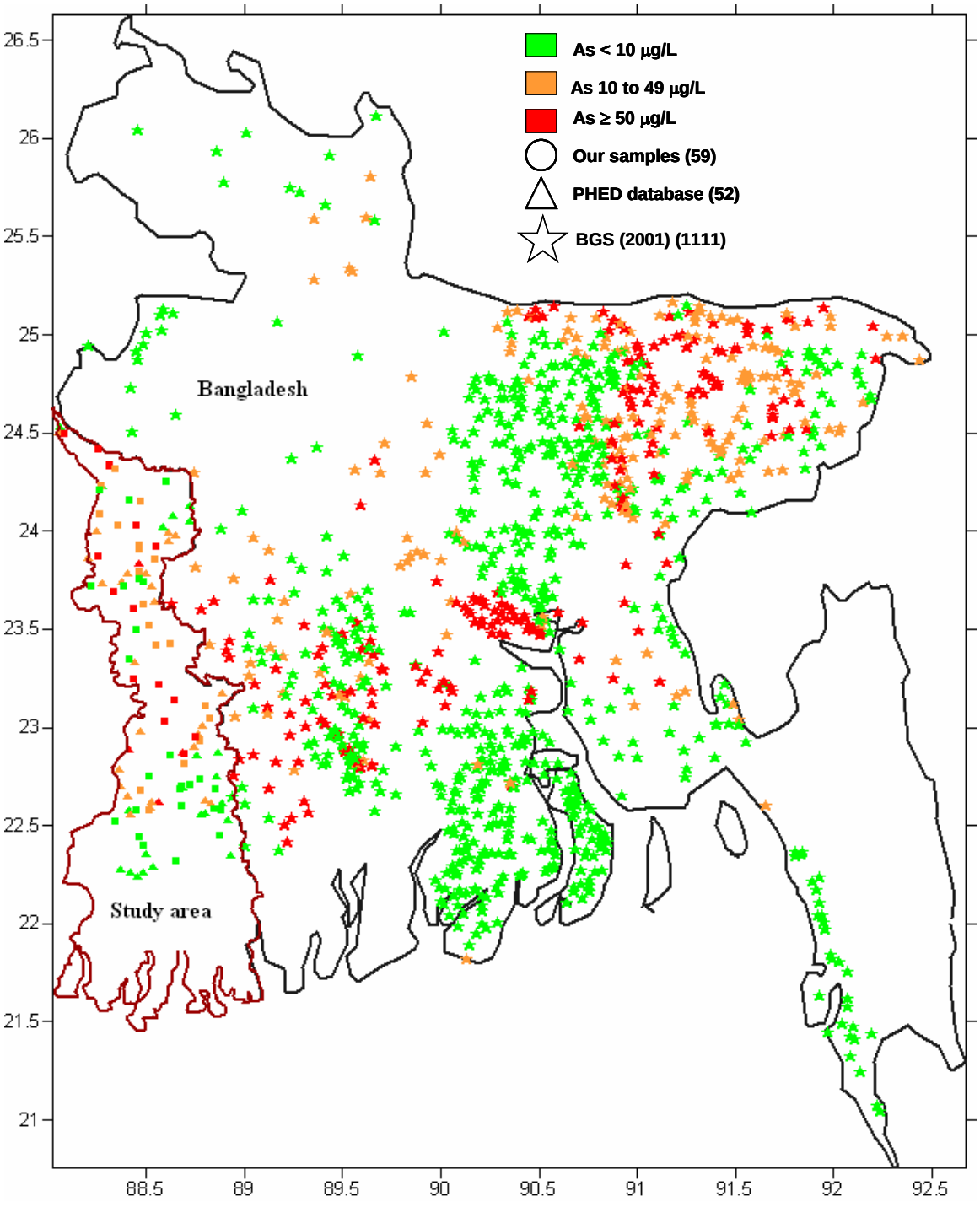

Figure 6.4: Map showing plot of arsenic concentrations of deeper wells of BGS/DPHE (2001) (≥50 m bgl) in Bangladesh and the data collected for the wells during this study and from PHED.

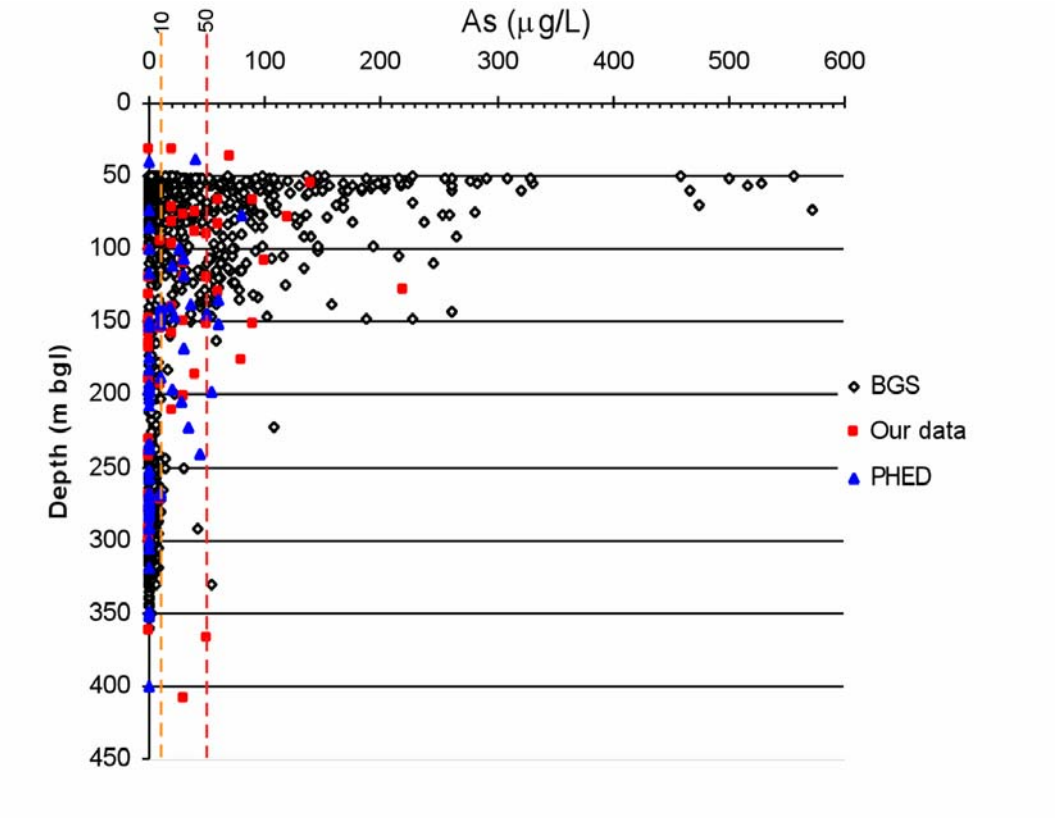

Figure 6.5: Comparison of arsenic concentrations as a function of depth for deeper wells of BGS/DPHE (2001) (≥50 m bgl) in Bangladesh and the data collected for the wells during this study and from PHED.

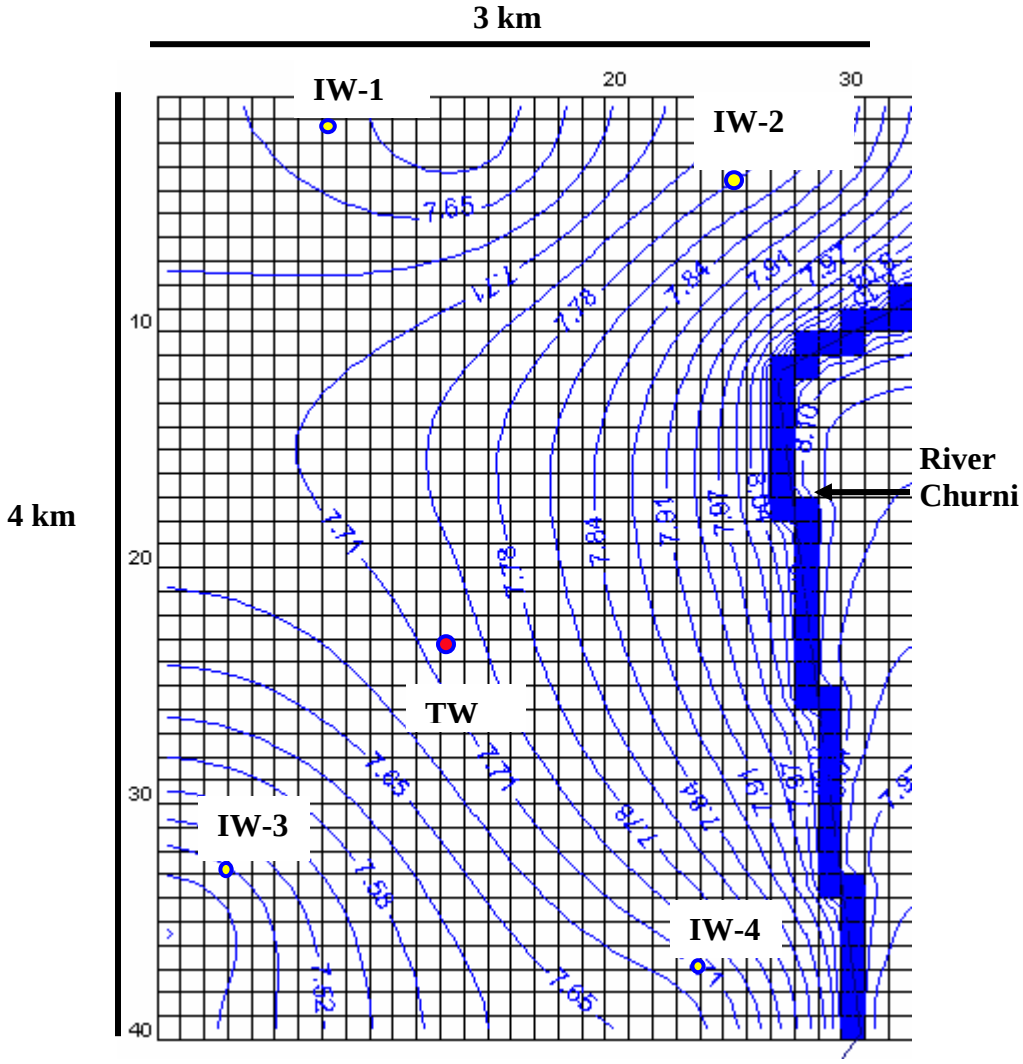

Figure 6.6: Map showing the discretization of the 12-km^2 area in and around Kamagachi (Ranaghat-I) that was used for particle tracking modeling. Horizontal grid spacing: 100 m × 100 m, vertical layers: 10 m (31 layers). The topography was defined by the SRTM-90 DEM. The irrigation wells (IW) were placed in arbitrary positions. The number of IWs was calculated per unit area from MID (2001). They were screened at 120 m bgl. The public supply well at Kamagachi (TW) was used as the target well and was placed in according to its global coordinates and screened at a depth of 150 m bgl. The rates of pumping are tabulated in Table 3.3a. The pumping rate inferred for the public TW was the same as those in Calcutta. The thin blue lines on the map indicate the simulated water-level contours with irrigational and public water-supply pumping (present-day conditions).

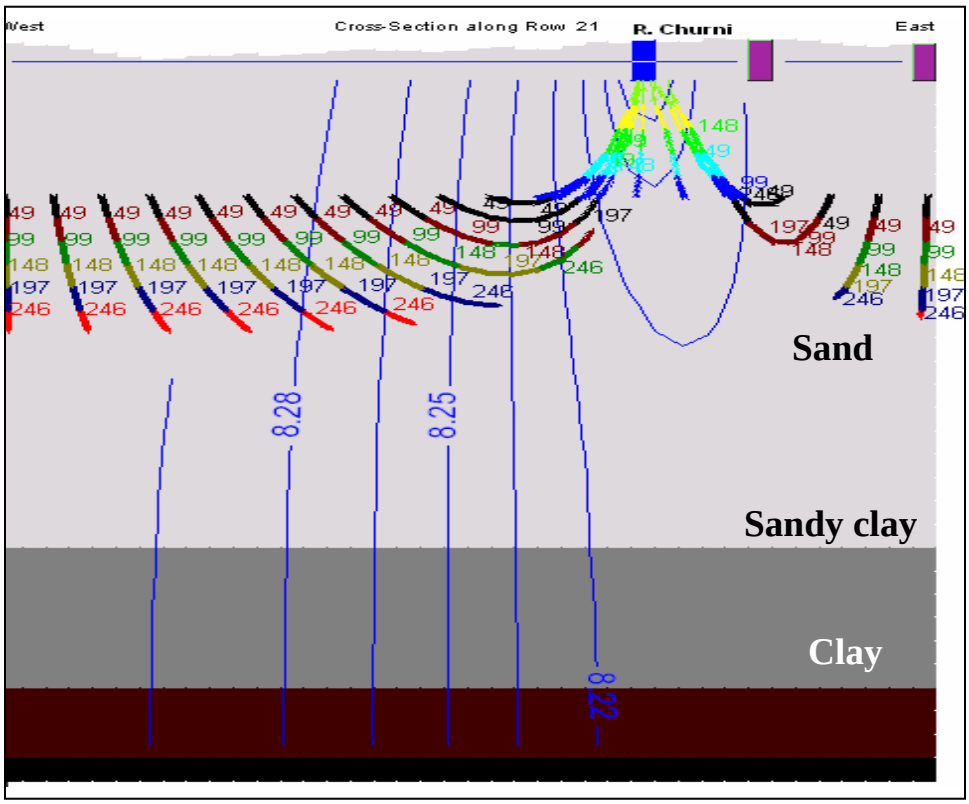

Figure 6.7a: Cross-section showing the results of particle-tracking modeling in the absence of pumping at Kamagachi (pre-1970s). The particles were placed horizontally at a depth of 50 m bgl. The numbers beside the flow paths indicate the numbers of years required to reach specific distances.

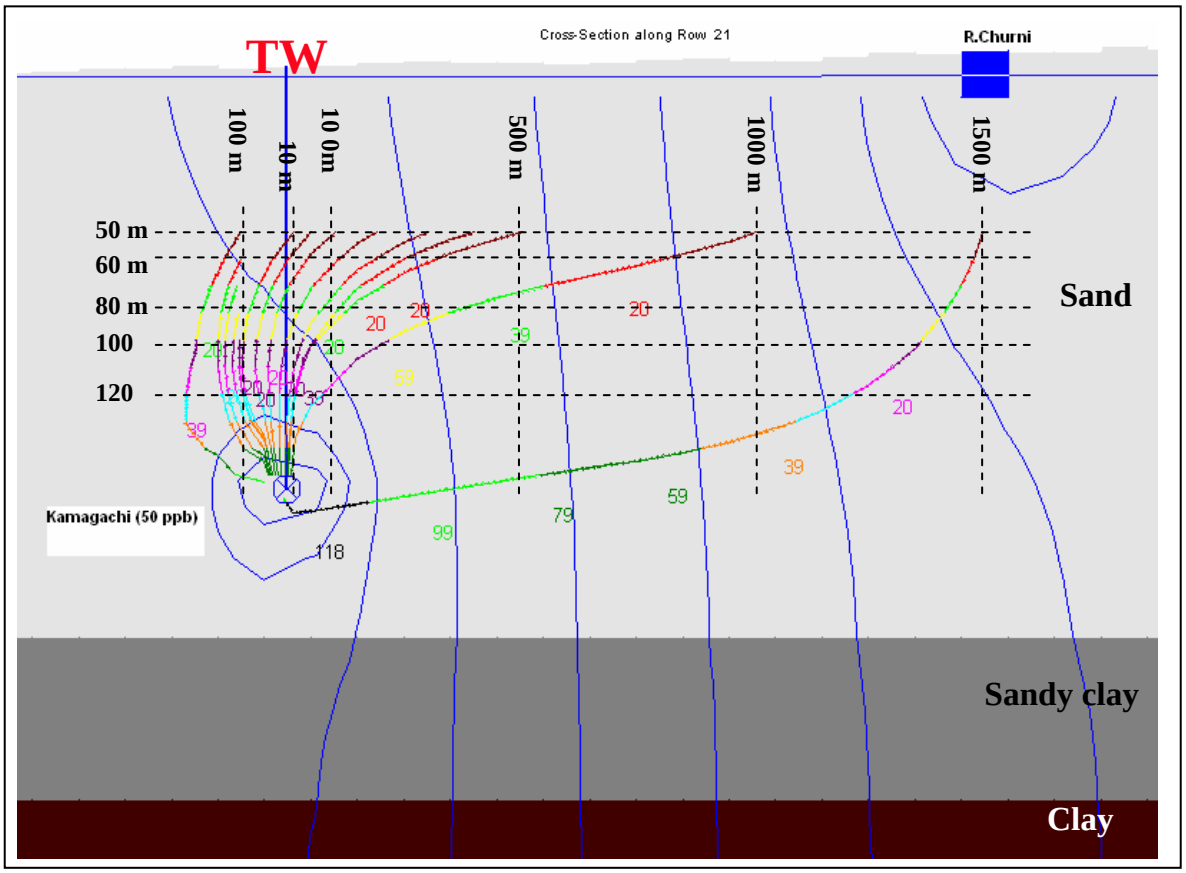

Figure 6.7b: Cross-section showing the results of particle-tracking modeling in presence of irrigation and water-supply pumping at Kamagachi (present day). The particles were placed horizontally at a depth of 50 m bgl, and vertically at every 10 m from 50 m to 120 m bgl. TW indicates the target well. The numbers beside the flow paths indicate the numbers of years required to reach specific distances.

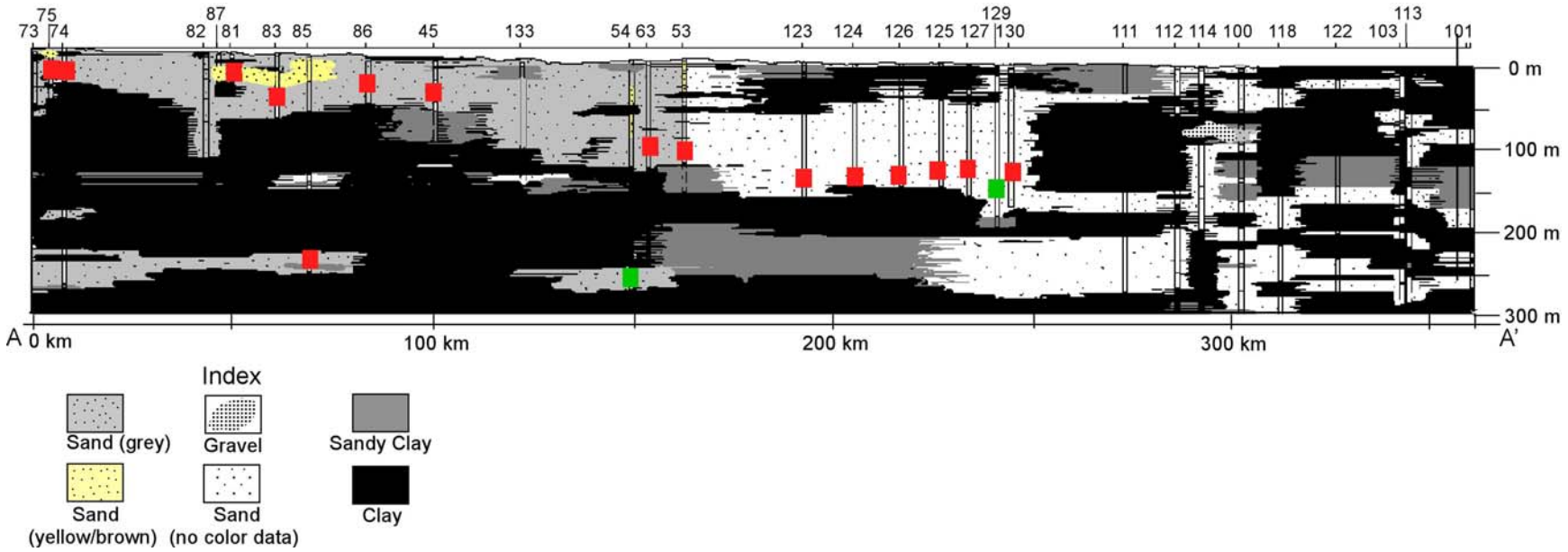

Figure 6.8a: Cross-section along section AA' (see figure 2.3) showing sediment color data and wells where As concentration data were available (with boxes). The boxes indicate the approximate tapped depth. Wells with red boxes had As ≥10 μg/L, and green boxes were ≤10 μg/L.

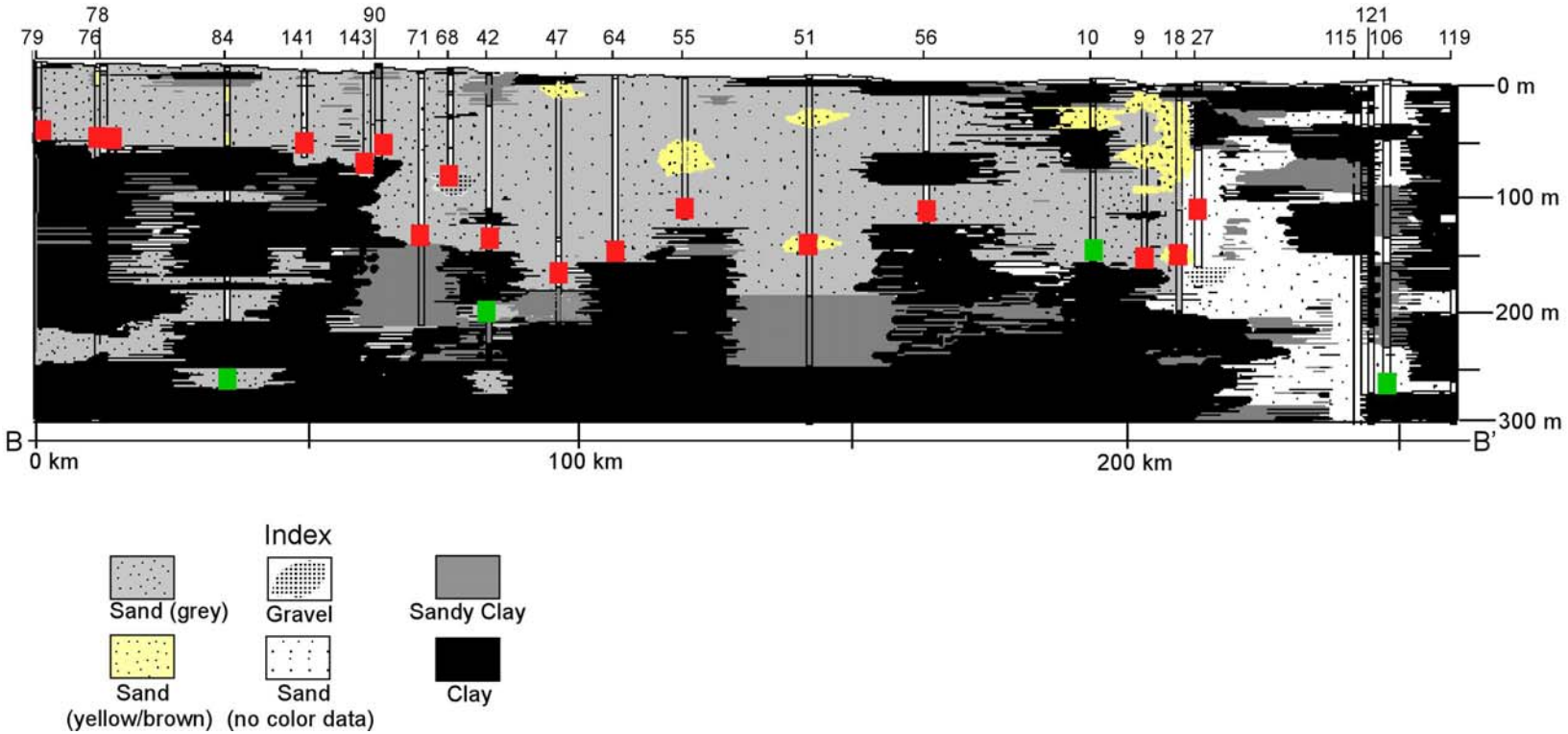

Figure 6.8b: Cross-section along section BB' (see figure 2.3) showing sediment color data and wells where As concentration data were available (with boxes). The boxes indicate the approximate tapped depths. Wells with red boxes had As ≥10 μg/L, and green boxes were ≤10 μg/L.

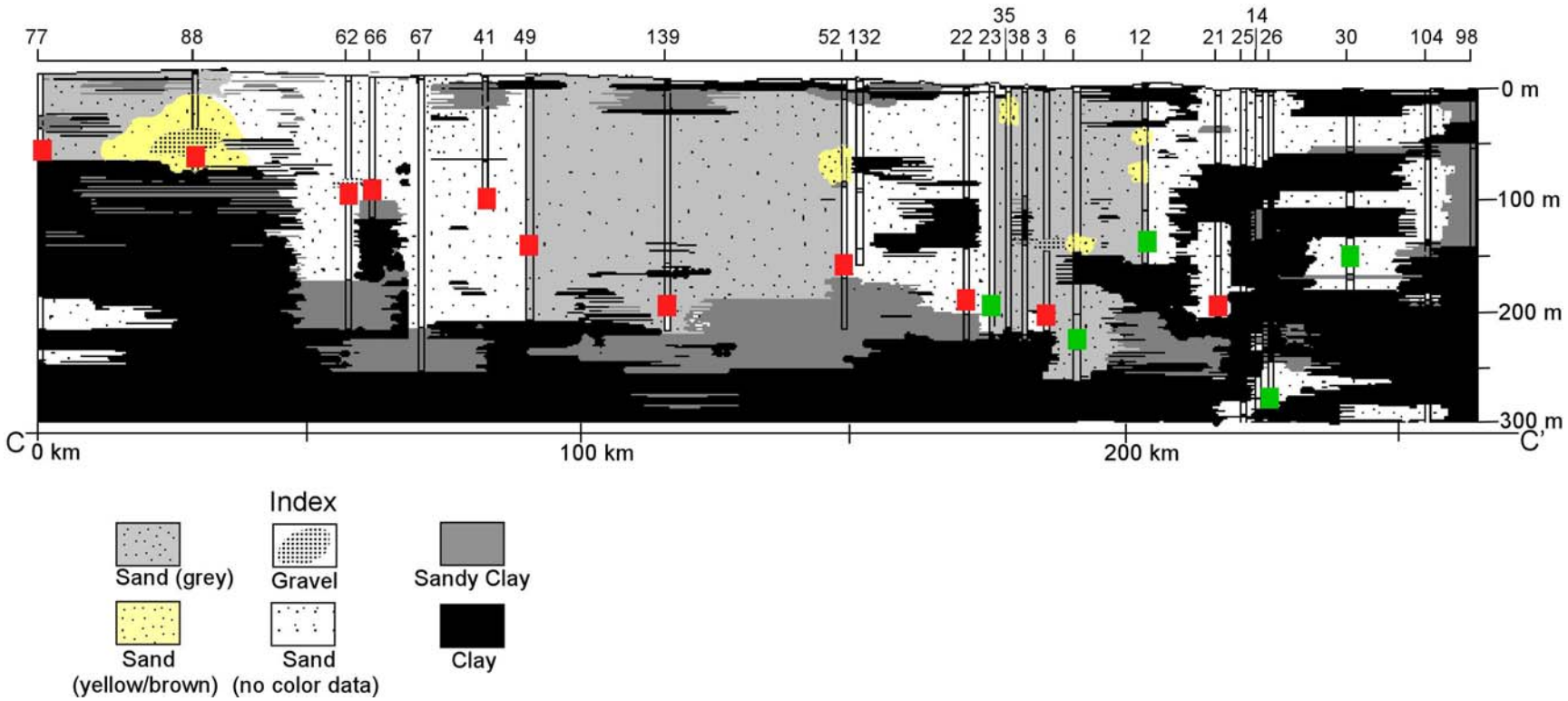

Figure 6.8c: Cross-section along section CC' (see figure 2.3) showing sediment color data and wells where As concentration data were available (with boxes). The boxes indicate the approximate tapped depths. Wells with red boxes had As ≥10 μg/L, and green boxes were ≤10 μg/L.

References

AAN, 2000. Arsenic contamination in groundwater and hydrogeology, Samta village, western Bangladesh. Asian Arsenic Network, report July 2000.

Abdullah, M.I., Shiyu, Z., Mosgren, K., 1995. Arsenic and selenium species in the oxic and anoxic waters of the Oslo-fjord, Norway. Mar. Pollut. Bull. 31, 116–126.

Acharyya, S.K., Lahiri, S., Raymahashay, B.C., Bhowmik, A., 1999. Arsenic poisoning in the Ganges delta. Nature 401, 545.

Acharyya, S.K., Lahiri, S., Raymahashay, B.C., Bhowmik, A., 2000. Arsenic toxicity of groundwater in parts of the Bengal basin in India and Bangladesh: the role of Quaternary stratigraphy and Holocene sea-level fluctuation. Environ. Geol. 39, 1127–1137.

Aggarwal, P.K., Basu, A.R., Kulkarni, K.M., Froehlich, K., Tarafdar, S.A., Ali, M., Hussain, A., 2000. A report on isotope hydrology of groundwater in Bangladesh: Implications for characterization and mitigation of arsenic in groundwater. International Atomic Energy Agency-TC Project BGD/8/016, 64 p.

Ahmed, K.M., 1994. Hydrogeology of the Dupi Tila Aquifer of the Barind Tract, NW Bangladesh. Unpublished Ph.D. thesis, Univ. London, London.

Ahmed, K.M., Hoque, M., Hasan, M.K., Ravenscroft, P., Chowdhury, L.R., 1998. Occurrence and origin of water well CH_4 gas in Bangladesh. J. Geol. Soc. India 51, 697–708.

Ahmed, K.M., Bhattacharya, K.M., Hasan, M.A., Akhter, S.H., Alam, M., Bhuyian, M.A.H., Imam, M.B., Khan, A.A., Sracek, O., 2004. Arsenic enrichment in groundwater of the alluvial aquifers in Bangladesh: an overview. Appl. Geochem. 19, 181–200.

AIP/PHED, 1991. National drinking water mission submission project on arsenic pollution in groundwater in West Bengal. Final report, Steering Committee, Arsenic Investigation Project (AIP) and Public Health Engineering Directorate, Government of West Bengal, India, 58 p.

AIP/PHED, 1995. Prospective plan for arsenic affected districts of West Bengal. Arsenic Investigation Project (AIP) and Public Health Engineering Directorate (PHED), Government of West Bengal, Calcutta, India.

Alam, M.K., Hassan, A.K.M.S., Khan, M.R., Whitney, J.W., 1990. Geological map of Bangladesh. Geological Survey of Bangladesh.

Alam, M., Alam, M.M., Curray, J.R., Chowdhury, M.L.R., Gani, M.R., 2003. An overview of the sedimentary geology of the Bengal basin in relation to the regional tectonic framework and basin-fill history. Sed. Geol. 155, 179–208.

Alley, W.M., Healy, R., LaBaugh, J.W., and Reilly, T.E., 2002. Flow and storage in groundwater systems. Science 296, 1985-1990.

Allison, G.B., 1982. The relationship between ^{18}O and deuterium in water and sand columns undergoing evaporation. J. Hydrol. 55, 163–176.

Allison, J.D., Brown, D.S., Novo-Gradac, K.J., 1990. MINTEQA2/PRODEFA2–A geochemical assessment model for environmental systems–version 3.0 user's manual. Environmental Research Laboratory, Office of Research and Development, U.S. Environmental Protection Agency, Athens, Georgia, 106 p.

Allison, M.A., 1998. Geologic framework and environmental status of the Ganges-Brahmaputra Delta. J. Coastal Res. 14(3), 826–836.

Allison, M.A., Khan, S.R., Goodbred, S.L., Kuehl, S.A., 2003. Stratigraphic evolution of the late Holocene Ganges-Brahmaputra lower delta plain. Sed. Geol. 155, 317–342.

Ananthakrishnan, R., 1977. Some aspects of the monsoon circulation and monsoon rainfall. In: Krishnamurti, T.N. (Ed.), Monsoon Dynamics. Birkhauses-Verlag, Basel and Stuttgart.

Andrews, J.N., Drimmie, R.J., Loosli, H.H., Hendry, M.J., 1991. Dissolved gases in the Milk River aquifer, Alberta, Canada. Appl. Geochem. 6(4), 393–403.

Anwar, H.M., Komaki, K., Akai, J., Takada, J., Ishizuka, T., Takahasi, T., Yoshioka, T., Kato, K., 2002. Diagenetic control on arsenic partitioning in sediments of the Meghna River delta, Bangladesh. Environ. Geol. 41, 816–825.

American Public Health Association, 1992. Standard Methods for the Examination of Water and Wastewater, 18th edition, method 4500-NH_3 C, pp. 4–78.

American Public Health Association, 1995a. Standard Methods for the Examination of Water and Wastewater, 19th edition, method 4500-NO_3-E, pp. 4–87.

American Public Health Association, 1995b. Standard Methods for the Examination of Water and Wastewater, 19th edition, method 4500-NO_2 B, pp. 4–85.

American Public Health Association, 1995c. Standard Methods for the Examination of Water and Wastewater, 19th edition, method 4500-S^{2-} D, pp. 4–124.

Appelo, C.A.J., Postma, D., 1994. Geochemistry, groundwater and pollution. A.A. Balkema, Rotterdam, 536 p.

Araguas-Araguas, L., Froehlich, K., Rozanski, K., 1998. Stable isotope composition of precipitation over Southeast Asia. J. Geophys. Res. 103, 721–742.

Aravena, R., Wassenaar, L.I., Plummer, L.N., 1995a. Estimating ^{14}C groundwater ages in a methanogenic aquifer. Water Resour. Res. 31, 2307–2317.

Aravena, R., Wassenaar, L. I., Barker, J. F., 1995b. Distribution and isotopic characterization of methane in a confined aquifer in southern Ontario, Canada. Canadian J. Hydrol. 173, 51–70.

Aswathanarayana, U., 1995. Geoenvironment: an introduction. A.A. Balkema, Rotterdam, 270 p.

ATSDR, 2005. CERCLA priority list of hazardous substances. Agency for Toxic Substance and Disease Registry, U.S. Department of Health and Human Services.

Back, W., 1966. Hydrochemical facies and groundwater flow patterns in the northern part of Atlantic Coastal Plain. U.S. Geol. Surv. Prof. Paper 498-C, 16 p.

Back, W., Hanshaw, B.B., 1970. Comparison of chemical hydrogeology of the carbonate peninsulas of Florida and Yucatan. J. Hydrol. 10, 330–368.

Bagchi, K., 1944. The Ganges Delta. University of Calcutta Press, Calcutta, 157 p.

Ball, F., 1877. Geology of the Rajmahal hills. Geol. Surv. Ind. Memoir 13, 1–94.

Banerjee, R.K., 1981. Cretaceous-Eocene sedimentation, tectonism and biofacies in the Bengal Basin, India. Palaeogeog. Palaeoclimat. Palaeoecol. 34, 57–85.

Banerjee, M., Sen, P.K., 1987. Palaeobiology in understanding the change in sea level and the coast line in Bengal basin during Holocene period. Ind. J. Earth Sci. 14, 307–320.

Barcelona, M.J., Holm, T.R., Schock, M.R., George, G.K., 1989. Spatial and temporal gradients in aquifer oxidation-reduction conditions. Water Resour. Res. 25, 991–1003.

Barker, J.A., Davies, J., Herbert, R., 1989. The pilot study into optimum well design: IDA 4000 Deep Tubewell II Project, vol. 4: Well and aquifer modeling: Part 1. A multi-layer model for long term pumping tests. British Geological Survey technical report WD/89/11.

Barker, J. F., Fritz, P., 1981. The occurrence and origin of methane in some groundwater flow systems. Canadian J. Earth Sci. 18, 1802–1816.

Barui, N.C., Chanda, S., 1992. Late Quaternary pollen analysis in relation to palaeoecology, biostratigraphy and dating of Calcutta peat. Proc. Ind. Nat. Sci. Acad. B54(4), 191–200.

Basu, A.R., Jacobsen, S.B., Poreda, R.J., Dowling, C.B., Aggarwal, P.K., 2001. Large groundwater strontium flux to the oceans from the Bengal Basin and marine strontium isotope record. Science 293, 1470–1473.

Basu, A.R., Jacobsen, S.B., Poreda, R.J., Dowling, C.B., Aggarwal, P.K., 2002. Response to Harvey, 2002: Groundwater flow in the Ganges delta. Science 296, 1563.

Baumler, R., Zech, W., 1994. Soils of the high mountain region of Eastern Nepal: classification, distribution and soil forming processes. Catena 22, 85–103.

Beck, K.C., Reuter, J.H., Perdue, E.M., 1974. Organic and inorganic geochemistry of some coastal plain rivers of the southeastern United States. Geochim. Cosmochim. Acta 38, 341–364.

Bednar, A.J., Garbarino, J.R., Ranville, J.F., Wildeman, T.R., 2002. Preserving the distribution of inorganic arsenic species in groundwater and acid mine drainage samples. Environ. Sci. Technol. 36, 2213–2218.

Bentley, H. W., Phillips, F.M., Davis, S.N., Habermehl, M., Airey, P.L., Calf, G.E., Elmore, D., Gove, H.E., Torgersen, T., 1986. Chlorine-36 dating of very old groundwater: 1. The Great Artesian basin, Australia. Water Resour. Res. 22, 1991–2001.

Berner, R.A., 1981. A new geochemical classification of sedimentary environments. J. Sed. Petrol. 51, 359–365.

BGS/DPHE, 2001. Arsenic contamination of groundwater in Bangladesh, vol. 2: final report. Kinniburgh, D.G., Smedley, P.L. (Eds.), British Geological Survey (BGS) Technical Report WC/00/19, Keyworth, 255 p.

BGS/DPHE/MML, 1999. Groundwater studies for arsenic contamination in Bangladesh, Phase I: Rapid investigation phase. Department of Public Health Engineering, Govt. of Bangladesh, British Geological Survey and Mott MacDonald Ltd., UK.

Bhattacharya, P., Chatterjee, D., Jacks, G., 1997. Occurrence of arsenic-contaminated groundwater in alluvial aquifers from the Bengal Delta Plain, Eastern India: options for a safe drinking water supply. Water Resour. Dev. 13, 79–92.

Bhattacharya, P., Jacks, G., Ahmed, K.M., Khan, A.A., Routh, J., 2002. Arsenic in groundwater of the Bengal Delta Plain aquifers in Bangladesh. Bull. Environ. Contam. Toxicol. 69, 538–545.

Bhattacharya, P., Von Bromssen, M., Jakariya, M., Ahmed, K.M., Jacks, G., 2005. Redox characteristics of sedimentary aquifers as a tool for targeting arsenic safe groundwater in Bangladesh. Geol. Soc. Am. Abstracts with Programs 37(7), 170.

Bhattacharya, S.K., Gupta, S.K., and Krishnamurthy, R.V., 1985. Oxygen and hydrogen isotope ratios in groundwaters and rivers from India. Proc. Ind. Acad. Sci. (Earth and Planetary Science) 94, 283–295.

Bhattacharya, S.K., Froehlich, K., Aggarwal, P.K., Kulkarni, K.M., 2003. Isotopic variation in Indian monsoon precipitation: records from Bombay and New Delhi. Geophys. Res. Let. 30, 2285–2288.

Biswas, B., 1963. Results of exploration for petroleum in the western part of Bengal basin, India. Proc. Symposium on Development of Petrology. Res., Mineral Resource Division, Service 18(1), 241–250.

Blanchon, P., and Shaw, J., 1995. Reef drowning during the last deglaciation: evidence from catastrophic sea level rise and ice sheet collapse. Geology, 23(1), 4-8.

Boswell, E.H., 1996. Hydrogeology of the Lower Mississippi Valley as related to the work of Harold N. Fisk. Eng. Geol. 45, 205–217.

Böttcher, J., Strebel, O., Voerkelius, S., Schmidt, H.L., 1990. Using isotope fractionation of nitrate-nitrogen and nitrate-oxygen for evaluation of microbial denitrification in sandy aquifer. J. Hydrol. 114, 413–424.

Brammer, H., 1990a. Floods in Bangladesh. I. Geographical background to the 1987 and 1988 floods. Geograph. J. 156, 12–22.

Brammer, H., 1990b. Floods in Bangladesh. II. Flood mitigation and environmental aspects. Geograph. J. 156, 158–165.

Brammer, H., 1996. The geography of soils of Bangladesh. University Press Ltd., Dhaka, 287 p.

Breit, G.N., Foster, A.L., Sanzalone, R.F., Yount, J.C., Whitney, J.W., Welch, A.H., Islam, M.K., Islam, M.N., 2001. Arsenic cycling in eastern Bangladesh: the role of phyllosilicates. Geol. Soc. Am. Abstracts with Programs 32(7), A192.

Burbank, D.W., 1992. Causes of recent Himalayan uplift deduced from deposited patterns in the Ganges basin. Nature 357, 680–683.

Butler, R.D., 1984. Hydrogeology of the Dakota aquifer system, Williston Basin, North Dakota. In: Jorgensen, D.G., Signor, D.N. (Eds.), Proc. Geohydrology of Dakota Aquifer Symposium. Water Well Journal Pub. Co., Worthington, Ohio, pp. 12–23.

Canfield, D.E., Thamdrup, B., Hansen, J.W., 1993. The anaerobic degradation of organic matter in Danish coastal sediments: Iron reduction, manganese reduction and sulfate reduction. Geochim. Cosmochim. Acta 57, 3867–3883.

Census, 2001. Provisional population totals. Census of India, chapter 3, series 1. Government of India, 16 p.

CGWB, 1994a. Hydrogeology and groundwater resource of Murshidabad district, West Bengal. Technical report, series D, Central Ground Water Board (CGWB), Eastern Region, Government of India.

CGWB, 1994b. Hydrogeology and groundwater resource of Nadia district, West Bengal. Technical report, series D, Central Ground Water Board (CGWB), Eastern Region, Government of India.

CGWB, 1994c. Hydrogeology and groundwater resource of North 24 Parganas district, West Bengal. Technical report, series D, Central Ground Water Board (CGWB), Eastern Region, Government of India.

CGWB, 1994d. Hydrogeology and groundwater resource of South 24 Parganas, West Bengal. Technical report, series D, Central Ground Water Board (CGWB), Eastern Region, Government of India.

CGWB, 1994e. Hydrogeological atlas of West Bengal, Scale 1:2,000,000. Central Ground Water Board (CGWB), Eastern Region, Government of India.

CGWB, 1997. High arsenic groundwater in West Bengal. Technical Report, series D, Central Ground Water Board (CGWB), Eastern Region, Calcutta, Government of India.

CGWB, 1999. High incidence of arsenic in groundwater in West Bengal. Central Ground Water Board, Ministry of Water Resources, Government of India.

Chakraborti, D., Basu, G.K., Biswas, B.K., Chowdhury, U.K., Rahman, M.M., Paul, K., Chowdhury, T.R., Chanda, C.R., Lodh, D., Ray, S.L., 2001. Characterization of arsenic-bearing sediments in the Gangetic delta of West Bengal, India. In: Chappell, W.R., Abernathy, C.O., Calderon, R.L. (Eds.), Arsenic Exposure and Health Effects IV. Elsevier Science Ltd., Oxford, pp. 27–52.

Chapelle, F.H., 1993. Ground Water Microbiology and Geochemistry. John Wiley & Sons, Inc., New York, 424 p.

Chapelle, F.H., McMahon, P.B., 1991. Geochemistry of dissolved inorganic carbon in a coastal plain aquifer: 1. Sulfate from confining beds as an oxidant in microbial CO_2 production. J. Hydrol. 127, 85–108.

Chapelle, F.H., Lovley, D.R., 1992. Competitive-exclusion of sulphate reduction by Fe(III)-reducing bacteria–a mechanism for producing discrete zones of high-iron groundwater. Ground Water 30, 29–36.

Chapelle, F.H., McMahon, P.B., Dubrovsky, N.M., Fujii, R.F., Oaksford, E.T., Vroblesky, D.A., 1995. Deducing the distribution of terminal electron-accepting processes in hydrologically diverse groundwater systems. Water Resour. Res. 31, 359–371.

Chatterjee, D., Jana, J., Jacks, G., Bhattacharya, P., 2004. Natural arsenic in groundwaters of West Bengal, India: Examples from the districts of Nadia and South 24 Parganas. Proc. 32nd IGC, Florence, Italy, BWO 06-42.

Chatterjee, S.P., 1949. Bengal in Maps. Oriental Longmans Ltd., Calcutta, 105 p.

Chowdhury, M.I., Hoque, M., Pramanik, A.H., 1985. Morphology and origin of Swatch of No Ground, Bay of Bengal. J. Nat. Oceanographic Marine Inst. 2, 19–29.

Chowdhury, T.R., Basu, G.K., Mandal, B.K., Biswas, B.K., Samanta, G., Chowdhury, U.K., Chanda, C.R., Lodh, D., Roy, S.L., Saha, K.C., Roy, S., Kabir, S., Quamrazzaman, Q., Chakraborti, D., 1999. Arsenic poisoning in the Ganges Delta. Nature 401, 545–546.

Clark, I.D., Fritz, P., 1997. Environmental Isotopes in Hydrogeology. Lewis Publishers, Boca Raton, Florida, 328 p.

Coleman, J.M., 1969. Brahmaputra river: channel processes and sedimentation. Sed. Geol. 3, 129–139.

Coleman, J.M., 1981. Deltas: Processes of Deposition and Models of Exploration, 2nd edition. Burgess, Minneapolis.

Coleman, D.D., Liu, D.L., Riley, K.M., 1988. Microbial methane in the shallow paleozoic sediments and glacial deposits of Illinois, USA. Chem. Geol. 71, 23–40.

Craig, H., 1961. Isotopic variations in meteoric water. Science 133, 1702–1703.

Cumming, D.E., Caccavo, F., Fendorf, S., Rosenzweig, R.F., 1999. Arsenic mobilization by the dissimilatory Fe(III) reducing bacterium Shewanella alga BrY. Environ. Sci. Technol. 33, 723–729.

Curray, J.R., Emmel, F.J., Moore, D.G., Raitt, R.W., 1982. Structure, tectonics and geological history of northern Indian Ocean. In: Nairn, A.E., Stehli, F.G. (Eds.), The Ocean Basins and Margins. New York, Plenum, 107–112.

Dansgaard, W., 1964. Stable isotopes in precipitation. Tellus 16, 436–467.

Das, D., Chatterjee, A., Mandal, B.K., Samanta, G., Chakraborti, D., Chanda, B., 1995. Arsenic in groundwater in 6 districts of West Bengal, India. Environ. Geochem. Health 18, 5–15.

Das, D., Chatterjee, A., Mandal, B.K., Samanta, G., Chakraborti, D., Chanda, B., 1996. Arsenic in groundwater in 6 districts of West Bengal, India: the biggest arsenic calamity in the world. Part 2: Arsenic concentration in drinking water, hair, nails, urine, skin-scale and liver tissue (biopsy) of the affected people. Analyst 120, 917–924.

Datta, D.K., Subramanian, V., 1997. Textures and mineralogy of sediments from the Ganges-Brahmaputra-Meghna river system in the Bengal basin, Bangladesh and their environmental implications. Environ. Geol. 30(3), 181–188.

Datta, D.K., Gupta, L.P., Subramanian, V., 1999. Distribution of C, N, and P in the sediments of the Ganges-Brahmaputra-Meghna river system in the Bengal basin. Org. Geochem. 30, 75–82.

Davis, J.C., 1986. Statistics and Data Analysis in Geology. John Wiley and Sons, New York, 550 p.

Derry, L.A., France-Lanord, C., 1996. Neogene Himalayan weathering history and river $^{87}Sr/^{86}Sr$: impact on the marine Sr record. Earth Planet. Sci. Let. 142, 59–74.

Dowling, C.B., Poreda, R.J., Basu, A.R., Peters, S.L., 2002. Geochemical study of arsenic release mechanisms in the Bengal basin groundwater. Water Resour. Res. 38(9), 1173–1191.

Dowling, C.B., Poreda, R.J., Basu, A.R., 2003. The groundwater geochemistry of the Bengal basin: weathering, chemosorption, and trace metal flux to the oceans. Geochim. Cosmochim. Acta 67, 2117–2136.

Downey, J.S., 1984. Geology and hydrology of the Madison limestone and associated rocks in parts of Montana, Nebraska, North Dakota, South Dakota, and Wyoming. U.S. Geol. Surv. Prof. Paper 1273-G, 152 p.

Dray, M., 1983. Contribution of isotopic techniques in the determination of the relationship of surface water/groundwater in Bangladesh (Ganges and Brahmaputra area). Proc. National Symposium on River Basin Development. Dacca, Bangladesh, 158–170.

Dreher, T., 2003. Comment on Güler et al., 2002, Evaluation of graphical and multivariate methods for classification of water chemistry data. Hydrogeol. J. 11, 605–606.

Drever, J.I., 1997. The Geochemistry of Natural Waters, 3rd edition. Prentice-Hall, Upper Saddle River, New Jersey, 388 p.

Eary, L.E., Schramke, J.A., 1990. Rates of inorganic oxidation reaction involving dissolved oxygen. In: Melchior, D.C., Bassett, R.L. (Eds.), Chemical Modeling of Aqueous Systems II. Am. Chem. Soc. Symp. Ser. 416, pp. 379–396.

EPA, 1979. Methods for Chemical Analysis of Water and Wastes, method 376.2, U.S. Environmental Protection Agency.

EPC/MMP, 1991. Dhaka region groundwater and subsidence study, Final report. Engineering and Planning Consultants, Dhaka, and Sir Mott MacDonald and Partners, UK.

Evans, P., 1964. The tectonic framework of Assam. J. Geol. Soc. Ind. 5, 80–96.

Fairbanks, R.G., 1989. A 17,000 glacio-eustatic sea level record: influence of glacial melting rates on the Younger Dryas event and deep ocean circulation. Nature 342, 637–642.

FAO, 1971. Soil survey project, Bangladesh. Food and Agricultural Organization (FAO), AGL:SF/PAK 6, Tech. Rep. 3, Rome.

Farmer, J.G., Lovell, M.A., 1986. Natural enrichment of arsenic in Loch Lomond sediments. Geochim. Cosmochim. Acta 50, 2059–2067.

Faure, G., 1998. Principles and Applications of Geochemistry, 2nd edition. Prentice Hall, Upper Saddle River, New Jersey, 600 p.

Ferguson, J.F., Anderson, M.A., 1974. Chemical form of arsenic in water supplies and their removal. In: Rubin, A.J. (Ed.), Chemistry of Water Supply, Treatment and Distribution. Ann Arbor Science, Ann Arbor, Michigan, pp. 137–158.

Fergusson, J., 1863. On recent changes in the delta of the Ganges. Quarterly J. Geol. Soc. London, 19, 321–354.

Fogg, G.E., Kreitler, C.W., 1982. Ground-water hydraulics and hydrochemical facies in Eocene aquifers of the East Texas basin. Rep. Invest. No. 127, Bureau of Economic Geology, Univ. Texas at Austin, 75 p.

Folk, R.L., Ward, W.C., 1957. Brazos river bar: a study in the significance of grain size parameters. J. Sed. Petrol. 22, 125–145.

Foster, A.L., Brown, G.E., Parks, G.A., 2003. X-ray absorption fine structure study of As(V) and Se(IV) sorption complexes on hydrous Mn oxides. Geochim. Cosmochim. Acta 67, 1937–1953.

Foster, M.D., 1950. The origin of high sodium bicarbonate waters in the Atlantic and Gulf Coastal Plains. Geochim. Cosmochim. Acta 1, 33–48.

France-Lanord, C., Derry, L., Michard, A., 1993. Evolution of the Himalayas since Miocene time: isotopic and sedimentological evidence from the Bengal Fan. In: Treloar, P.J., Searle, M.P. (Eds.), Himalayan Tectonics. Geological Society Special Publication 74, 603–621.

Freeze, R.A., Cherry, J.A., 1979. Groundwater. Prentice Hall, Englewood Cliffs, New Jersey, 604 p.

Fryar, A.E., Mullican III, W.F., Macko, S.A., 2001. Groundwater recharge and chemical evolution in the southern High Plains of Texas, USA. Hydrogeol. J. 9, 522–542.

Gaillardet, J., Dupre, B., Louvat, P., Allegre, C.J., 1999. Global silicate weathering and CO_2 consumption rates deduced from the chemistry of large rivers. Chem. Geol. 159, 3–30.

Gallagher, P.A., Schegel, C.A., Wei, X., Creed, J.T., 2001. Speciation and preservation of inorganic arsenic in drinking water sources using EDTA with IC separation and ICP-MS detection. J. Environ. Monitor. 3, 371–376.

Galy, A., France-Lanord, C., 1999. Weathering processes in the Ganges-Brahmaputra basin and the riverine alkalinity budget. Chem. Geol. 159, 31–60.

Garai, R., Chakraborty, A.K., Dey, S.B., Saha, K.C., 1984. Chronic arsenic poisoning from tube-well water. J. Indian Med. Assoc. 82, 32–35.

Garrels, R.M., 1967. Genesis of some ground waters from igneous rocks. In: Abelson, P.H. (Ed.), Researches in Geochemistry. John Wiley & Sons, New York, pp. 405–421.

Gasse, F., Arnold, M., Fontes, J.C., Fort, M., Bingyan, L., Quinsang, Z., 1991. A 13,000 year record from western Tibet. Nature 353, 742–745.

Gavrieli, I., Zheng, Y., van Geen, A., Stute, M., Dhar, R., Ahmed, K.M., Simpson, J., Goldstein, S.L., 2000. Hydrogeochemical study of arsenic contamination in Bangladesh groundwater–role of redox condition. J. Conf. Abstract 5, 435.

GHCN, 2005. The Global Historical Climatology Network version 2, accessed December, 2005. URL: http://www.ncdc.noaa.gov/oa/climate/research/ghcn/ghcn.html.

Ghosh, A.R., and Mukherjee, A., 2002. Arsenic contamination of groundwater and human health impacts in Burdwan District, West Bengal, India. Geol. Soc. Am. Abstracts with Programs 34(2), 107.

Ghosh, N.C., Chakraborty, B., and Mazumder, P.K., 1999. Groundwater flow model of Yamuna sub-basin. Proc. Workshop on Groundwater and Its Protection with Special Reference to Arsenic Contamination, CGWB, Calcutta, India.

Glynn, P.D., Plummer, L.N., 2005. Geochemistry and the understanding of ground-water systems. Hydrogeol. J. 13(1), 263–287.

Goodbred, S.L., Kuehl, S.A., 2000. The significance of large sediment supply, active tectonism, and eustasy of margin sequence development: Late Quaternary stratigraphy and evolution of the Ganges-Brahmaputra delta. Sed. Geol. 133, 227–248.

Goodbred, S.L., Kuehl, S.A., Steckler, M.S., Sarkar, M.H., 2003. Controls on facies distribution and stratigraphic preservation in the Ganges-Brahmaputra delta sequence. Sed. Geol. 155, 301–316.

Goswami, D.C., 1985. Brahmaputra river, Assam, India: physiography. Basin denudation and channel aggradation. Water Resour. Res. 21(7), 959–978.

Griffin, J.J., Windhom, H., Goldberg, E.D., 1968. The distribution of clay minerals in the world ocean. Deep Sea Research 15, 433–459.

Grossman, E.L., Coffman, B. K., Fritz, S.J., Wada, H., 1989. Bacterial production of methane and its influence on ground-water chemistry in east-central Texas aquifers. Geology 17, 495–499.

Grout, H., 1995. Characterisation physique, mineralogique, chimique et signification de la charge particulaire et colloýdale derivieres de la zone subtropicale. Unpublished PhD thesis, Aix-Marseille, France.

Guha Mazumder, D.N., Haque, R., Ghosh, N., De, B.K., Santra, A., Chakraborty, D., Smith, A.H., 1998. Arsenic level in drinking water and the prevalence of skin lesions in West Bengal, India. Int. J. Epidem. 27, 871–877.

Gulen, J., Champ, D.R., Jackson, R.E., 1979. Influence of redox environments on the mobility of arsenic in groundwater. In: Jenne, E.A. (Ed.), Chemical Modeling in Aqueous Systems. Am. Chem. Soc. Symp. Ser. 81, pp. 95.

Güler, C., Thyne, G.D., McCray, J.E., Turner, A.K., 2002. Evaluation of graphical and multivariate statistical methods for classification of water chemistry data. Hydrogeol. J. 10, 455–474.

Hait, A.K., Das, J.K., Ghosh, S., Ray, A.K., Saha, A.K., Chanda, S., 1996. New dates of Pleisto-Holocene subcrop samples from South Bengal, India. Indian J. Earth Sci. 23(2), 79–82.

Handa, B.K., 1972, Geochemical characteristics and quality of groundwater in Gangetic West Bengal. Proc. Geohydrology and Geotechniques of the Lower Ganga Basin, IIT Kharagpur, West Bengal, B65–B81.

Hansen, L.K., Jakobsen, R., Postma, D., 2001. Methanogenesis in a shallow sandy aquifer, Rømø, Denmark. Geochim. Cosmochim. Acta 65, 2925–2935.

Harvey, C.F., 2002. Groundwater flow in the Ganges delta. Science 296, 1563.

Harvey, C.F., Swartz, C.H., Badruzzaman, A.B.M., Keon-Blute, N., Yu, W., Ali, M.A., Jay, J., Beckie, R., Niedan, V., Brabander, D., Oates, P.M., Ashfaque, K.N., Islam, S., Hemond, H.F., Ahmed, M.F., 2002. Arsenic mobility and groundwater extraction in Bangladesh. Science 298, 1602–1606.

Harvey, C.F., Swartz, C.H., Badruzzaman, A.B.M., Keon-Blute, N., Yu, W., Ali, M.A., Jay, J., Beckie, R., Niedan, V., Brabander, D., Oates, P.M., Ashfaque, K.N., Islam, S., Hemond, H.F., Ahmed, M.F., 2005. Groundwater arsenic contamination on the Ganges Delta: biogeochemistry, hydrology, human perturbations, and human suffering on a large scale. Compt. Rend. Geosci. 337, 285–296.

Harvey, C.F., Ashfaque, K.N., Yu, W., Badruzzaman, A.B.M., Ali, M.A., Oates, P.M., Michael, H.A., Neumann, R.B., Beckie, R., Islam, S., Ahmed, M.F., 2006. Groundwater dynamics and arsenic contamination in Bangladesh. Chem. Geol. 228, 112–136.

Hem, J.D., 1992. Study and interpretation of the chemical characteristics of natural water. U.S. Geol. Surv. Water-Supply Paper 2254, 264 p.

Hendry, M.J., Schwartz, F.W., 1990. The chemical evolution of ground water in the Milk River aquifer, Canada. Ground Water 28, 253–261.

Hendry, M.J., Schwartz, F.W., Robertson, C., 1991. Hydrogeology and hydrogeochemistry of the Milk River aquifer system, Alberta, Canada: a review. Appl. Geochem. 6(4), 369–380.

Heroy, D.C., Kuehl, S.A., Goodbred, S.L., 2003. Mineralogy of the Ganges and Brahmaputra Rivers: implications for river switching and Late Quaternary climate change. Sed. Geol. 155, 343–359.

Horneman, A., van Geen, A., Kent, D.V., Mathe, P.E., Zheng, Y., Dhar, R.K., O'Connell, S., Hoque, M.A., Aziz, Z., Shamsudduha, M., 2004. Decoupling of As and Fe release to Bangladesh groundwater under reducing conditions. Part I: Evidence from sediment profiles. Geochim. Cosmochim. Acta 68(17), 3459–3473.

Hossain, M., D. Lewis, M. Bose, A. Chowdhury, 2003. Rice research: Technological progress and impacts on the poor: The Bangladesh case (Summary Report), International Food Policy Research Institute (IFPRI).

Huizing, H.G.J., 1971. A reconnaissance study of the mineralogy of sand fractions from East Pakistan sediments and soils. Geoderma 6, 109–133.

Imam, M.B., Shaw, H.F., 1985. The diagenesis of Neogene clastic sediments from Bengal basin, Bangladesh. J. Sed. Petrol. 55, 665–671.

Inskeep, W.P., McDermott, T.R., Fendorf, S., 2002. Arsenic(V)/(III) cycling in soils and natural waters: Chemical and microbiological processes. In: Frankenberger Jr., W.T. (Ed.), Environmental Chemistry of Arsenic, Marcel Dekker, pp. 183–215.

Ishiga, H., Dozen, K., Yamazaki, C., Ahmed, F., Islam, M.B., Rahman, M.H., Sattar, M.A., Yamamoto, H., Itoh, K., 2000. Geological constraints on arsenic contamination of groundwater in Bangladesh. Abstracts of 5th Forum on Asian Arsenic Contamination, Yokohama, Japan. RGAG, Saitama, pp. 53–62.

Islam, M.S., Tooley, M.J., 1999. Coastal and sea level changes during the Holocene in Bangladesh. Quat. Int. 55, 61–75.

Islam, F.S., Gault, A.G., Boothman, C., Polya, D.A., Charnock, J.M., Chatterjee, D., Lloyd, J.R., 2004. Role of metal-reducing bacteria in arsenic release from Bengal delta sediments. Nature 430, 68–71.

Jacks, G., Sharma, V.P., Trossander, P., Aberg, G., 1994. Origin of sulfur in soil and water in a Precambrian terrain, South India. Geochem. J. 28, 351–358.

Jackson, R.E., Patterson, R.J., 1982. Interpretation of pH and Eh trends in a fluvial-sand aquifer system. Water Resour. Res. 18, 1255–1268.

Jakobsen, R., Postma, D., 1999. Redox zoning, rates of sulfate reduction and interactions with Fe-reduction and methanogenesis in a shallow sandy aquifer, Rømø, Denmark. Geochim. Cosmochim. Acta 63, 137–151.

JICA, 2000. The study on the ground water development of deep aquifers for safe drinking water supply to arsenic affected areas in western Bangladesh. Progress report, book 1-3. Japan International Cooperation Agency, Kokusai Kogyo Co. Ltd. and Mitsui Mineral Development Engineering Co. Ltd.

JICA, 2002. The study on the ground water development of deep aquifers for safe drinking water supply to arsenic affected areas in western Bangladesh. Draft final report, book 1-3. Japan International Cooperation Agency, Kokusai Kogyo Co. Ltd. and Mitsui Mineral Development Engineering Co. Ltd.

Johnson, T.M., Roback, R.C., McLing, T.L., Bullen, T.D., DePaolo, D.J., Doughty, C., Hunt, R.J., Murrell, M.T., Smith, R.W., 2000. Groundwater ‘‘fast paths’’ in the Snake River Plain aquifer: Radiogenic isotope ratios as natural groundwater tracers. Geology, 28, 871–874.

Jain, A., Klaus, R.P., Loeppert, R.H., 1999. Arsenite and arsenate adsorption on ferrihydrite: surface charge reduction and net OH-release stoichiometry. Environ. Sci. Technol. 33, 1179–1184.

Klump, S., Kipfer, R., Olaf, A.C., Harvey, C.F., Brennwald, M.S., Khandkar, N.A., Badruzzaman, A.B.M., Hug, S., Imboden, D.M., 2006. Groundwater dynamics and arsenic mobilization in Bangladesh assessed using noble gases and tritium. Environ. Sci. Technol. 40, 243–250.

Korte, N.E., Fernando, Q., 1991. A review of arsenic(III) in groundwater. Crit. Rev. Environ. Contr. 21, 1–39.

Krishnamurthy, R.V., Bhattacharya, S.K., 1991. Stable oxygen and hydrogen isotope ratios in shallow groundwater from India and a study of the role of evapotranspiration in the Indian monsoon. In: Taylor, H.P., O’Neil, J.R., Kaplan, I.R. (Eds.), Stable Isotope Geochemistry. A Tribute to Samuel Epstein. Special Publication No. 3, The Geochemical Society, San Antonio, Texas, pp. 187–194.

Kuehl, S.A., Hairu, T.M., Moore, W.S., 1989. Shelf sedimentation off the Ganges-Brahmaputra river system: evidence of sediment bypassing to the Bengal fan. Geology 17, 1132–1135.

Kuhn, A., Sigg, L., 1993. Arsenic cycling in eutrophic Lake Greifen, Switzerland-influence of seasonal redox processes. Limnol. Oceanog. 38, 1052–1059.

Kuivila, K.M., Murray J.W., Devol A.H., Novelli, P.C., 1989. Methane production, sulfate reduction and competition for substrates in the sediments of Lake Washington. Geochim. Cosmochim. Acta 53, 409–416.

Kumar, S., Singh, I.B., 1978. Sedimentological study of Gomti river sediments, Uttar Pradesh, India: example of a river in alluvial plain. Senckenb Marit 10(6), 145–211.

Lahm, T.D., Bair, E.S., Vanderkwaak, J., 1998. Role of salinity-derived variable-density flow in the displacement of brine from a shallow, regionally extensive aquifer. Water Resour. Res. 34, 1469–1480.

Land, L.S., Prezbindowski, D., 1981. The origin and evolution of saline formation waters, Lower Cretaceous carbonates, south-central Texas, USA. J. Hydrol. 54, 51–74.

Langmuir, D., 1997. Aqueous Environmental Geochemistry. Prentice Hall, Upper Saddle River, New Jersey, 600 p.

Lehmann, B.E., Davis, S.N., Fabryka-Martin, J., 1993. Atmospheric and subsurface sources of stable and radioactive nuclides used for groundwater dating, Water Resour. Res. 29, 2027–2040.

Leuchs, W., 1988. Vorkommen, Abfolge und Auswirkungen anoxischerredoxreaktionen in einem Pleistozänen Porengrundwasserleiter. Bes. Mitt. Dtsch. Gewass. Jahrbuch (Dusseldorf) 52, 106 p.

Lindsay, J.F., Holiday, D.W., Hulbert, A.G., 1991. Sequence stratigraphy and the evolution of the Ganges-Brahmaputra complex. Am. Assoc. Petrol. Geol. Bull. 75, 1233–1254.

Mallick, S., Rajgopal, N.R., 1995. Groundwater development in the arsenic affected alluvial belt of West Bengal–some questions. Curr. Sci. 70, 956–958.

Malmstrom, V.H., 1969. A new approach to classification of climate. J. Geog. 68, 351–357.

Mance, G., O'Donnell, A.R., Smith, P.R., 1988. Proposed environmental quality standards for List II substances in water: Boron. Water Res. Center, Tech. Rep. no. 256.

Mandal, B.K., Chowdhury, T.R., Samanta, G., Mukherjee, D., Chanda, C.R., Saha, K.C., Chakraborti, D., 1998. Impact of safe water for drinking on five families for 2 years in West Bengal, India. Sci. Tot. Environ. 218, 185–201.

Manning, B.A., Fendorf, S.E., Bostick, B., Suarez, D.L., 2002. Arsenic(III) oxidation and arsenic(V) adsorption reactions on synthetic birnessite. Environ. Sci. Technol. 36, 976–981.

Martens, C.S., Goldhaber, M.B., 1978. Early diagenesis in transitional sedimentary environments of the White Oak Estuary, North Carolina. Limnol. Oceanogr. 23, 428–441.

Masscheleyen, P.H., DeLaune, R.D., Patrick, W.H., 1991. Effect of redox potential and pH on arsenic speciation and solubility in a contaminated soil. Environ. Sci. Technol. 25, 1414–1419.

Maxey, G.B., 1964. Hydrostratigraphic units. J. Hydrol. 2, 124–129.

McArthur, J.M., Ravenscroft, P., Safiullah, S., Thirlwall, M.F., 2001. Arsenic in groundwater: testing pollution mechanisms for aquifers in Bangladesh. Water Resour. Res. 37, 109–117.

McArthur, J.M., Banerjee, D.M., Hudson-Edwards, K.A., Mishra, R., Purohit, R., Ravenscroft, P., Cronin, A., Howarth, R.J., Chatterjee, A., Talukder, T., Lowry, D., Houghton, S., Chadha, D., 2004. Natural organic matter in sedimentary basins and its relation to arsenic in anoxic groundwater: the example of West Bengal and its worldwide implications. Appl. Geochem. 19, 1255–1293.

McDonald, M.G., Harbaugh, A.W., 1988. A modular three-dimensional finite-difference ground-water flow model. U.S. Geol. Surv. Techniques Water-Resour. Invest., Book 6, Chap. A1, 586 p.

Meade, R.H., and Parker, R.S., 1985. Sediments in rivers of the United States. National Water Summary, 1984. U.S. Geol. Surv. Water Sup. Paper 2275, 49–60.

Mehta, B.C., Bhattacharya, M., c. 2000. Hydrogeochemistry of mobilization of arsenic in groundwater of West Bengal, India. Central Ground Water Board, Calcutta.

Miah, M.M., 1988. Flood in Bangladesh: A hydromorphological study of the 1987 flood. Academic Publishers, Dhaka.

MID, 2001. Report of 3rd Minor Irrigation Census in West Bengal 2000-2001. Minor Irrigation Department, Government of West Bengal, India.

Milliman, J.D., Meade, R.H., 1983. World-wide delivery of river sediments to the oceans. J. Geol. 91, 1–22.

Milliman, J.D., Rutkowski, C., Meybeck, M., 1995. River discharge to sea: a global river index (GLORI). Texel, NIOZ, 125 p.

Morgan, C.O., Winner Jr., M.D., 1962. Hydrochemical facies in the 400 foot and 600 foot sands of Baton Rouge area, Louisiana. U. S. Geol. Surv. Prof. Paper 450-B, B120-121.

Morgan, J.P., McIntire, W.G., 1959. Quaternary geology of Bengal Basin, East Pakistan and India. Geol. Soc. Am. Bull. 70, 319–342.

Mukherjee, S., 2004, Prerequisite studies for numerical flow modeling to locate safe drinking water wells in the zone of arsenic polluted groundwater in the Yamuna sub-basin, West Bengal, India. Proc. 32nd IGC, Florence, Italy, BWO 06-42.

Muller, G., 1979. Schermetalle in den sedimenten des Rhines. Varenderungen seit 1971, Umaschau 79, 778–785.

Neumann, T., Raush, N., Leipe, T., Dellwig, O., Berner, Z., Bottcher, M.E., 2005. Intense pyrite formation under low-sulfate conditions in the Achterwasser lagoon, SW Baltic Sea. Geochim. Cosmochim. Acta 14, 3619–3630.

Nickson, R., McArthur, J.M., Ravenscroft, P., Burgess, W.G., Rahman, M., 1998. Arsenic poisoning of groundwater in Bangladesh. Nature 395, 338.

Nickson, R., McArthur, J.M., Ravenscroft, P., Burgess, W.G., Ahmed, M., 2000. Mechanism of arsenic release to groundwater, Bangladesh and West Bengal. Appl. Geochem. 15, 403–411.

Nordstrom, D.K., 2004. Modeling low-temperature geochemical processes. In: Drever, J.I., Holland, H.D., Turekian, K.K. (Eds.), Treatise on Geochemistry, vol. 5, Surface and Groundwater, Weathering and Soils. Elsevier Ltd., pp. 37–72.

Nordstrom, D.K., Plummer, L.N., Wigley, T.M.L., Wolery, T.J., Ball, J.W., Jenne, E.A., Bassett, R.L., Crerar, D.A., Florence, T.M., Fritz, B., Hoffman, M., Holdren, G.R., Jr., Lafon, G.M., Mattigod, S.V., McDuff, R.E., Morel, F., Reddy, M.M., Sposito, G., Thrailkill, J., 1979, A comparison of computerized chemical models for equilibrium calculations in aqueous systems. In: Jenne, E.A. (Ed.), Chemical Modeling in Aqueous Systems, Speciation, Sorption, Solubility, and Kinetics, Am. Chem. Soc. Symp. Ser. 93, pp. 857–892.

Oremland, R.S., 1988. Biogeochemistry of methanogenic bacteria. In: Zehnder, A.J.B. (Ed.), Biology of Anaerobic Microorganisms. John Wiley & Sons, New York, pp. 641–706.

Oremland, R.S., Newman, D.K., Kail, B.W., Stolz, J.F., 2002. Bacterial respiration of arsenate and its significance in the environment. In: Frankenberger Jr, W.T. (Ed.), Environmental Chemistry of Arsenic. Marcel Dekker, pp. 273–295.

Oscarson, D.W., Huang, P.M., Defosse, D., Herbillion, A., 1981. Oxidative power of Mn(IV) and Fe(III) oxides with respect to As(III) in terrestrial and aquatic environments. Nature 291, 50–51.

Pal, T., Mukherjee, P.K., Sengupta, S., Bhattacharya, A.K., Shome, S., 2002. Arsenic pollution in groundwater of West Bengal, India–An insight into the problem by subsurface sediment analysis. Gondwana Res. 5, 501–502.

Parkes, R.J., Cragg, B.A., Fry, J.C., Herbert, R.A., Wimpenny, J.W.T., 1990. Bacterial biomass and activity in deep sediment layers from the Peru margin. Phil. Trans. R. Soc. Lond. A331, 139–153.

Parkhurst, D.L., Appelo, C.A.J., 1999. User's guide to PHREEQC (version 2): A computer program for speciation, batch-reaction, one-dimensional transport, and inverse geochemical calculations. U.S. Geol. Surv. Water Resour. Invest. Rep. 99-4259, 312 p.

Parkhurst, D.L., Christenson, S., Breit, G.N., 1996. Ground-water quality assessment of the Central Oklahoma aquifer, Oklahoma–geochemical and geohydrologic investigations. U.S. Geol. Surv. Water-Supply Paper 2357-C, 101 p.

Penny, E., Lee, M.K., Morton, C., 2003. Groundwater and microbial processes of Alabama coastal plain aquifers. Water Resour. Res. 39(11), 1320, doi:10.1029/2003WR001963.

Peter, K.L., 1984. Hydrogeochemistry of lower Cretaceous sandstone aquifers, Northern Great Plains. In: Jorgensen, D.G., Signor, D.N. (Eds.), Proc. Geohydrology of Dakota Aquifer Symp. Water Well J. Pub. Co., Worthington, Ohio, pp. 163–174.

PHED, 2003a. Tubewell particulars of water supply schemes, district Murshidabad. Public Health Engineering Directorate, Government of West Bengal, India.

PHED, 2003b. Tubewell particulars of water supply schemes, district Nadia. Public Health Engineering Directorate, Government of West Bengal, India.

PHED, 2003c. Tubewell particulars of water supply schemes, district North 24 Parganas. Public Health Engineering Directorate, Government of West Bengal, India.

PHED, 2003d. Tubewell particulars of water supply schemes, district South 24 Parganas. Public Health Engineering Directorate, Government of West Bengal, India.

PHED, 2004. Map showing arsenic affected blocks in West Bengal. Public Health Engineering Directorate, Government of West Bengal, India.

Pierce, M.L., Moore, C.B., 1980. Adsorption of arsenite on amorphous iron hydroxide from dilute aqueous solution. Environ. Sci. Technol. 14, 214–216.

Pike, J.G., 1964. The estimation of annual runoff from meteorological data in a tropical climate, J. Hydrol. 2, 116–123.

Piper, A.M., 1944. A graphic procedure in the geochemical interpretations of water analyses. Trans. Amer. Geophys. Union 25, 914–923.

Plummer, L.N., Busby, J.F., Lee, R.W., Hanshaw, B.B., 1990. Geochemical modeling of the Madison aquifer in parts of Montana, Wyoming, and South Dakota. Water Resour. Res. 26(9), 1981–2014.

Plummer, L.N., Prestemon, E.C., Parkhurst, D.L., 1994. An interactive code (NETPATH) for modeling net geochemical reactions along a flow path, version 2.0. U.S. Geol. Surv. Water-Resour. Invest. Rep. 94-4169, 130 p.

Plummer, L.N., Sprinkle, C.L., 2001. Radiocarbon dating of dissolved inorganic carbon in groundwater from confined parts of the Upper Floridan aquifer, Florida, USA. Hydrogeol. J. 9, 127–150.

Polizzotto, M.L., Harvey, C.F., Sutton, S.R., Fendorf, S., 2005. Processes conducive to the release and transport of arsenic into aquifers of Bangladesh. Proc. Nat. Acad. Sci. 102(52), 18819-18823

Postma, D., Jakobsen, R., 1996. Redox zonation: Equilibrium constraints on the Fe(III)/SO_4^{2-} reduction interface. Geochim. Cosmochim. Acta 60, 3169–3175.

Potter, P.E., 1978. Petrology and chemistry of modern big river sands. J. Geol. 86, 423–449.

Quade, J., Roe, L., DeCelles, P.G., Ojha, T.P., 1997. The late Neogene $^{87}Sr/^{86}Sr$ record of lowland Himalayan rivers. Science 276, 1828–1831.

Ramesh, R., and Sarin, M.M., 1992. Stable isotope study of the Ganga (Ganges) river system. J. Hydrol. 139, 49–62.

Ranganathan, V., Hanor, J.S., 1987. A numerical model for the formation of saline waters due to diffusion of dissolved NaCl in subsiding sedimentary basins with evaporates. J. Hydrol. 92, 97–120.

Rao, K.N., 1981. Tropical cyclones of the Indian Seas. In: Arakawa, H., Takahasi, K. (Eds.), World Survey of Climatology 9, Elsevier, Amsterdam, pp. 257–281.

Ravenscroft, P., McArthur, J.M., Hoque, B., 2001. Geochemical and palaeohydrological controls on pollution of groundwater by arsenic. In: Chappell, W.R., Abernathy, C.O., Calderon, R.L. (Eds.), Arsenic Exposure and Health Effects IV. Elsevier Science, Oxford, pp. 53–77.

Ravenscroft, P., Burgess, W.G., Ahmed, K.M., Burren, M., Perrin, J., 2005. Arsenic in groundwater of the Bengal basin, Bangladesh: Distribution, field relations, and hydrogeologic setting. Hydrogeol. J. 13, 727–751.

Ray, A.K., 1999. Chemistry of arsenic and arsenic minerals relevant to contamination of groundwater and soil from subterranean source. Everyman's Science 35(1).

Rea, D.K., 1992. Delivery of the Himalayan sediments to the Northern Indian Ocean and its relation to global climate, sea level, uplift and sea water strontium. In: Duncan, R.A. et al. (Eds.), Synthesis of Results from Scientific Drilling in the Indian Ocean. Am. Geophys. Un. Geophysical Monograph 70, pp. 387–402.

Redman, A.D., Macalady, D.L., Ahmann, D., 2001. Influence of natural organic matter on sorption of arsenic oxyanions onto metal oxides. Geol. Soc. Am. Abstracts with Programs 33(6).

Reimann, K.U., 1993. The Geology of Bangladesh. Gebruder Borntraeger, Berlin.

Rhine, E.D., Phelps, C.D., Young, L.Y., 2006. Anaerobic arsenite oxidation by novel denitrifying isolates. Environ. Microbiol. 8, 899–908.

Rittle, K.A., Drever, J.I., Colberg, P.J.S., 1995. Precipitation of arsenic during bacterial sulphate reduction. Geomicrobiol. J. 13, 1–11.

Roback, R.C., Johnson, T.M., McLing, T.L., Murrell, M.T., Luo, S., Ku, T.L., 2001. Uranium isotopic evidence for groundwater chemical evolution and flow patterns in the eastern Snake River Plain aquifer, Idaho. Geol. Soc. Am. Bull. 113, 1133–1141.

Ronen, D., Magaritz, M., Almon, E., Amiel, A.J., 1987. Anthropogenic anoxification ("eutrophication") of water table region of a phreatic aquifer. Water Resour. Res. 23, 1554–1560.

Ross, B., Parrott, K., Woodard, J., 1999. Household water quality: hydrogen sulfide in household water. Virginia Polytechnic Institute and State University, Virginia Cooperative Extension pub. no. 356-488, 2 p.

Safiullah, S., 1998. CIDA arsenic project report: monitoring and mitigation of arsenic in the groundwater of Faridpur Municipality. Jahangirnagar University, Dhaka, Bangladesh, 96 p.

Saha, A.K., 1991. Genesis of arsenic in groundwater in parts of West Bengal. Center for Studies on Man and Environment, Calcutta, annual volume.

Saheed, S.M., 1995. Bangladesh. In: Zink, J.A. (Ed.), Soil Survey: Perspective and Strategies of 21st century FAO, Rome, 51–56.

Salati, E., Oall'Olio, A., Matsui, E., Gat, J.R., 1979. Recycling of water in the Amazon basin, an isotope study. Water Resour. Res. 15, 1250–1258.

Sanford, R.F., Pierson, C.T., Crovelli, R.A., 1993. An objective replacement method for censored geochemical data. Math. Geol. 25, 59–80.

Sanyal, J., Lu, X.X., 2003. Application of GIS in flood hazard mapping: a case study of Gangetic West Bengal, India. Map Asia Conference, GIS development.net, 8 pp.

Sarin, M.M., Krisnaswami, S., Dilli, K., Somayajulu, B.L.K., Moore, W.S., 1989. Major ion chemistry of the Ganges-Brahmaputra river system: weathering processes and fluxes to the Bay of Bengal. Geochim. Cosmochim. Acta 54, 1387–1396.

Schwartz, F.W., Zhang, H., 2002. Fundamentals of Ground Water. John Wiley & Sons, Inc., New York, 582 p.

Scott, M.J., Morgan, J.J., 1995. Reactions at oxide surfaces. 1. Oxidation of As(III) by synthetic birnessite. Environ. Sci. Technol. 29, 1898–1905.

Seaber, P.R., 1988. Hydrostratigraphic units. In: Back, W., Rosenshein, J.S., Seaber, P.R. (Eds.), The Geology of North America, vol. O-2, Hydrogeology. The Geological Society of America, Boulder, Colorado, pp. 9–14..

Segall, M.P., Kuehl, S.A., 1992. Sedimentary processes of the Bengal continental shelf as revealed by clay size mineralogy. Cont. Shelf Res. 12(4), 517–541.

Sen, P.K., Banerjee, M., 1990. Palyno-plankton stratigraphy and environmental changes during the Holocene in the Bengal Basin, India. Rev. Palaeobot. Palynol. 65, 25–35.

Sengupta, S., 1966. Geological and geophysical studies in the western part of the Bengal Basin, India. Am. Assoc. Petrol. Geol. Bull. 50, 1001–1017.

Seyler, P., Martin, J.M., 1989. Biogeochemical processes affecting arsenic species distribution in a permanently stratified lake. Environ. Sci. Technol. 23, 1258–1263.

Shivanna, K., Sharma, S., Sinha, U.K., Nair, A.R., Navada, S.V., Ray, A., Talukdar, T., Mehta, B.C., Ghosh, A.K., 1999. Arsenic pollution in ground water of West Bengal. Proc. Workshop on Groundwater Pollution and Its Protection with Special Reference to Arsenic Contamination. CGWB, Calcutta.

Sikdar, P.K., Sarkar, S.S., Palchoudhury, S., 2001. Geochemical evolution of groundwater in the Quaternary aquifer of Calcutta and Howrah, India. J. Asian Earth Sci. 19, 579–594.

Simpkins, W.W., Parkin, T.B., 1993. Hydrogeology and redox geochemistry of CH_4 in a late Wisconsinan till and loess sequence in central Iowa. Water Resour. Res. 29, 3643–3657.

Singh, S.K., Trivedi, K.P., Ramesh, R., Krishnaswami, K., 1998. Chemical and strontium, oxygen and carbon isotopic compositions of carbonates from the lesser Himalaya: Implications to the strontium isotopic composition of the source waters of the Ganga, Ghagra, and Indus rivers. Geochim. Cosmochim. Acta 62, 743–755.

Smedley, P.L., Kinniburgh, D.G., 2002. A review of the source, behaviour and distribution of arsenic in natural waters. Appl. Geochem. 17, 517–568.

Smith, A.H., Lingas, E.O., Rahman, M., 2000. Contamination of drinking-water by arsenic in Bangladesh: a public health emergency. Bull. WHO 78(9), 1093–1103.

Sracek, O., Bhattacharya, P., Ahmed, K.M., Bromsen, M.V., 2004a. Geochemistry of arsenic-enriched groundwater of Brahmanbaria district, Bangladesh: speciation modeling and multivariate statistics. In: Proc. 32nd IGC, Florence, Italy, BWO 06–24.

Sracek, O., Bhattacharya, P., Jacks, G., Gustafsson, J., Bromsen, M.V., 2004b. Behavior of arsenic and geochemical modeling of arsenic enrichment in aqueous environment. Appl. Geochem. 19, 169–180.

Stallard, R.F., Edmond, J.M., 1983. Geochemistry of Amazon 2. The influence of geology and weathering environment on the dissolved load. J. Geophys. Res. 88, 9671–9688.

Stallard, R.F., Edmond, J.M., 1987. Geochemistry of Amazon 3. Weathering chemistry and limits to dissolved load. J. Geophys. Res. 92, 8293–8302.

Stüben, D., Berner, Z., Chandrashekharam, D., Karmakar, J., 2003. Arsenic enrichment in groundwater of West Bengal, India: geochemical evidence for mobilization of As under reducing conditions. Appl. Geochem. 18(9), 1417–1434.

Stumm, W., Morgan, J.J., 1996. Aquatic Chemistry, 3rd edition. John Wiley and Sons, New York, 1022 p.

Survey of India, 1971. Map of West Bengal, scale 1:1,000,000. Publishing Group of Survey of India, Government of India.

Swartz, C.H., Blute, N.K., Badruzzaman, B., Ali, A., Brabander, D., Jay, J., Besancon, J., Islam, S., Hemond, H.F., Harvey, C.F., 2004. Mobility of arsenic in a Bangladesh aquifer: Inferences from geochemical profiles, leaching data, and mineralogical characterization. Geochim. Cosmochim. Acta 66, 4539–4557.

SWID, 1998. A comprehensive hydrogeological information of Murshidabad district. Geologic Division No. III, State Water Investigation Directorate (SWID), Government of West Bengal, 43 p.

Tagore, R., 1905. Amar Sonar Bangla (My Golden Bengal). Baul (Folk Singer), Visva-Bharati Publications, Calcutta, India.

Tardy, Y., 1971. Characterization of the principal weathering types by the geochemistry of waters from some European and African crystalline massifs. Chem. Geol. 7, 253–271.

Tareq, S.M., Safiullah, S., Anwar, H.M., Rahman, M.M., Ishazuka, T., 2003. Arsenic pollution in groundwater: a self organizing complex geochemical process in the deltaic sedimentary environment, Bangladesh. Sci. Tot. Environ. 313, 213–226.

Taylor, S.R., McLennan, S.M., 1985. The Continental Crust: Its Composition and Evolution. Blackwell, London, 312 p.

Tetlow, J.A., Wilson, A.L., 1958. Determination of iron in boiler feedwater. Analyst.

Tóth, J., 1963. A theoretical analysis of groundwater flow in small drainage basins. J. Geophys. Res. 68, 4795–4812.

Uddin, A., Lundberg, N., 1998. Unroofing history of the eastern Himalayas and the Indo-Burma ranges: heavy mineral study of Cenozoic sediments from the Bengal Basin, Bangladesh. J. Sed. Res. 68(3), 465-472.

Umitsu, M., 1985. Natural levees and landform evolution in the Bengal lowland. Geograph. Rev. Jap. 58(2), 149–164.

Umitsu, M., 1987. Late Quaternary sedimentary environment and landform evolution in the Bengal Lowland. Geograph. Rev. Jap. Series B 60, 164–178.

Umitsu, M., 1993. Late Quaternary sedimentary environments and landforms in the Ganges Delta. Sed. Geol. 83, 177–186.

UNDP, 1982. Groundwater survey: The hydrogeological conditions of Bangladesh. UNDP technical report DP/UN/BGD-74-009/1, 113 p.

van Geen, A., Ahmed, K.M., Seddique, A.A., Shamsudduha, M., 2003. Community wells to mitigate the arsenic crisis in Bangladesh. Bull. WHO 81, 632–638.

van Geen, A., Rose, J., Thoral, S., Garnier, J.M., Zheng, Y., Bottero, A., 2004. Decoupling of As and Fe release to Bangladesh groundwater under reducing conditions. Part II: Evidence from sediment incubations. Geochim. Cosmochim. Acta 68, 3475–3486.

Varner, D., Skipton, S., Jasa, P., Dvorak, B., 2004. Drinking water: Sulfates and hydrogen sulfide. University of Nebraska-Lincoln Extension Webguide pub. no. G1275, 3 p.

Vishnu-Mittre, S., Guputa, H. P., 1979. Pollen analytical study of Quaternary deposits in the Bengal Basin. Paleobotanist 19, 297–306.

Wadia, D.N., 1949. Geology of India, 2nd edition. MacMillan and Co., Ltd., London, 460 p.

Wadia, D.N., 1981. Geology of India. Tata McGraw-Hill, New Delhi, 508 p.

Ward, J.H., 1963. Hierarchical grouping to optimize an objective function. J. Am. Stat. Assoc. 69, 236–244.

Weber, M.E., Wiedicke, M.H., Kudgrass, H.R., Hubsher, C., Erienkeuser, H., 1997. Active growth of Bengal Fan during sea level rise and highstand. Geology 25, 315–318.

Wersin, P., Hohener, P., Giovanoli, R., Stumm, W., 1991. Early diagenetic influences on iron transformations in a freshwater lake sediment. Chem. Geol. 90, 233–252.

West, W.D., 1949. Geological map of India. Geol. Surv. India records, vol. 81, pt. 1, 222 p.

Whiticar, M.J., 1999. Carbon and hydrogen isotope systematics of bacterial formations and oxidation of methane. Chem. Geol. 161, 291–314.

Whittemore, D.O., 2004. Geochemical identification of the saltwater source affecting surface and ground waters near the Washita River, Garvin County, Oklahoma. Kansas Geol. Surv. Open File Rep. 2004-58.

Wood, W.W., 1981, Guidelines for collection and field analysis of ground-water samples for selected unstable constituents: U.S. Geol. Surv. Techniques Water-Resources Investigations, Book 1, Chap. D2, 11 p.

WHO, 1993. Guidelines for Drinking-Water Quality. Vol. 1 Recommendations, 2nd edn. World Health Organization, Geneva.

WHO, 2001. WHO Guidelines for Drinking-Water Quality: Arsenic in Drinking Water. Fact Sheet No. 210. World Health Organization, Geneva.

Yu, W., Harvey, C.M., Harvey, C.F., 2003. Arsenic in groundwater in Bangladesh: A geostatistical and epidemiological framework for evaluating health effects and potential remedies. Water Resour. Res. 39, 1146.

Zachara, J.M., Fredrickson, J.K., Li, S.M., Kennedy, D.W., Smith, S.C., Gassman, P.L., 1998. Bacterial reduction of crystalline Fe(III) oxides in single phase suspensions and subsurface materials. Am. Mineral. 83, 1426–1443.

Zhang, C., Grossman, E.L., Ammerman, J.W., 1998. Factors influencing methane distribution in Texas ground water. Ground Water 36, 58–66.

Zheng, Y., Stute, M., van Geen, A., Gavrieli, I., Dhar, R., Simpson, H.J., Schlosser, P., Ahmed, K.M., 2004. Redox control of arsenic mobilization in Bangladesh groundwater. Appl. Geochem. 19, 201–214.

Zheng, Y., Datta, S., Stute, M., Dhar, R., Hoque, M.A., Rahman, M.W., Ahmed, K.M., Schlosser, P., van Geen, A., 2005a. Stable isotopes (^{18}O, ^{2}H) and arsenic distribution in the shallow aquifers in Araihazar, Bangladesh. Eos Trans. AGU, 86(52), Fall Meeting Supplement, Abstract H31B-1305.

Zheng, Y., van Geen, A., Stute, M., Dhar, R., Mo, Z., Cheng, Z., Horneman, A., Gavrieli, A., Simpson, H.J., Versteeg, R., Steckler, M., Grazioli-Venier, A., Goodbred, S., Shanewaz, M., Shamsudduha, M., Hoque, M., Ahmed, K.M., 2005b. Geochemical and hydrogeological contrasts between shallow and deeper aquifers in two villages of Araihazar, Bangladesh:

Implications for deeper aquifers as drinking water sources. Geochim. Cosmochim. Acta 69, 5203–5218.

ZoBell, C.E., 1946. Studies on redox potential of marine sediments. Am. Assoc. Petrol. Geol. Bull. 30, 477–513.

Vita

Personal Details
Date of Birth: 23 February 1976
Place of Birth: Calcutta, India

Education
- **Master of Science** (M.S.) in Geology, University of Kentucky, USA, 2003

Thesis title: Identification of natural attenuation of trichloroethene and technetium-99 along Little Bayou Creek, McCracken County, Kentucky.
Advisor: Dr. Alan E. Fryar
- **Post Graduate Diploma** in Software Engineering, National Institute of Information Technology, India, 2000
- **Master of Science** (M.Sc.) in Geology, University of Calcutta, India, 1999

Thesis title: Geotechnical study of landslides in and around the approach road to Kalimpang, Darjeeling district, West Bengal.
Advisor: Prof. Arup K. Mitra
- **Bachelor of Science with Honors** (B.Sc.[Hons]) in Geology, University of Calcutta, India, 1997

Special/Short Courses
- MODFLOW, International Ground Water Modeling Center, Colorado School of Mines, November 2004
- Quaternary Geology, remote sensing and GIS, International Union of Quaternary Research (INQUA), Indian Chapter, January 1999
- Basic computer applications, Indian Institute of Computer Engineers, Asutosh College, 1994-1995
- Petrographic slide preparation and ore polishing, Asutosh College, 1994

Research Experience
- Regional hydrogeology and groundwater quality in the western Bengal basin, India by computer-generated simulations, and chemical and stable isotopic characterizations (for ongoing Ph.D.)
- Groundwater/surface-water interactions and fate of organic and radioactive contaminants by conservative and non-conservative tracer tests and simulations at a U.S. Department of Energy nuclear enrichment facility in the northern Gulf Coastal Plain, USA (for M.S., 2001-2003)
- Environmental geotechnical studies of lower Ganges river, India (for post-masters research at the University of Calcutta, 1999-2001)
- Geotechnical studies on causes, effects and remediation of landslides in Eastern Himalayas, India (for M.Sc., 1997-1999)

Honors/Grants
- Selected as Earth Institute Fellow at the Columbia University, 2006
- Dissertation Enhancement Award, University of Kentucky, 2005 ($3000)
- Ferm Grant for field research, Department of Geological Sciences, University of Kentucky, 2005 ($600)

- Graduate Student Research Grant Award, Hydrogeology Division, Geological Society of America, 2004 ($2815)
- Pirtle Fellowship, Department of Geological Sciences, University of Kentucky, 2004-2006 ($3000 each year)
- Departmental nominee, Outstanding Master's Thesis Award in Physical Sciences and Engineering, Council of Southern Graduate Schools, 2003
- Student research grant, Geological Society of America, Southeastern Section, 2002 ($600), 2005 ($900)
- Student research grant, Graduate School, University of Kentucky, 2002 ($400), 2004 ($400)
- Brown-McFarlan Grant for research, Department of Geological Sciences, University of Kentucky, 2002 ($400)
- Nominated for "International Man of the Year" by International Biographical Center, Cambridge, UK, 2001
- Selected as "One of the 2000 Outstanding Scientists and Intellectuals" by International Biographical Center, Cambridge, UK, 2001
- Nominated for "Young Scientist Award" by Indian Science Congress Association, 2001
- All India Rank 20th in Graduate Aptitude Test in Engineering (GATE), Government of India, 2001
- National Scholarship from Government of India for excellence in graduate studies, 1999
- Total Freedom Scholarship from National Institute of Information Technology (NIIT), India, for software engineering study, 1997

Professional Affiliations

- American Association of Petroleum Geologists
- Geological Society of America
- Indian Science Congress Association

Professional Services

- Co-Chair (with Prosun Bhattacharya, KTH, Stockholm, Sweden, Kaye Savage, Vanderbilt University, and Andrea Foster, U.S. Geological Survey) topical session on "Arsenic and metalloids in groundwater and surface water systems" Geological Society of America Annual Meeting, Philadelphia, PA, 2006
- Co-Chair (with Alan E. Fryar, University of Kentucky, and Alan Welch, U.S. Geological Survey) of "Arsenic occurrence and fate in hydrogeologic systems" topical session (3 sessions), Geological Society of America Annual Meeting, Salt Lake City, Utah, 2005
- Co-convener, Graduate and undergraduate research symposium, Department of Geological Sciences, University of Kentucky, 2003
- Convener, Green Circle of India (a non-governmental environmental research organization), 1999-2001

List of Publications

Refereed Journal Articles

Mukherjee, A., Fryar, A.E., and Howell, P. (in review). Regional hydrostratigraphy and groundwater flow modeling of the arsenic contaminated aquifers of the western Bengal basin, West Bengal, India. Hydrogeology Journal.

Mukherjee, A., Fryar, A.E., and Rowe, H.D. (in review). Characterizing the regional scale stable isotopic ($\delta^{18}O$-$\delta^{2}H$) signature and recharge of the deeper water of the arsenic affected areas of the Gangetic West Bengal, India. Journal of Hydrology.

Mukherjee, A., and Fryar, A.E. (in review). Deeper groundwater chemistry and geochemical modeling of the arsenic affected western Bengal basin, West Bengal, India. Applied Geochemistry.

Mukherjee, A., Fryar, A.E., and LaSage, D.M., 2005. Using tracer tests to assess natural attenuation of contaminants along a channelized Coastal Plain stream. Environmental & Engineering Geoscience, vol. 11, no. 4, 371-381.

Mukherjee, A., and Mitra, A.K., 2001. Geotechnical study of mass movements along the Kalimpong approach road in the eastern Himalayas. Indian Journal of Geology, vol. 73, no. 4, 271-279.

Ghosh, D., Deb, A., Fryar, A.E., **Mukherjee, A.,** Patra, K., and Sengupta, R., (in revision). Deeper groundwater alpha radioactivity and related chemistry of the arsenic polluted areas of West Bengal, India. Journal of Environmental Radiation.

Mukherjee, A., Fryar, A.E., and Bhattacharya, A. (in preparation). Arsenic contamination of western Bengal basin: Is deeper groundwater an alternate safe drinking-water source?

LaSage, D.M., Fryar, A.E., and **Mukherjee, A.** (in preparation). Contaminated ground-water discharge along a channelized Coastal Plain stream. To be submitted to Journal of Contaminant Hydrology

Book Chapter

Mukherjee, A., Fryar, A.E. (in preparation). Arsenic in hydrologic systems. In Henke, K., Atwood, D., Blue, L. (eds): Chemistry, Geology and Biology of Arsenic. John Wiley & Sons, Ltd (UK)

Unpublished Theses

Mukherjee, A., 2003. Identification of natural attenuation of trichloroethene and technetium-99 along Little Bayou Creek, McCracken County, Kentucky. University of Kentucky, Lexington, 177 p. (M.S. thesis)

Mukherjee, A., 2001. Geotechnical study of landslides in and around the approach road to Kalimpang, Darjeeling district, West Bengal. University of Calcutta, Kolkata, 126 p. (M.Sc. thesis)

Conference Papers

Fryar, A.E., and **Mukherjee, A**., 2006. Arsenic pollution in western Bengal basin: Is deeper water an alternate safe source? In Proceedings of the International Congress on Integrated Water Resources Management and Challenges of the Sustainable Development (GIRE3D), Marrakech, Morocco.

Mukherjee, A., Fryar, A.E., and Chakraborti A., 2004. Regional groundwater chemistry and its relation to arsenic contamination in the western Bengal basin. In Proceedings

XXXIII Congress IAH & 7º Congress ALHSUD, International Association of Hydrogeologists, Zacatecas, Mexico, paper WS-AS-04, 4 p.

Abstracts

Mukherjee, A., and Fryar, A.E., 2006. Arsenic mobilization and retention caused by partial redox equilibrium in deeper groundwater of the western Bengal basin, West Bengal, India. Geological Society of America, Abstracts with Programs, in press.

Mukherjee, A., Von Brömssen, M, Jacks, G, Ahmed, K.M., Fryar, A.E., Hasan, M.A., Bhattacharya, P., 2006. Hydrochemical contrast between two arsenic affected areas near the eastern and western margins of Bengal basin: some preliminary results. Geological Society of America, Abstracts with Programs, in press.

Gupta, N.N., **Mukherjee, A.**, White, E. R., Fryar, A.E., Atwood, D.A., 2006. Use of water insoluble thiols for arsenic remediation—a field Study. Geological Society of America, Abstracts with Programs, in press.

Mukherjee, A., and Fryar, A.E., 2005. A composite approach to characterize the deeper aquifer of the arsenic contaminated western Bengal basin, India. Geological Society of America, Abstracts with Programs, vol. 37, no. 7, p. 170.

Mukherjee, A., and Fryar, A.E., 2005. Status of arsenic contamination and hydrogeochemistry of deeper groundwater in eastern part of River Bhagirathi, West Bengal, India. In Proceedings of the National Conference on Arsenic Pollution in West Bengal, Srikrishna College, Bagula, West Bengal, India.

Mukherjee, A., and Fryar, A.E., 2005. Arsenic in deeper groundwater of the western Bengal basin, India: a contradiction of conventional belief. In Proceedings of the Kentucky Water Resources Annual Symposium, Kentucky Water Resources Research Institute, 29-30.

Mukherjee, A., and Fryar, A.E., 2005. Understanding the regional scale groundwater flow and chemistry in the arsenic affected western Bengal basin, India. In Proceedings, 92nd Session, Indian Science Congress. Earth System Sciences, Indian Science Congress Association.

Ghosh, D., Deb, A., Patra, K.K., Sengupta, R., **Mukherjee, A**., and Fryar, A.E., 2005. Double health risk in arsenic contaminated drinking water—evidence of enhanced alpha radioactivity: Geological Society of America Abstracts with Programs, v. 37, no. 7, p. 170.

Mukherjee, A., and Fryar, A.E., 2004. Regional-scale hydrostratigraphy and groundwater chemistry in the western Bengal basin, India. Geological Society of America Abstracts with Programs, vol. 36, no. 5, p. 566.

Mukherjee, A., and Fryar, A.E, 2004. Trends in arsenic and other solutes in deep groundwater along a topographic gradient within the western Bengal basin, India. In Proceedings of the Kentucky Water Resources Annual Symposium, Kentucky Water Resources Research Institute, 9-10.

Mukherjee, A., Fryar, A.E., and Chakrabarti, A., 2004. Study on spatial distribution of arsenic in Bengal groundwater as a function of regional groundwater flow and palaeogeomorphology: A curtain raiser. In Proceedings, 91st Session, Indian Science Congress. Earth System Sciences, Indian Science Congress Association.

Mukherjee, A., 2003. An overview of probable mechanism of arsenic mobilization in Bengal basin groundwater. In Proceedings, 90th Session, Indian Science Congress. Earth System Sciences, Indian Science Congress Association.

Mukherjee, A., and Fryar, A.E., 2003. Evaluating natural attenuation of contaminants along a first order coastal plain stream. Geological Society of America Abstracts with Programs, vol. 35, no. 6, p. 375.

Mukherjee, A. and Fryar, A.E., 2003. Identification of natural attenuation of trichloroethene and technetium along Little Bayou Creek, Kentucky, by tracer tests. Geological Society of America Abstracts with Programs, vol. 35, no. 1, p. 73.

Mukherjee, A., and Fryar, A.E., 2003. Natural attenuation of trichloroethene and technetium along Little Bayou Creek, Kentucky by tracer tests. In Proceedings of the Kentucky Water Resources Annual Symposium, Kentucky Water Resources Research Institute.

Mukherjee, A., 2002. Hydrogeological study on causes and effects and remediation of arsenic contamination of Bengal basin ground water. In Proceedings, 89th Session, Indian Science Congress. Earth System Sciences, Indian Science Congress Association.

Ghosh, A.R., and **Mukherjee, A**., 2002. Arsenic contamination and human health impacts in Burdwan district, West Bengal, India. Geological Society of America Abstracts with Programs, vol. 34, no. 2, p. 107.

Mukherjee, A., 2001. Assessment of causal factors and suggested remedial measures for the landslides of the west slope of Kalimpong hills. In Proceedings, 88th Session, Indian Science Congress, Earth System Sciences.

Popular Science Articles

Mukherjee, A., 1999. Triggering the ages of ice. Breakthrough, vol. 8, no. 2.

Mukherjee, A., 1995. March toward extinction. Scan, vol. 8.

Invited Lectures

- Rast-Holbrook Lecture Series, Department of Earth and Environmental Sciences, University of Kentucky, February 2006: Hydrologic characterization of the arsenic contaminated western Bengal basin, India.
- Kentucky Geological Survey, November 2004: Regional Quaternary hydrostratigraphy, groundwater flow, hydrochemistry and arsenic contamination of the Indian part of the Bengal basin: interim results.
- Arsenic Core Committee, Government of West Bengal, October 2004: Study of hydrogeochemical evolution of groundwater and fate of arsenic along regional flow path in the western Bengal basin, India.

Extracurricular Activities

- Chairman, University of Kentucky Graduate and Family Housing Resident Council, 2005-2006
- Vice-Chairman, University of Kentucky Graduate and Family Housing Resident Council, 2004-2005
- Committee member, Student Activity Board, University of Kentucky, 2002-2003
- Publicity Secretary, Jubamaitry (a social organization), Calcutta, India, 1994-2001